AD-A141 904 TWO-DIMENSIONAL AND QUASI THREE-DIMENSIONAL EXPERIMENTAL STANDARD CONFIGU..(U) ECOLE POLYTECHNIQUE FEDERALE DE LAUSANNE (SWITZERLAND) LAB DE.. 1/3

UNCLASSIFIED T FRANSSON ET AL. 30 SEP 83 F/G 20/4 NL

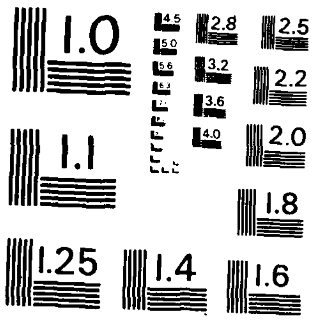

MICROCOPY RESOLUTION TEST CHART
NATIONAL BUREAU OF STANDARDS-1963-A

ECOLE POLYTECHNIQUE FEDERALE DE LAUSANNE

Laboratoire de Thermique Appliquée

TWO-DIMENSIONAL AND QUASI THREE-DIMENSIONAL EXPERIMENTAL STANDARD CONFIGURATIONS FOR AEROELASTIC INVESTIGATIONS IN TURBOMACHINE-CASCADES.

Compiled by T. Fransson and P. Suter

ECOLE POLYTECHNIQUE FEDERALE
DE LAUSANNE

Laboratoire de Thermique Appliquée

TWO-DIMENSIONAL AND QUASI THREE-DIMENSIONAL EXPERIMENTAL STANDARD CONFIGURATIONS FOR AEROELASTIC INVESTIGATIONS IN TURBOMACHINE-CASCADES.

Compiled by T. Fransson and P. Suter

September 30, 1983

This work is jointly sponsored by the United States Air Force under GRANT AFOSR 81-0251, AFOSR 83-0063 with Dr. Anthony Amos as program manager and by the Lausanne Federal Institute of Technology.

Report
LTA-TM-83-2

Preface

At the 1980 "Symposium on Aeroelasticity in Turbomachines", held in Lausanne, Switzerland, it became clear that it was virtually impossible to compare different analytical models for flutter and forced vibration prediction and to establish their validity.

The Scientific Committee (*) of this meeting has decided to initiate a workshop on "Standard Configurations for Aeroelasticity in Turbomachine-Cascades". The aim of this project is to establish a data base with a few well documented experimental data, and to initialize and coordinate future experimental investigations in existing test facilities. The standard configurations to be compiled should also serve as test cases for present and future prediction models for aeroelastic phenomena in turbomachine-cascades.

This report constitutes the first product, a standard set of two-dimensional and quasi three-dimensional experimental configurations. These configurations will be treated by calculation models from several research groups during 1983, whereafter a second report with a comparison between the experimental and the theoretical results will be established and presented at the Third Symposium on Aeroelasticity in Turbomachines (1984). It is the hope of the Scientific Committee that these reports will constitute a bench-mark for the validation of both experimental and theoretical aeroelastic investigations in turbomachines.

September 30, 1983

P. Suter
Chairman of the Scientific Committee
of the 1980 "Symposium on Aeroelasticity in Turbomachines"

(*)

The members of the Scientific Committee at the 1980 Symposium are:

H. Försching, Germany
G. Gyarmathy, Switzerland
R. Legendre, France
A.A. Mikolajczak, USA
M. Roy, France
P. Suter, Switzerland (chairman)
Y. Tanida, Japan
D.S. Whitehead, United Kingdom

Abstract

The aeroelastician needs reliable, efficient methods for the calculation of unsteady blade forces in turbomachines. The validity of such theoretical or empirical prediction models can only be established if researchers apply their flutter and forced vibration predictions to a number of well documented experimental test cases.

In the present report, the geometrical and time-averaged flow conditions of nine two-dimensional or quasi three-dimensional experimental standard configurations for aeroelasticity in turbomachine cascades are given. For each configuration some aeroelastic test cases are defined, comprising different incidence angles, Mach numbers, interblade phase angle, reduced frequencies, etc.

Furthermore a proposal for unified nomenclature and reporting formats is included, in order to facilitate the comparison between the different experimental data and theoretical results.

Contents page

Nomenclature

Note:

a) Throughout this report, "standard configuration" will designate a cascade geometry and "aeroelastic case" or "aeroelastic test case" will indicate the different time dependant (and, in some cases time averaged) conditions within a standard configuration.

b) The tables and figures will be numbered as the chapters. For example, Figure 3.7-2 denotes the second figure in chapter 3.7.

Symbol	Explanation	Dimension
Latin Alphabet		
A	amplitude ($A=\vec{h}$ for pure sinusoidal heaving) ($A=\vec{\alpha}$ for pure sinusoidal pitching)	- rad
A	Fourier coefficient	
c	chord length	m
$\vec{C}_F(t)$	unsteady perturbation force coefficient vector per unit amplitude, positive in positive coordinate directions: $\vec{C}_F(t)=\vec{\bar{C}}_F e^{i(wt-\phi_F)}$	-
$C_L(t)$	unsteady perturbation lift coefficient per unit amplitude, positive in positive y-direction: $C_L(t)=\bar{C}_L e^{i(wt-\phi_L)}$ Note: In the present work, the lift coefficient is defined as the force component perpendicular to the chord!	-
$C_M(t)$	unsteady perturbation moment coefficient per unit amplitude, positive in clockwise direction: $C_M(t)=\bar{C}_M e^{i(wt-\phi_M)}$	-
$C_p(x,t)$	unsteady perturbation blade surface pressure coefficient per unit amplitude: $C_p(x,t)=\bar{C}_p(x) e^{i(wt-\phi_p)}$	-
C_W	coefficient for aerodynamic work done on the airfoil during the cycle of oscillation	-
d	maximum blade thickness (dimensionless with chord)	-

f	vibration frequency	Hz
f	function	-
$h(x,y,t)$	dimensionless (with chord) bending vibration, positive in positive coordinate directions	
$\bar{h}$	dimensionless (with chord) bending amplitude	-
i	$\sqrt{-1}$	-
i	indicence	deg
k	reduced frequency = $\frac{C\,w}{2V_{ref}}$	-
k	harmonic in Fourier series	-
M	Mach number	-
$\vec{n}$	unit vector normal to blade surface, positive inwards	-
$p(x,y,t)$	pressure (without superscript:time dependant perturbation) (with superscript $\sim$:time averaged)	N/m^2
$\vec{R}_\alpha$	dimensionless vector from mean pivot axis to an arbitrary point on the mean blade surface	-
R	real part of complex value	-
Re	Reynolds number = $\frac{V_1 c}{\nu}$	-
$\vec{s}$	unity vector tangent to blade surface, positive in positive coordinate-directions	-
Str	Strouhal number = $\frac{f \cdot c}{V_{ref}}$ $(=k/\pi)$	-
T	dimensionless time: $T = t/T_0$	-
T_0	period of a cycle	s
t	time	s
V	velocity	m/s

V_{ref}	reference velocity for reduced frequency and Strouhal number: $V_{ref} = V_1$ for compresor cascade $V_{ref} = V_2$ for turbine cascade	m/s
w	circular frequency = $2\pi f$	rad/s
x	dimensionless (with chord) chord-wise coordinate	-
x	dimensionless (with chord) chord-wise position of torsion axis	-
y	dimensionless (with chord) normal-to-chord coordinate	-
y	dimensionless (with chord) normal-to-chord position of torsion axis	-
z	dimensionless (with chord) span-wise coordinate	-

Greek Alphabet

$\alpha(t)$	pitching vibration, positive nose-up	rad
$\bar{\alpha}$	pitching amplitude	rad
β	flow angle	deg
γ	chordal stagger angle	deg
δ	heaving vibration direction = $\tan^{-1}(\bar{h}_y/\bar{h}_x)$	deg
$\Delta C_p(x,t)$	unsteady perturbation pressure difference coefficient $\Delta C_p(x,t) = C_p^{(ls)}(x,t) - C_p^{(us)}(x,t) = \overline{\Delta C_p}(x) e^{i(wt + \phi_{\Delta p})}$	-
$\theta_{\alpha}^{(m)}$	phase lead of pitching motion towards heaving motion of blade (m)	deg,rad
ν	kinematic viscosity	m/s
Ξ	aerodynamic damping coefficient, positive for stable motion	-

$\delta^{(m)}$	interblade phase angle between blade "m-1" and blade "m". $\delta^{(m)}=\delta$ for constant interblade phase angle. $\delta^{(m)}$ is positive when blade "m" preceeds blade "m-1". For idealized conditions (constant interblade phase angle between adjacent blades, δ , and identical blade vibration amplitude for all blades) the motion of the (m)th blade, for flexion, is given by: $\vec{h}^{(m)}(x,y,t)=\vec{h}(x,y)^{(O)}e^{i\{wt+m\sigma\}}$	deg,rad
τ	dimensionless (with chord) blade pitch = gap-to-chord ratio	
ϕ_F	phase lead of perturbation force coefficient towards motion	deg,rad
ϕ_L	phase lead of perturbation lift coefficient towards motion	deg,rad
ϕ_M	phase lead of perturbation moment coefficient towards motion	deg,rad
$\phi_p(x)$	phase lead of perturbation pressure coefficient towards motion	deg,rad
$\phi_{\Delta p}(x)$	phase lead of perturbation pressure difference coefficient towards motion	deg,rad
φ	phase angle in the Fourier series	deg

Subscripts:

A	A = h for heaving α for pitching
G	center of gravity
global	*global* (= time dependant + time averaged) (see eq. 7)
I	imaginary part
is	isentropic values
LE	leading edge
k	k-th harmonic in Fourier series
R	real part
ref	reference velocity for reduced frequency $V_{ref} = V_1$ *for compressor cascade* $V_{ref} = V_2$ for turbine cascade
TE	trailing edge
t	total head value
x	component in x-direction
y	component in y-direction
z	component in z-direction
α	position of pitch axis (see Fig. 1)
1	measuring station upstream of cascade
2	measuring station downstream of cascade
$-\infty$	values at "infinity" upstream
$+\infty$	values at "infinity" downstream

Superscripts:

(B)	(B) designates lower or upper surface of profile (B) = (ls) for lower surface of profile (us) " upper " " "
(ls)	lower surface of profile
(m)	blade number m = 0, 1, 2, ... If the amplitude, interblade phase angle, ... are constant for the blader under consideration, this superscript will not be used
(us)	upper surface of profile
$\sim$	time averaged (= steady) values. This superscript will only be used in ambiguous context
$-$	amplitude of unsteady complex value

1. Introduction

In axial-flow turbomachines considerable dynamic blade loads may occur as a result of the unsteadiness of the flow. The trend towards ever greater mass flows or smaller diameters in the turbomachines leads to higher flow velocities and to more slender blades. It is therefore likely that aeroelastic phenomena, which concerns the motion of a deformable structure in a fluid stream, will increase ever more in future turboreactors (fan stage) and industrial turbines (last stage) |10|.

The large complications, and high costs, of unsteady flow measurements in actual turbomachines makes it necessary for the aeroelastician to rely on cascade experiments and theoretical prediction methods for minimizing blade failures due to aeroelastic phenomena. It is therefore of great importance to validate the accuracy of flutter and forced vibration predictions as well as experimental cascade data and to compare theoretical results with cascade tests and trends in actual turbomachines.

Several well documented unsteady experimental cascade data exists throughout the world, as well as many different promising calculation methods for solving the problem of unsteady flow in two-dimensional and quasi three-dimensional cascades. However, due to different basic assumptions in these prediction methods, as well as many different ways of representing the obtained results, no real effort has been made to compare the different theoretical methods with each other. Furthermore, the validity of these theoretical prediction analysis can only, since hardly any exact solutions are known, be verified by comparison with experiments. This is very seldom done, partly because of the reasons mentioned above, partly as well documented experimental data normally are of proprietary nature.

It is the purpose of the present project to partly remedy this situation by selecting a certain number of standard configurations for aeroelastic investigations in turbomachine-cascades and to define an unified reporting format to facilitate the comparison between different theoretical results and the experimental standard configurations.

The final objective of a comparative work of the present kind is of course to validate theoretical prediction models with experiments performed under actual conditions in the turbomachine, i.e. under consideration of unsteady rotor-stator interaction, flow separation, viscosity, shock-boundary layer interaction, three dimensionality etc. Such a far-reaching objec-

tive does however not correspond with the present state-of-art of aeroelastic knowledge, neither for prediction models nor as regards well documented experimental data to be used as standard configurations.

The scope of the present report will thus be limited to fully aeroelastic phenomena under idealized flow conditions in two-dimensional or quasi three-dimensional cascades. Such interesting phenomena as rotor-stator interactions, stalled flutter and fully three-dimensional effects will thus be excluded, unless as an extension from the idealized two-dimensional cascade flow.

In this first report, nine standard configurations, ranging from flat plates to highly cambered turbine bladings and from incompressible to supersonic flow conditions, are selected and a certain number of aeroelastic test cases, mostly based upon existing experimental data, are defined for analysis by existing prediction methods for flutter and forced vibrations. It is intended that an extensive number of "blind test" calculations by different prediction methods (see chapter 4) should be performed in the autumn of 1983. The experimental data will thereafter be distributed (in beginning of 1984) to all researchers having performed the recommended analysis; the comparison of the experimental and theoretical results will so prepare a base for detailed discussions of the different experimental and theoretical results during the "Third Symposium on Aeroelasticity in Turbomachines" (1984) |1|, |2|.

In the beginning of 1984 it will also be possible for the participants to eventually refine some aspects of their experimental or theoretical procedure and to prepare, if possible, a contribution to the 1984 Symposium on Aeroelasticity.

The final comparison of the experimental and theoretical results will be distributed at the 1984 Symposium on Aeroelasticity. Attention will then also be focused upon still unresolved aeroelastic problems and a coordination of future experimental and theoretical investigations may be initiated.

2. Recommendations for Unified Representation of the Results

The physical reasons for self excited blade vibrations in turbomachines are not presently understood in detail. Various representations of experimental and theoretical results are thus used by different researchers. The number of different reporting formats used may be very large, as various importance is attached to different results, depending upon the scope of the aeroelastic investigation.

However, as the main objective for both experimental and theoretical aeroelastic studies is to provide a tool for the designer of turbomachines to minimize blade failures, the important results from the different investigations should be standarized to allow for interpretation of non-specialists in aeroelasticity.

In order to facilitate the comparison and to establish the mutual validity of both theoretical and experimental results, a certain amount of information must be unified. This is also desirable in order to avoid misinterpretation of some results.

In the present project, a minimum number of prescriptions have been defined. Both the nomenclature and the representation formats are based upon references |3| - |9|, especially the publication by Carta |3| (|7|). It has been chosen, furthermore, as similar as possible to the presentation previously used for the experiments serving as standard configurations, this to avoid excessive retreatment of the data.

2.1 Steady Two-Dimensional Cascade Nomenclature

The profiles under investigation are arranged, in a two-dimensional section of the cascade, as in Fig. 2.1-1. In this figure, all the physical lengths are scaled with the chordlength "c", and the nomenclature in Table 2.1-1 is used.

It is here important to note that the chord is defined as the straight line between the intersections of the camber line and the profile surface, and that the x-coordinate is aligned with the chord.

Throughout this report, extensive use will be made of the time averaged blade surface pressure coefficient, which will be defined as

$$\tilde{C}_p = \frac{\tilde{p} - \tilde{p}_{-\infty}}{\tilde{p}_{t-\infty} - \tilde{p}_{-\infty}} \tag{1}$$

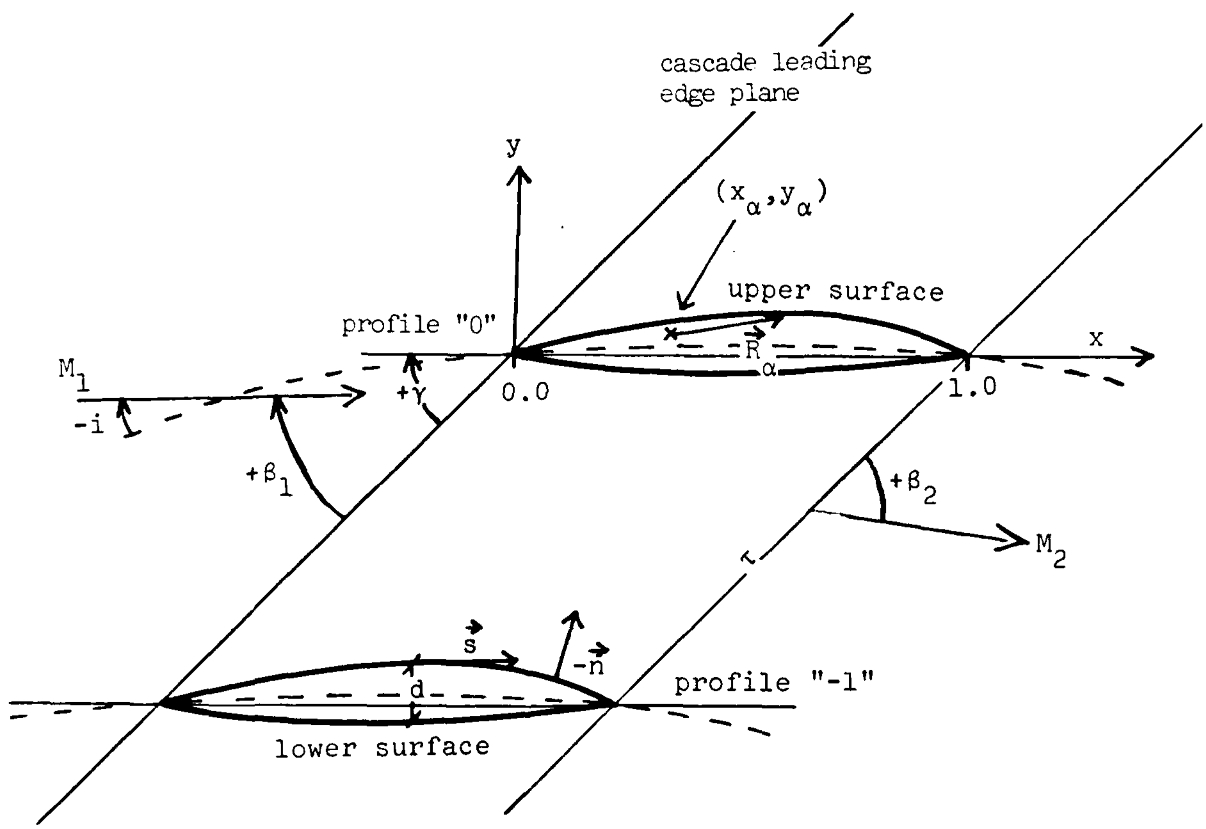

Figure 2.1-1 Steady two-dimensional cascade geometry

Symbol	Explanation	Dimension
c	chord lenght	m
d	maximum blade thickness (dimensionless with chord)	-
$\tilde{C}_p$	time averaged pressure coefficient $= \dfrac{\tilde{p}-\tilde{p}_{-\infty}}{\tilde{p}_{t-\infty}-\tilde{p}_{-\infty}}$	-
i	incidence	deg
M	Mach number	-
$\vec{n}$	unity vector normal to blade surface, positive inwards	-
$\tilde{p}$	time averaged pressure	N/m^2
$\vec{R}_{\alpha}$	dimensionless vector from mean pivot to an arbitrary point on the mean blade surface	-
Re	Reynolds number $= \dfrac{V_1 c}{\nu}$	-
$\vec{s}$	unity vector tangent to blade surface, positive in positive coordinate directions	-
V	velocity	m/s
V_{ref}	reference velocity for reduced frequency and Strouhal number: "V_{ref}" = "V_1" for compressor cascade "V_{ref}" = "V_2" " turbine "	m/s
x	dimensionless (with chord) chord-wise coordinate	-
y	dimensionless (with chord) normal-to-chord coordinate	-
z	dimensionless (with chord) span-wise coordinate	-
β	flow angle	deg
γ	chordal stagger angle	deg
ν	kinematic viscosity	m /s
τ	dimensionless blade pitch = grap-to-chord ratio	-

Table 2.1-1 (continuation on next page)

Subscripts

G	center of gravity
is	isentropic values
t	total head value
x	component in x-direction
y	component in y-direction
z	component in z-direction
1	measuring station upstream of cascade
2	measuring station downstream of cascade
$-\infty$	values at "infinity" upstream
$+\infty$	values at "infinity" downstream
α	pitch axis (see Fig. 1)

Superscripts

(m)	mth blade, m=0, 1, 2,....If the amplitude, interblade phase angle,... are constant for the blades under consideration, this superscript will not be used
(ls)	lower surface of profile
(us)	upper surface of profile
$\sim$	steady (time averaged) values. This superscript will only be used in ambigous context.

Table 2.1-1 Steady two-dimensional cascade nomenclature

2.2 Unsteady Two-Dimensional Cascade Nomenclature

Blade Motion

Fig. 2.2-1 is a schematic representation of cascaded two-dimensional airfoils; the form of the profiles is considered to remain rigidly fixed during heaving and/or pitching oscillations, $\vec{h}\,(x,y,t)$ and $\vec{\alpha}(t)$ resp., in which the components h_x, h_y and α of the motion vectors $\vec{h}$ and $\vec{\alpha}$ are noted in complex form to account for phase differences between the translation and the rotation.

We will therefore define

$$\vec{h}^{(m)}(x,y,t)=\vec{\bar{h}}(x,y)^{(m)}e^{i\{w^{(m)}t\}} \qquad \text{for heaving motion}$$

$$\vec{\alpha}^{(m)}(t)=\vec{\bar{\alpha}}^{(m)}e^{i\{w^{(m)}t+\Theta_\alpha^{(m)}\}} \qquad \text{for pitching motion} \tag{2}$$

where $\bar{h}^{(m)}$, $\bar{\alpha}^{(m)}$ are the dimensionless amplitudes, and $w^{(m)}$ the circular frequency, of the vibration of blade (m).

It is also assumed that the torsional motion, for the (m)th blade, preceeds the bending motion by a phase angle $\Theta_\alpha^{(m)}$. Furthermore, if the amplitude, circular frequency or phase lead is identical for all blades, the superscript (m) will be omitted on the corresponding symbol (see Table 2.2-1).

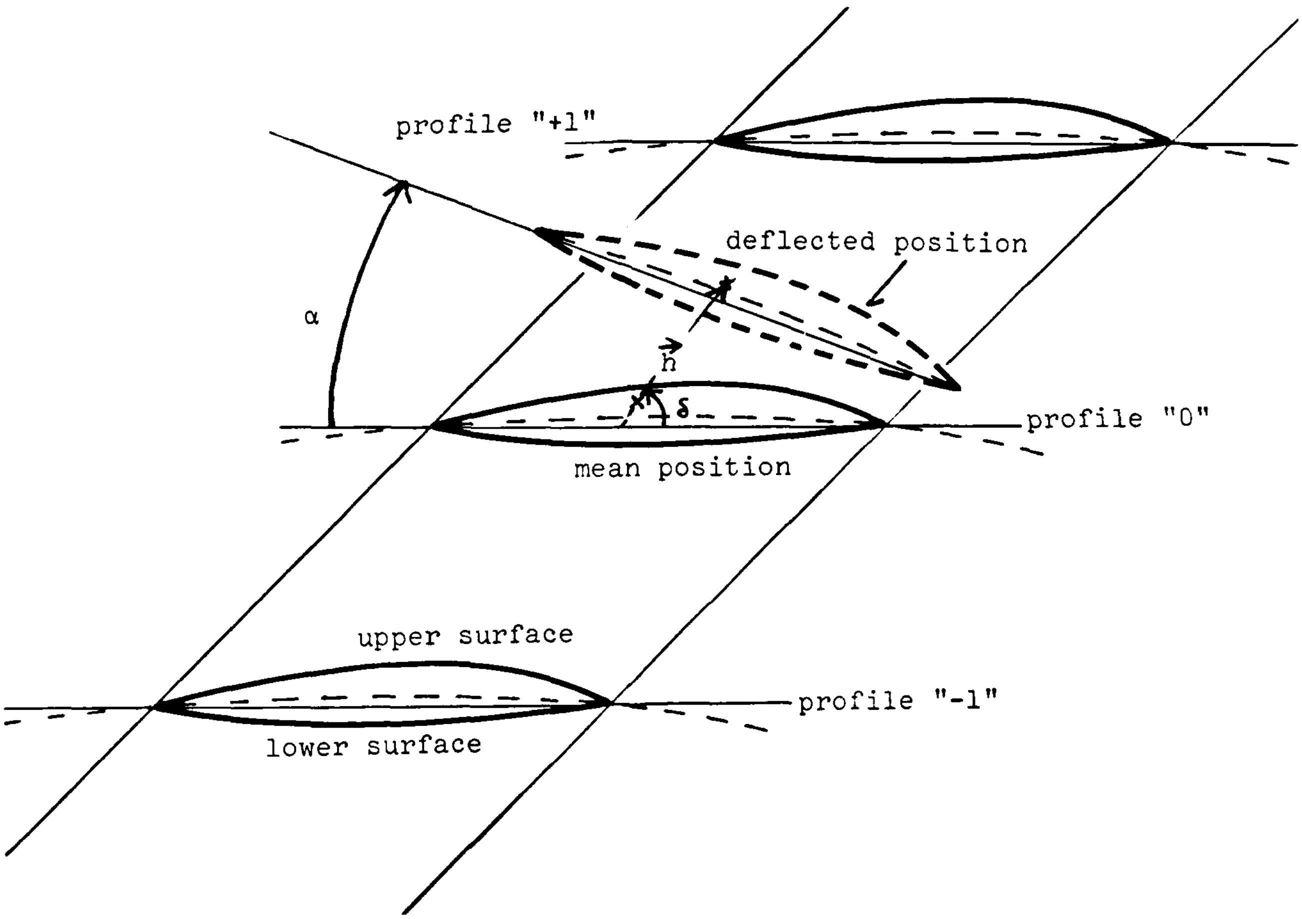

Figure 2.2-1 Unsteady two-dimensional cascade nomenclature

Symbol	Explanation	Dimension
A	amplitude $A_{\bar{h}}$ for pure sinusoidal heaving $A_{\bar{\alpha}}$ " " " pitching	- rad
$\vec{C}_F(t)$	unsteady perturbation force coefficient vector per unit amplitude, positive in positive coordinate directions: $$\vec{C}_F(t)=\bar{\vec{C}}_F e^{i(\omega t+\phi_F)}$$	-
$C_L(t)$	unsteady perturbation lift coefficient per unit amplitude, positive in positive y-direction: $$C_L(t)=\bar{C}_L e^{i(\omega t+\phi_L)}$$ Note: In the present report, the lift coefficient is defined as the force component perpendicular to the chord!	-
$C_M(t)$	unsteady perturbation moment coefficient per unit amplitude, positive in clockwise direction: $$C_M(t)=\bar{C}_M e^{i(\omega t+\phi_M)}$$	-
$C_p(x,t)$	unsteady perturbation pressure coefficient per unit amplitude: $$C_p(x,t)=\bar{C}_p(x)e^{i(\omega t+\phi_p)}$$	-
C_w	coefficient for aerodynamic work done on the system during one cycle of oscillation	-
f	vibration frequency	Hz
$\vec{h}(x,y,t)$	dimensionless (with chord) bending vibration, positive in positive coordinate directions	-
$\bar{\vec{h}}(x,y)$	dimensionless (with chord) bending amplitude	-
k	reduced frequency $= \dfrac{c\,\omega}{2V_{ref}}$	-
p	time dependant perturbation pressure	N/m^2
Str	Strouhal number $= \dfrac{f\cdot c}{V_{ref}}$ $(=k/\pi)$	-

Table 2.2-1 (continuation on next page)

T	dimensionless time $T=t/T_o$	-
T_o	period of a cycle	s
t	time	s
w	circular frequency = $2\pi f$	rad/s
$\alpha(t)$	pitching vibration, positive nose up	rad
$\bar{\alpha}$	pitching amplitude	rad
δ	heaving vibration direction = $\tan^{-1}(\bar{h}_y/\bar{h}_x)$	deg
$\Delta C_p(x,t)$	unsteady perturbation blade surface pressure difference coefficient: $\Delta C_p(x,t)=C_p^{(ls)}(x,t)-C_p^{(us)}(x,t)=\overline{\Delta C_p}(x)e^{i(wt-\phi_{\Delta p})}$	-
$\Theta_\alpha^{(m)}$	phase lead of pitching motion towards heaving motion of blade (m)	deg or rad
Ξ	aerodynamic damping coefficient, positive for stable motion	-
ϕ_F	phase lead of perturbation force coefficient towards motion	deg or rad
ϕ_L	phase lead of perturbation lift coefficient towards motion	deg or rad
ϕ_M	phase lead of perturbation moment coefficient towards motion	deg or rad
$\phi_p(x)$	phase lead of perturbation pressure coefficient towards motion	deg or rad
$\phi_{\Delta p}(x)$	phase lead of perturbation blade surface pressure difference coefficient towards motion	deg or rad
$\sigma^{(m)}$	interblade phase angle between blade "m-l" and blade "m"	deg or rad

Table 2.2-1 (continuation on next page)

$\sigma^{(m)} = \sigma$ for constant interblade phase angle. $\sigma^{(m)}$ is positive when blade "m" leads blade "m-1".
Under idealized conditions constant interblade phase angle between adjacent blades, σ, and identical vibration amplitude for all blades) the motion of the m^{th} blade is given, for flexion, by

$$\vec{h}^{(m)}(x,y,t) = \vec{\bar{h}}(x,y)^{(O)} e^{i\{wt - m\sigma\}}$$

and similar for torsion, by

$$\vec{\alpha}^{(m)}(t) = \vec{\bar{\alpha}}^{(O)} e^{i\{wt - m\sigma - \Theta_\alpha\}}$$

Subscripts

A	A = h for heaving A = α for pitching
global	global (= time dependant - time averaged) (see eq. 7)
I	imaginary part
R	real part

Superscript

(ls)	lower blade surface
(m)	blade number m 0, 1, 2, ...
(us)	upper blade surface
—	amplitude of unsteady complex value

Table 2.2-1 Unsteady two-dimensional cascade nomenclature

Two-Dimensional Aerodynamic Coefficients

The unsteady (complex) blade surface pressure coefficient C_p, as well as the lift C_L, force C_F and moment C_M coefficients (per unit span), are scaled with the amplitude of the corresponding motion (amplitude ="A", where A=h$^{(m)}$ or $\alpha^{(m)}$). According to the conventional definitions of these parameters, we thus have:

$$C_{p_A}^{(B)}(x,t)=\frac{1}{A}\left\{\frac{p^{(B)}(x,t)}{\tilde{p}_{t-\infty}-\tilde{p}_{-\infty}}\right\} \tag{3}$$

$$\vec{C}_{L_A}(t)=\frac{1}{A}\cdot\frac{1}{\tilde{p}_{t-\infty}-\tilde{p}_{-\infty}}\cdot\oint_{\substack{\text{profile}\\ \text{surface}}} p(x,t)\cdot\{\vec{n}\cdot\vec{e}_y\}\cdot ds=\int_{X_{Le}}^{X_{Te}}\{C_{p_A}^{(ls)}(x,t)-C_{p_A}^{(us)}(x,t)\}\cdot dx \tag{4}$$

$$\vec{C}_{F_A}(t)=\frac{1}{A}\cdot\frac{1}{\tilde{p}_{t-\infty}-\tilde{p}_{-\infty}}\cdot\oint_{\substack{\text{profile}\\ \text{surface}}} p(x,t)\cdot\vec{n}\cdot ds \tag{5}$$

$$\vec{C}_{M_A}(t)=-\frac{1}{A}\cdot\frac{1}{\tilde{p}_{t-\infty}-\tilde{p}_{-\infty}}\cdot\oint_{\substack{\text{profile}\\ \text{surface}}}\{\vec{R}_\alpha\times\{p(x,t)\cdot ds\cdot\vec{n}\}\}\cdot\vec{e}_z \tag{6}$$

where

- p is the unsteady (=perturbation) pressure
- "lift" coefficient is defined normal to chord
- force components are positive when acting in positive coordinate directions
- C_M is positive when acting in clockwise direction
- superscript (B) denotes the blade lower surface (ls) or blade upper surface (us).

Furthermore, the global (=time averaged + time dependant) blade surface pressure coefficient is defined as

$$C_{p_{global}}=\tilde{C}_p+A\cdot C_p=\frac{\tilde{p}-\tilde{p}_{-\infty}}{\tilde{p}_{t-\infty}-\tilde{p}_{-\infty}}+\frac{p}{\tilde{p}_{t-\infty}-\tilde{p}_{-\infty}}=\frac{(\tilde{p}+p)-\tilde{p}_{-\infty}}{\tilde{p}_{t-\infty}-\tilde{p}_{-\infty}} \tag{7}$$

A further important quantity, for slender blades, is the normalized unsteady pressure difference along the blade chord, $\Delta C_p(x)$.
This is defined as the difference of the time dependant pressures on the blade lower and upper surfaces:

$$\Delta C_p(x,t)=C_p^{(ls)}(x,t)-C_p^{(us)}(x,t) \tag{8}$$

All of the above mentioned variables can be expressed in either complex exponential form or in component form as:

$$C_p(x,t)=\bar{C}_p(x)e^{i\{wt+\phi_p(x)\}}=\{C_{pR}(x)+iC_{pI}(x)\}e^{iwt} \tag{9}$$

Here, the subscripts "R" and "I" denotes the real and imaginary parts of the pressure coefficient $C_p(x,t)$. Physically, these two parts can be interpreted as the components of the pressure coefficient which are in-phase (real part) and out-of-phase (imaginary part) with the blade motion. Furthermore, the phase angles $\phi_p(x)$, $\phi_{\Delta p}(x)$, ϕ_L, ϕ_F, ϕ_M are all defined positive when the pressure (pressure difference, lift, force or moment, resp.) leads the motion.

The amplitude and phase relationships in eq. (9) are defined in the usual manner, that is:

$$\begin{cases} \bar{C}_p(x)=\sqrt{C_{pR}(x)^2+C_{pI}(x)^2} \\ \phi_p(x)=\tan^{-1}\{C_{pI}(x)/C_{pR}(x)\} \end{cases} \tag{10a}$$

$$\begin{cases} C_{pR}(x)=\bar{C}_p(x)\cdot\cos(\phi_p(x)) \\ C_{pI}(x)=\bar{C}_p(x)\cdot\sin(\phi_p(x)) \end{cases} \tag{10b}$$

It should here be noted that, in computing the blade surface pressure distribution, only components, and not amplitudes or phase angles may be differentiated (/3/). Therefore

$$\begin{cases} \Delta C_{pR}(x)=C_{pR}^{(ls)}(x)-C_{pR}^{(us)}(x) \\ \Delta C_{pI}(x)=\bar{C}_{pI}^{(ls)}(x)-C_{pI}^{(us)}(x) \end{cases} \tag{11a}$$

$$\begin{cases} \overline{\Delta C_p}(x)\neq\overline{C_p}^{(ls)}(x)-\overline{C_p}^{(us)}(x) \\ \phi_{\Delta p}(x)\neq\phi_p^{(ls)}(x)-\phi_p^{(us)}(x) \end{cases} \tag{11b}$$

Two-Dimensional Aerodynamic Work

The two-dimensional differential work, per unit span, done on a rigid system by the aerodynamic forces and moments is conventionally expressed by the product of the real parts (in phase with motion components) of force and differential translation, as well as moment and differential

torsion. Thus, the total aerodynamic work coefficient per period of oscillation, done on the system is obtained by computing

$$C_W = C_{Wh} + C_{W\alpha} + C_{Wh\alpha} + C_{W\alpha h} \tag{12}$$

Expressed in this way, the aerodynamic work coefficients c_w, c_{wh}, $c_{w\alpha}$, $c_{w\alpha h}$, $c_{wh\alpha}$ are all in nondimensionalized form, with the product of the pressure difference ($\tilde{p}_{t\infty} - \tilde{p}_{\infty}$) and chord[3] as normalizing factor.

From the definition (eq. 12 and 13) it is seen that these coefficients become negative for a stable motion.

As the force and moment coefficients each have time dependant parts from both the heaving and pitching oscillations, c_{wh} *is defined as the* work done on the profile during a pure heaving cycle (no torsion). Similarly, $c_{w\alpha}$ is the work done on the blade during a pure pitching cycle (no bending); $c_{w\alpha h}$ and $c_{wh\alpha}$ is the work done by the pitching force due to heaving and by the heaving moment due to pitching, respectively. Thus, the work coefficients may be expressed in conventional form as

$$
\begin{aligned}
C_{Wh} &= \oint_{\substack{\text{Cycle of}\\ \text{oscillation}}} Re\{\bar{h}\cdot\vec{C}_{Fh}(t)\}\cdot Re\{d\vec{h}(t)\} \\
C_{W\alpha} &= \oint_{\substack{\text{Cycle of}\\ \text{oscillation}}} Re\{\bar{\alpha}\cdot\vec{C}_{M\alpha}(t)\}\cdot Re\{d\vec{\alpha}(t)\} \\
C_{Wh,\alpha} &= \oint_{\substack{\text{Cycle of}\\ \text{oscillation}}} Re\{\bar{h}\cdot\vec{C}_{Mh}(t)\}\cdot Re\{d\vec{\alpha}(t)\} \\
C_{W\alpha,h} &= \oint_{\substack{\text{Cycle of}\\ \text{oscillation}}} Re\{\bar{\alpha}\cdot\vec{C}_{F\alpha}(t)\}\cdot Re\{d\vec{h}(t)\}
\end{aligned}
\tag{13}
$$

In the case of pure sinusoidal *normal-to-chord* bending or pure sinusoidal torsional vibration, as well as sinusoidal lift and moment responses, respectively, the expressions (13) may be integrated to give the following simple formulas

$$
\begin{aligned}
C_{Wh} &= \pi\bar{h}^2\cdot C_{LI} = \pi\bar{h}^2\cdot\bar{C}_L\cdot\sin(\phi_L) \\
C_{W\alpha} &= \pi\bar{\alpha}^2\cdot C_{MI} = \pi\bar{\alpha}^2\cdot\bar{C}_M\cdot\sin(\phi_M) \\
C_{Wh,\alpha} &= 0 \\
C_{W\alpha,h} &= 0
\end{aligned}
\tag{14}
$$

It is thus seen that the aerodynamic work only depends upon the value of the out of phase component of the lift and moment coefficients, and that the airfoil damps the motion when the imaginary part of the lift

and moment coefficient, resp. is negative.

The aerodynamic work can be expressed in normalized form as the aerodynamic damping parameter Ξ /3/. With the same assumptions as in eq. (14), this parameter is defined as

$$\begin{cases} \Xi_h = -C_{Wh}/\pi \bar{h}^2 = -C_{LI} \\ \Xi_\alpha = -C_{W\alpha}/\pi \bar{\alpha}^2 = -C_{MI} \end{cases} \tag{15}$$

The normalized parameter Ξ is thus positive for a stable motion.

Non-Harmonic Pressure Response

All theoretical prediction methods for flutter and forced vibrations available today make a few basic assumptions.

Most of the methods are submitted to restrictions regarding

- sinusoidal blade vibrations
- sinusoidal pressure response
- identical vibration frequencies for all blades
- identical vibration amplitudes for all blades
- constant interblade phase angles

In experiments, however, these assumption can never be exactly fullfilled. The large energy input needed to drive a cascade with prescribed frequencies, amplitudes and phase angles makes it impossible to satisfy the three latter assumptions, apart from in tests with low frequencies and/or small amplitudes. Even in this case though, the pressure response on the profiles will, in general, not be sinusoidal.

For the detailed comparison between the experimental data and the prediction model, it is thus important to realize how well the theoretical assumptions approximate the experiment.

The non-sinusoidal pressure response on the vibrating blades does not hinder the computation of the aerodynamic work and damping coefficients, as only the frequency of the pressure response spectra corresponding to the blade vibration frequency contributes to the aerodynamic work. The validity of this statement can be demonstrated if we suppose that the blade motion is sinusoidal with angular frequency w, and as any periodic signal F(wt), of which f(wt) is the unsteady part, can be represented as a Fourier series

$$F(wt) = A_0 + f(wt) = A_0 + \sum_{k=1}^{\infty} A_k e^{i(kwt \cdot \varphi_k)} \tag{16}$$

As exemple of proof of the statement, let us consider a pure sinusoidal pitching mode ($\bar{\alpha}$ real)

$$\alpha(t)=\bar{\alpha}e^{iwt}$$

with a moment signal

$$\bar{\alpha}C_{M\alpha}(t)=\bar{\alpha}\left\{\sum_{k=1}^{\infty}\bar{C}_{M\alpha,k}e^{i(kwt+\phi_M k)}\right\}$$

The aerodynamic work coefficient $c_{w\alpha}$ becomes thus

$$C_{W\alpha}=\oint_{\substack{\text{Cycle of}\\ \text{oscillation}}}\mathrm{Re}\{\bar{\alpha}C_{M\alpha}(t)\}\cdot\mathrm{Re}\{d\vec{\alpha}(t)\}=\int_0^{2\pi}\mathrm{Re}\left\{\bar{\alpha}\sum_{k=1}^{\infty}\bar{C}_{M\alpha,k}\,e^{i(kwt+\phi_M k)}\right\}\cdot\mathrm{Re}\{i\bar{\alpha}e^{iwt}\}d(wt)=$$

$$=\int_0^{2\pi}\bar{\alpha}\left\{\sum_{k=1}^{\infty}\bar{C}_{M\alpha,k}\cos(kwt+\phi_M k)\right\}\{-\bar{\alpha}\sin(wt)\}d(wt)=$$

$$=-\bar{\alpha}^2\sum_{k=1}^{\infty}\bar{C}_{M\alpha,k}\left\{\int_0^{2\pi}\cos(kwt+\phi_M k)\ \sin(wt)\,d(wt)\right\}=$$

$$=\left\{\begin{matrix}\pi\bar{\alpha}^2\,\bar{C}_{M\alpha,k}\sin(k\phi_M) & \text{if } k=1\\ 0 & \text{if } k\neq 1\end{matrix}\right\}\rightarrow C_{W\alpha}=\pi\bar{\alpha}^2\,\bar{C}_{M\alpha,1} \tag{17}$$

Thus, in the computation of the work coefficients only the first harmonic of the force or moment response appears (compare eq. 14).

This simplification of a non sinusoidal pressure response is however only possible due to the existence of a pure sinusoidal motion and the integration over a cycle of vibration. A verification of the actual time histories of the experiments is thus needed.

This is even more important in experiments with non-identical blade vibration amplitudes and interblade phase angles, as these differences largely may contribute to discrepancies between the experimental and theoretical (idealized) results.

On the basis of detailed time recordings, a statistical evaluation or a discrete Fourier analysis may be used to appreciate how well the different idealizations in the prediction models approximate the real cascade flow conditions.

It is thus recommended that the amplitude of all the physical quantities α, h, c_p,... be defined:

o as the amplitude of the first harmonic, if a Fourier analysis is used

o as the root-mean-square value (RMS) times a factor $\sqrt{2}$, if a statistical evaluation is used (example: $\bar{h} = \sqrt{2} \cdot \sqrt{\frac{1}{T}\int_0^T h(t)^2 \, d(t)}$ (*)). The factor $\sqrt{2}$ is here introduced in order to equalize the statistical amplitude with the full amplitude for a purely sinusoidal fluctuation.

In both cases, an indication of the quality of the signal should, if possible, be given. This criteria can, for example be established as

o higher harmonics for Fourier analysis

o fluctuation of result with different averaging times for a narrow-band filter

o shape of spectral peak at a distance of, e.g., 20 dB relative to peak for spectrum analysis

In order to evaluate eventual discrepancies between the experimental data and theoretical results, it is of importance that an analysis of the above mentioned kind accompany the data.

(*) This RMS-value may occur e.g. as the output of a narrow-band filter applied to the unsteady pressure signal, centered at the blade oscillation frequency.

2.3 Precise Reporting Formats

One of the main problems for the comparison of experimental and theoretical aeroelastic investigations at the 1980 "Symposium on Aeroelasticity in Turbomachines" was the lack of coherency in the reporting formats; the researchers participating in the present project are therefore invited to follow the guide-lines for a standarized reporting format, given in this chapter.

Two main groups of representation will be used:

I: The first concerns the detailed comparison of the measured and calculated blade pressure distributions.

II. The second representation is directed towards the physical mechanism of the flutter phenomena, its important parameters and towards the establishment of the flutter boundaries for the different cascades.

It is evident that all participants are encouraged to use any further reporting formats in order to establish other comparisons or to emphasize any special point of interest in their investigations.

I: Detailed comparison of experimental results and theoretical approaches

The establishment of the validity of theoretical results can only be done by a mutual agreement between the measured and calculated unsteady pressure distributions on both blade surfaces. This detailed comparison will be performed on the basis of Figure 2.3-1 which is to be presented for different combinations of

- o interblade phase angle
- o reduced frequency
- o inlet conditions
- o cascade geometry

depending upon the existing experimental data for the configuration under investigation.

Quite a few prediction models for flutter or forced vibrations are based upon small perturbation theories, where the steady pressure distribution on the blade is an input data. The experimentally determined time averaged blade surface pressure distributions is therefore specified for such studies, as in Fig. 2.3-2.

Furthermore the comparison between the steady (Fig 2.3-2) and unsteady (Fig 2.3-1) blade pressure distributions may in some cases give a quantita-

tive notion about the aeroelastic phenomena under investigation (instabilities due to stall, choke, shockwaves, coupling effects between the steady and unsteady flow fields...).

The distribution of the blade surface pressure difference coefficient along the blade, $\Delta C_p(x)$, indicates the presence of stable and unstable zones. This information is thus also of interest, and will be plotted as in Figure 2.3-3.

II. Flutter boundaries

The second form of representation concerns the values of the resultant aerodynamic blade forces and moments, as well as the aerodynamic work and damping coefficients.

Two different representations (see Figures 2.3-4 and 2.3-5) will be used to elaborate the influence of several important parameters on the flutter boundaries

- o reduced frequency
- o interblade phase angle
- o inlet flow velocity
- o inlet flow angle
- o outlet flow velocity
- o cascade geometry

First, the unsteady blade pressure coefficients will be integrated to yield the aerodynamic force, or lift, and moment coefficients as in Figure 2.3-4. The phase angles ϕ_F and ϕ_M resp., give in this representation immediate information about the aeroelastic stability of the system (see chapter 2.2).

Secondly, the aerodynamic work and damping coefficients per cycle of oscillation may be calculated if the mode-shape of the motion is well known. Most of the problems treated in the present work will concern motion of nondeformed profiles (at least for the theoretical predictions), wherefore the aerodynamic damping coefficient can be easily computed and plotted. This information is useful for the turbomachine designer for the judgement of the aeroelastic behaviour of a specific cascade (Figure 2.3-5).

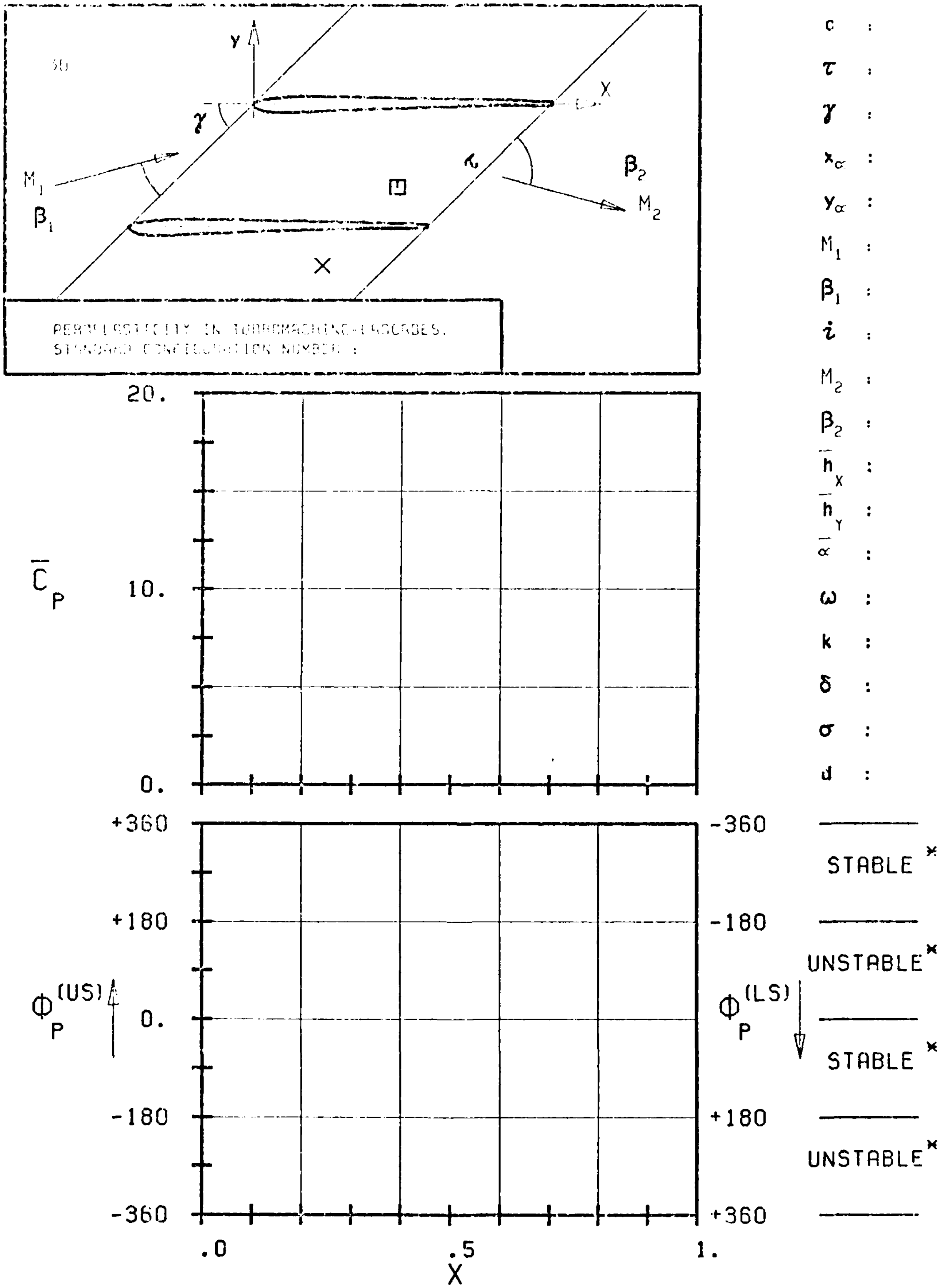

FIG. 2.3-1: MAGNITUDE AND PHASE LEAD OF UNSTEADY BLADE SURFACE PRESSURE DISTRIBUTION.

(*: IN PITCH MODE, NOTATION VALID UPSTREAM OF PITCH AXIS)

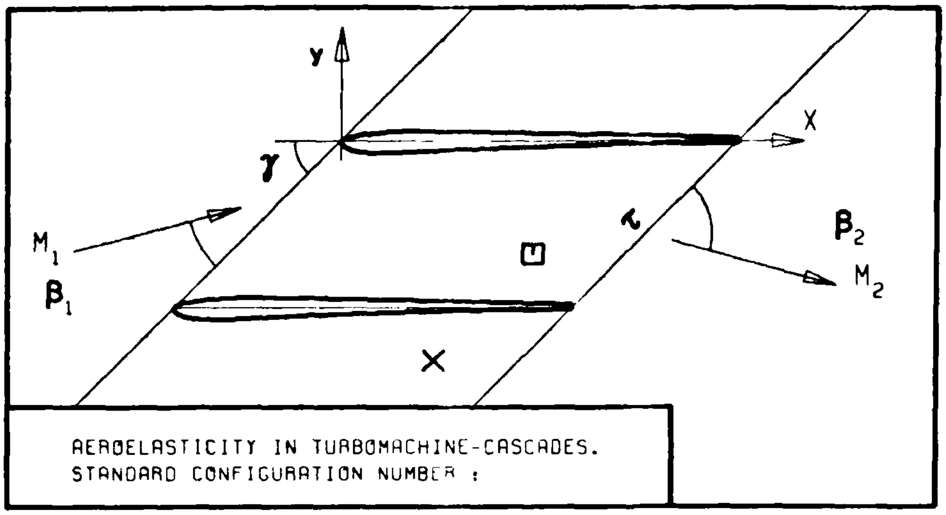

c :
τ :
γ :
x_α :
y_α :
M_1 :
β_1 :
i :
M_2 :
β_2 :
$\bar{h}_X$:
$\bar{h}_Y$:
$\bar{\alpha}$:
ω :
k :
δ :
σ :
d :

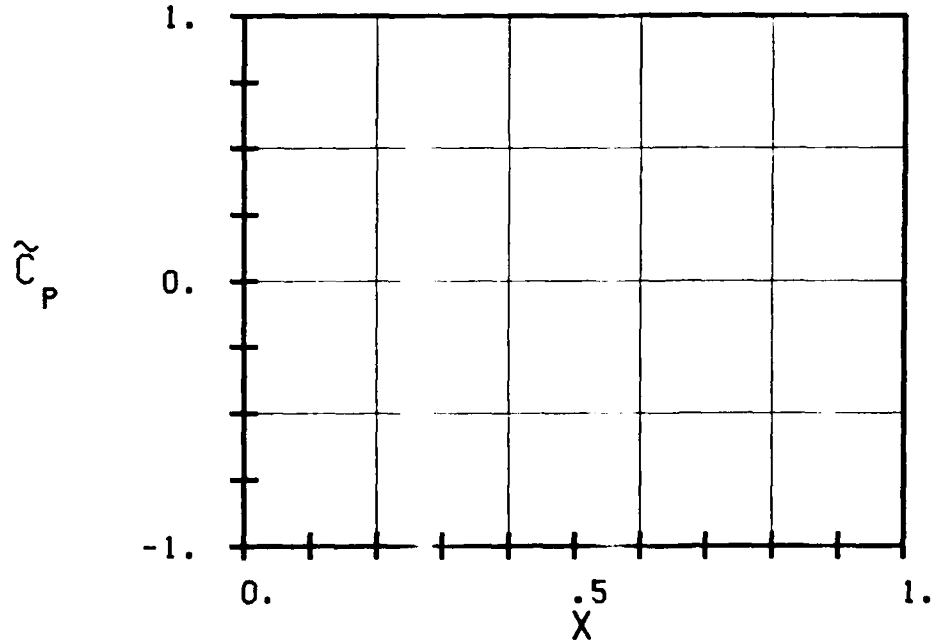

FIG. 2.3-2: TIME AVERAGED BLADE SURFACE PRESSURE COEFFICIENT.

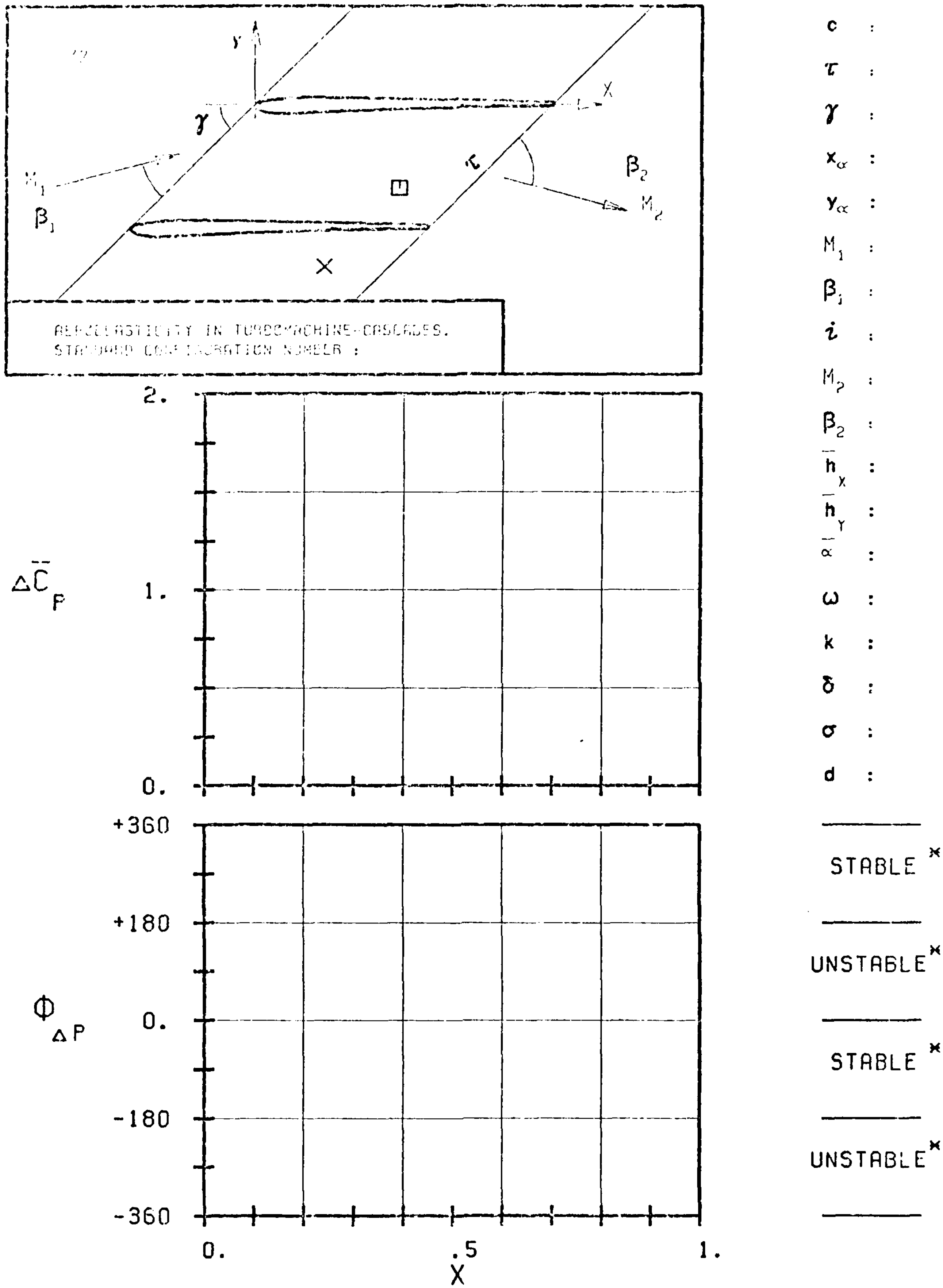

FIG. 2.3-3: MAGNITUDE AND PHASE LEAD OF UNSTEADY BLADE SURFACE PRESSURE DIFFERENCE COEFFICIENT.

(*: IN PITCH MODE, NOTATION VALID UPSTREAM OF PITCH AXIS)

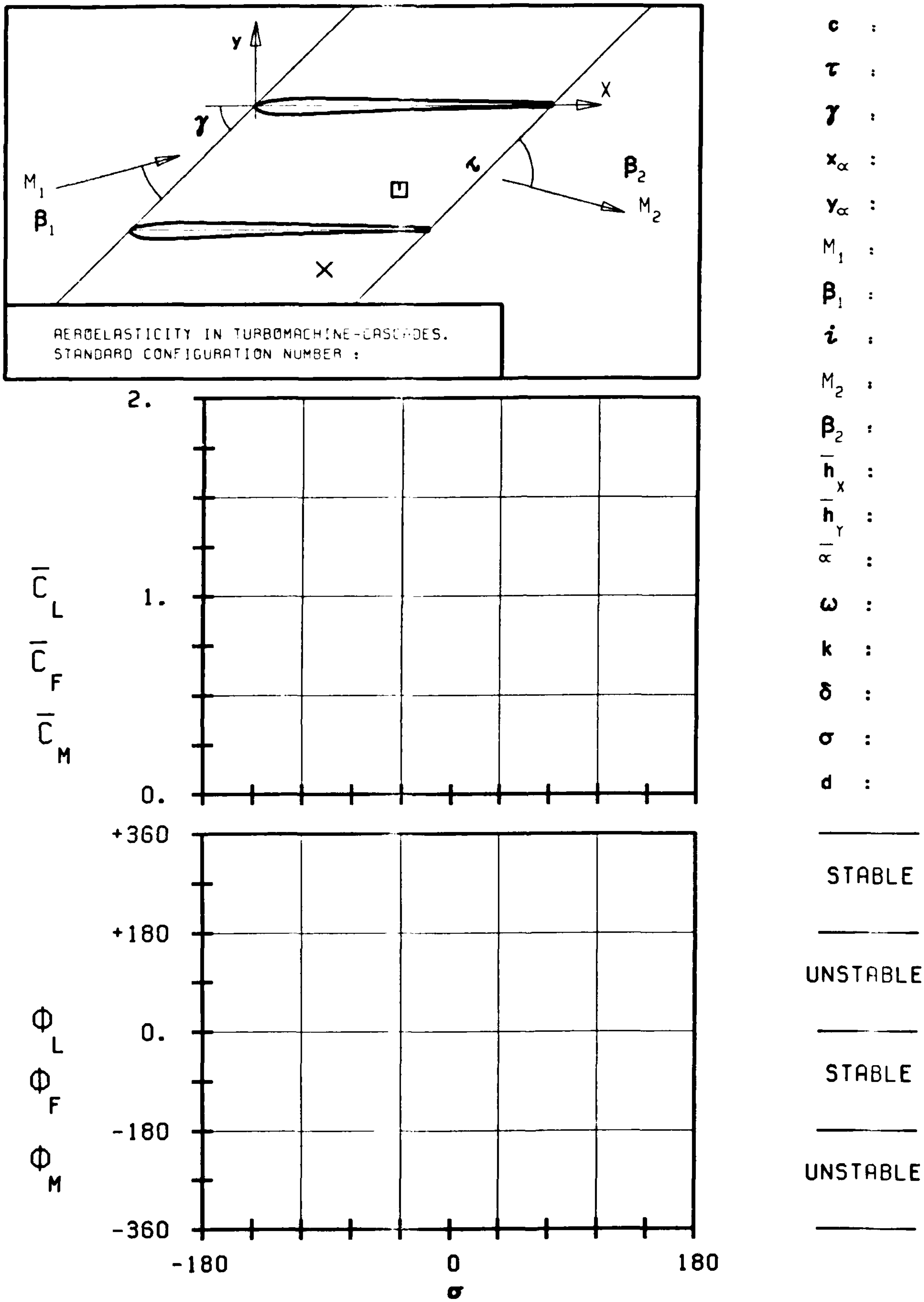

FIG. 2.3-4: AERODYNAMIC FORCE, LIFT AND MOMENT COEFFICIENTS TOGETHER WITH THE CORRESPONDING PHASE LEADS IN DEPENDANCE OF CASCADE GEOMETRY AND FLOW QUANTITIES.

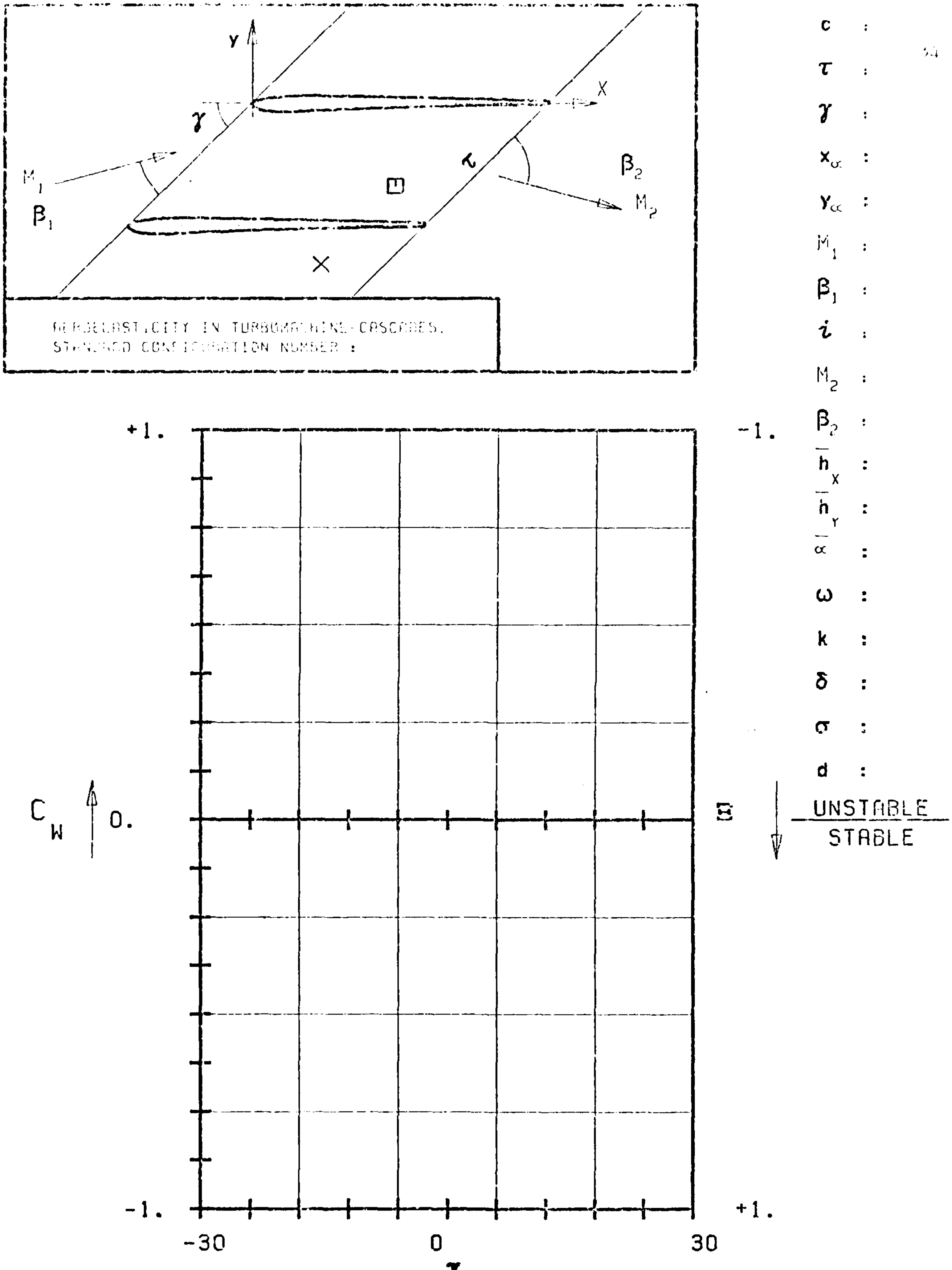

FIG. 2.3-5: AERODYNAMIC WORK AND DAMPING COEFFICIENTS IN DEPENDANCE OF CASCADE GEOMETRY AND FLOW QUANTITIES.

3. Standard Configurations

On the basis of existing test facilities of the participating laboratories, and in relationship with the state-of-art of theoretical methods, nine standard configurations(*) for establishing the mutual validity of two-dimensional and quasi three-dimensional aeroelastic cascade experiments and prediction models have been selected. The configurations should approximate idealized flows, wherefore stall effects have been excluded, except as extensions of unstalled experiments.

In order to guarantee a correct validation of the theoretical models, the quality of the experimental results must also be verified. If possible, two rather similar experimental cascade geometries have therefore been identified as standard configurations for each of the following flow regimes:

- o low subsonic (~ incompressible)
- o subsonic
- o transonic
- o supersonic

Out of the nine standard configurations, which are summarized in tables 3.0-1, seven are based upon experimental cascade results; the eighth is directed towards the establishment of validity for prediction models in the limiting case of flat plates and for comparison of the large number of existing flat plate theories. The final configuration (ninth) is defined as to investigate blade thickness effects upon the aeroelastic behaviour of the cascade, and upon the theoretical results, especially at high subsonic flow velocities.

Each of the standard configurations selected allow for a systematic variation of one or several aerodynamic and/or aeroelastic parameters. However, a too large number of aeroelastic cases in each standard configuration would limit the usefulness in this report in providing comparisons for experimentalists and analysts working independently of each other.

For this reason, a restricted number of aeroelastic configurations for each test case, based upon available experimental data, has been chosen

---

(*) Throughout this report, "standard configuration" will designate a cascade geometry and "aeroelastic case" or "aeroelastic test case" will indicate the different time dependant (and, in some cases, time averaged) conditions within a standard configuration.

Experimental Configuration	Institution	Geometry						Profile		Flow Field								Kinematics									Results						
		Cascade		Flow			Profile			Mach Regime					Separation			Excitation		Motion				Mode									
		Linear Cascade	Annular Cascade	[illegible]	Quasi Three-dimensional	[illegible]	[illegible]	Thickness	[illegible]	Incompressible	[illegible]	[illegible]	Supersonic	[illegible]	[illegible]	Partial stall	Fully stalled	[illegible]	[illegible]	[illegible]	[illegible]	[illegible]	[illegible]	[illegible]	[illegible]	[illegible]	[illegible]	[illegible]	[illegible]	[illegible]	[illegible]	[illegible]	[illegible]
1	United Technologies Research Center	X		X				X	X	X					X			X		X		X	X		X		X	X		X	X		[illegible]
2	University of Tokyo	X		X				X	X	X					X	X	X	X		X		X	X		X		X		X	X			[illegible]
3	Tokyo National Aerospace Laboratory		X		X			X	X			X			X	X	X	X		X		X	X		X		X	X		X			[illegible]
4	Lausanne Institute of Technology		X		X			X	X		X				X	X		X		X		X	X	X	X		X	X					[illegible]
5	Office National d'Etudes et de Recherches Aérospatiales	X		X				X			X				X	X	X	X		X		X	X		X		X	X		X	X	X	[illegible]
6	Lausanne Institute of Technology		X		X			X	X			X			X	X		X	X	X		X	X	X	X		X	X				X	[illegible] vibration mode, [illegible]
7	NASA Lewis Research Center	X		X				X	X				X	X	X			X		X		X	X		X		X	X		X	X	X	[illegible]
Theoretical Flat Plate Configuration 9				X			X			X	X		X	X	X			X		X		X	X		X			X	X	X	X		
Theoretical [illegible] Configuration [illegible]				X				X		X	X		X	X	X			X		X		X	X		X		X	X	X	X	X		[illegible]

Table 3.0-1a Summary of Nine Standard Configurations for Two-Dimensional and Quasi Three-Dimensional Aeroelastic Investigations in Turbomachine-Cascades

Standard Conf. No	Courtesy of	Velocity domain(s)	Compressor/ Turbine Configur.	Profile % thickness ° camber	Linear/ Annular Configur.	Instrument on reference blade	Mode Torsion/ Bending	Representation
1	UTRC (F.O. Carta)	Incompress.	C	6% 10^{o}	Linear (Air)	• 20 transducers • Strain gages	T	$C_p(x)$, $\Delta C_p(x)$ for $\begin{cases} 2\lambda \\ 2\bar{\sigma} \end{cases}$ C_M, Ξ= f(σ) C_M, Ξ= f(k)
2	Tokyo Univ. (H. Tanaka)	Incompress.	C + T	5% 16^{o}	Linear (Water)	• Strain gages	T	C_M, Ξ= f(σ) C_M, Ξ= f(k) C_M, Ξ= f(γ) C_M, Ξ= f(i)
3	NAL-Tokyo (H. Kobayashi)	Transonic (Sub+Super)	T	12 % 60^{o}	Annular (Freon)	• 10 transducers • Strain gages	T	$C_p(x)$ C_M, Ξ= f(M_2) C_M, Ξ= f(k) C_M, Ξ= f(σ)
4	EPF-Lausanne (M. Degen)	Subsonic	T	17% 45^{o}	Annular (Air)	• 12 transducers • Strain gages	B,T	C_M, Ξ= f(σ) C_M, Ξ= f(β_1) C_M, Ξ= f(p_2/p_{t1})
5	ONERA (E. Szechenyi)	Subsonic	C	3% 0^{o}	Linear (Air)	• 26 transducers • Strain gages	T	$C_p(x)$, $\Delta C_p(x)$ C_M, Ξ= f(M_1) C_M, Ξ= f(i) C_M, Ξ= f(k)
6	EPF-Lausanne (D. Schläfli)	Transonic (Sub+Super)	T	5% 14^{o}	Annular (Air)	• 5 transducers each on two blades • Strain gages	B,T	$C_p(x)$ C_F, Ξ= f(β_1) C_F, Ξ= f(M_2) C_F, Ξ= f(σ) C_F, Ξ= f(k)
7	NASA LeRC (D.R. Boldman)	Supersonic Transonic (Super+Sub)	C	3% -1.3^{o}	Linear (Air) Strain gages	• 12 transducers • Strain gages	T	$C_p(x)$, $\Delta C_p(x)$ C_M, Ξ= f([illegible]) C_M, Ξ= f(p_2/p_{t1})

Table 3.0-1b Summary of the Seven Experimental Standard Configurations

for priority analyses, giving a total of 293 test cases. This number still seems to be rather large, but it concerns configurations over the whole velocity domain from incompressible to supersonic flow velocities. It is therefore not likely that any participant will calculate more than a small number of these cases.

Furthermore, some of the standard configurations, especially those with fairly thick blades and large deviations, do probably not correspond with the present state-of-art of aeroelasticity. If this is so, they may instead serve as a base for future developments.

Configurations 1 and 2 (see tables 3.6-1) treat the cascaded airfoils of rather low camber in the low subsonic velocity domain. The blades oscillate in torsion mode with a relatively low frequency.

Standard configurations 3 and 4 concern modern high turning turbine rotor hub sections; they have therefore relatively thick blades, with subsonic inlet and subsonic or supersonic outlet conditions. In both configurations, the blade vibration frequencies correspond to the ones found in the actual turbomachine-blade.

Configuration 6 concern low turning transonic turbine rotor tip sections with relatively thin blades with low stagger angle. The inlet condition is subsonic, with subsonic, transonic or supersonic outlet conditions.

Configurations 5 and 7 treat tip sections of fan stages in modern jet-engines and have thus rather thin profiles. The inlet flow conditions in configuration 5 are subsonic, with incidence ranging from attached to stalled flow conditions on the blades. In configuration 7, the inlet conditions are supersonic followed, in most cases, by strong in-passage shock waves.

The profiles in configurations 3-7 correspond to sections of actual turbomachine bladings. Both linear (configurations 1, 2, 5 and 7) and annular (configurations 3, 4 and 6) cascade test facilities are used.

The two last standard configurations (8 and 9) are of theoretical nature only. They are included to validate numerical methods against each other, especially in the high subsonic velocity domain, and to look into some physical aspects of the flutter phenomena.

3.1 First Standard Configuration

This configuration is compiled from two-dimensional cascade experiments in the low subsonic flow region. It is therefore mainly directed towards the validation of incompressible predictions.

The experiments have been performed, in air, in the linear low subsonic oscillating cascade wind tunnel at the United Technologies Research Center and are included in the present work by courtesy of F.O. Carta.

The cascade configuration consists of eleven vibrating NACA 65-series blades, each having a chord c=0.1524 m and a span of 0.254 m, with a 10 degree circular arc camber and a thickness-to-chord ratio of 0.06. The gap-to-chord ratio is 0.750 and the stagger angle for the experiments here presented is 35°.

The cascade geometry and profile coordinates are given in Figure and Table 3.1-1.

The airfoils oscillates in pitching mode around a pivot axis at (0.5, 0.0115). Experiments have been performed with oscillation frequencies between 6 and 26 Hz and with two pitching amplitudes (0.5° and 2°). Both the time averaged and time dependant instrumentation on this cascade is very complete, and a large number of well documented data have been obtained during the tests. The instrumentation allows for determination of both local and global unsteady forces on the blades (i.e. several high response pressure transducers and integration of these signals for global effects), and the results are presented in several ways.

From these tests, 15 aeroelastic cases have been retained as recommendations for off-design calculations. The cases are contained in Table 3.1-2, together with the proposal for representation of the results. They correspond to two different mean settings of the cascade (see Table 3.1-2), for each of which the steady blade surface pressure distribution is given in Figures 3.1-2 and Table 3.1-3.

According to the recommended representation, the test data concerning the unsteady blade surface pressures as well as the moment coefficient and aerodynamic damping shall be given in dependance of the reduced frequency and interblade phase angle. An example of the representation in the standarized reporting format (to be used for the representation of the experimental and theoretical data) of the time dependant results for this cascade are shown in Figures 3.1-3 and Table 3.1-4.

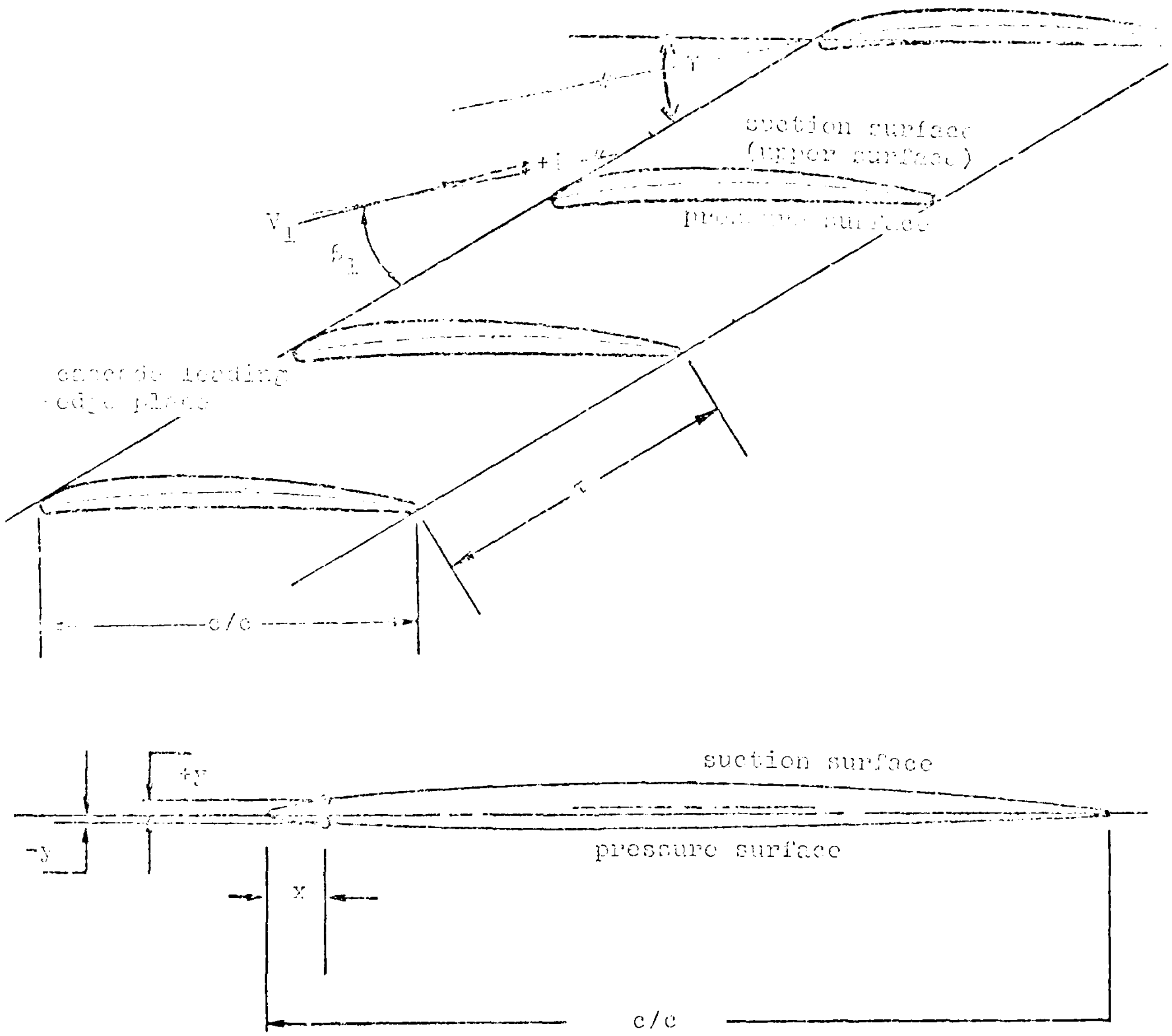

c	= 0.1524 m	τ	= 0.75
span	= 0.254 m	x_α	= 0.5
camber	= 10.°	y_α	= 0.0115
γ	= 35.°	$\frac{\text{thickness}}{\text{chord}}$	= 0.06

Figure 3.1-1 First Standard Configuration: Cascade Geometry

c = 15.24 cm (6 in.)			
SUCTION SURFACE		PRESSURE SURFACE	
X	Y	X	Y
0.0008	0.0020	0.0012	-0.0019
0.0046	0.0053	0.0054	-0.0042
0.0070	0.0064	0.0080	-0.0050
0.0120	0.0083	0.0130	-0.0061
0.0244	0.0116	0.0256	-0.0077
0.0494	0.0164	0.0507	-0.0098
0.0743	0.0204	0.0757	-0.0115
0.0993	0.0237	0.1007	-0.0129
0.1494	0.0290	0.1506	-0.0150
0.1994	0.0331	0.2006	-0.0165
0.2495	0.0364	0.2505	-0.0177
0.2996	0.0387	0.3004	-0.0185
0.3998	0.0411	0.4002	-0.0188
0.5000	0.0406	0.5000	-0.0176
0.6002	0.0370	0.5998	-0.0146
0.7003	0.0306	0.6997	-0.0104
0.8003	0.0223	0.7997	-0.0069
0.8503	0.0176	0.8497	-0.0053
0.9003	0.0127	0.8997	-0.0040
0.9502	0.0078	0.9497	-0.0032
0.9975	0.0030	0.9973	-0.0025

	RADIUS CENTER COORDINATES
L.E. RADIUS/c = 0.0024	X = 0.0024, Y = 0.0002
T.E. RADIUS/c = 0.0028	X = 0.9972, Y = 0.0003

Table 3.1-1 First Standard Configuration: Dimensionless Airfoil Coordinates

Case No	Inlet Air Velocity M_1 (-)	Incidence Angle i (^{o})	p_1/p_{t1} (-)	p_2/p_{t1} (-)	Outlet Flow Angle β_2 (^{o})	Reduced Frequency k (-)	Amplitude α (rad)	Interblade Phase σ (^{o})	Frequency f (Hz)	c_p	Δc_p	C_M	[illegible]
1	0.18	2	0.9774	0.5818	28	0.122	0.5	-45^o	15.3	1	2	-	-
2	↓	2	↓	↓	↓	↓	0.5	$+45^o$	↓	↓	↓	-	-
3	0.17	6	0.9730	0.9852	27.5		0.5	-45^o				-	-
4	↓	↓	↓	↓	↓		2.0	$+45^o$				4	6
5							↓	-45^o				↓	↓
6								-180^o		-	-		
7								-135^o		1	2		
8								-90^o		-	-	3,	5,
9								-0^o		1	2		
10								$+90^o$		-	-		
11								$+135^o$		1	2		
12						0.072		-90^o	9.2	-	-	3	3
13						0.151		↓	19.2	-	-	↓	↓
14						0.301			38.4	-	-		
15						0.603			76.8				

Column groups: Time averaged values (M_1 to β_2); Time dependant values (k to f); Recommended representation (c_p to last column).

NOTES : 1) c_p as a function of x
2) Δc_p " " " " x
3) C_M " " " " k
4) C_M as a function of -
5) [illegible] " " " " k
6) - " " " " -

Table 3.1-2 First Standard Configuration: 15 recommended aeroelastic cases

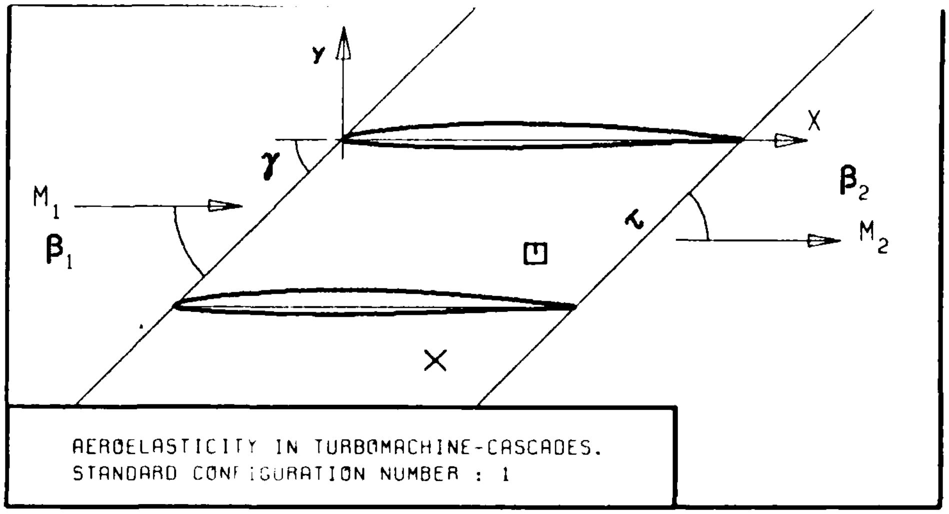

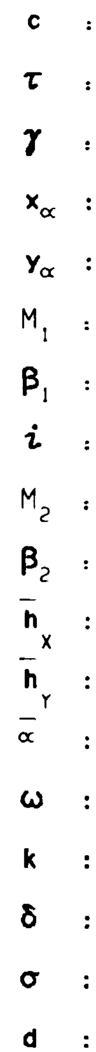

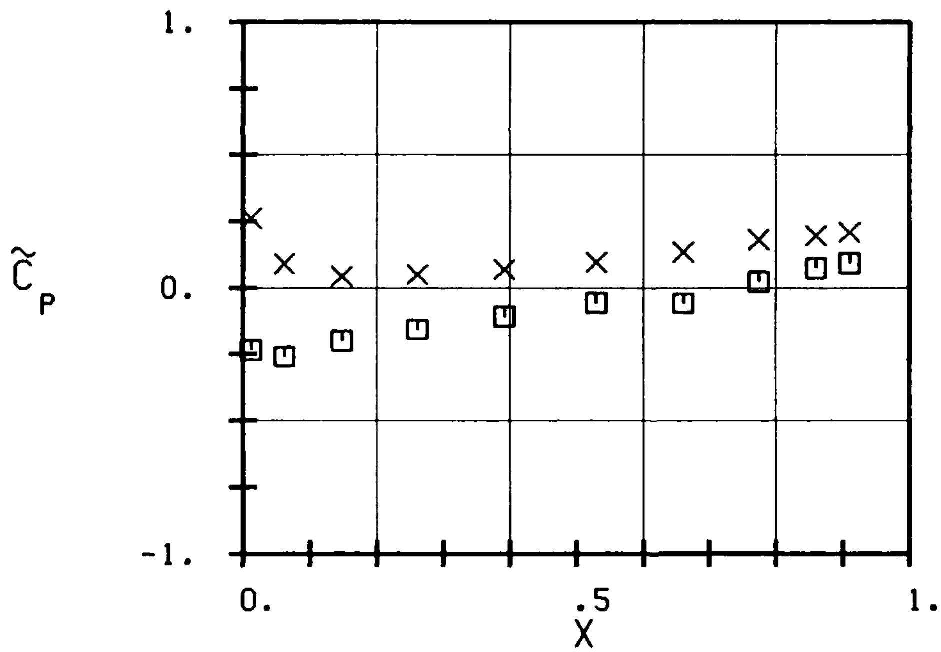

FIG. 3.1-2A: FIRST STANDARD CONFIGURATION.
TIME AVERAGED BLADE SURFACE PRESSURE
COEFFICIENT FOR INCIDENCE 2. DEGREES.

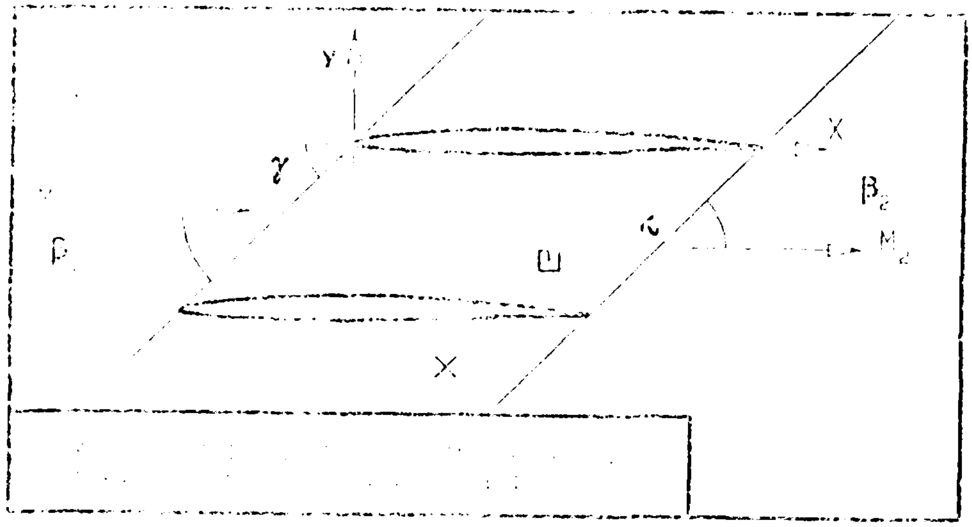

c :
τ :
γ :
x_α :
y_α :
M_1 :
β_1 :
i :
M_2 :
β_2 :
$\bar{h}_X$:
$\bar{h}_Y$:
$\bar{\alpha}$:
ω :
k :
δ :
σ :
d :

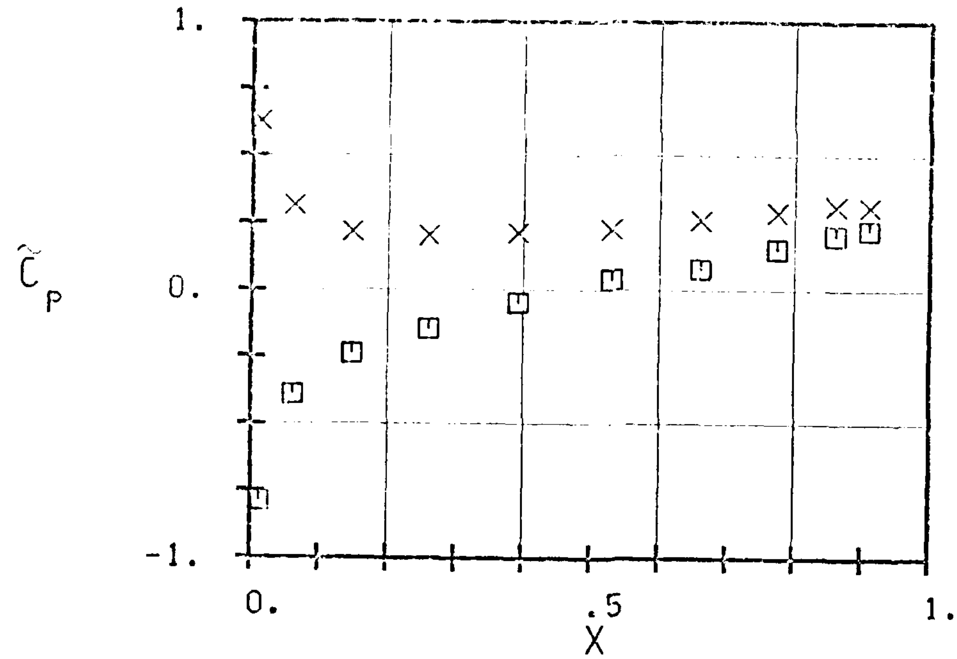

FIG. 3.1-2B: FIRST STANDARD CONFIGURATION.
TIME AVERAGED BLADE SURFACE PRESSURE
COEFFICIENT FOR INCIDENCE 6. DEGREES.

Aeroelasticity in Turbomachine-Cascades First Standard Configuration Time Averaged Blade Surface Pressure Distributions				
M_1 (-)	0.18		0.17	
i (°)	2		6	
p_2/p_{t1} (-)	0.9818		0.9852	
β_2 (°)	28		27.5	
$\bar{x}$ (-)	Upper surface $\tilde{C}_p$ (-)	Lower surface $\tilde{C}_p$ (-)	Upper surface $\tilde{C}_p$ (-)	Lower surface $\tilde{C}_p$ (-)
.012	-.2341	.2618	-.7874	.6278
.062	-.2587	.0904	-.3910	.3139
.148	-.1992	.0441	-.2390	.2148
.261	-.1561	.0503	-.1465	.2015
.392	-.1078	.0688	-.0485	.2115
.530	-.0565	.0955	.0385	.2269
.661	-.0585	.1345	.0782	.2599
.774	.0236	.1817	.1531	.2896
.860	.0739	.1961	.2037	.3128
.910	.0934	.2094	.2247	.3106

Table 5.1-5 First Standard Configuration: Time Averaged Blade Surface Pressure Distributions for the 15 Recommended Aeroelastic Cases

Aeroelasticity in Turbomachine-Cascades.
First Standard Configuration.
Aeroelastic test case N^{o}:______

M_1=_____ $\quad$ i= _____^{o}. $\quad$ k= _____ .

$\bar{\alpha}^{(-2)}$=_____ • $\bar{\alpha}^{(-1)}$=_____ • $\bar{\alpha}^{(0)}$=_____ • $\bar{\alpha}^{(+1)}$=_____ • $\bar{\alpha}^{(+2)}$=_____ • (rads)

$\sigma^{(-2)}$=_____ • $\sigma^{(-1)}$=_____ • $\sigma^{(0)}$=_____ • $\sigma^{(+1)}$=_____ • $\sigma^{(+2)}$=_____ • (^{o})

a) Global Aeroelastic Coefficients

$\bar{C}_M$=_______ • $\bar{C}_L$=_______ • C_W=_______ • Ξ =_______ • (-)

Φ_M=_______ • Φ_L=_______ • $\quad$ (^{o})

b) Local Time Dependant Blade Surface Pressure Coefficients

X (-)	$C_p^{(ls)}$ (-)	$\Phi_p^{(ls)}$ (^{o})	$C_p^{(us)}$ (-)	$\Phi_p^{(us)}$ (^{o})	$\Delta\bar{C}_p$ (-)	$\Phi_{\Delta p}$ (^{o})

Table 3.1-4 First Standard Configuration: Table for Representation of the Recommended Aeroelastic Test Cases

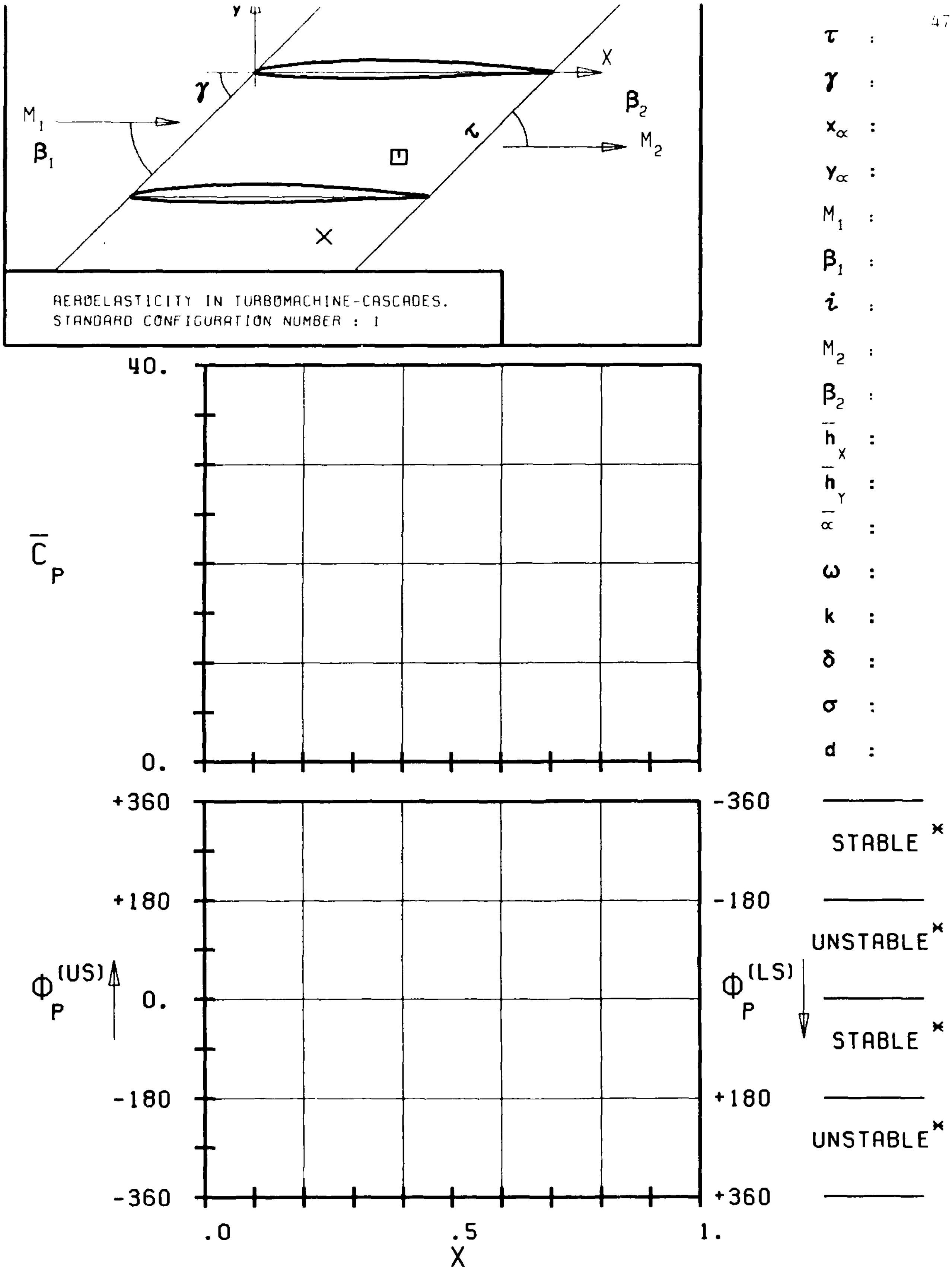

FIG. 3.1-3A: FIRST STANDARD CONFIGURATION.
MAGNITUDE AND PHASE LEAD OF UNSTEADY BLADE
SURFACE PRESSURE COEFFICIENT.

(*: IN PITCH MODE, NOTATION VALID UPSTREAM OF PITCH AXIS)

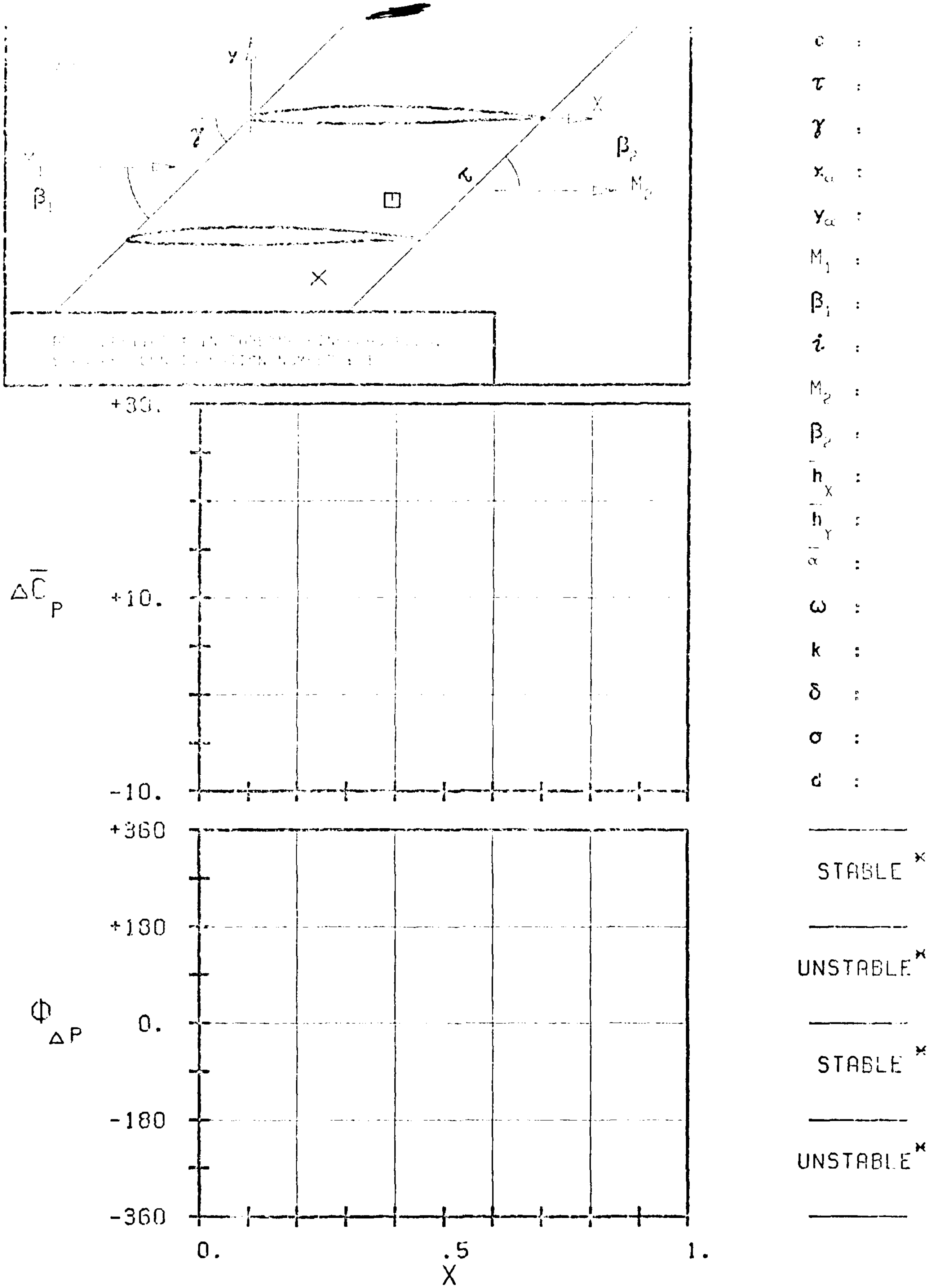

FIG. 3.1-3B: FIRST STANDARD CONFIGURATION.
MAGNITUDE AND PHASE LEAD OF UNSTEADY
SURFACE PRESSURE DIFFERENCE COEFFICIENT.

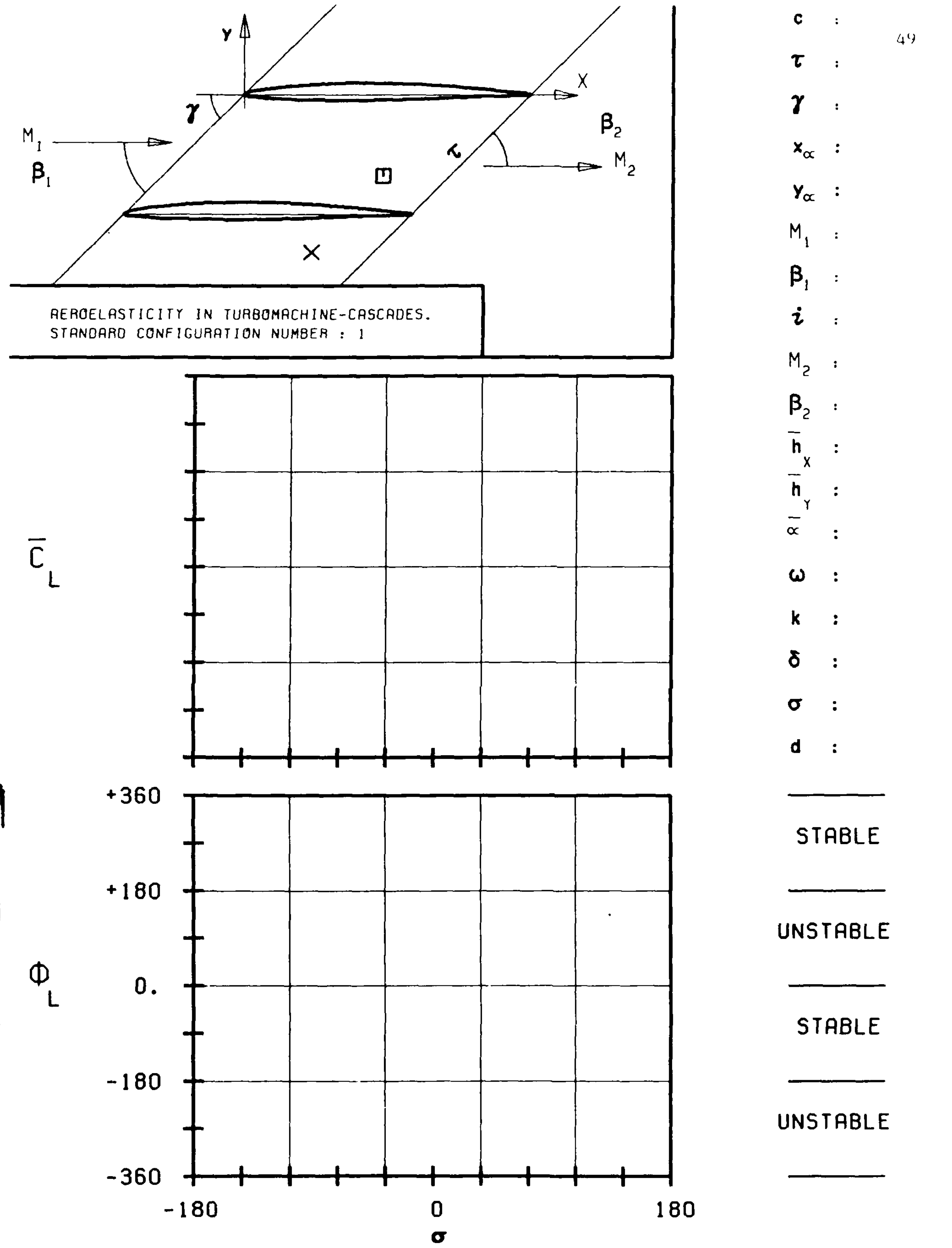

FIG. 3.1-3C: FIRST STANDARD CONFIGURATION.
AERODYNAMIC LIFT COEFFICIENT AND PHASE LEAD
IN DEPENDANCE OF INTERBLADE PHASE ANGLE.

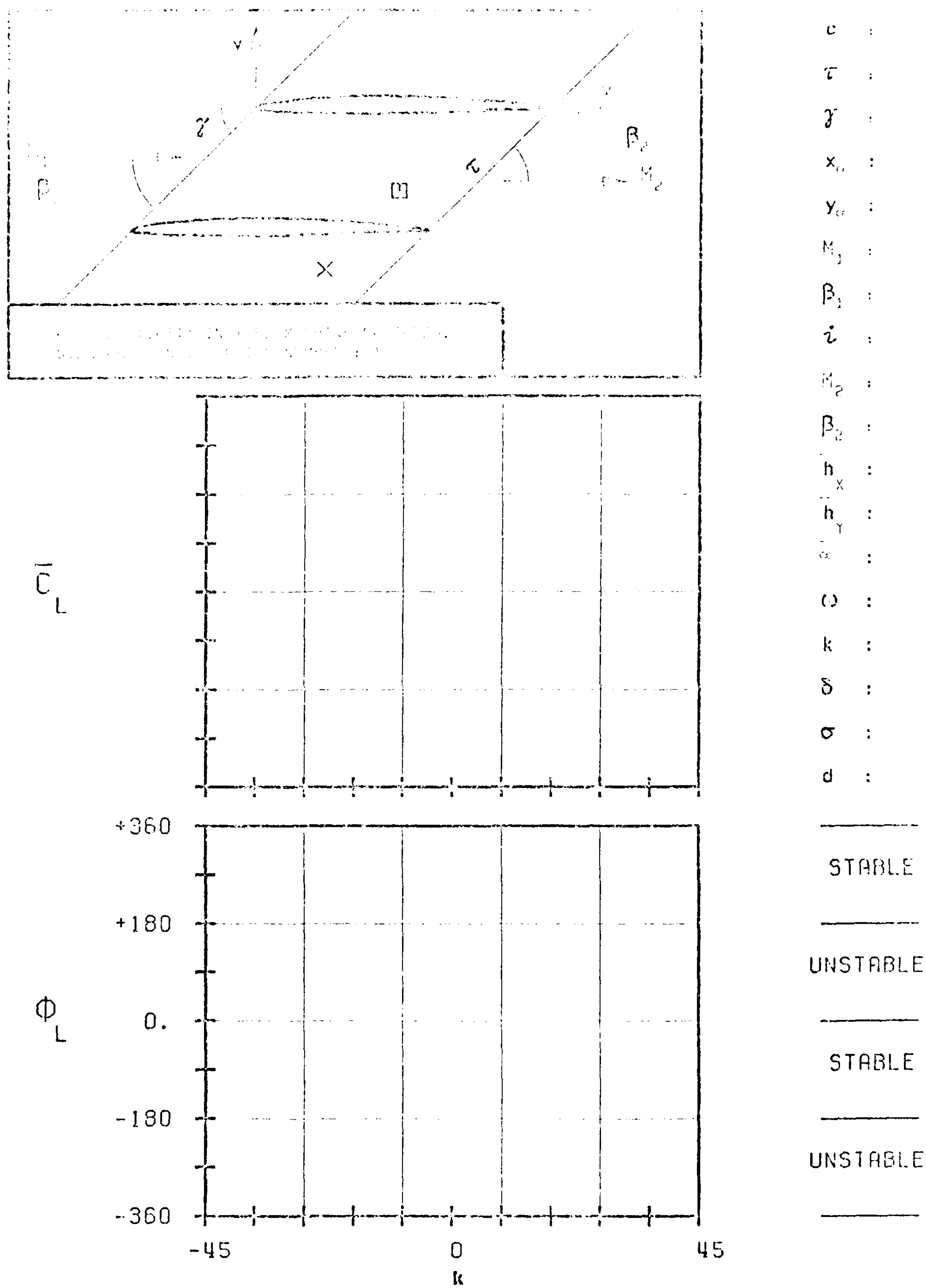

FIG. 3.1-3D: FIRST STANDARD CONFIGURATION.
AERODYNAMIC LIFT COEFFICIENT AND PHASE LEAD
IN DEPENDANCE OF REDUCED FREQUENCY.

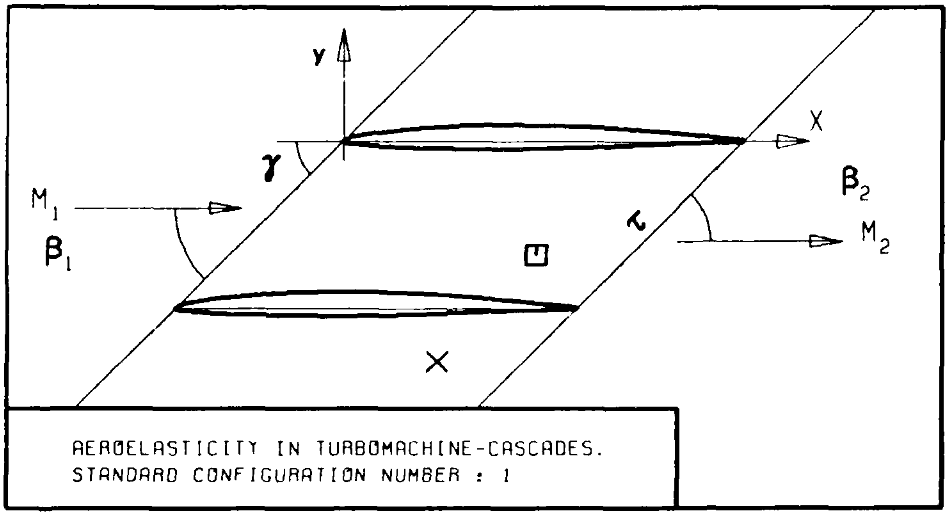

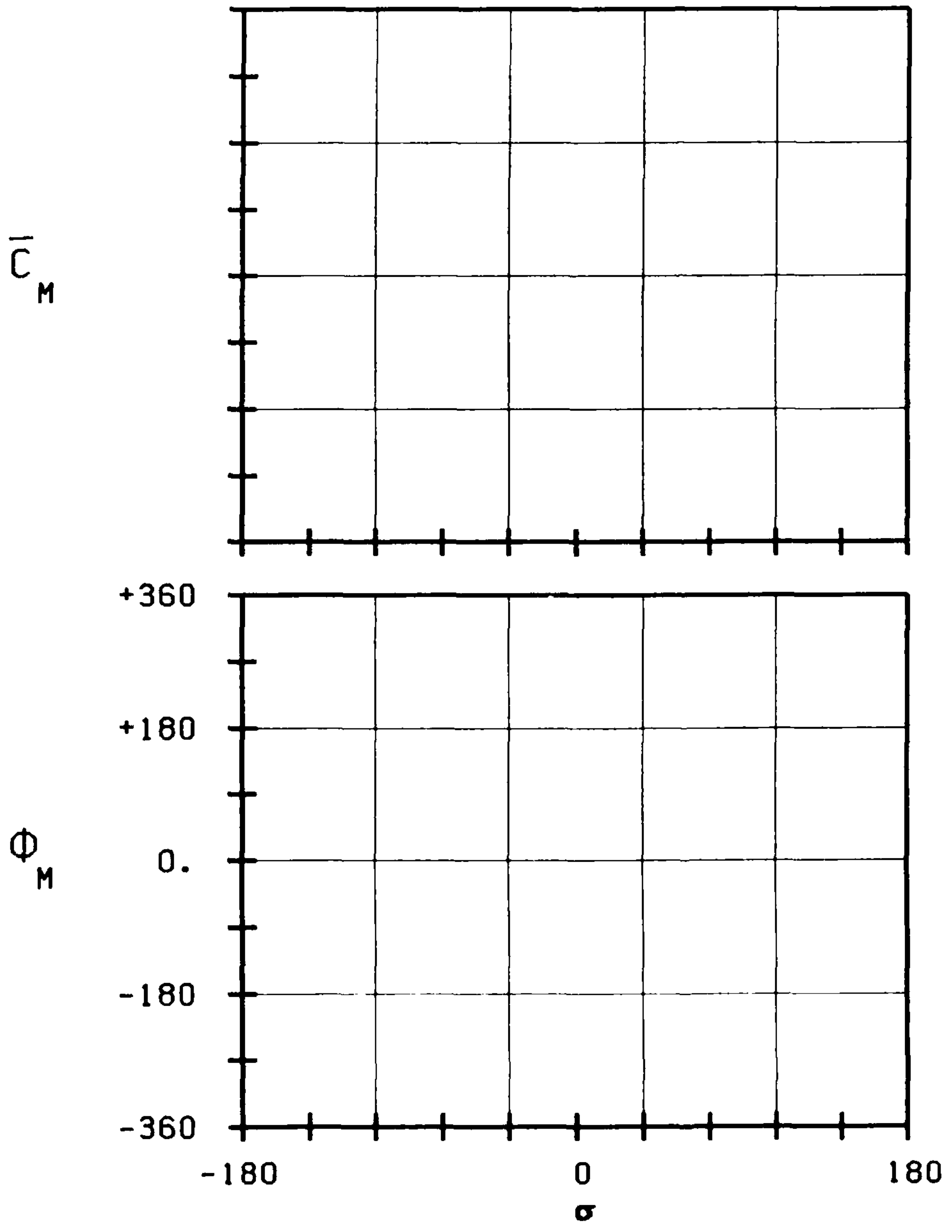

c :

τ :

γ :

x_α :

y_α :

M_1 :

β_1 :

i :

M_2 :

β_2 :

$\bar{h}_X$:

$\bar{h}_Y$:

$\bar{\alpha}$:

ω :

k :

δ :

σ :

d :

STABLE

UNSTABLE

STABLE

UNSTABLE

FIG. 3.1-3E: FIRST STANDARD CONFIGURATION.
AERODYNAMIC MOMENT COEFFICIENT AND PHASE LEAD
IN DEPENDANCE OF INTERBLADE PHASE ANGLE.

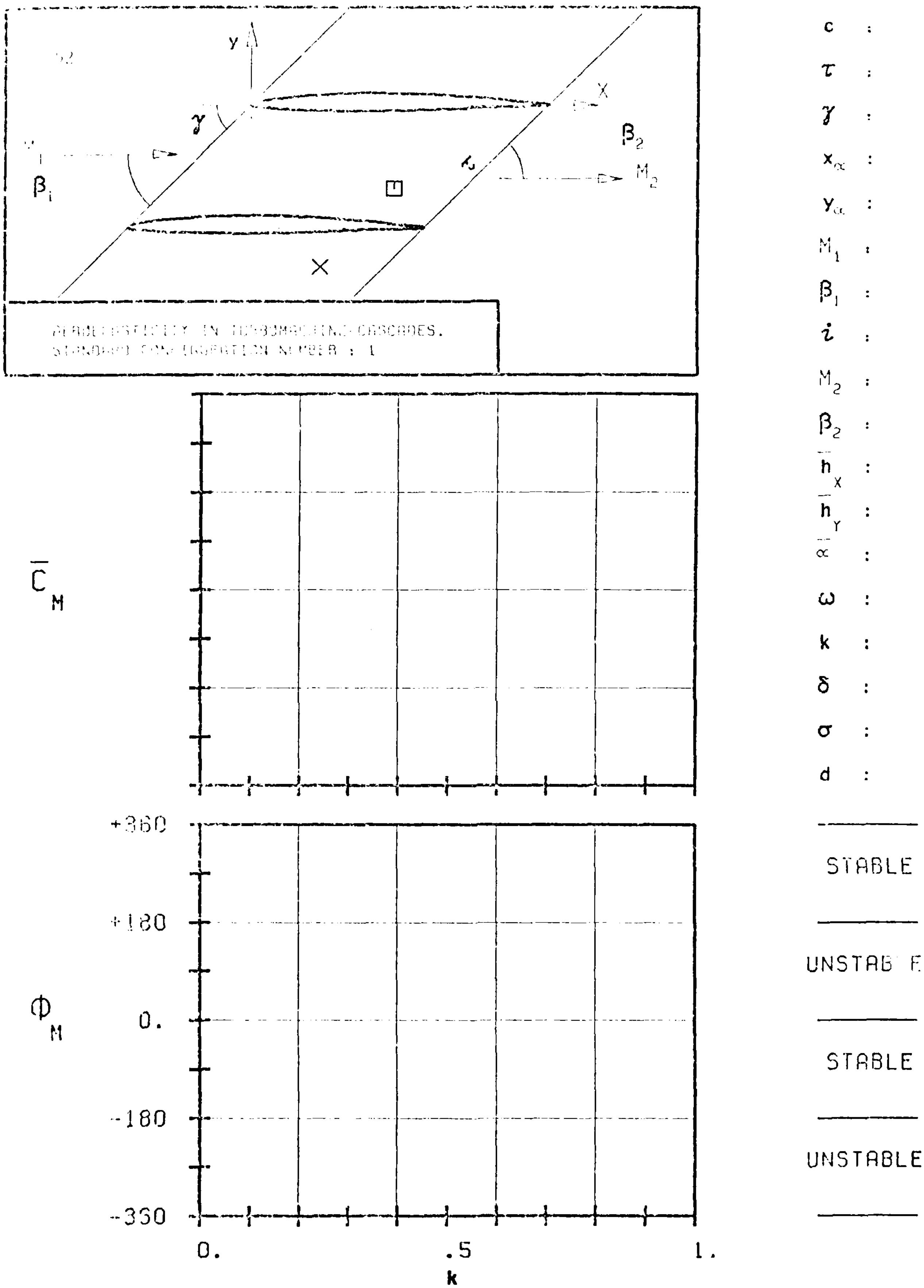

FIG. 3.1-3F: FIRST STANDARD CONFIGURATION.
AERODYNAMIC MOMENT COEFFICIENT AND PHASE LEAD
IN DEPENDANCE OF REDUCED FREQUENCY.

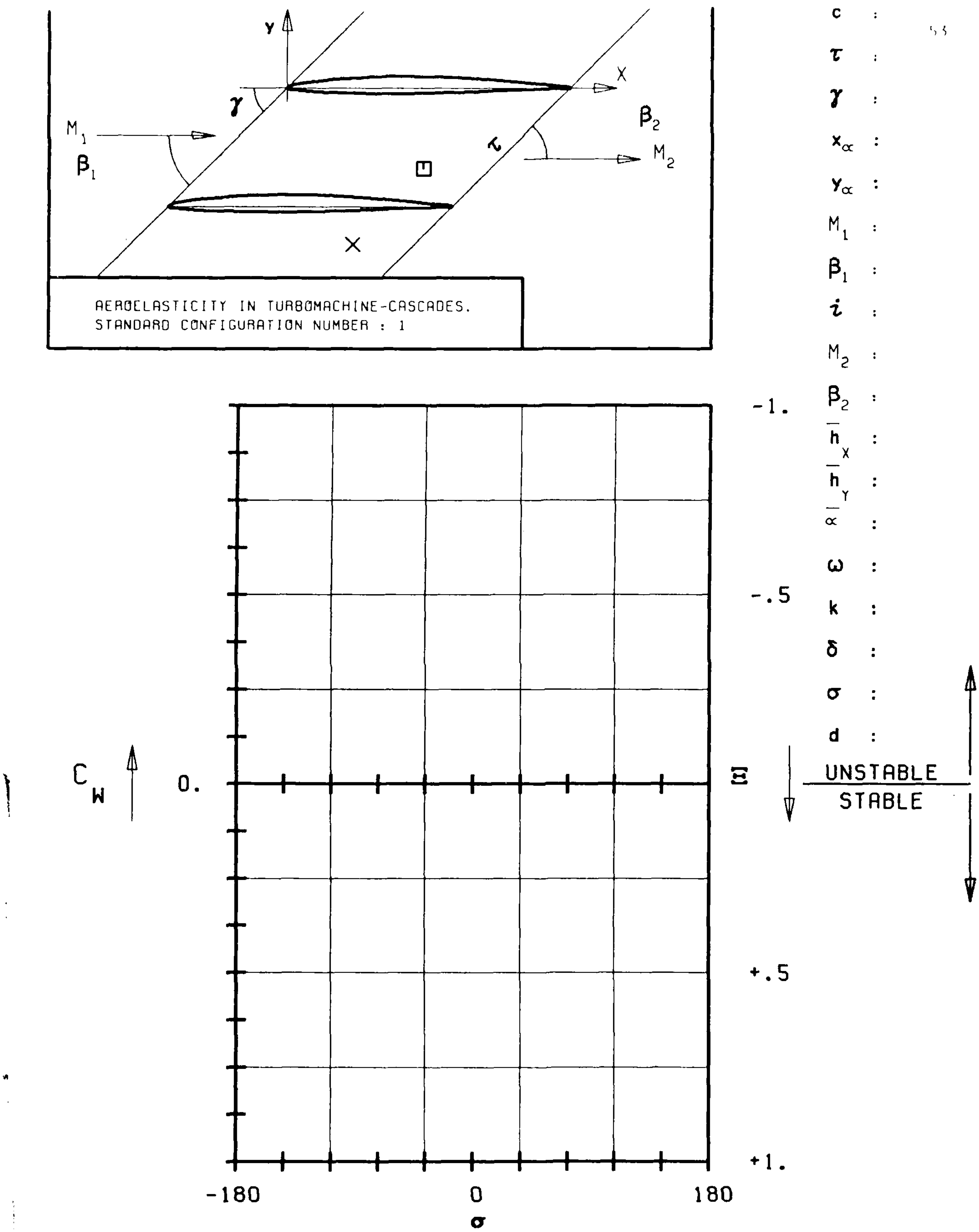

FIG. 3.1-3G: FIRST STANDARD CONFIGURATION.
AERODYNAMIC WORK AND DAMPING COEFFICIENTS
IN DEPENDANCE OF INTERBLADE PHASE ANGLE

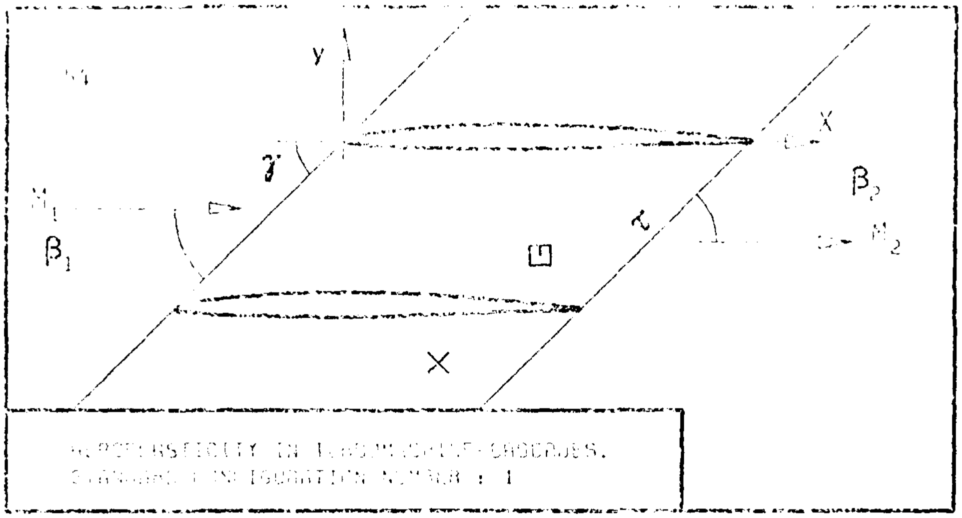

c :
τ :
γ :
x_{α} :
y_{α} :
M_1 :
β_1 :
i :
M_2 :
β_2 :
$\bar{h}_X$:
$\bar{h}_Y$:
$\bar{\alpha}$:
ω :
k :
δ :
σ :
d :

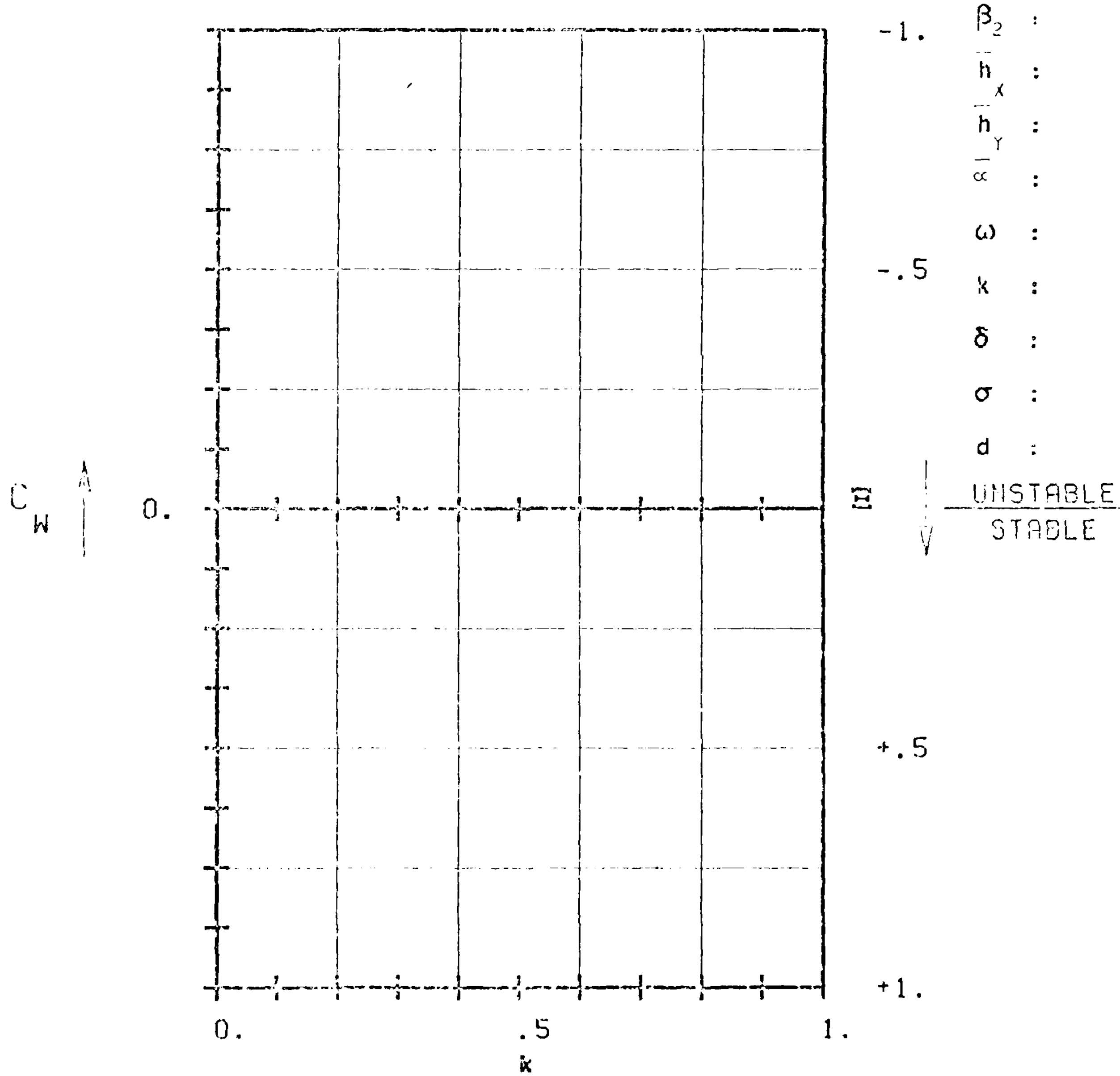

FIG. 3.1-3H: FIRST STANDARD CONFIGURATION.
AERODYNAMIC WORK AND DAMPING COEFFICIENTS
IN DEPENDENCE OF REDUCED FREQUENCY.

3.2 Second Standard Configuration

This incompressible two-dimensional cascade configuration has been measured in a water cascade tunnel at the University of Tokyo. The results have been submitted by courtesy of H. Tanaka.

The cascade consists of eleven vibrating and six stationary double circular arc profiles. Each of the blades have a chord of c=0.050 m and a span of 0.100 m, with a camber angle of 16° and a gap-to-chord ratio of 1.00. The water velocity during the tests was V_1=2 m/s, with the Reynolds number situated at Re 1.2 . 10^5. The eleven vibrating blades oscillate in pitch, with an amplitude of 0.06 rad (3.4°) and a frequency between 1.3 and 13Hz. Thus, the reduced frequency lies in the domain 0.1 to1.0. The cascade geometry is given in Figure 3.2-1 and the profile coordinates in Table 3.2-1.

Experiments have been performed with incidence ranging from attached to partly separated and fully separated flow. Further, the stagger angle as well as the interblade phase angle and pivot axis have been varied systematically.

The experimental data indicates the unsteady lift and moment coefficients (amplitudes together with the corresponding phase lead angles). These coefficients are computed from strain gage measurements; no time dependant pressures are measured on the blade surfaces.

From the experiments, 22 aeroelastic cases are selected for "prediction". These aeroelastic test cases are summarized in Table 3.2-2, together with the proposal for representation of the results.

The 22 aeroelastic cases correspond to 5 cascade geometries (see Table 3.2-2). The recommended representation of the results of the second standard configuration includes therefore trends of lift and moment coefficients for aeroelastic parameters, such as interblade phase angle and reduced frequency, but also for cascade parameters such as incidence and stagger angle.

The time-averaged blade pressure distributions was not measured during the experiments.

It is recommended that the results should be represented as in Figures 3.2-2 and Table 3.2-3.

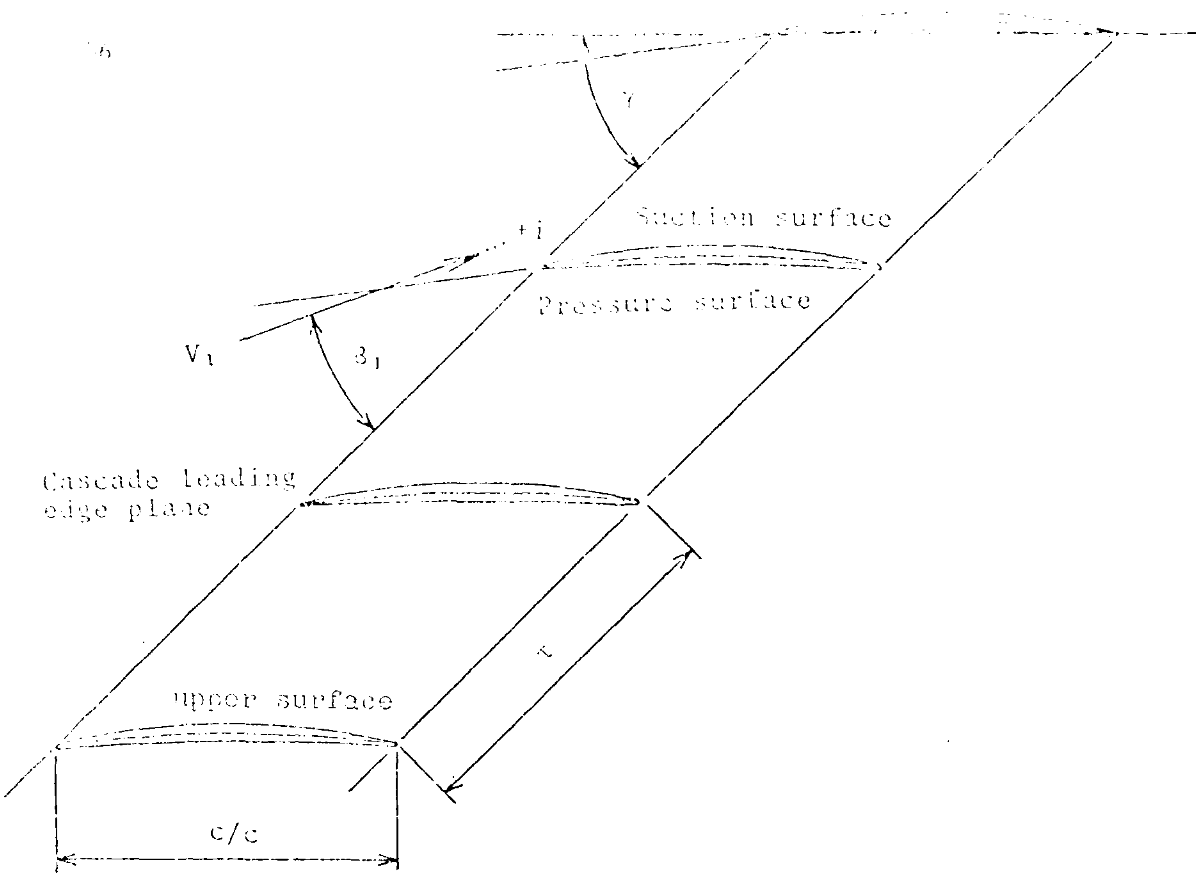

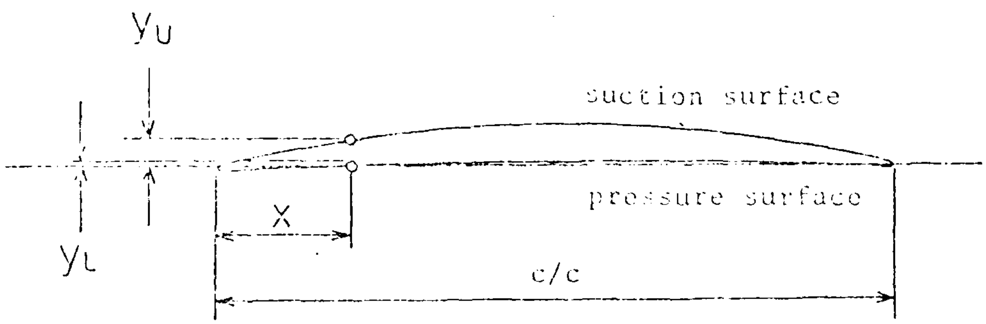

c	= 50 mm	τ	= 1.00
Span	=100 mm	x	= 0.5
Camber	= 16°46'	y	= 0.0362
γ	= 90°, 60°, -30°	$\frac{\text{Thickness}}{\text{chord}}$	= 0.0524

Figure 3.2-1 Second Standard Configuration Cascade Geometry

Double Circular Arc Blade c=0.050 m (1.968 in.)		
	Suction surface (upper surface)	Pressure surface (lower surface)
x (%)	y (%)	y (%)
0	0	0
5	1.644	-0.404
10	2.637	-0.127
15	3.509	0.115
20	4.262	0.326
25	4.897	0.505
30	5.416	0.650
35	5.818	0.764
40	6.105	0.845
45	6.272	0.893
50	6.334	0.910
55	6.272	0.893
60	6.105	0.845
65	5.818	0.764
70	5.416	0.650
75	4.897	0.505
80	4.262	0.326
85	3.509	0.115
90	2.637	-0.127
95	1.644	-0.404
100	0	0

L.E. and T.E. RADIUS			RADIUS CENTER COORDINATES
L.E.	RADIUS/c	0.666 (%)	x 0.666 (%), y 0 (%)
T.E.	RADIUS/c	0.666 (%)	x 0.993 (%), y 0 (%)

Table 3.2-1 Second Standard Configuration: Dimensionless Airfoil Coordinates

Aeroelastic case No.	Water velocity V_1 (m/s)	Incidence (a) i (°)	Stagger angle γ (°)	Pivot axis x_α (-)	y_α (-)	Frequency f (Hz)	Reduced frequency k (-)	Amplitude α (rad)	Interblade phase angle σ (°)	Moment coefficient C_M (-)	Lift coefficient C_L (-)	Aerodynamic damping Ξ (-)
1	2.0	2	90	0.5	[illegible]	6.5	.5	[illegible]	180	3	3	3
2			60							1,2,[illegible],4	1,2,[illegible],4	1,2,[illegible],4
3			30									
4			-60									
5			-30									
6		0	60							4	4	4
7		-5										
8		-8										
9		+5										
10		2				1.3	0.1			2	2	2
11						3.9	0.3					
12						10.4	0.8					
13						13.0	1.0					
14						19.5	1.5					
15						26.0	2.0					
16						6.5	0.5	0		1	1	1
17									45			
18									90			
19									135			
20									225			
21									[illegible]			
22									315			

(a) the flow was attached for all these incidences

(b) A total of 4 blades vibrate with indentical amplitudes, frequencies and interblade phase angles

NOTES: 1) C_M, C_L and Ξ as a function of σ
2) " k
3) " γ
4) " i

Table 5.2-2 Second Standard Configuration: recommended aeroelastic test cases

Aeroelasticity in Turbomachine-Cascades.
Second Standard Configuration.
Aeroelastic test case N^o: _______

V_1 = 2 m/s. γ = _____ ^{o}. i= _____ ^{o}. k= _____.

$\bar{\alpha}^{(-2)}$= _____ • $\bar{\alpha}^{(-1)}$= _____ • $\bar{\alpha}^{(0)}$= _____ • $\bar{\alpha}^{(+1)}$= _____ • $\bar{\alpha}^{(+2)}$= _____ • (rads)

$\sigma^{(-2)}$= _____ • $\sigma^{(-1)}$= _____ • $\sigma^{(0)}$= _____ • $\sigma^{(+1)}$= _____ • $\sigma^{(+2)}$= _____ • (^{o})

a) Global Aeroelastic Coefficients

$\left\{ \begin{array}{l} \bar{C}_M = \_\_\_\_\_ \\ \Phi_M = \_\_\_\_\_ \end{array} \right.$ • $\left\{ \begin{array}{l} \bar{C}_L = \_\_\_\_\_ \\ \Phi_L = \_\_\_\_\_ \end{array} \right.$ • C_W= _____ • Ξ = _____ • (-)

• (^{o})

b) Local Time Dependant Blade Surface Pressure Coefficients

X (-)	$C_p^{(ls)}$ (-)	$\Phi_p^{(ls)}$ (^{o})	$C_p^{(us)}$ (-)	$\Phi_p^{(us)}$ (^{o})	$\Delta\bar{C}_p$ (-)	$\Phi_{\Delta p}$ (^{o})

Table 3.2-3 Second Standard Configuration. Table for Representation of the 22 Recommended Aeroelastic Test Cases

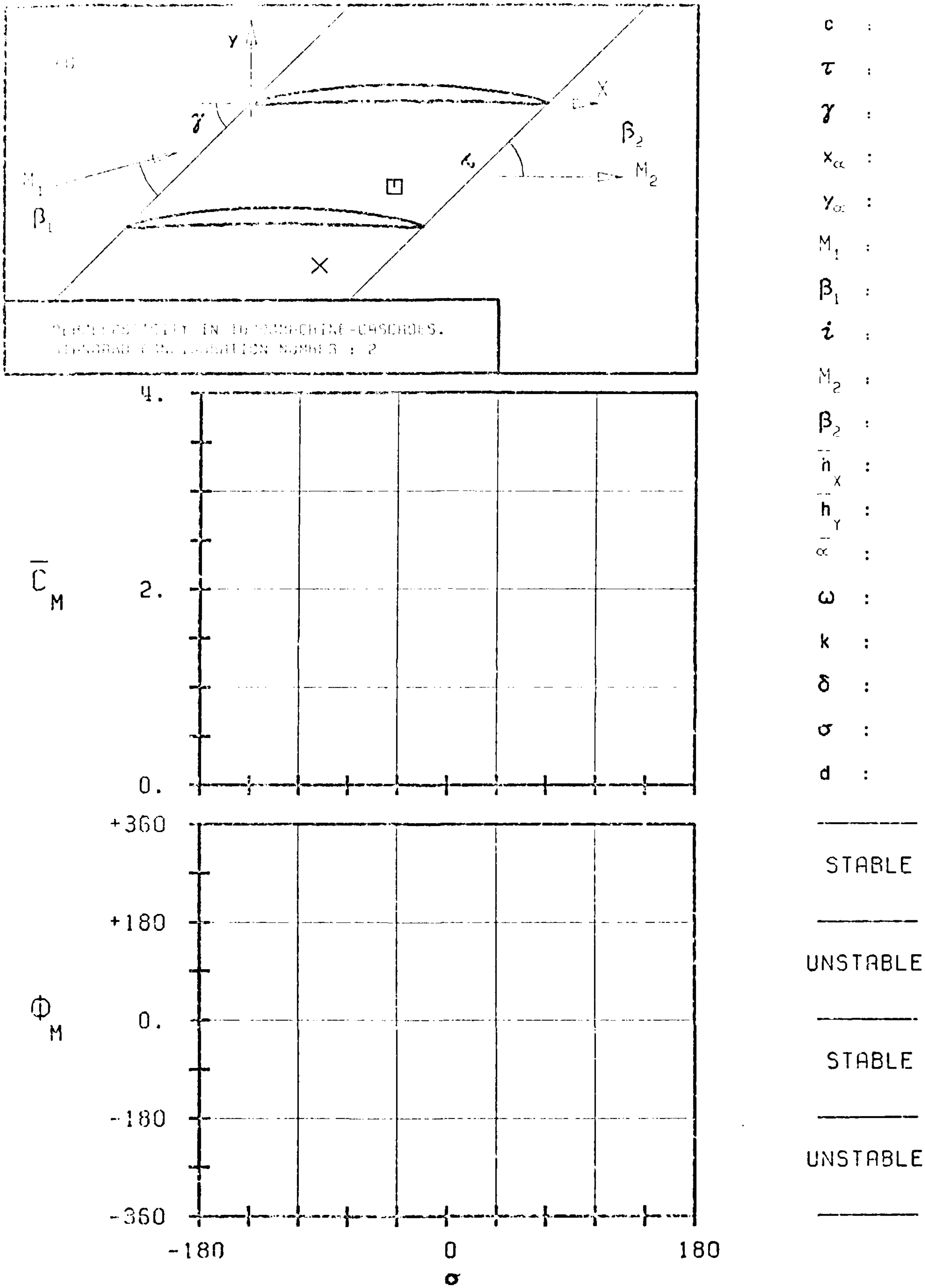

FIG. 3.2-2A: SECOND STANDARD CONFIGURATION:
AERODYNAMIC MOMENT COEFFICIENT AND PHASE LEAD
IN DEPENDANCE OF INTERBLADE PHASE ANGLE.

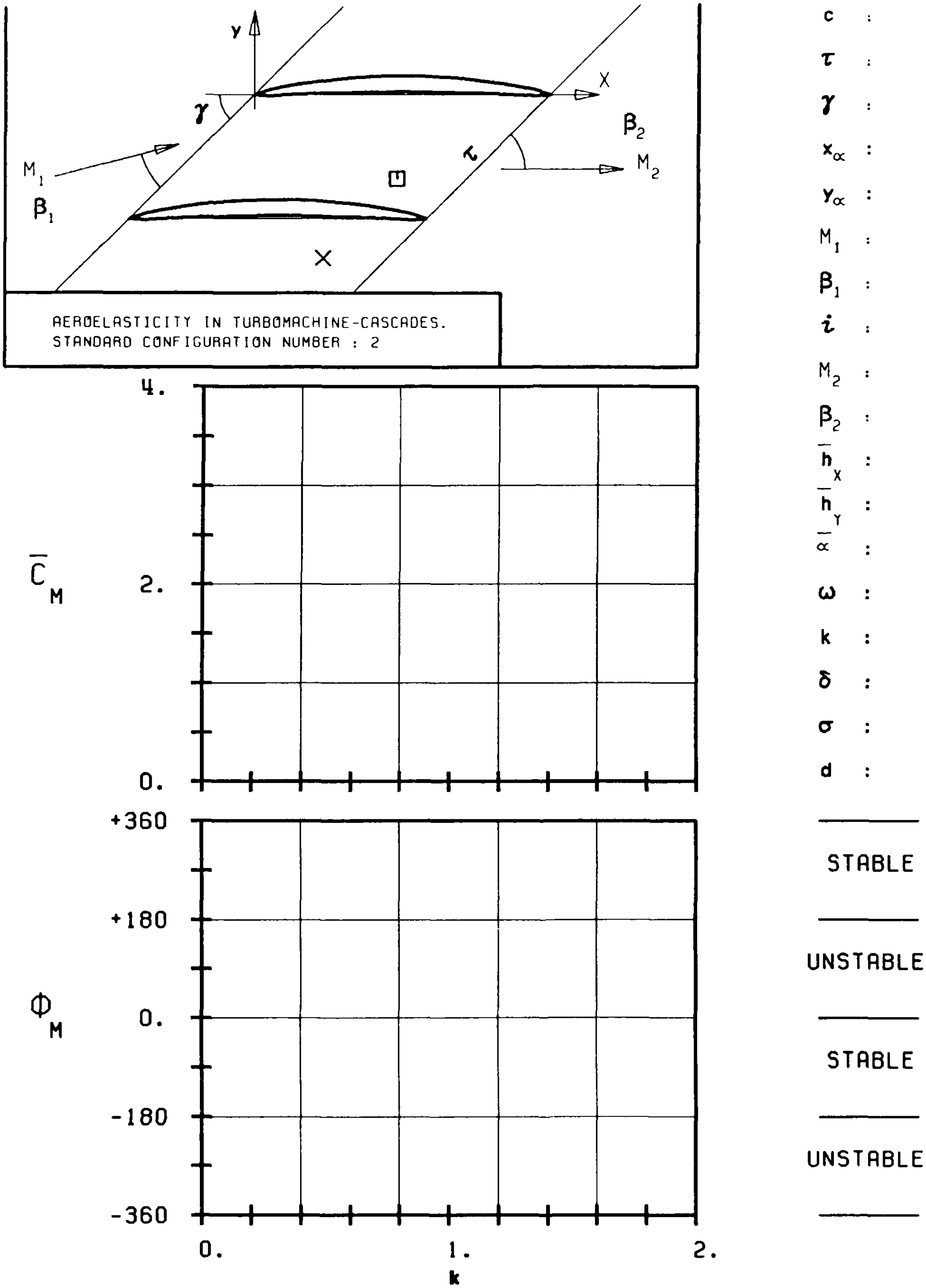

FIG. 3.2-2B: SECOND STANDARD CONFIGURATION:
AERODYNAMIC MOMENT COEFFICIENT AND PHASE LEAD
IN DEPENDANCE OF REDUCED FREQUENCY.

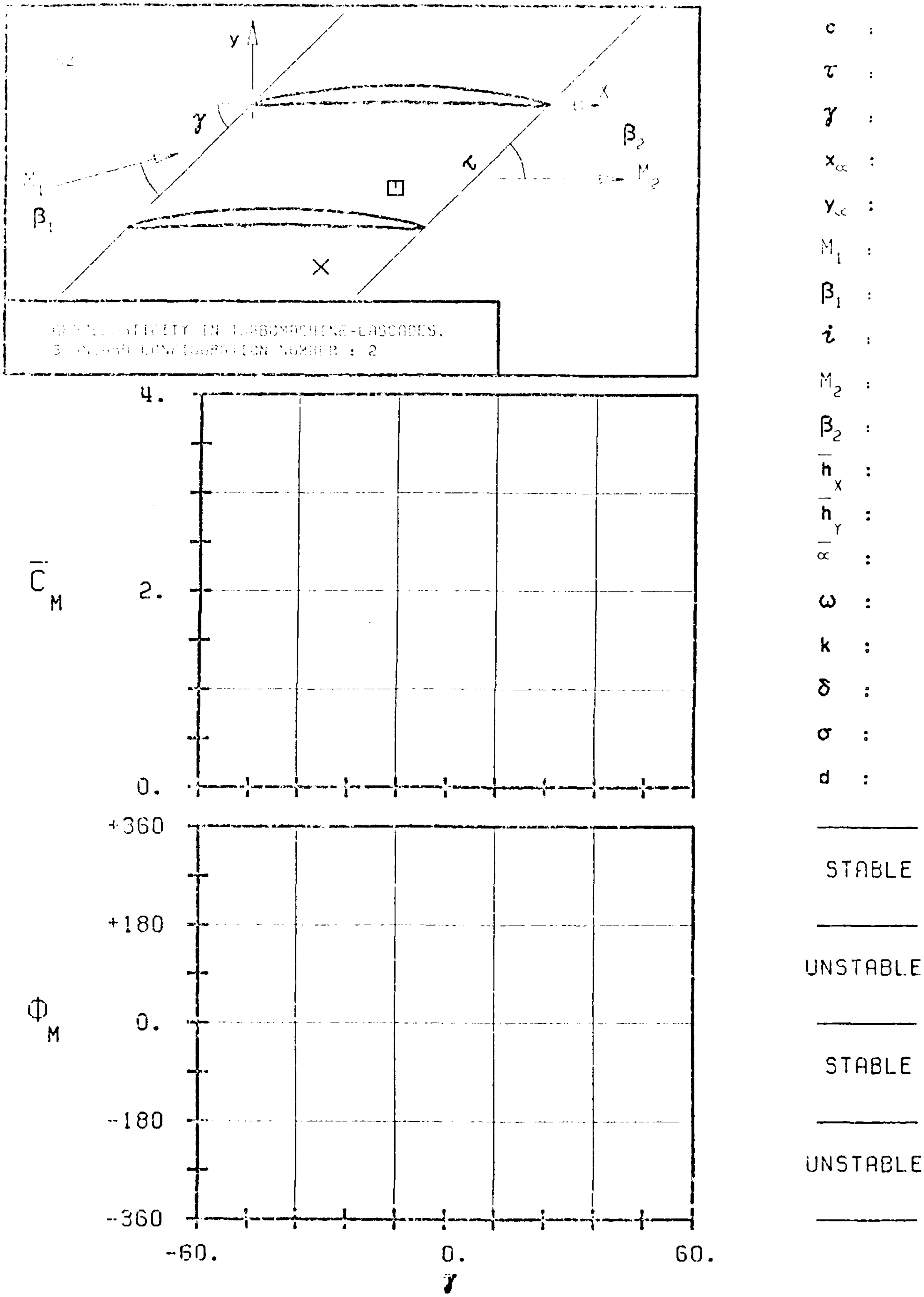

FIG. 3.2-2C: SECOND STANDARD CONFIGURATION:
AERODYNAMIC MOMENT COEFFICIENT AND PHASE LEAD
IN DEPENDANCE OF STAGGER ANGLE.

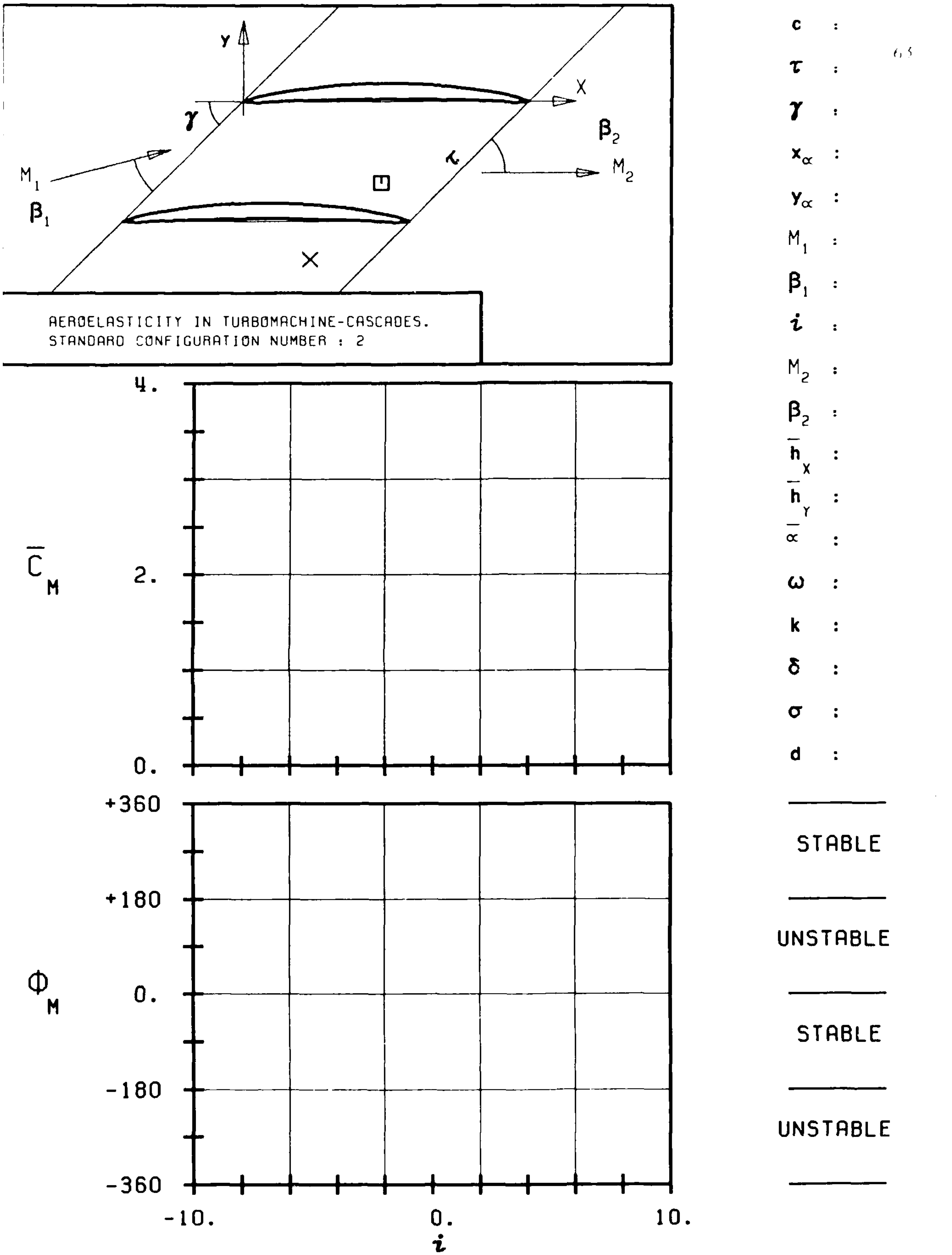

FIG. 3.2-2D: SECOND STANDARD CONFIGURATION:
AERODYNAMIC MOMENT COEFFICIENT AND PHASE LEAD
IN DEPENDANCE OF INCIDENCE ANGLE.

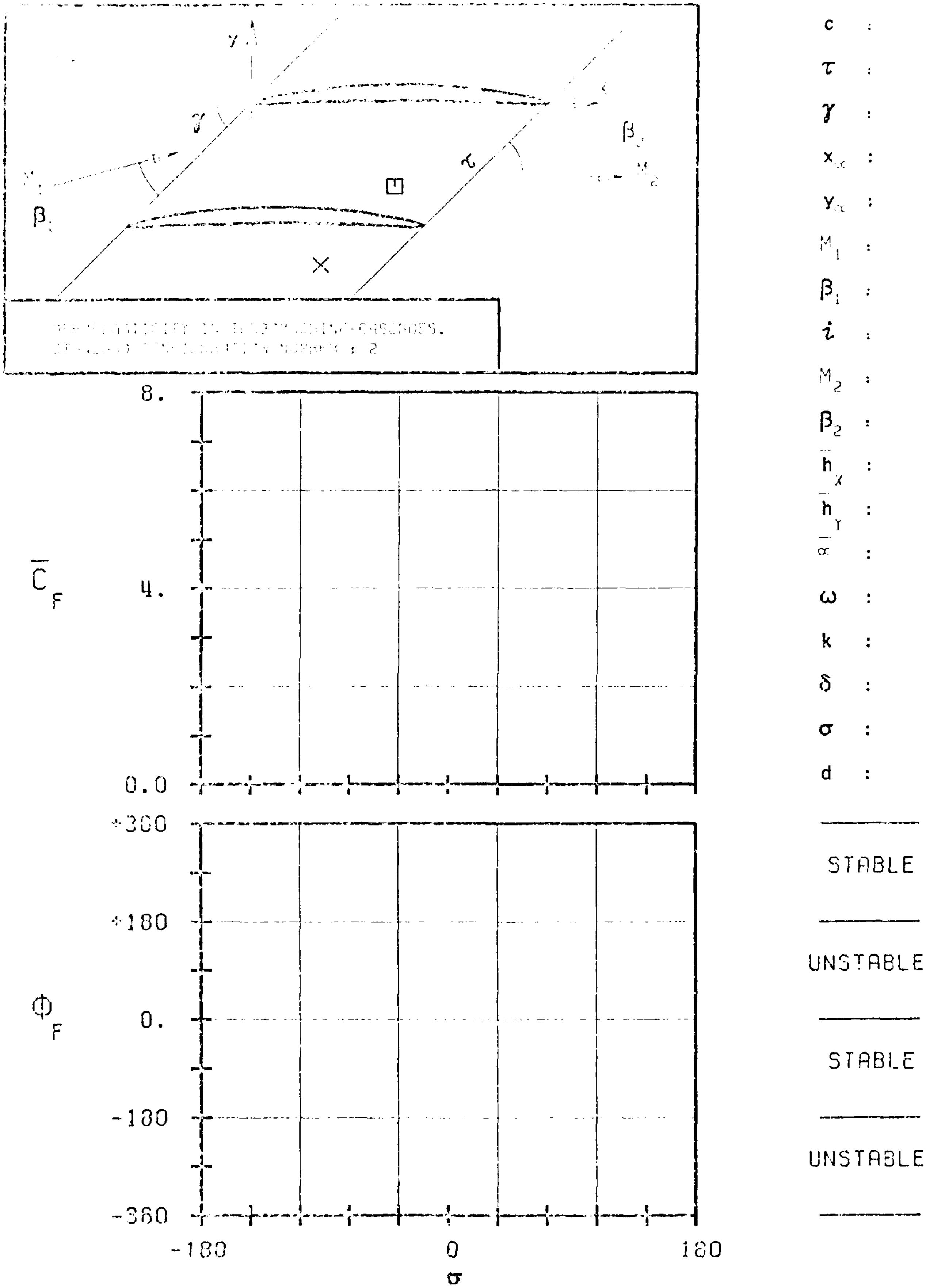

FIG. 3.2-2E: SECOND STANDARD CONFIGURATION:
AERODYNAMIC FORCE COEFFICIENT AND PHASE LEAD
IN DEPENDANCE OF INTERBLADE PHASE ANGLE.

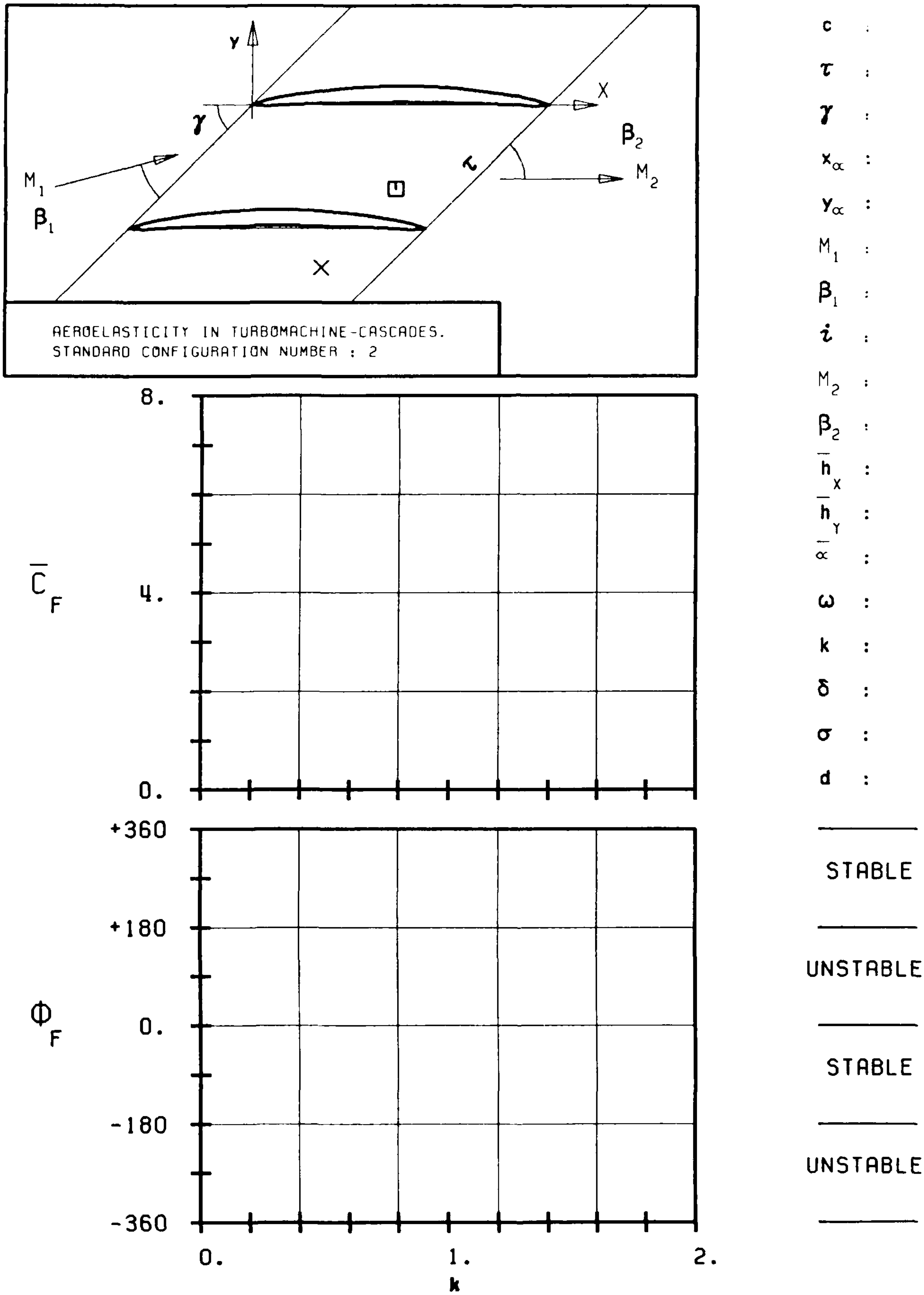

FIG. 3.2-2F: SECOND STANDARD CONFIGURATION:
AERODYNAMIC FORCE COEFFICIENT AND PHASE LEAD
IN DEPENDANCE OF REDUCED FREQUENCY.

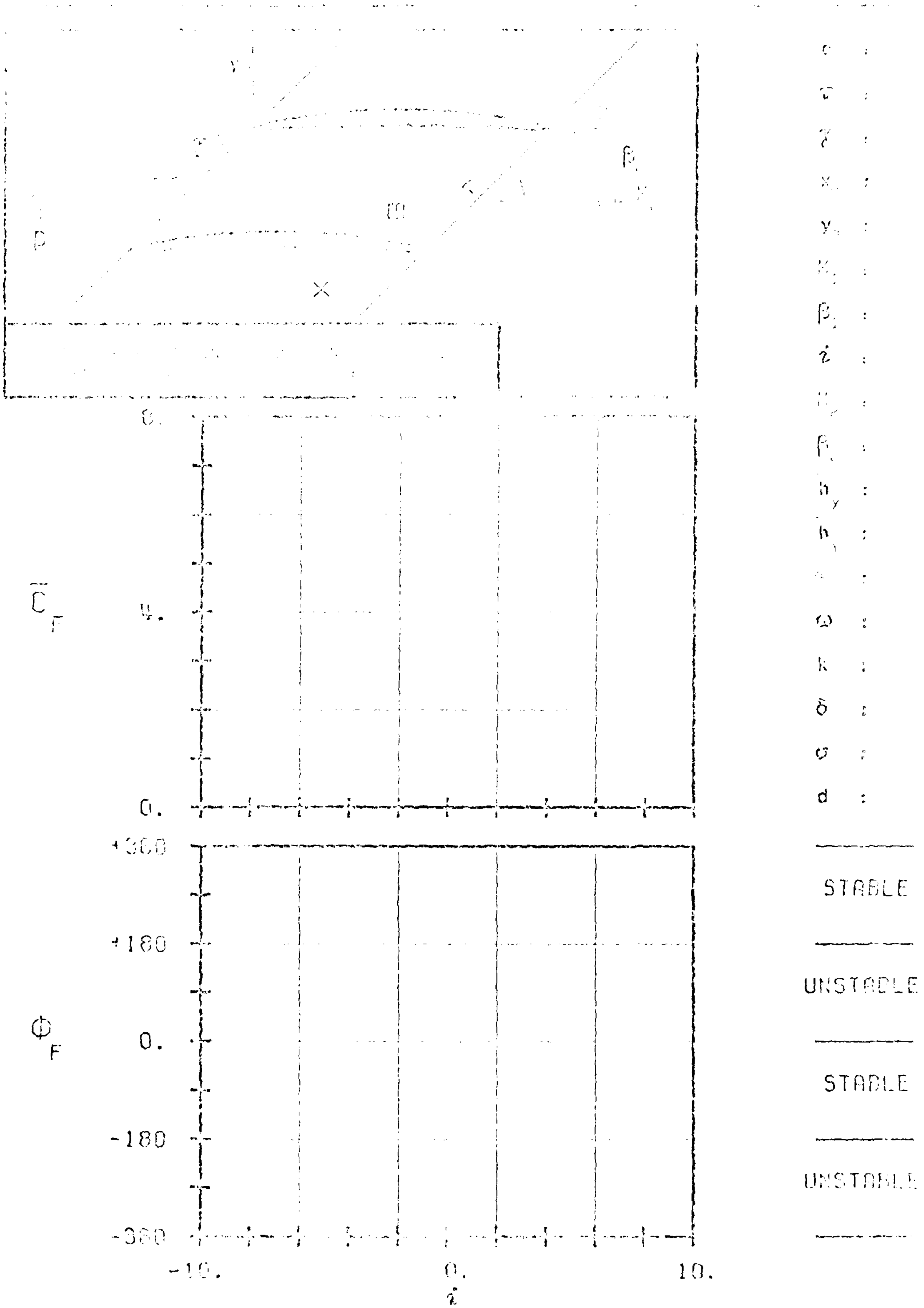

FIG. 3.2-[illegible] [illegible] STANDARD CONFIGURATION:
AERODYNAMIC FORCE COEFFICIENT AND PHASE LEAD
IN [illegible] OF [illegible] ANGLE.

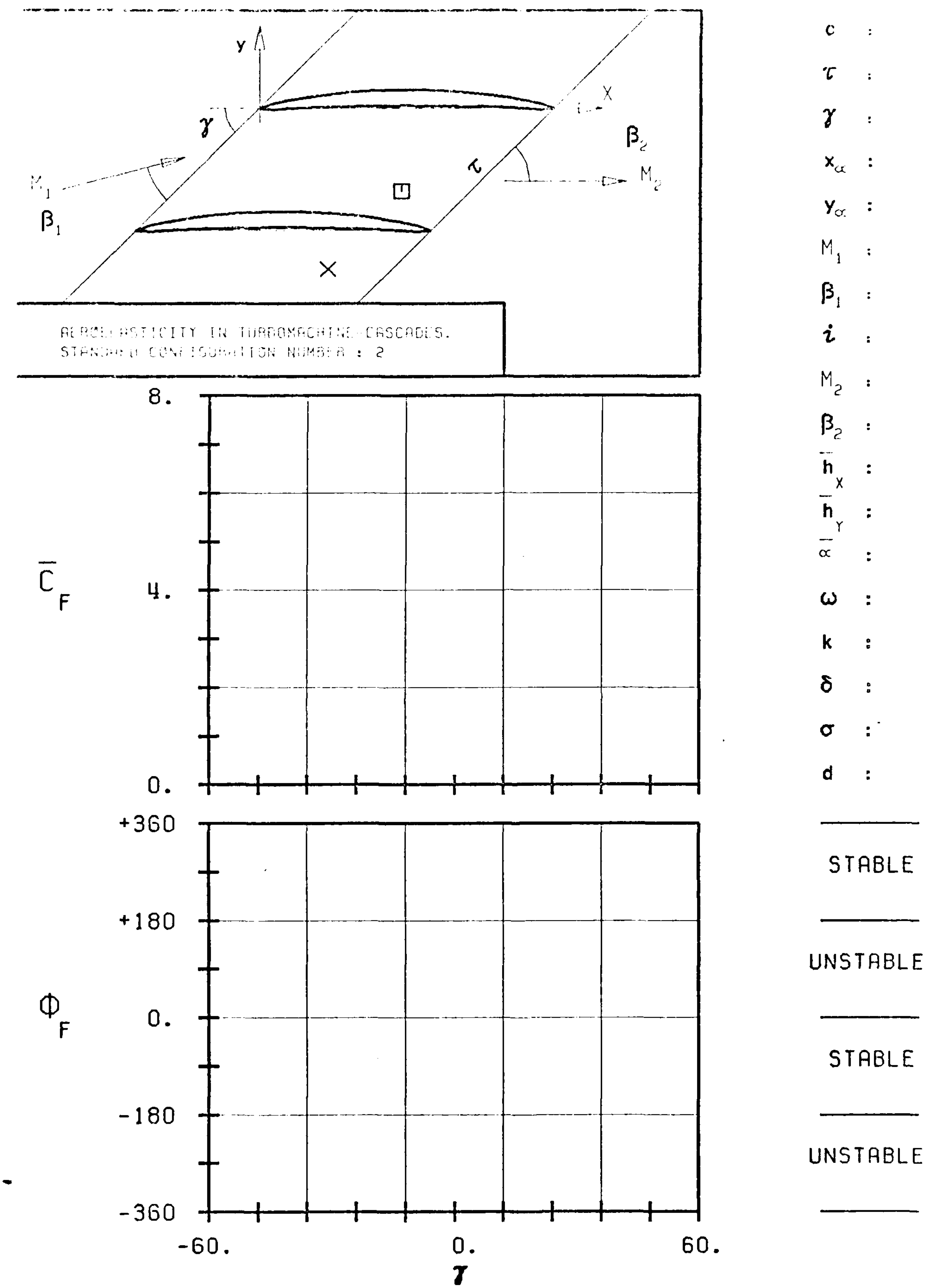

FIG. 3.2-2H: SECOND STANDARD CONFIGURATION:
AERODYNAMIC FORCE COEFFICIENT AND PHASE LEAD
IN DEPENDANCE OF STAGGER ANGLE.

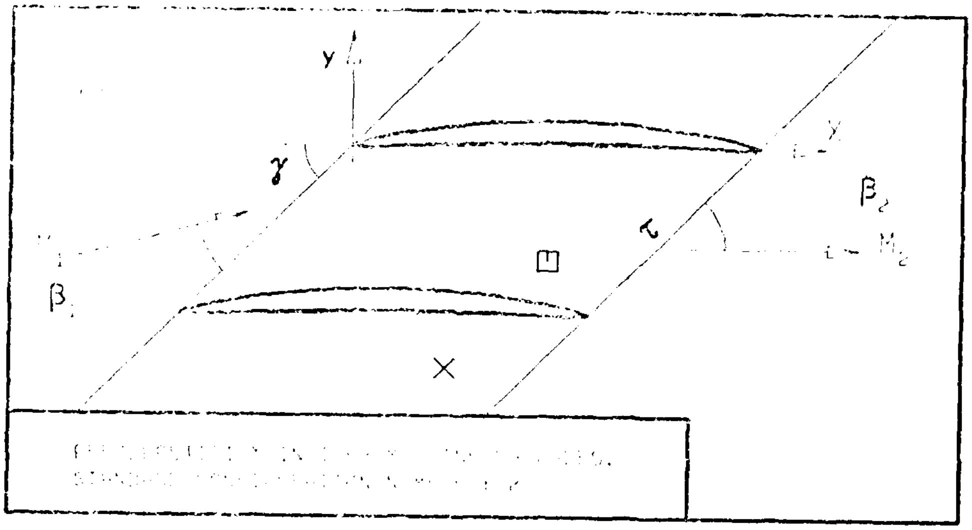

c :
τ :
γ :
x_0 :
y_0 :
M_1 :
β_1 :
i :
M_2 :
β_2 :
$\bar{h}_X$:
$\bar{h}_Y$:
$\bar{\alpha}$:
ω :
k :
δ :
σ :
d :

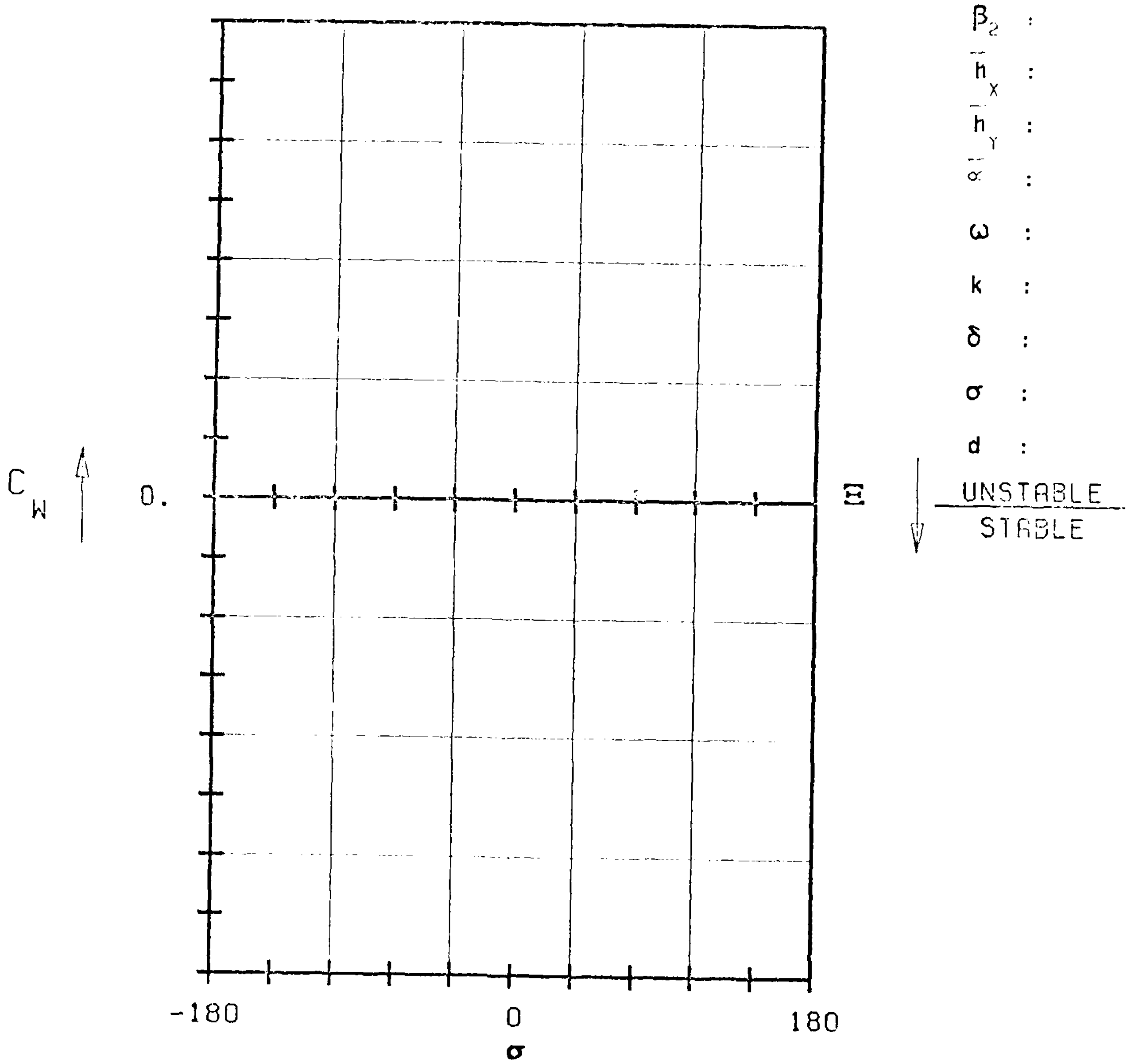

FIG. 3.2-21: SECOND STANDARD CONFIGURATION:
AERODYNAMIC WORK AND DAMPING COEFFICIENTS
IN DEPENDANCE OF INTERBLADE PHASE ANGLE.

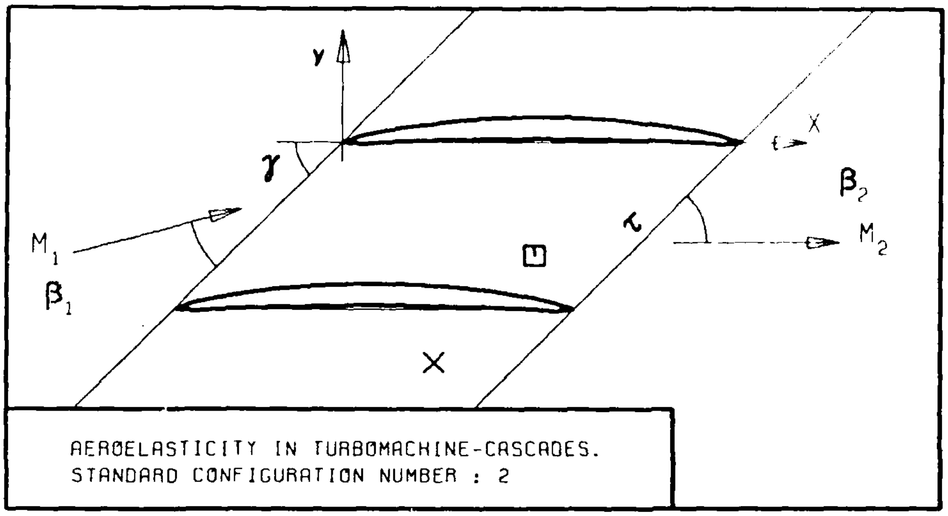

c :
τ :
γ :
x_α :
y_α :
M_1 :
β_1 :
i :
M_2 :
β_2 :
$\bar{h}_X$:
$\bar{h}_Y$:
$\bar{\alpha}$:
ω :
k :
δ :
σ :
d :

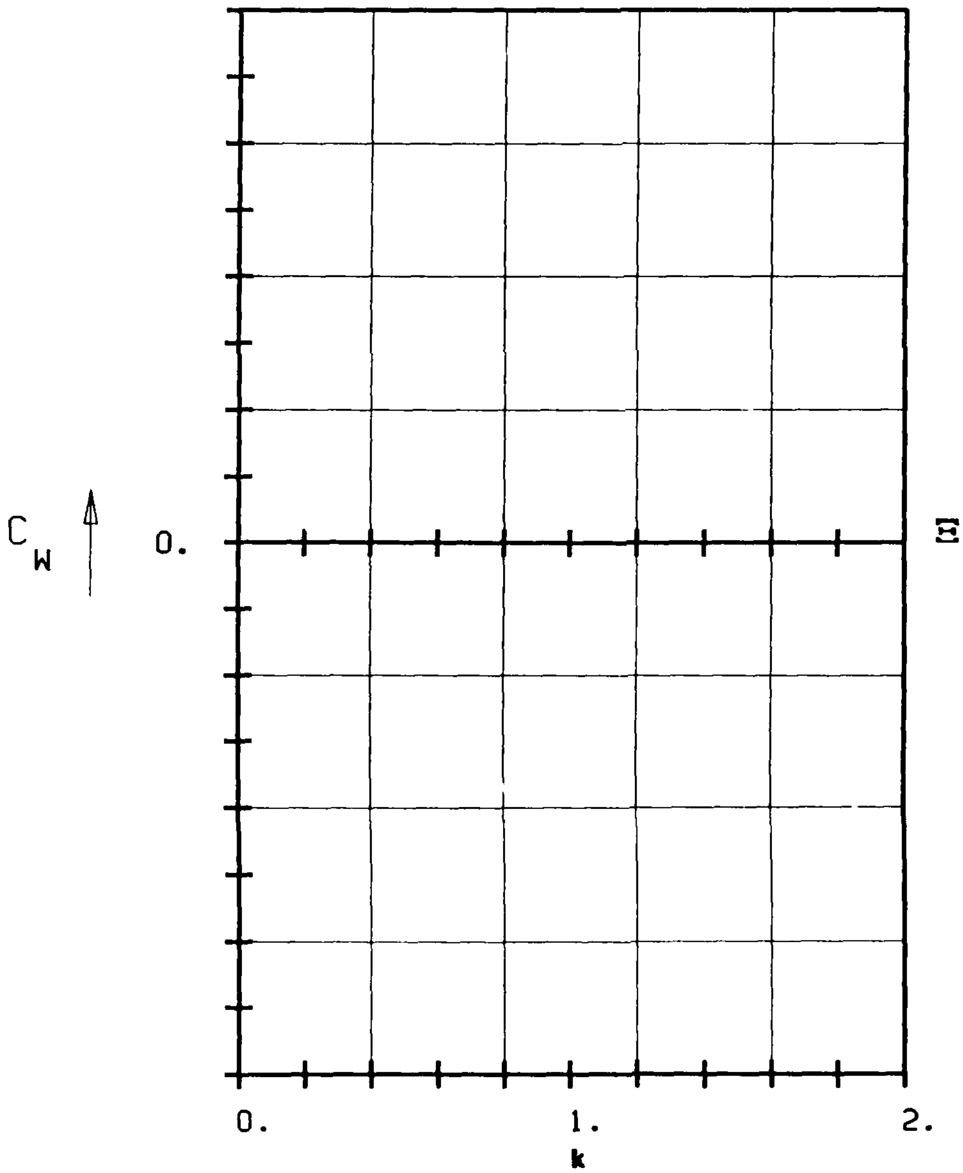

UNSTABLE
STABLE

FIG. 3.2-2K: SECOND STANDARD CONFIGURATION
AERODYNAMIC WORK AND DAMPING COEFFICIENTS
IN DEPENDANCE OF REDUCED FREQUENCY.

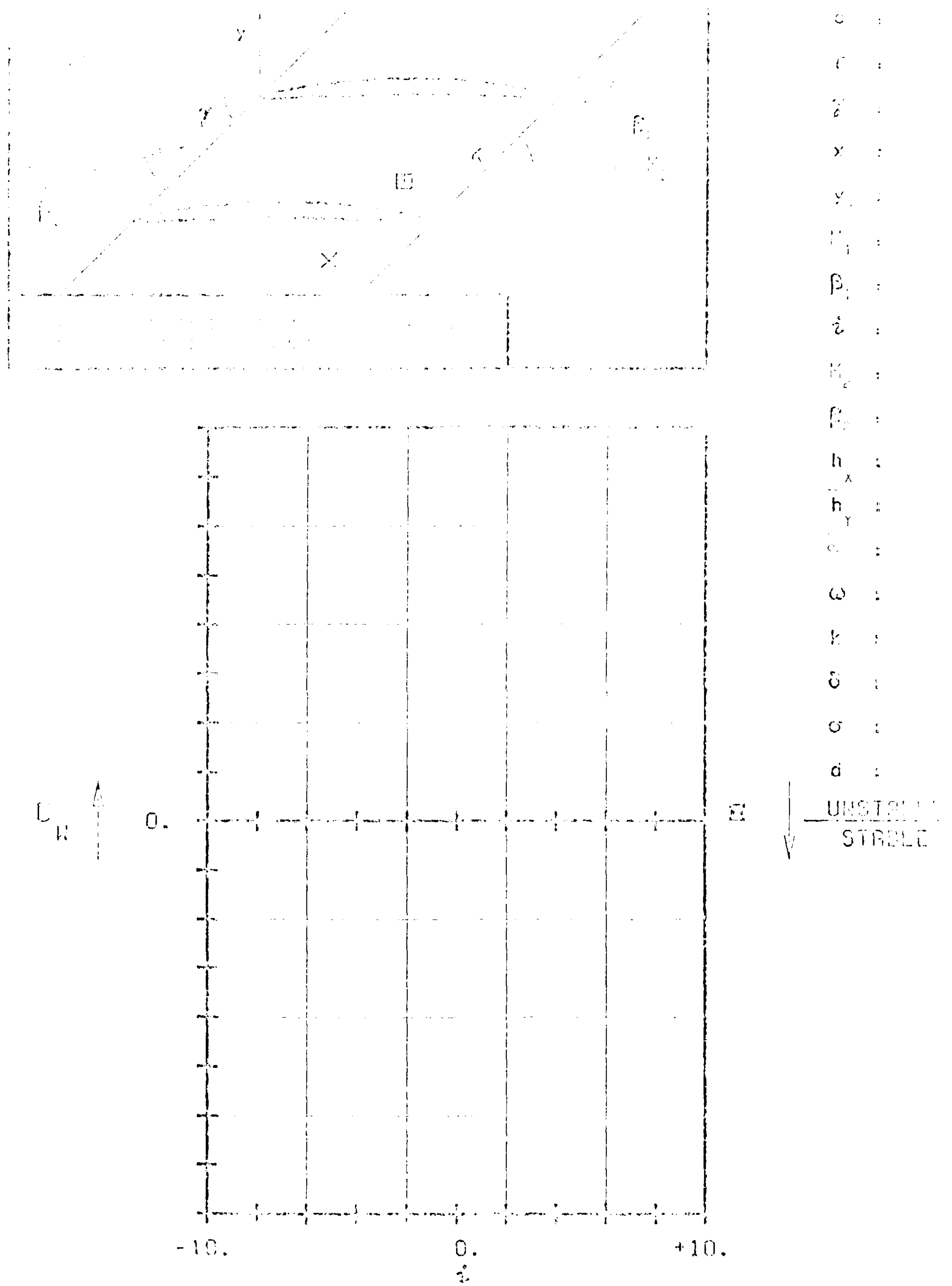

FIG. 3.2-[illegible]L: SECOND STANDARD CONFIGURATION:
AERODYNAMIC WORK AND DAMPING COEFFICIENTS
IN DEPENDENCE OF INCIDENCE ANGLE.

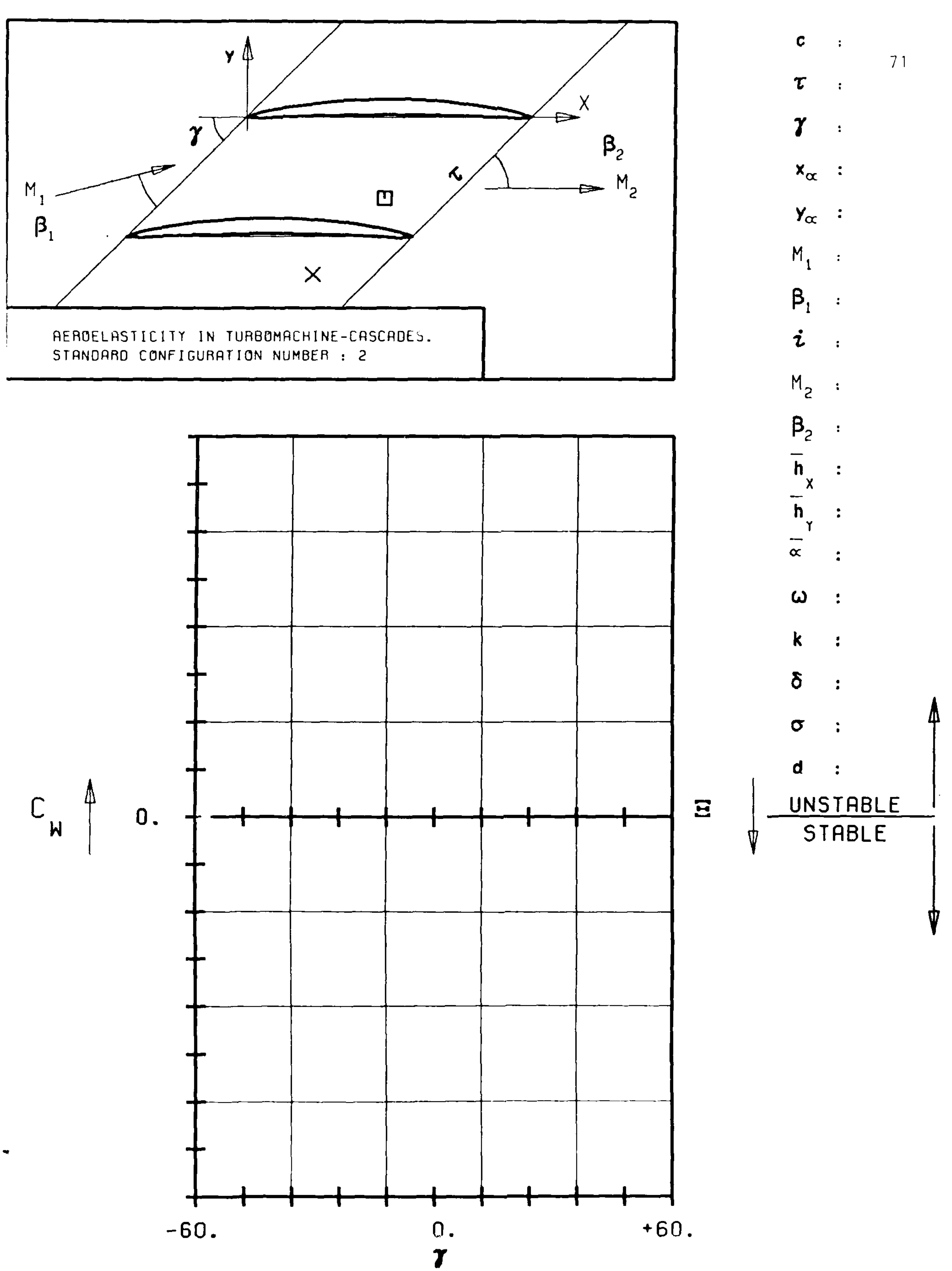

FIG. 3.2-2M: SECOND STANDARD CONFIGURATION: AERODYNAMIC WORK AND DAMPING COEFFICIENTS IN DEPENDANCE OF STAGGER ANGLE.

5.5 [illegible] Configuration

[illegible] configuration [illegible] [illegible] [illegible] [illegible] [illegible] [illegible] [illegible]

[illegible] [illegible] [illegible] [illegible] [illegible] [illegible] of the blade [illegible] [illegible] [illegible] [illegible] [illegible] [illegible] [illegible]

[illegible] [illegible] [illegible] [illegible] [illegible] [illegible] pressure [illegible] [illegible] [illegible] blade [illegible] [illegible] [illegible] with a span [illegible] [illegible] [illegible] [illegible] [illegible] [illegible] [illegible] [illegible] points were presented [illegible] and the [illegible] chord [illegible]

[illegible] [illegible] [illegible] [illegible] [illegible] [illegible] [illegible] [illegible] [illegible] [illegible] [illegible] [illegible] [illegible] [illegible] [illegible] [illegible]

The [illegible] are oscillated in pitching mode around the [illegible] [illegible]

The [illegible] geometry is given in Figure 5.5-1 and the [illegible] [illegible] in Table 5.5-1.

The [illegible] fluid is [illegible] gas with the specific heat ratio 1.137 [illegible]

[illegible] have been performed with variable expansion ratio P_2/P_1, M_2, [illegible] frequency and interblade phase angle.

The [illegible] instrumentation [illegible] pressure transducers [illegible] a blade midspan and strain gages. The [illegible] moment coefficient [illegible] [illegible] with [illegible] [illegible] data.

From [illegible] results obtained during these tests 10 aeroelastic cases are recommended for [illegible] calculations. These cases are contained in Table 5.5-2 together with the proposal for representation of the results. The 10 aeroelastic cases correspond to 5 different time averaged [illegible] [illegible] Table 5.5-2, for each of which the steady blade pressure [illegible] [illegible] in Figures 5.5-2 and Table 5.5-3.

[illegible] [illegible] [illegible] [illegible] performed with constant [illegible] [illegible] [illegible] velocity.

[illegible] [illegible] [illegible] [illegible] [illegible] of the results of the [illegible] standard

configuration allows detailed comparison of the local time dependant blade surface pressures and trends of global effects (moment and aerodynamic damping coefficients) in dependance of expansion ratio (P_2/P_{t_1}), blade vibration frequency and interblade phase angle (see Table 3.3-4 and Figure 3.3-3).

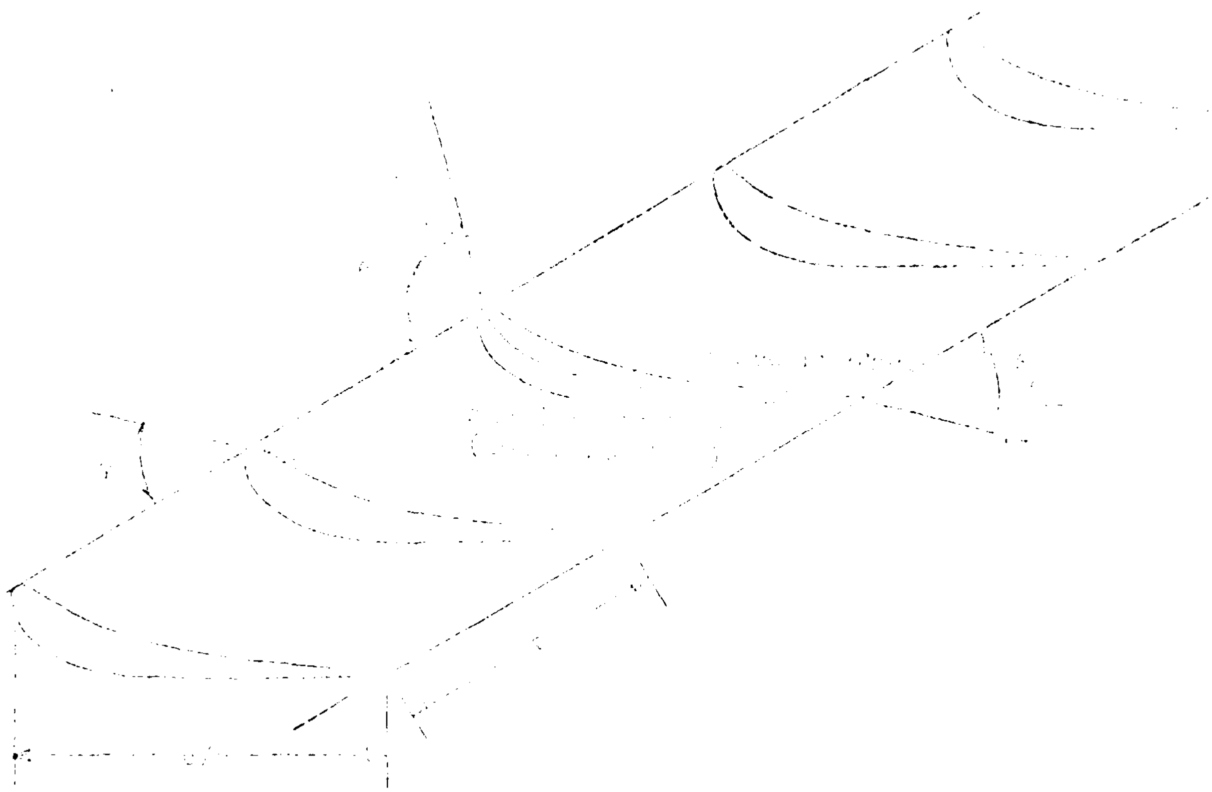

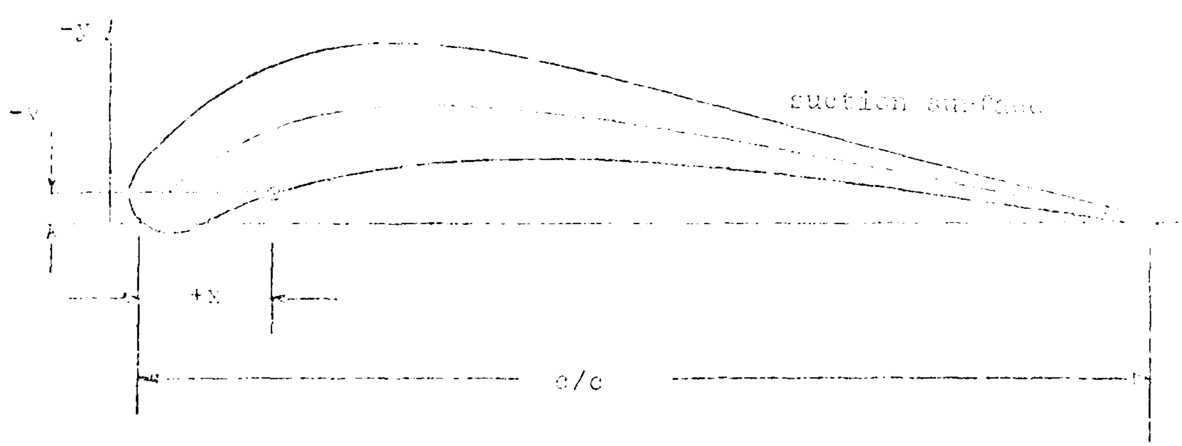

c	= 0.072 m		γ	= 44.33°
[illegible]	= 0.0[illegible] m		(x_α, y_α)	= (0.195, -0.1097)
camber	= 60.[illegible]°		τ	= 0.7[illegible] (hub)
[illegible]	= 0.[illegible]			0.8[illegible] (midspan)
				0.873 (tip)

[illegible]

[illegible]

C = 0.072 m			
SUCTION SURFACE (Lower surface)		PRESSURE SURFACE (Upper surface)	
X	Y_s	X	Y_p
0.0	0.0	0.0	0.0
-0.073	-0.0096	0.0247	+0.0108
-0.0115	-0.0290	0.0439	+0.0066
-0.0051	-0.0487	0.0718	-0.0073
0.0102	-0.0698	0.0932	-0.0144
0.0296	-0.0918	0.1213	-0.0265
0.0462	-0.1080	0.1478	-0.0356
0.0668	-0.1240	0.1742	-0.0434
0.0887	-0.1384	0.2014	-0.0502
0.1117	-0.1508	0.2289	-0.0538
0.1358	-0.1610	0.2563	-0.0601
0.1606	-0.1693	0.2840	-0.0637
0.1864	-0.1749	0.3119	-0.0660
0.2122	-0.1781	0.3395	-0.0674
0.2354	-0.1797	0.3676	-0.0676
0.2584	-0.1800	0.3891	-0.0669
0.2814	-0.1793	0.4113	-0.0662
0.3046	-0.1772	0.4329	-0.0657
0.3274	-0.1745	0.4547	-0.0646
0.3432	-0.1719	0.4765	-0.0639
0.3591	-0.1692	0.4982	-0.0623
0.3748	-0.1657	0.5201	-0.0613
0.3904	-0.1621	0.5419	-0.0596
0.4058	-0.1580	0.5633	-0.0579
0.4806	-0.1396	0.5850	-0.0562
0.5552	-0.1208	0.6069	-0.0540
0.6291	-0.1018	0.6285	-0.0519
0.7038	-0.0829	0.6502	-0.0497
0.7780	-0.0640	0.6721	-0.0470
0.8525	-0.0452	0.6939	-0.0446
0.9270	-0.0264	0.7152	-0.0419
1.0	-0.0075	0.7368	-0.0388
		0.7583	-0.0359
		0.7986	-0.0295
		0.8387	-0.0237
		0.8792	-0.0176
		0.9195	-0.0118
		0.9597	-0.0060
		1.0	0.0

Table 5.3-1 Third Standard Configuration.Dimensionless Airfoil Coordinates identical over the whole Span

[illegible]	M_1 (–)	β (°)	p_{t2}/p_{t1} (–)	p_2/p_{t1} (–)	M_2 (–)	[illegible]
[illegible]	[illegible]	91.7	[illegible]	[illegible]	[illegible]	[illegible]
[illegible]	[illegible]	90.5	[illegible]	[illegible]	[illegible]	[illegible]

[illegible] given [illegible] at mid_span

1) [illegible] x

2) [illegible]

3) [illegible] M_1

4) [illegible]

5) [illegible]

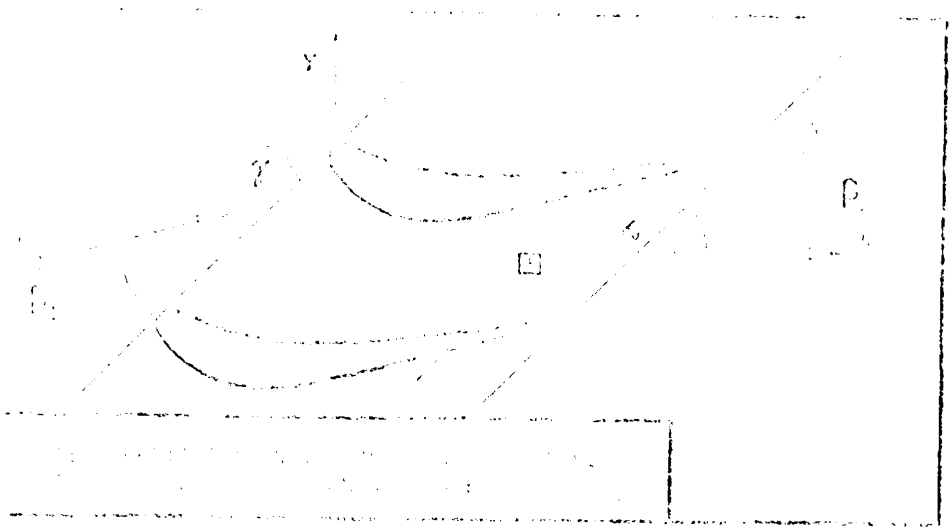

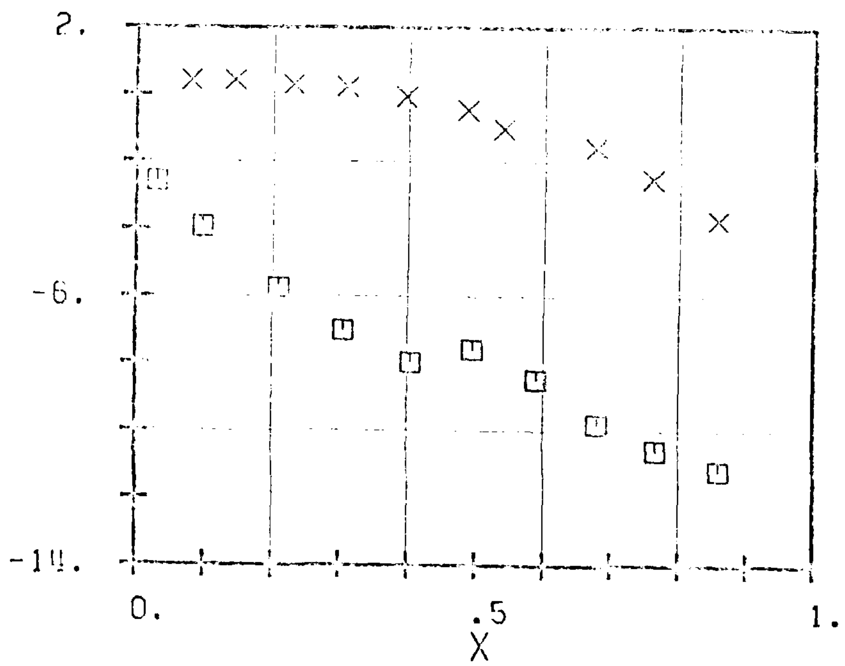

α :
τ :
γ :
x_o :
y_o :
M_1 :
β_1 :
i :
M_2 :
β_2 :
$\bar{h}_x$:
$\bar{h}_Y$:
$\bar{\alpha}$:
ω :
k :
δ :
σ :
d :

FIG. 3.3-24: THIRD STANDARD CONFIGURATION.
TIME AVERAGED BLADE SURFACE PRESSURE
DISTRIBUTION FOR OUTLET FLOW MACH NUMBER = 1.20 .

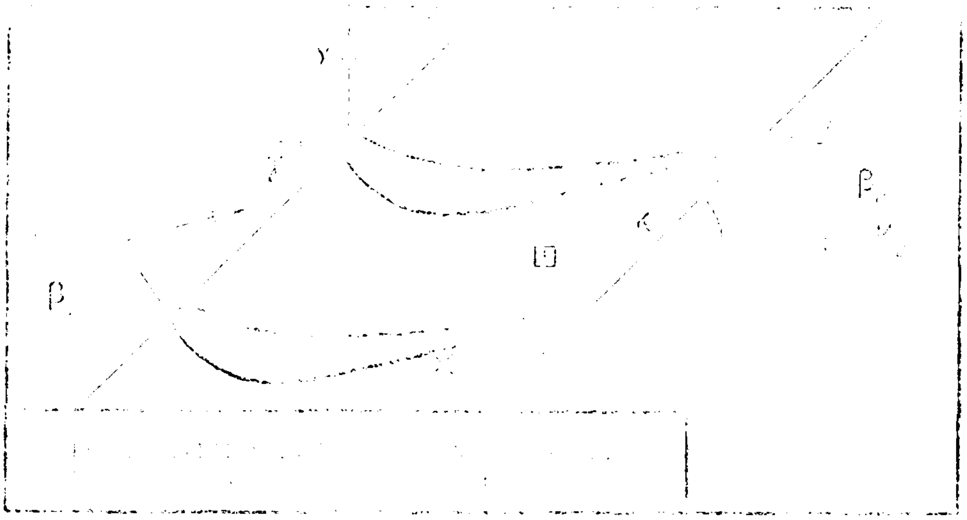

α :
γ :
x :
y :
:
β :
i :
:
β :
h_y :
h_x :
:
ω :
k :
δ :
σ :
d :

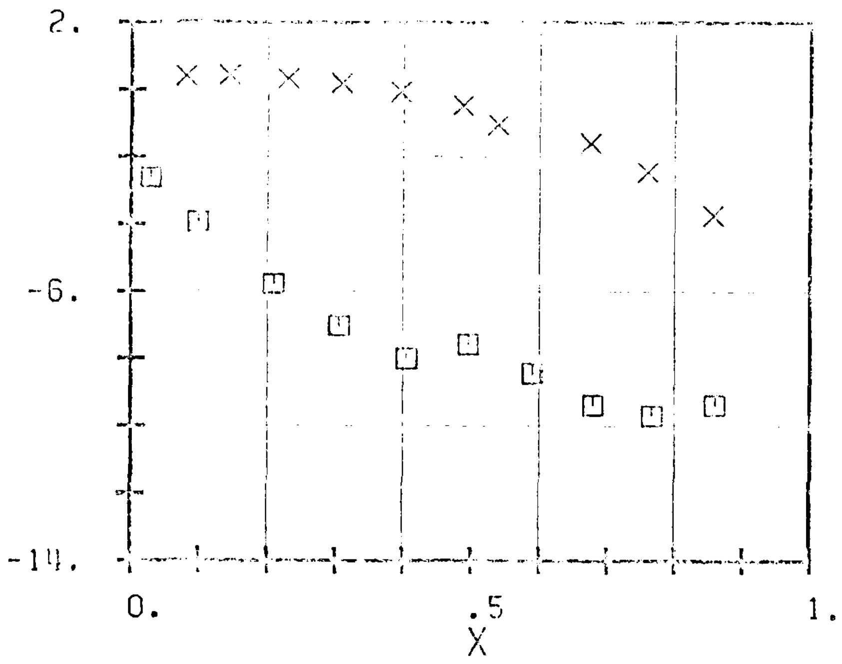

FIG. 3.3-26: THIRD STANDARD CONFIGURATION.
TIME AVERAGED BLADE SURFACE PRESSURE
DISTRIBUTION FOR OUTLET REGION MACH NUMBER = 1.0

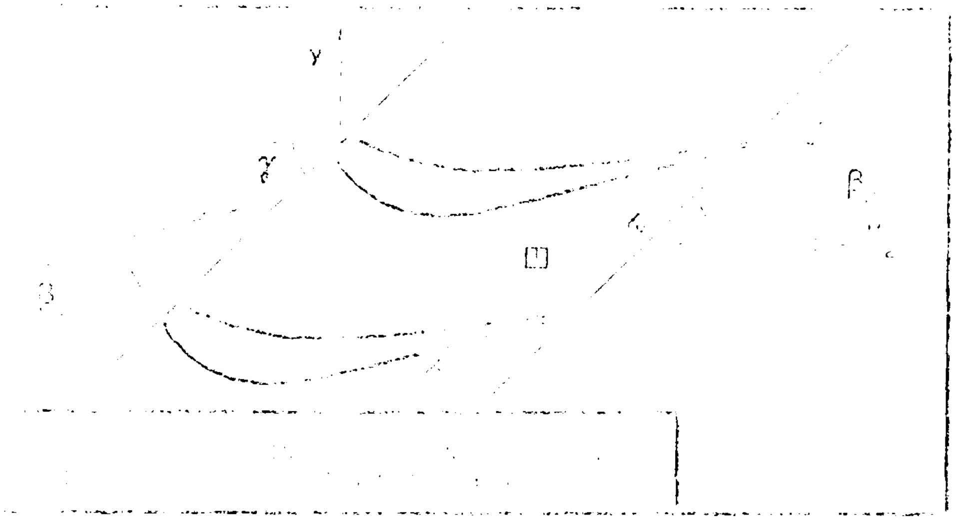

c	:
τ	:
γ	:
[illegible]	:
y	:
M_1	:
β_1	:
i	:
M_2	:
β_2	:
$\bar{h}_x$	:
$\bar{h}_y$	:
[illegible]	:
ω	:
k	:
δ	:
σ	:
d	:

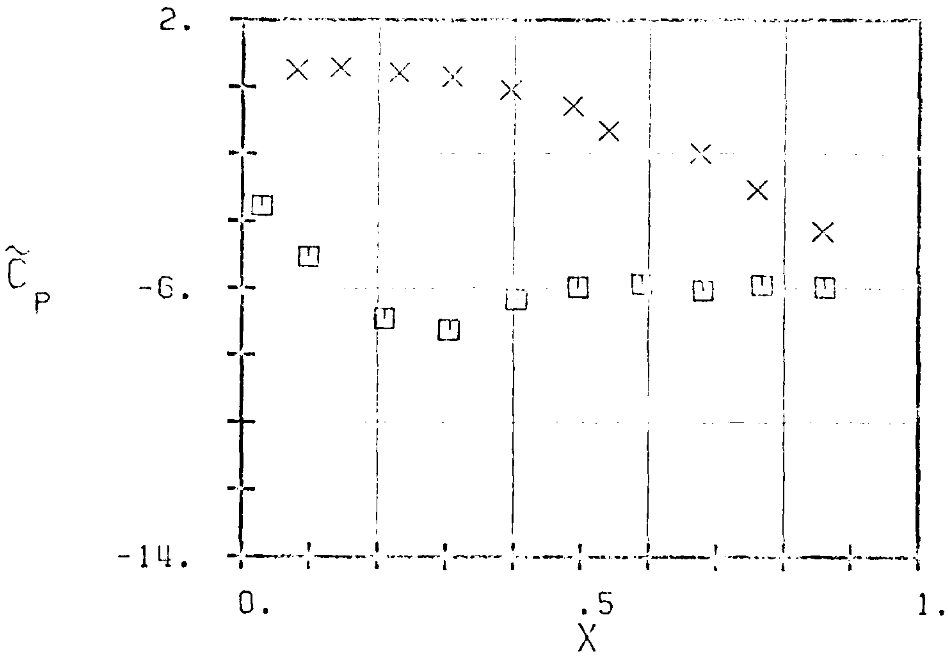

FIG. 3.3-20: TH[illegible] [illegible] CONFIGURATION.
TIME AVERAGED [illegible] SURFACE PRESSURE
DIS[illegible] FOR OUTLET [illegible] MACH NUMBER = 0.[illegible] .

[illegible]	[illegible]		[illegible]		[illegible]	
[illegible]	[illegible]		[illegible]		[illegible]	
[illegible]	[illegible]		[illegible]		[illegible]	
[illegible]	[illegible]		[illegible]		[illegible]	
[illegible]	[illegible]		[illegible]		[illegible]	
[illegible] (-)	[illegible]°		55°		[illegible]°	
X	[illegible]	$\bar{C}_p$	[illegible]	$\bar{C}_p$	[illegible]	$\bar{C}_p$
(-)	(-)	(-)	(-)	(-)	(-)	(-)
[illegible]						
[illegible]	[illegible]	[illegible]	[illegible]	[illegible]	[illegible]	[illegible]
[illegible]	[illegible]	[illegible]	0.758	[illegible]	[illegible]	[illegible]
[illegible]	[illegible]	[illegible]	0.662	-5.771	[illegible]	[illegible]
[illegible]	[illegible]	-7.212	0.576	-7.019	0.611	[illegible]
[illegible]	[illegible]	[illegible]	[illegible]	[illegible]	0.541	-7.965
[illegible]	0.701	-5.970	[illegible]	-7.566	[illegible]	[illegible]
[illegible]	[illegible]	[illegible]	[illegible]	[illegible]	0.503	[illegible]
[illegible]	[illegible]	-6.651	[illegible]	-9.578	[illegible]	[illegible]
[illegible]	[illegible]	[illegible]	[illegible]	[illegible]	0.346	[illegible]
[illegible]	[illegible]	-5.970	[illegible]	[illegible]	0.302	-11.19
[illegible]						
[illegible]	[illegible]	[illegible]	[illegible]	[illegible]	1.161	[illegible]
[illegible]	[illegible]	[illegible]	[illegible]	[illegible]	1.165	[illegible]
[illegible]	[illegible]	[illegible]	[illegible]	[illegible]	1.156	0.298
[illegible]	[illegible]	[illegible]	[illegible]	[illegible]	1.147	[illegible]
[illegible]	[illegible]	[illegible]	[illegible]	[illegible]	[illegible]	[illegible]
[illegible]	[illegible]	[illegible]	[illegible]	[illegible]	[illegible]	[illegible]
[illegible]	[illegible]	[illegible]	[illegible]	[illegible]	[illegible]	[illegible]
[illegible]	[illegible]	[illegible]	[illegible]	[illegible]	[illegible]	[illegible]
[illegible]	[illegible]	[illegible]	[illegible]	[illegible]	[illegible]	[illegible]
[illegible]	[illegible]	[illegible]	[illegible]	[illegible]	[illegible]	[illegible]
[illegible]	[illegible]		[illegible]		[illegible]	

Table [illegible] [illegible]

Aeroelasticity in Turbomachine-Cascades.
Third Standard Configuration.

Aeroelastic test case N^{o}: ______

M_1 = ______ • p_2/p_{t1} = ______ • M_2 = ______ • β_1 = ______ ^{o} • β_2 = ______ ^{o} • k = ______ •

$\bar{\alpha}^{(-2)}$ = ______ • $\bar{\alpha}^{(-1)}$ = ______ • $\bar{\alpha}^{(0)}$ = ______ • $\bar{\alpha}^{(+1)}$ = ______ • $\bar{\alpha}^{(+2)}$ = ______ • (rads)

$\sigma^{(-2)}$ = ______ • $\sigma^{(-1)}$ = ______ • $\sigma^{(0)}$ = ______ • $\sigma^{(+1)}$ = ______ • $\sigma^{(+2)}$ = ______ • $(^{o})$

a) Global Aeroelastic Coefficients

$\bar{C}_M$ = ______ • $\bar{C}_L$ = ______ • C_W = ______ • Ξ = ______ • (-)

Φ_M = ______ • Φ_L = ______ • $(^{o})$

b) Local Time Dependant Blade Surface Pressure Coefficients

X (-)	$C_p^{(ls)}$ (-)	$\Phi_p^{(ls)}$ $(^{o})$	$C_p^{(us)}$ (-)	$\Phi_p^{(us)}$ $(^{o})$	$\Delta\bar{C}_p$ (-)	$\Phi_{\Delta p}$ $(^{o})$

Table 5.3-4. Third Standard Configuration. Table for Presentation of the 10 Recommended Aeroelastic Test Cases

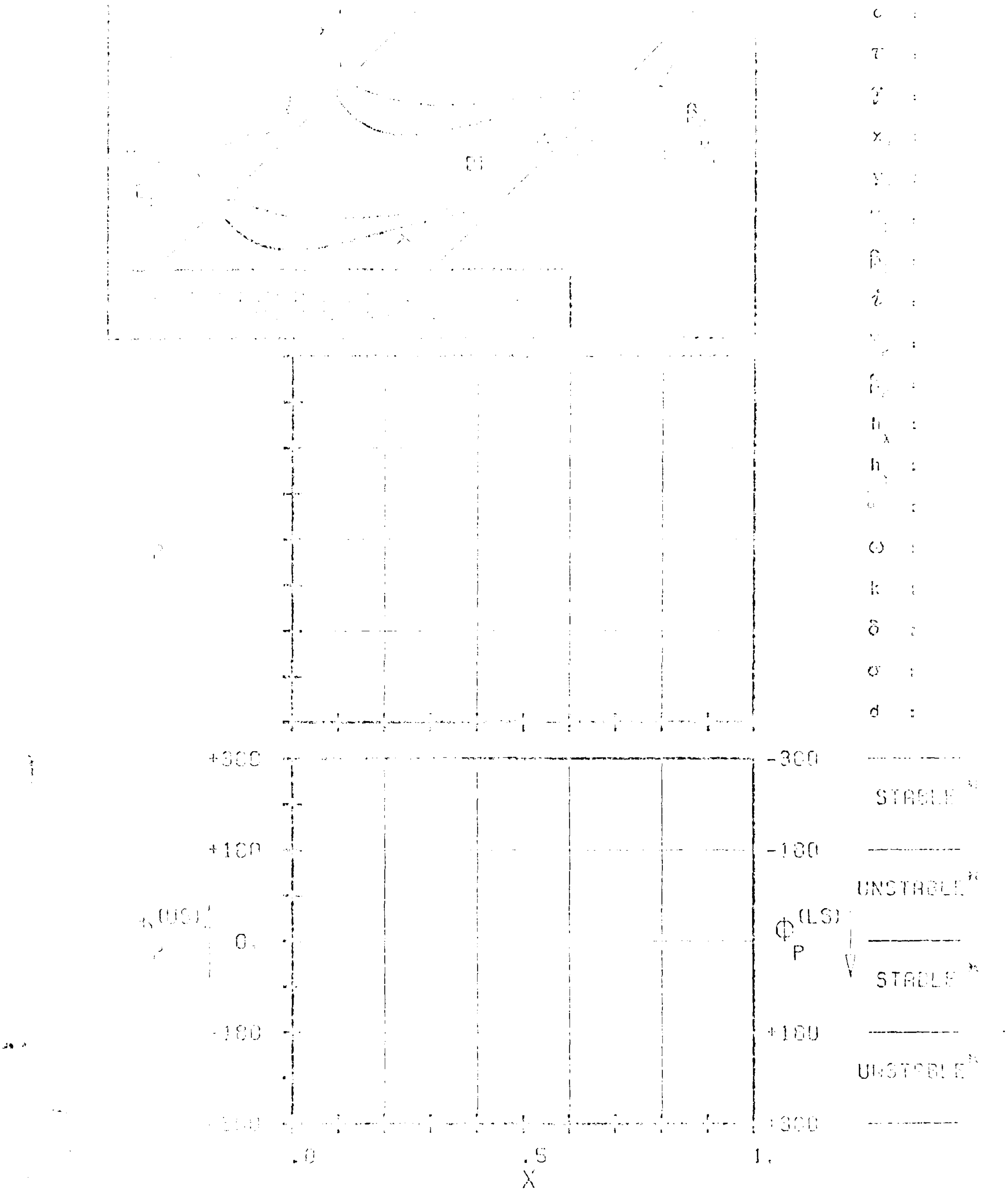

+300
+100
0.
-100
-300
-100
+100
+300
.0
.5
1.
X
STABLE
UNSTABLE
STABLE
UNSTABLE

[illegible]

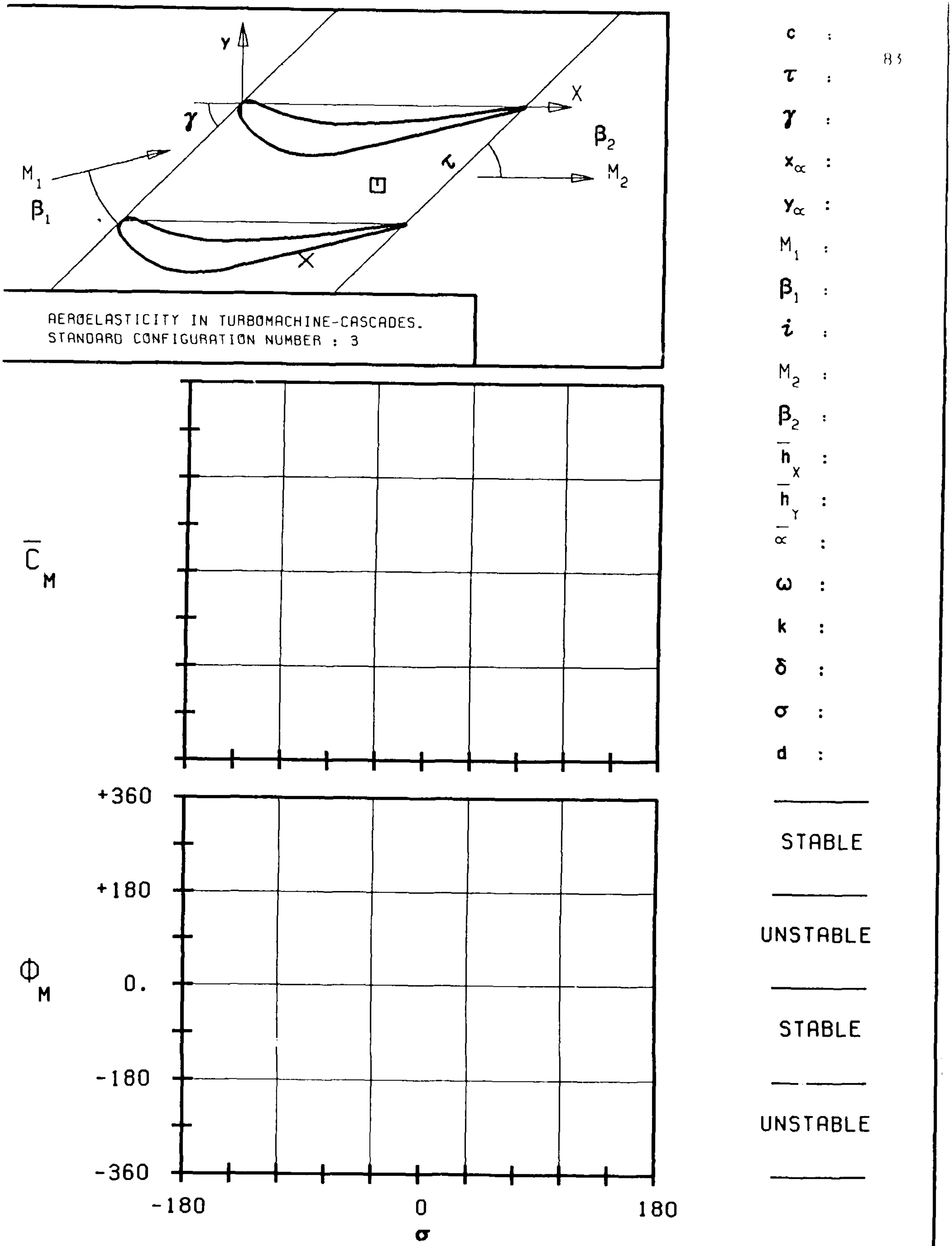

FIG. 3.3-3B: THIRD STANDARD CONFIGURATION.
AERODYNAMIC MOMENT COEFFICIENT AND PHASE LEAD
IN DEPENDANCE OF INTERBLADE PHASE ANGLE.

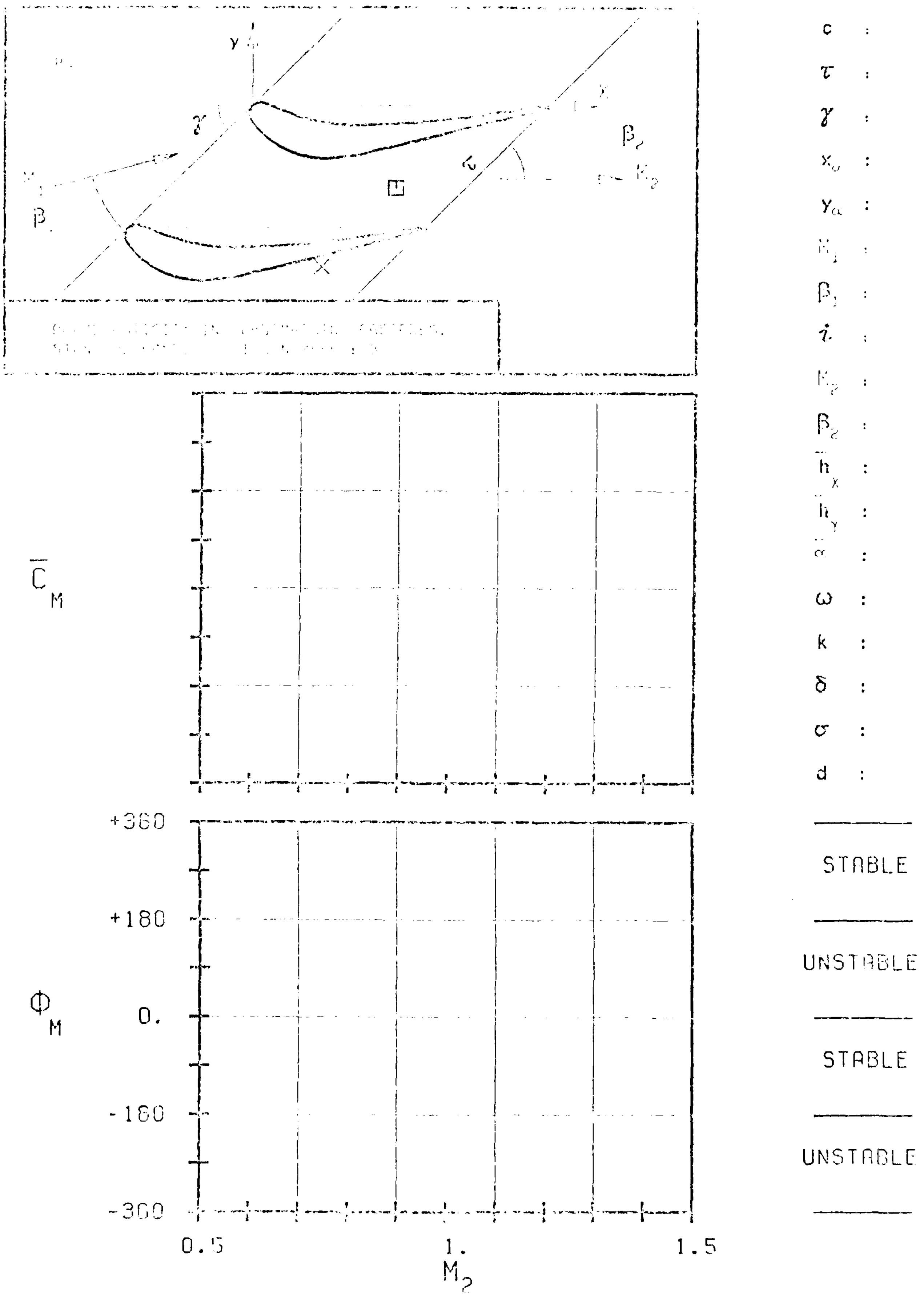

FIG. 3.3-3C: THIRD STANDARD CONFIGURATION.
AERODYNAMIC MOMENT COEFFICIENT AND PHASE LEAD
IN DEPENDANCE OF OUTLET FREON MACH NUMBER.

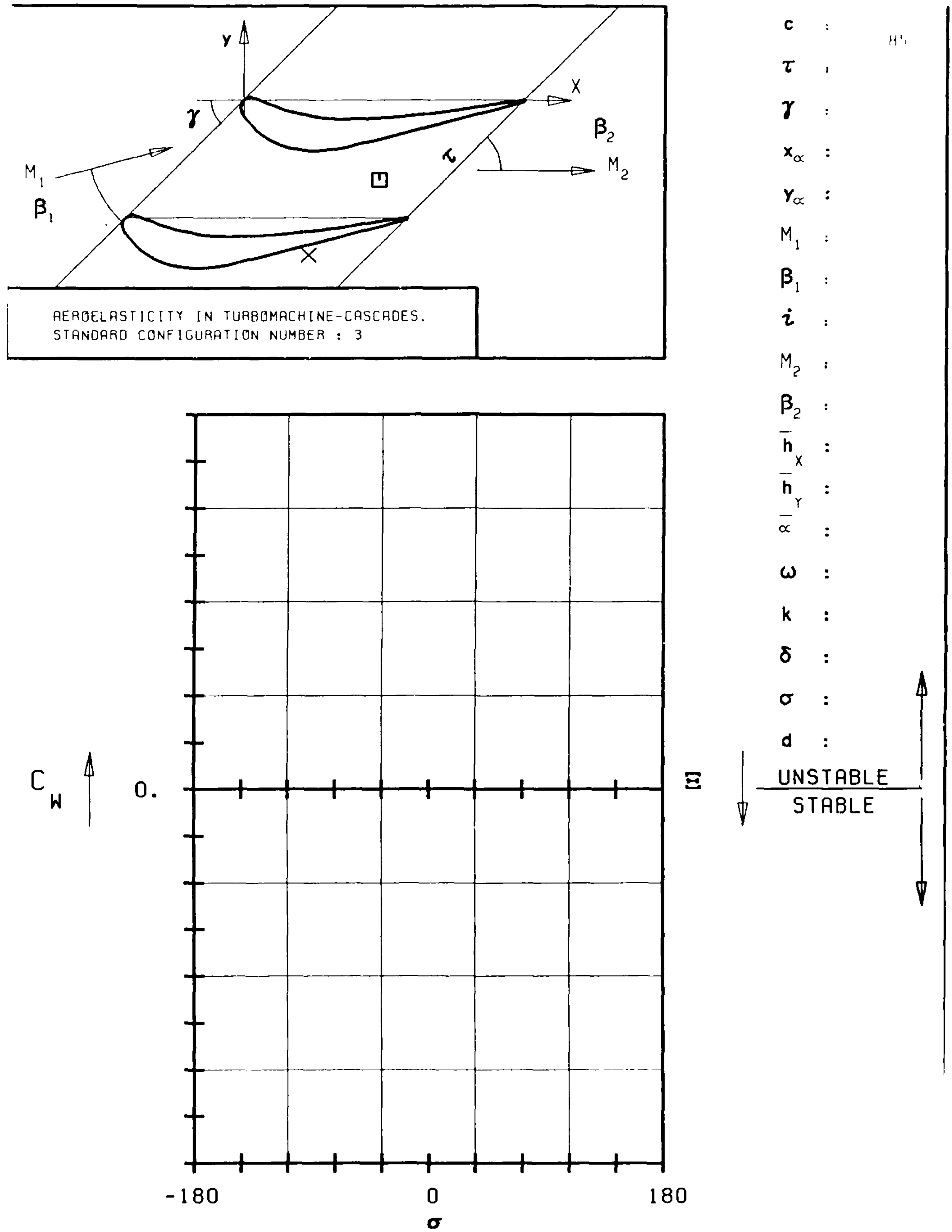

FIG. 3.3-3D: THIRD STANDARD CONFIGURATION.
AERODYNAMIC WORK AND DAMPING COEFFICIENTS IN
DEPENDANCE OF INTERBLADE PHASE ANGLE.

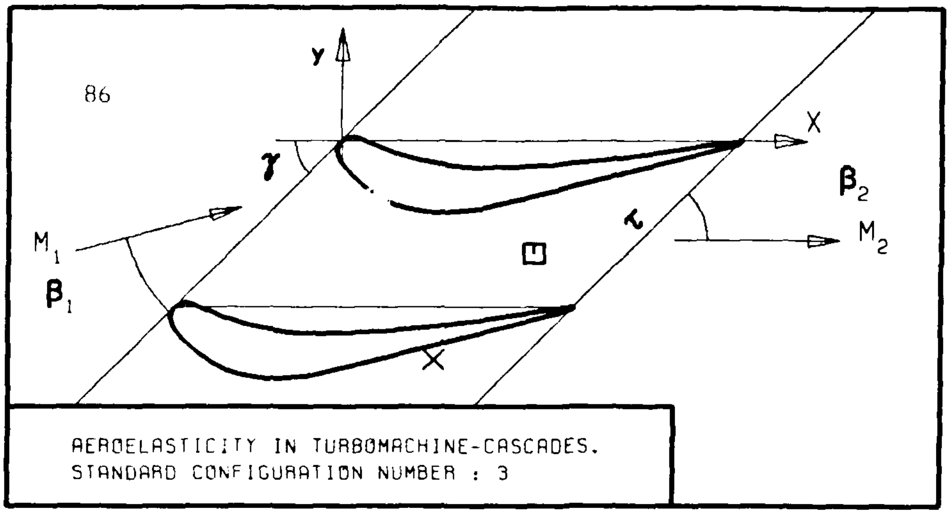

c :
τ :
γ :
x_α :
y_α :
M_1 :
β_1 :
i :
M_2 :
β_2 :
$\bar{h}_X$:
$\bar{h}_Y$:
$\bar{\alpha}$:
ω :
k :
δ :
σ :
d :

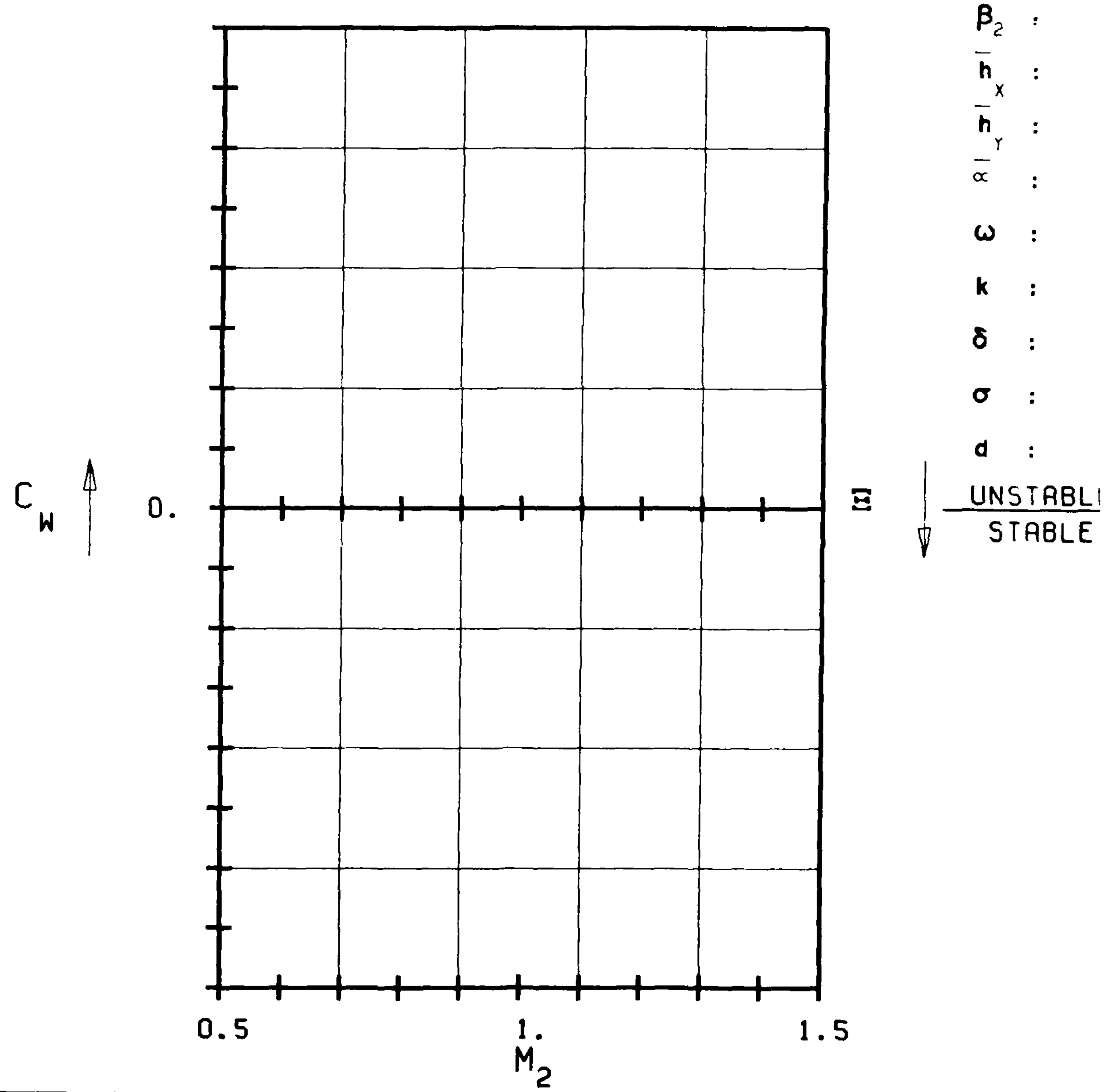

FIG. 3.3-3E: THIRD STANDARD CONFIGURATION.
AERODYNAMIC WORK AND DAMPING COEFFICIENTS IN DEPENDANCE OF OUTLET FREON MACH NUMBER.

3.4 Fourth Standard Configuration

Presently, quasi three-dimensional cascade experiments on highly loaded turbine rotor sections are performed in the annular cascade facility at the Lausanne Institute of Technology by M. Degen.

This fourth standard configuration is of interest mainly because of the relative high blade thickness and camber, the high subsonic flow conditions and for its resemblance with the third standard configuration.

Detailed test results will be available at the end of 1983, so that theoretical results can be validated against the data from this configuration simultaneously as against other standard configurations.

The cascade configuration consists of twenty vibrating prismatic blades, each having a chord of c=0.0744 m and a span of 0.040 m, with 45° turning and a maximum thickness-to-chord ratio of 0.17 .

The stagger angle is 33.4°, with the gap-to-chord ratio of the cascade:

0.67 (hub)
0.76 (midspan)
0.84 (tip)

The hub-tip ratio in the test facility is 0.8.

The cascade geometry is given in Figure 3.4-1 and the profile coordinates are tabulated in Table 3.4-1.

Experiments are performed with variable inlet flow angle (M_1, i), expansion ratio (p_2/p_{t_1}, M_2), vibration mode, oscillation frequency and interblade phase angle. All the experiments presently performed have constant spanwise flow conditions upstream. The time dependent instrumentation includes pressure transducers on one blade (midspan) and strain gages.

The aeroelastic cases for this standard configuration are not yet fully defined, wherefore they will be distributed together with the corresponding time averaged blade surface pressure distributions towards the end of 1983.

The recommended presentation format will be similar to the one used in standard configuration six.

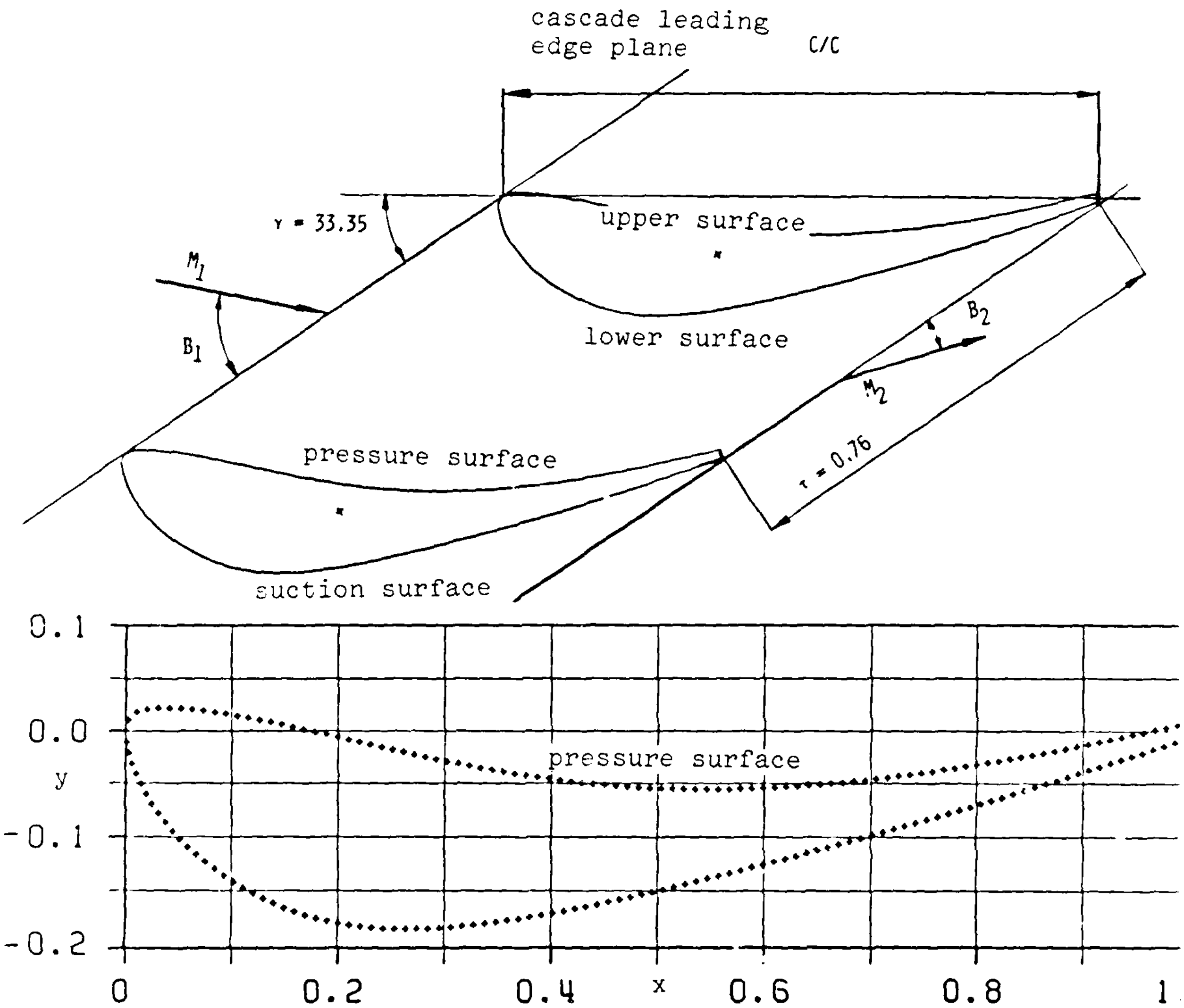

c = 0.0744 m
span = 0.040 m
τ = 0.67 (hub)
0.76 (midspan)
0.84 (tip)

γ = 33.35°
camber = 45°
$\frac{\text{thickness}}{\text{chord}}$ = 0.17
hub/tip = 0.8

Nominal values: M_1 = 0.31 M_2 = 0.90
β_1 = 45.9° β_2 = 17.6°

Figure 3.4-1 Fourth Standard Configuration: Cascade Geometry

C = .0744 M

UPPER SURFACE				LOWER SURFACE			
X	Y	X	Y	X	Y	X	Y
0.000	0.000	.514	-.055	0.000	0.000	.443	-.163
.003	.010	.524	-.055	.001	-.011	.453	-.160
.010	.018	.535	-.055	.003	-.021	.464	-.158
.020	.021	.546	-.055	.006	-.031	.474	-.156
.031	.022	.556	-.055	.010	-.041	.485	-.154
.042	.022	.567	-.055	.014	-.051	.495	-.151
.052	.021	.578	-.055	.020	-.060	.505	-.149
.063	.020	.588	-.055	.025	-.069	.516	-.146
.074	.019	.599	-.054	.031	-.078	.526	-.144
.084	.018	.610	-.054	.038	-.087	.536	-.141
.095	.016	.620	-.053	.044	-.095	.547	-.139
.105	.014	.631	-.052	.052	-.102	.557	-.136
.116	.012	.642	-.052	.059	-.110	.568	-.134
.126	.010	.652	-.051	.067	-.117	.578	-.131
.136	.008	.663	-.050	.076	-.124	.588	-.129
.147	.006	.673	-.049	.084	-.130	.598	-.126
.157	.004	.684	-.048	.093	-.136	.609	-.123
.168	.001	.695	-.047	.102	-.142	.619	-.121
.178	-.001	.705	-.046	.111	-.147	.629	-.118
.188	-.003	.716	-.044	.120	-.153	.640	-.115
.199	-.006	.726	-.043	.130	-.157	.650	-.113
.209	-.008	.737	-.042	.139	-.162	.660	-.110
.220	-.011	.747	-.040	.149	-.166	.671	-.107
.230	-.013	.758	-.039	.159	-.170	.681	-.104
.240	-.015	.768	-.037	.169	-.173	.691	-.101
.251	-.018	.779	-.036	.179	-.176	.701	-.099
.261	-.020	.790	-.034	.190	-.179	.712	-.096
.271	-.022	.800	-.032	.200	-.181	.722	-.093
.282	-.025	.811	-.030	.211	-.182	.732	-.090
.292	-.027	.821	-.029	.221	-.184	.742	-.087
.303	-.029	.832	-.027	.232	-.185	.753	-.084
.313	-.031	.842	-.025	.243	-.185	.763	-.081
.324	-.033	.852	-.023	.253	-.186	.773	-.078
.334	-.035	.863	-.021	.264	-.186	.783	-.075
.345	-.037	.873	-.019	.274	-.186	.794	-.072
.355	-.039	.884	-.017	.285	-.186	.804	-.069
.365	-.041	.894	-.015	.296	-.185	.814	-.066
.376	-.043	.905	-.013	.306	-.184	.824	-.063
.387	-.044	.915	-.010	.317	-.183	.834	-.060
.397	-.046	.926	-.008	.328	-.182	.844	-.057
.408	-.047	.936	-.006	.338	-.181	.855	-.054
.418	-.048	.946	-.004	.349	-.179	.865	-.050
.429	-.049	.957	-.001	.359	-.178	.875	-.047
.439	-.051	.967	.001	.370	-.176	.885	-.044
.450	-.051	.978	.003	.380	-.175	.895	-.041
.461	-.052	.988	.006	.391	-.173	.905	-.037
.471	-.053			.401	-.171	.926	-.031
.482	-.054			.412	-.169	.936	-.028
.493	-.054			.422	-.167	.946	-.024
.503	-.055			.433	-.165	.956	-.021
						.966	-.017
						.976	-.014
						.986	-.011
						.996	-.007

Table 3.4-1 For the Standard Configuration: Dimensionless Airfoil Coordinates (identical over the whole span)

3.5 Fifth Standard Configuration

This two-dimensional subsonic/transonic cascade configuration has been tested in a rectilinear cascade air tunnel at the Office National d'Etudes et de Recherches Aérospaciales (ONERA). The configuration and experimental results are included by courtesy of E. Szechenyi.

The cascade configuration consists of six fan stage tip sections, each blade having a chord of c=0.090 m and a span of 0.120 m. The maximum thickness-to-chord ratio is 0.027, with no camber and a gap-to-chord ratio of 0.95. The present configuration was measured with a stagger angle of 30.7°.

The cascade geometry is given in Figure 3.5-1 and the profile coordinates in Table 3.5-1.

The two center blades can vibrate in pitch about several axis, whereafter the aeroelastic coefficients for different interblade phase angles are computed by linearized summation of the unsteady pressure responses on all six blades.

Experiments have been performed with oscillation frequencies between 75 and 550 Hz, inlet Mach numbers between 0.5 and 1.0 and with incidence angles between attached and fully separated flow (2° to 15°).

Both the time averaged and time dependant instrumentation on this cascade is very extensive and a large number of well documented data have been obtained during the experiments. The large amount of flush mounted high response pressure transducers on one blade allows the determination of resultant time dependant blade forces.

From the results obtained during these tests, 27 aeroelastic cases are recommended for off-design calculations. They are contained in Table 3.5-2, together with a recommendation for representation of the results.

The 27 cases correspond to 11 different settings of the cascade (see Table 3.5-2).

The steady blade surface pressure distributions of the 11 time-averaged settings are given as a basis for time-variant calculations by small perturbation prediction models in Figure 3.5-2 and Table 3.5-3.

Of special interest in this fifth standard configuration is the extensive variation of time-averaged parameters, such as inlet flow velocity (M_1) and incidence (i).

The inlet Mach number is varied from M_1 0.5 to M_1=1.0, and the range

of incidence is from fully attached (incidence less than 5°) up to fully separated (incidence greater than 10°) flow conditions.

The recommended representation of the results includes detailed comparison of unsteady blade surface pressure coefficients as well as aerodynamic damping and moment coefficients in dependance of the parameters incidence (i), flow velocity (M_1) and reduced frequency (k), as proposed in Figure 3.5-3 and Table 3.5-4.

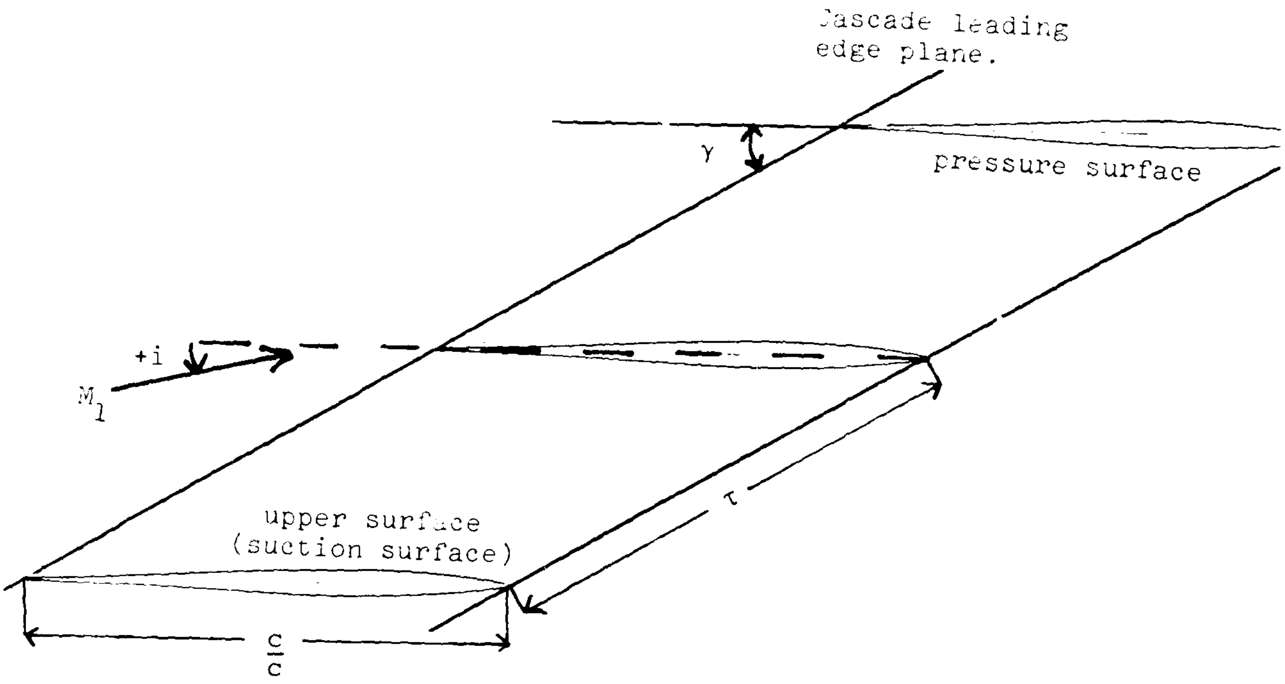

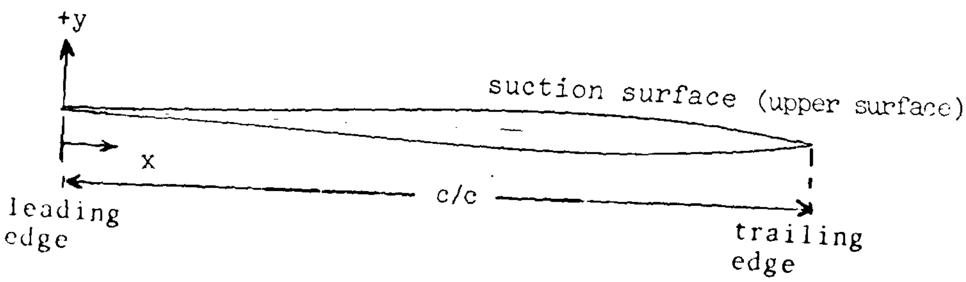

c = 0.090 m

span = 0.120 m

camber = 0°

τ = 0.95

γ = 30.7°

$\frac{\text{thickness}}{\text{chord}}$ = 0.027

Figure 3.5-1 Fifth Standard Configuration: Cascade Geometry

c 0.090 m		
	Upper surface (Suction surface)	Lower surface (Pressure surface)
x	y	y
0.	0.	0.
0.0124	0.0016	-0.0016
0.0250	0.0018	-0.0018
0.0500	0.0026	-0.0026
0.0750	0.0033	-0.0033
0.1000	0.0041	-0.0041
0.1500	0.0053	-0.0053
0.2000	0.0062	-0.0062
0.2500	0.0079	-0.0079
0.3000	0.0101	-0.0101
0.3500	0.0103	-0.0103
0.4000	0.0111	-0.0111
0.4500	0.0119	-0.0119
0.5000	0.0124	-0.0124
0.5500	0.0128	-0.0128
0.6000	0.0133	-0.0133
0.6500	0.0135	-0.0135
0.7000	0.0135	-0.0135
0.7500	0.0128	-0.0128
0.8000	0.0116	-0.0116
0.8500	0.0098	-0.0098
0.9000	0.0076	-0.0076
0.9500	0.0048	-0.0048
1.0000	0.	0.
$\frac{\text{LE radius}}{c}$ $\frac{\text{TE radius}}{c}$ 0.002		

Table 3.5-1 Fifth Standard Configuration: Dimensionless Airfoil Coordinates

Aeroelastic case	Time averaged Parameters					Time Dependant Parameters					Recommended Representation			
	M_1 (b) (-)	i (°)	$p_2^{(c)}/p_{t1}$	x_1 (-)	$y_{..}$ (-)	Amplitude (a) (rad)	Interblade phase angle (a) (°)	Frequency f (Hz)	Reduced Frequency k (-)	Flow	C_p	ΔC_p	C_M	Ξ
1	0.5	2	0.84	0.5	0.	.00524	180	200	0.33	Attached	1	1	2	2
2	↓	4	0.86	↓	↓	↓	↓	↓	↓	"	↓	↓	↓ ,4	↓ ,4
3		6	0.87							Part. sep			,4	,4
4		8	0.87							"				
5		10	0.88							Fully sep			3,4	3,4
6		12	0.89							"				
7		4	0.86					75	0.12	Attached	1	1	4	4
8		↓	↓					125	0.21	↓	↓	↓	↓	↓
9								300	0.50					
10								550	0.91					
11		6	0.87					75	0.12	Part. sep	-	-	4	4
12		↓	↓					125	0.21	↓	-	-	↓ ,5	↓ ,5
13								300	0.50		-	-		
14								550	0.91		-	-		
15		12	0.88					75	0.12	Fully sep	-	-	4	4
16		↓	↓					125	0.21	↓	-	-	↓ ,5	↓ ,5
17								300	0.50		-	-		
18								550	0.91		-	-		
19	0.6	↓	0.84					200	0.28		-	-	3	3
20	0.7		0.80					↓	0.24		-	-	↓	↓
21	0.8		0.77						0.21		-	-		
22	0.9	10	0.72						0.18		-	-	3	3
23	1.0	10	0.69						0.17		-	-	3	3
24	0.5	6	0.87	0.				125	0.21	Part. sep	1	1	5	5
25	0.5	6	0.87	0.92				↓	↓	"	1	1	5	5
26	0.5	10	0.88	0.						Fully sep	-	-	5	5
27	0.5	10	0.88	0.92						"	-	-	5	5

NOTES:

(a) Only center blade oscillates

(b) Measured at 2 chord distances upstream of leading edge

(c) " " 0.5 " " downstream of trailing edge

1) C_p and ΔC_p as a function of x

2) C_M and Ξ as a function of i

3) C_M and Ξ as a function of M_1

4) C_M and Ξ as a function of k

5) C_M and Ξ as a function of x_1

Table 3.5-2 Fifth Standard Configuration: 27 Recommended Aeroelastic Cases

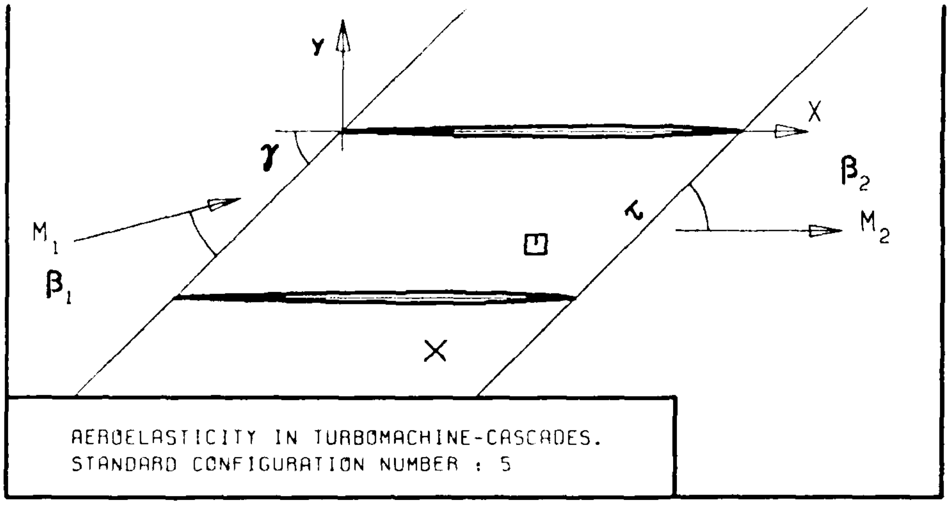

c :
τ :
γ :
x_α :
y_α :
M_1 :
β_1 :
i :
M_2 :
β_2 :
$\bar{h}_X$:
$\bar{h}_Y$:
$\bar{\alpha}$:
ω :
k :
δ :
σ :
d :

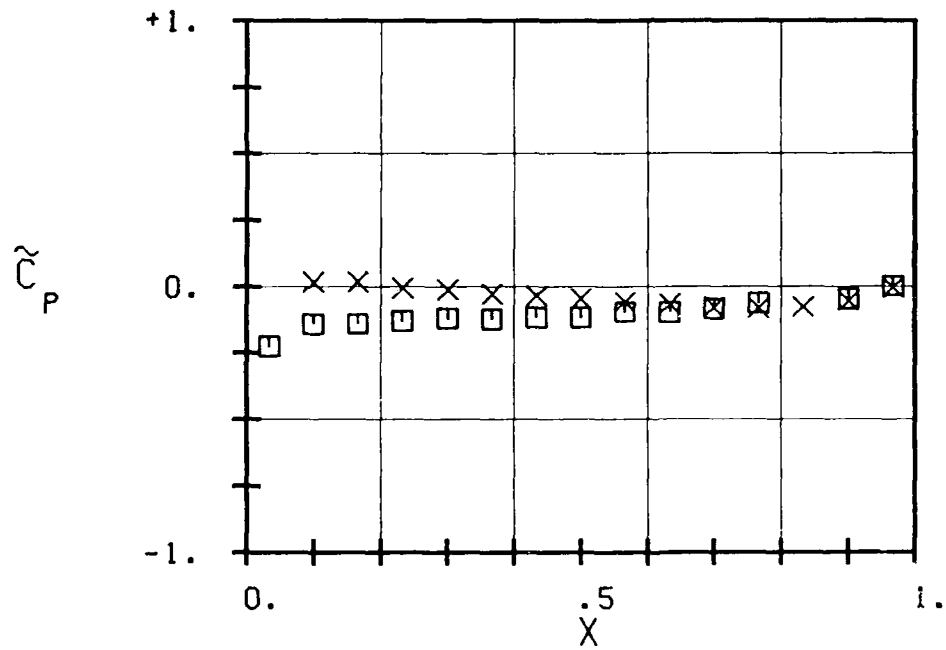

FIG. 3.5-2A: FIFTH STANDARD CONFIGURATION:
TIME AVERAGED BLADE SURFACE
DISTRIBUTION FOR M1=0.5

AD-A141 904 TWO-DIMENSIONAL AND QUASI THREE-DIMENSIONAL EXPERIMENTAL STANDARD CONFIGU..(U) ECOLE POLYTECHNIQUE FEDERALE DE LAUSANNE (SWITZERLAND) LAB DE.. 2/3

UNCLASSIFIED T FRANSSON ET AL. 30 SEP 83 F/G 20/4 NL

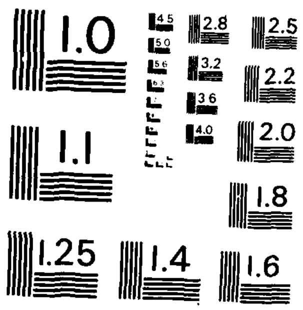

MICROCOPY RESOLUTION TEST CHART
NATIONAL BUREAU OF STANDARDS-1963-A

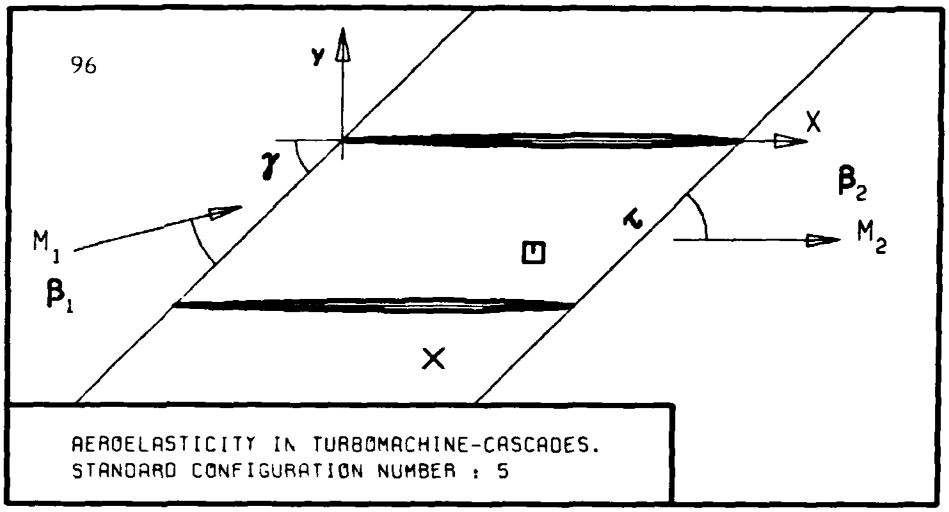

c :
τ :
γ :
x_α :
y_α :
M_1 :
β_1 :
i :
M_2 :
β_2 :
$\bar{h}_X$:
$\bar{h}_Y$:
$\bar{\alpha}$:
ω :
k :
δ :
σ :
d :

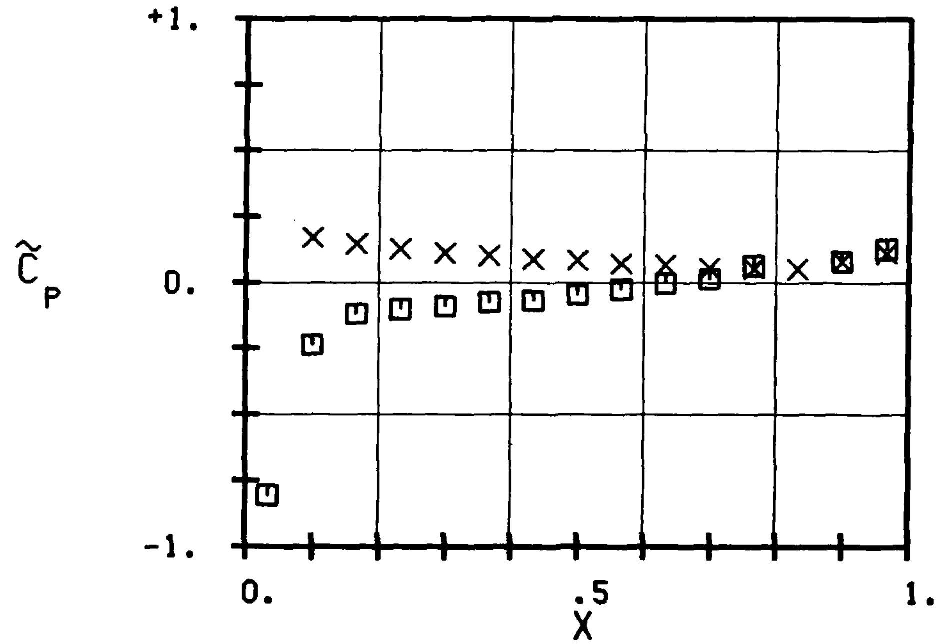

FIG. 3.5-2B: FIFTH STANDARD CONFIGURATION:
TIME AVERAGED BLADE SURFACE PRESSURE
DISTRIBUTION FOR M1=0.5 AND INCIDENCE=4 DEG.

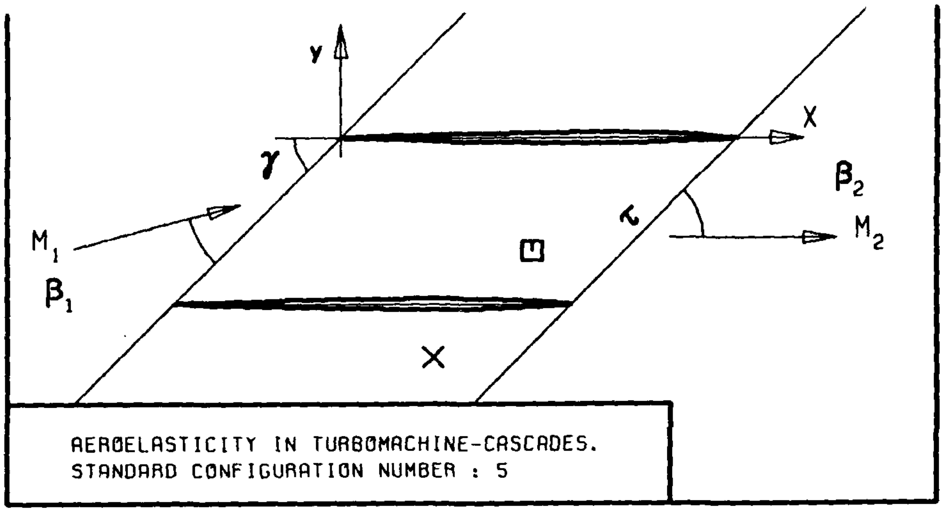

c :
τ :
γ :
x_α :
y_α :
M_1 :
β_1 :
i :
M_2 :
β_2 :
$\bar{h}_X$:
$\bar{h}_Y$:
$\bar{\alpha}$:
ω :
k :
δ :
σ :
d :

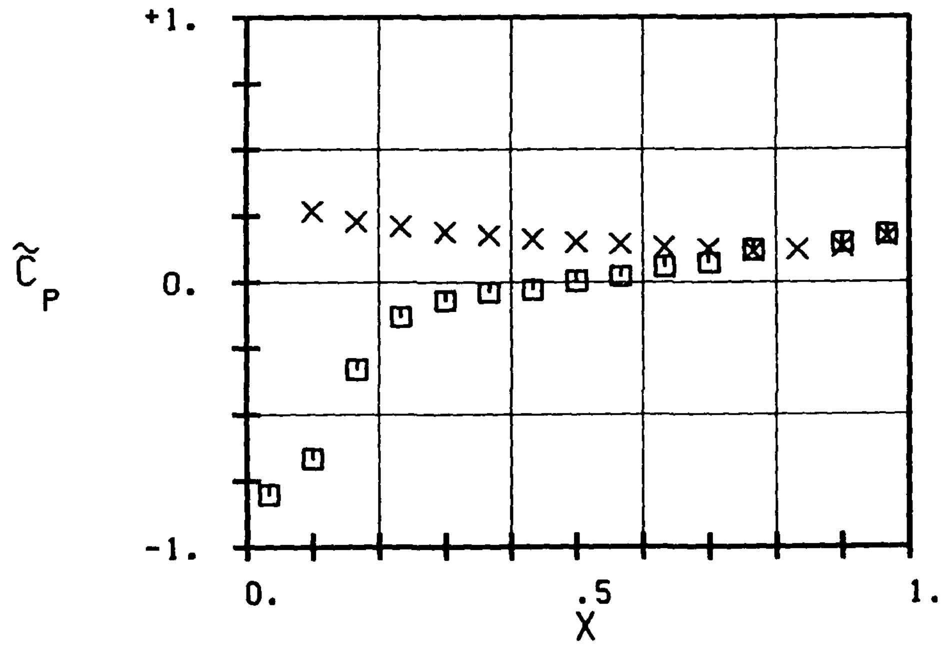

FIG. 3.5-2C: FIFTH STANDARD CONFIGURATION:
TIME AVERAGED BLADE SURFACE PRESSURE
DISTRIBUTION FOR M1=0.5 AND INCIDENCE=6 DEG.

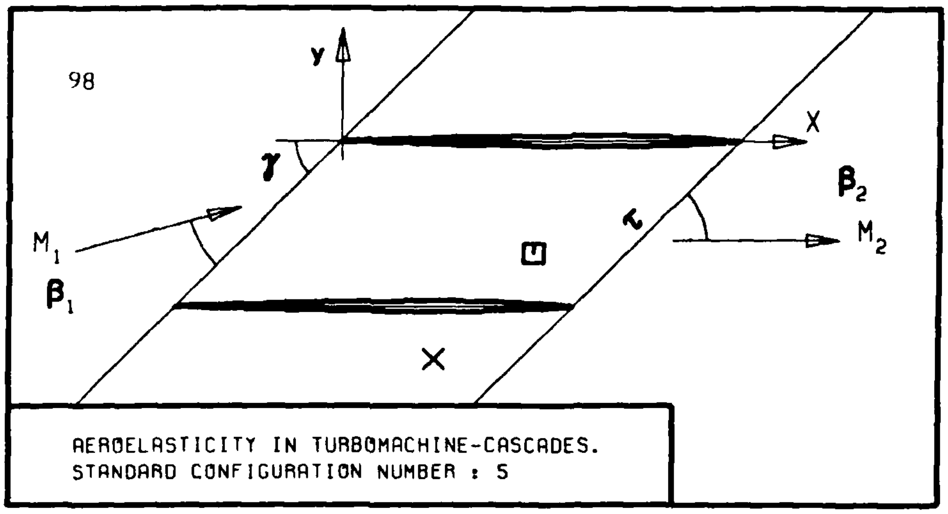

c :
τ :
γ :
x_α :
y_α :
M_1 :
β_1 :
i :
M_2 :
β_2 :
$\bar{h}_X$:
$\bar{h}_Y$:
$\bar{\alpha}$:
ω :
k :
δ :
σ :
d :

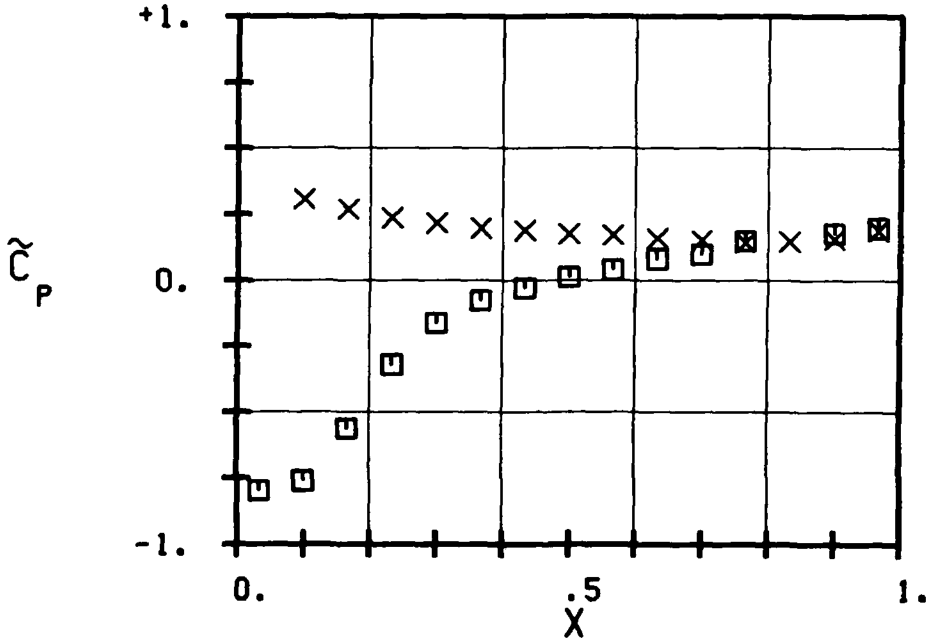

FIG. 3.5-2D: FIFTH STANDARD CONFIGURATION:
TIME AVERAGED BLADE SURFACE PRESSURE
DISTRIBUTION FOR M1=0.5 AND INCIDENCE=8 DEG.

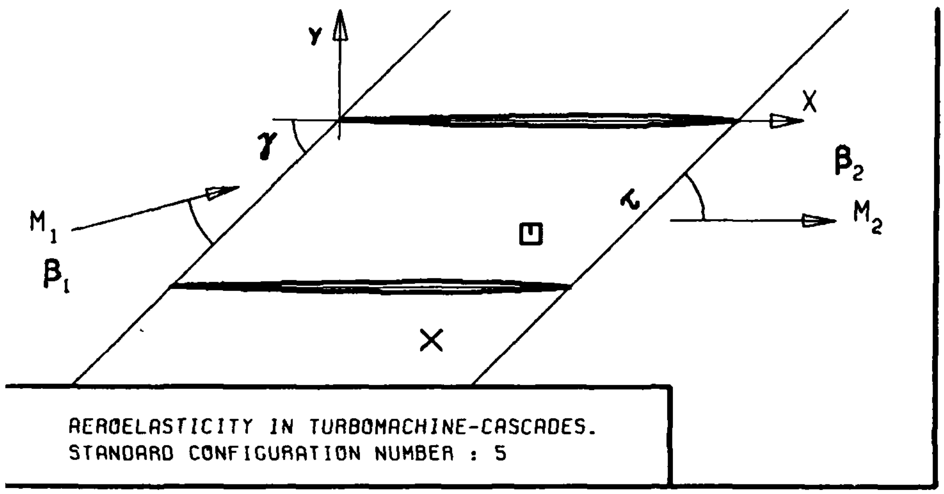

c :
τ :
γ :
x_α :
y_α :
M_1 :
β_1 :
i :
M_2 :
β_2 :
$\bar{h}_X$:
$\bar{h}_Y$:
$\bar{\alpha}$:
ω :
k :
δ :
σ :
d :

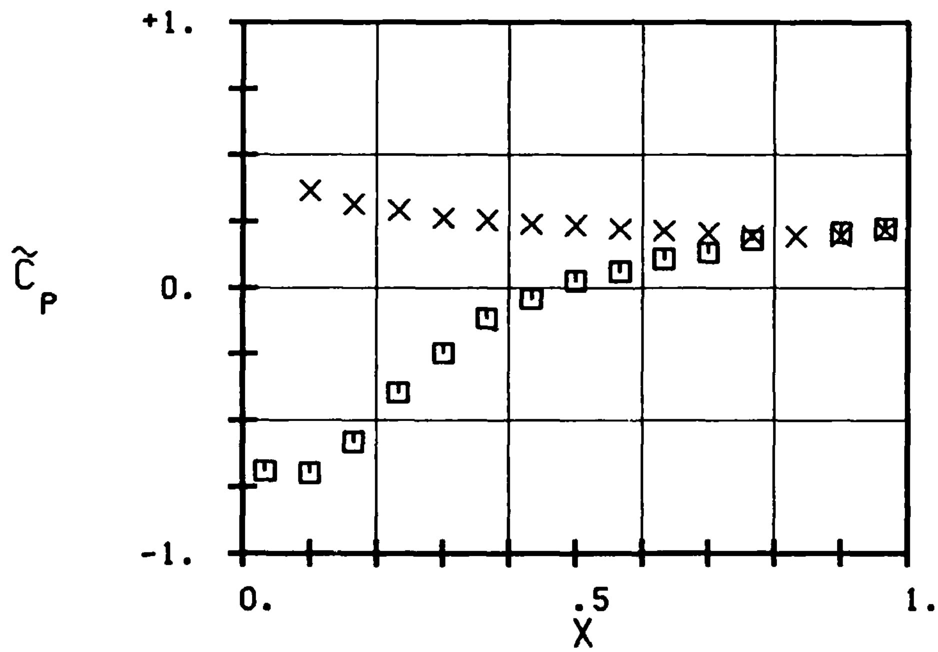

FIG. 3.5-2E: FIFTH STANDARD CONFIGURATION:
TIME AVERAGED BLADE SURFACE PRESSURE
DISTRIBUTION FOR M1=0.5 AND INCIDENCE=10 DEG.

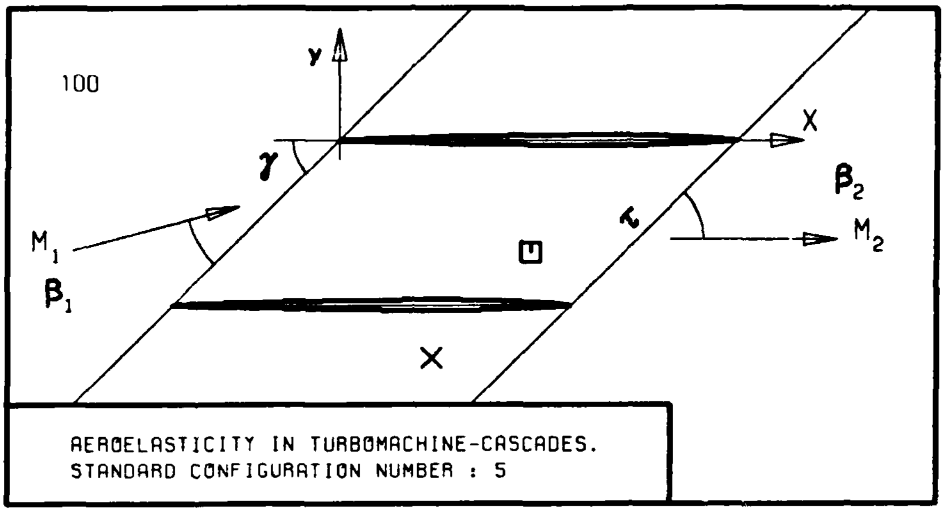

c :
τ :
γ :
x_α :
y_α :
M_1 :
β_1 :
i :
M_2 :
β_2 :
$\bar{h}_x$:
$\bar{h}_y$:
$\bar{\alpha}$:
ω :
k :
δ :
σ :
d :

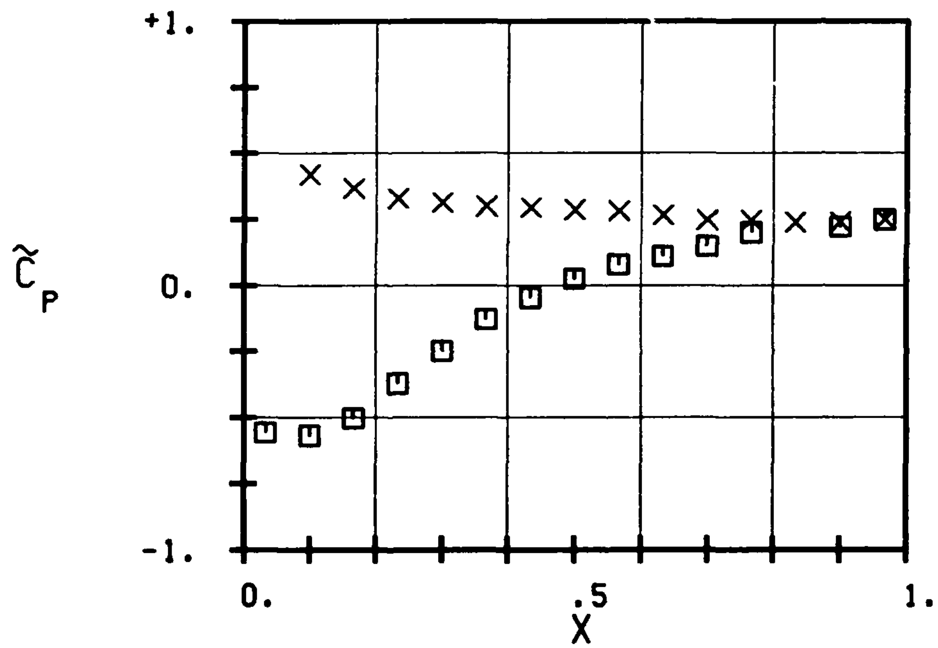

FIG. 3.5-2F: FIFTH STANDARD CONFIGURATION:
TIME AVERAGED BLADE SURFACE PRESSURE
DISTRIBUTION FOR M1=0.5 AND INCIDENCE=12 DEG.

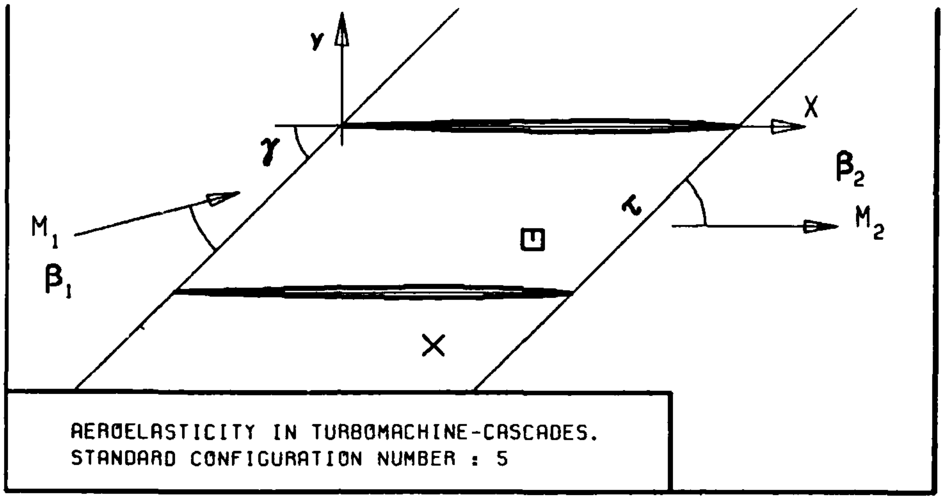

c :
τ :
γ :
x_α :
y_α :
M_1 :
β_1 :
i :
M_2 :
β_2 :
$\bar{h}_X$:
$\bar{h}_Y$:
$\bar{\alpha}$:
ω :
k :
δ :
σ :
d :

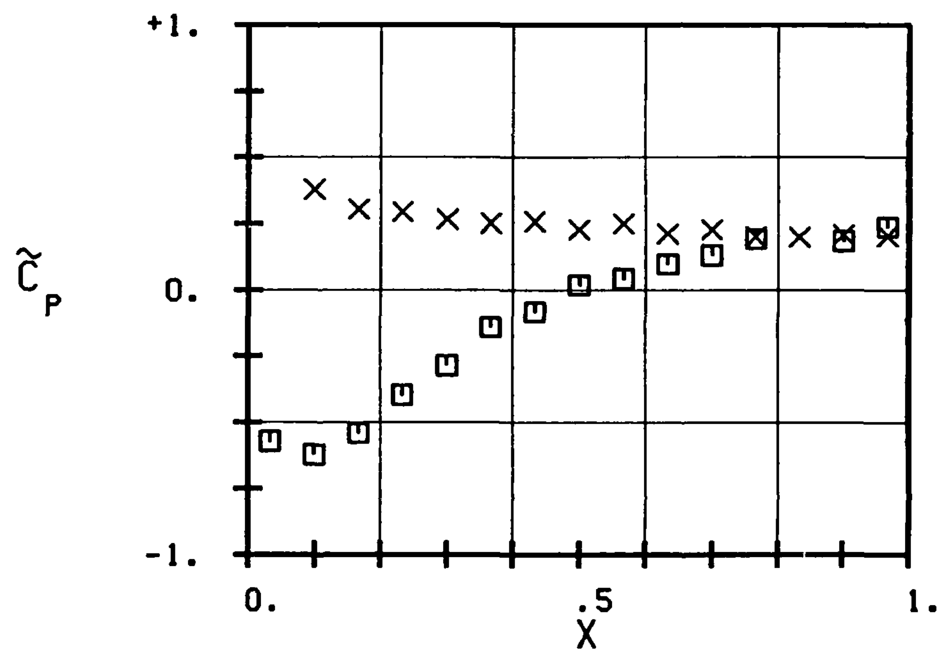

FIG. 3.5-2G: FIFTH STANDARD CONFIGURATION:
TIME AVERAGED BLADE SURFACE PRESSURE
DISTRIBUTION FOR M1=0.6 AND INCIDENCE=10 DEG.

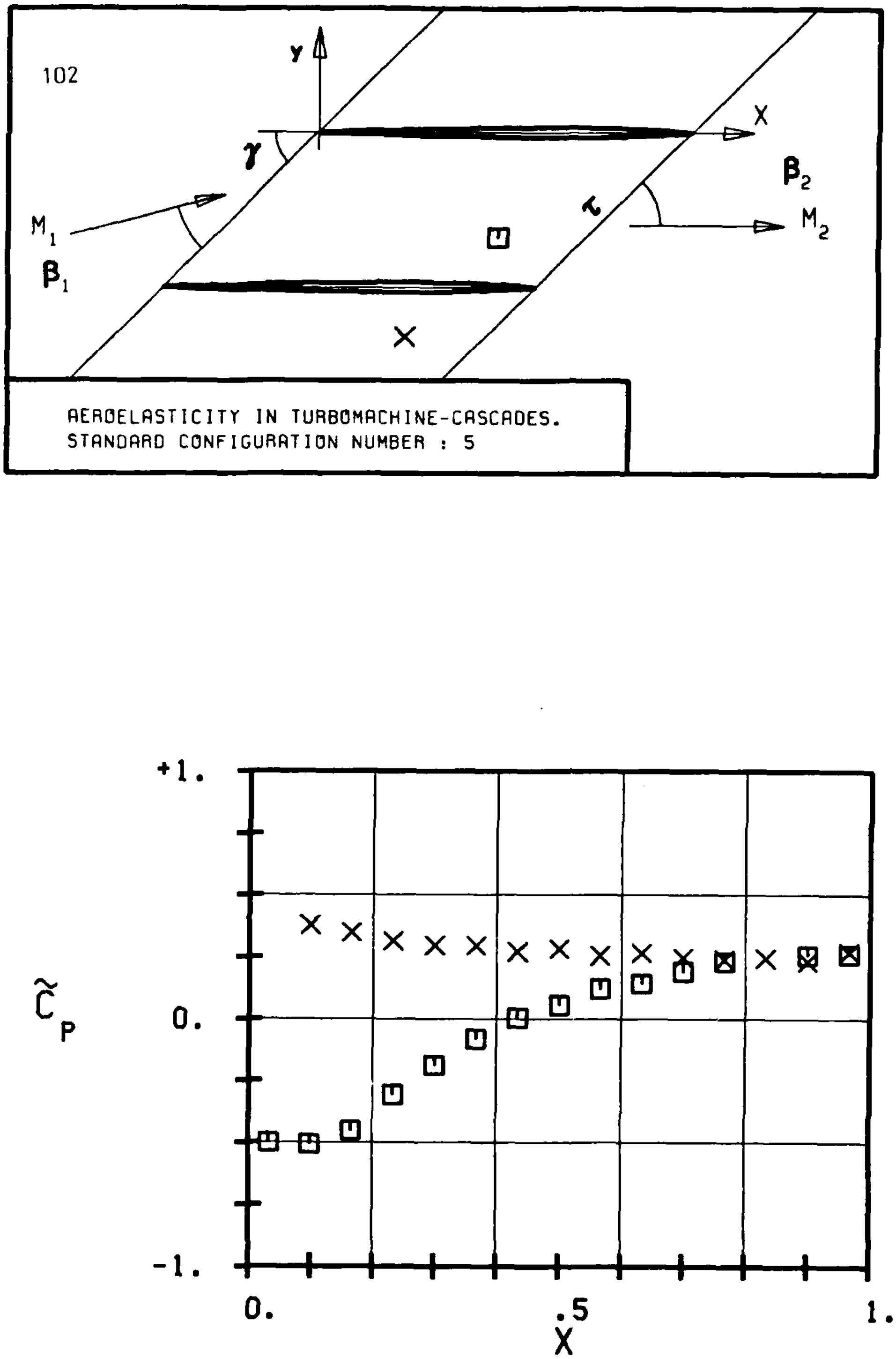

c :
τ :
γ :
x_α :
y_α :
M_1 :
β_1 :
i :
M_2 :
β_2 :
$\bar{h}_X$:
$\bar{h}_Y$:
$\bar{\alpha}$:
ω :
k :
δ :
σ :
d :

FIG. 3.5-2H: FIFTH STANDARD CONFIGURATION:
TIME AVERAGED BLADE SURFACE PRESSURE
DISTRIBUTION FOR M1=0.7 AND INCIDENCE=10 DEG.

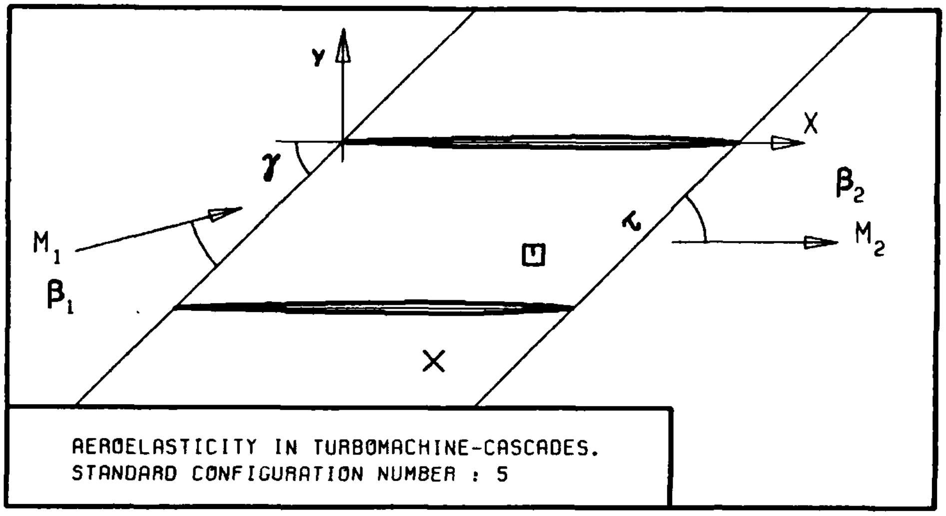

c :
τ :
γ :
x_α :
y_α :
M_1 :
β_1 :
i :
M_2 :
β_2 :
$\bar{h}_X$:
$\bar{h}_Y$:
$\bar{\alpha}$:
ω :
k :
δ :
σ :
d :

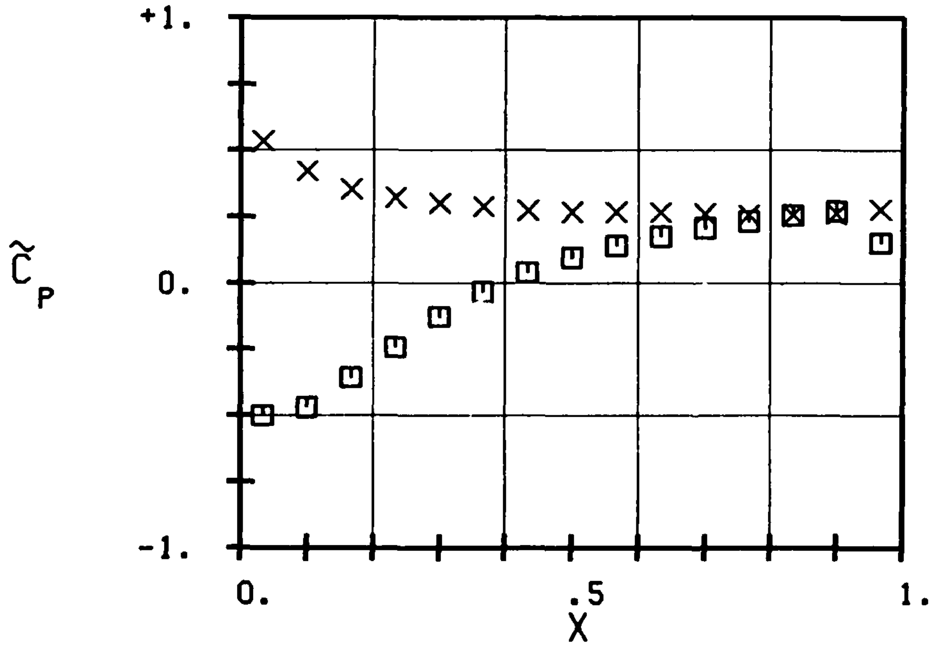

FIG. 3.5-21: FIFTH STANDARD CONFIGURATION:
TIME AVERAGED BLADE SURFACE PRESSURE
DISTRIBUTION FOR M1=0.8 AND INCIDENCE=10 DEG.

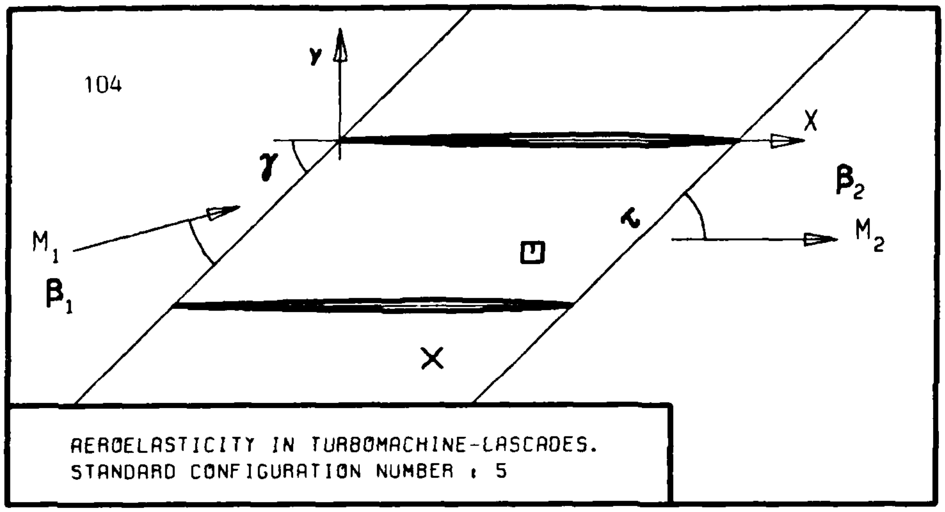

c :

τ :

γ :

x_α :

y_α :

M_1 :

β_1 :

i :

M_2 :

β_2 :

$\bar{h}_X$:

$\bar{h}_Y$:

$\bar{\alpha}$:

ω :

k :

δ :

σ :

d :

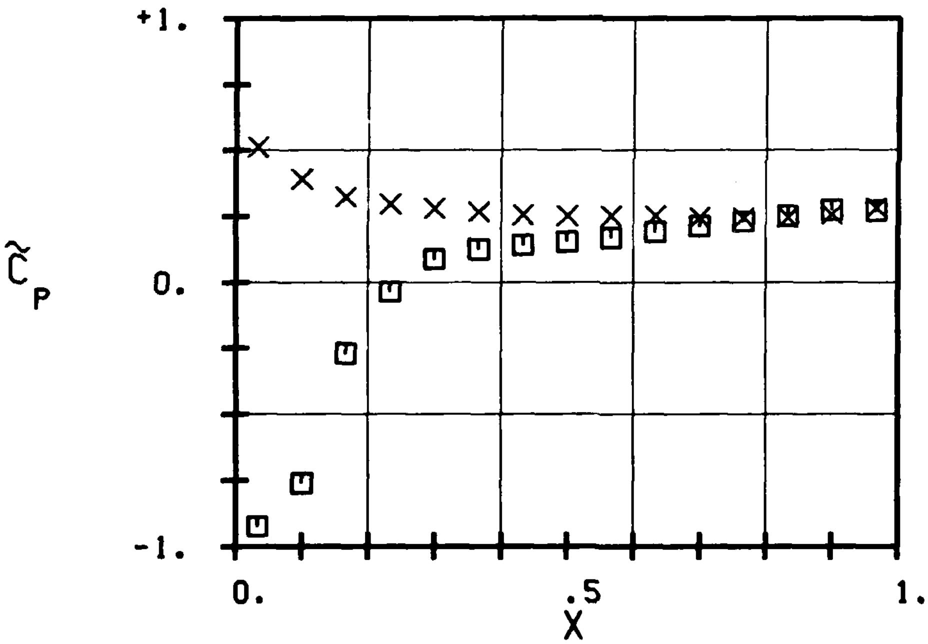

FIG. 3.5-2K: FIFTH STANDARD CONFIGURATION:
TIME AVERAGED BLADE SURFACE PRESSURE
DISTRIBUTION FOR M1=0.9 AND INCIDENCE=10 DEG.

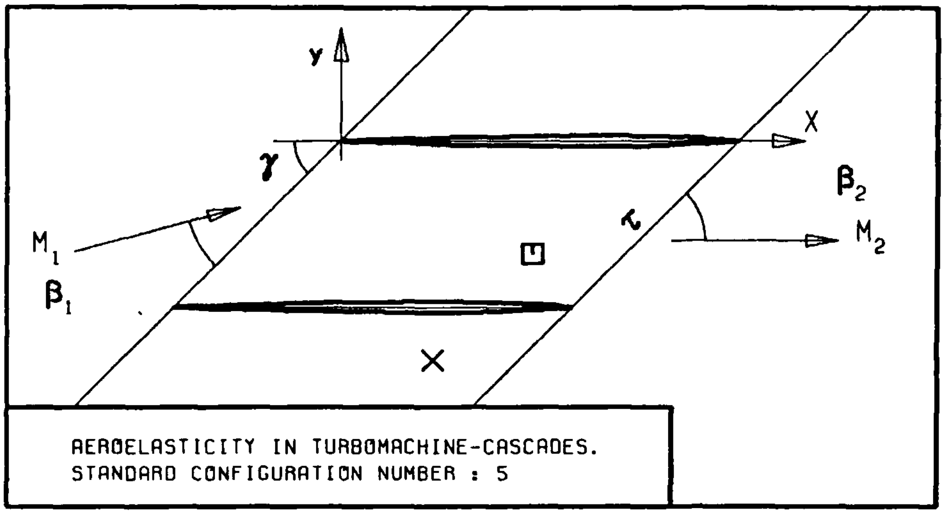

c :
τ :
γ :
x_α :
y_α :
M_1 :
β_1 :
i :
M_2 :
β_2 :
$\bar{h}_X$:
$\bar{h}_Y$:
$\bar{\alpha}$:
ω :
k :
δ :
σ :
d :

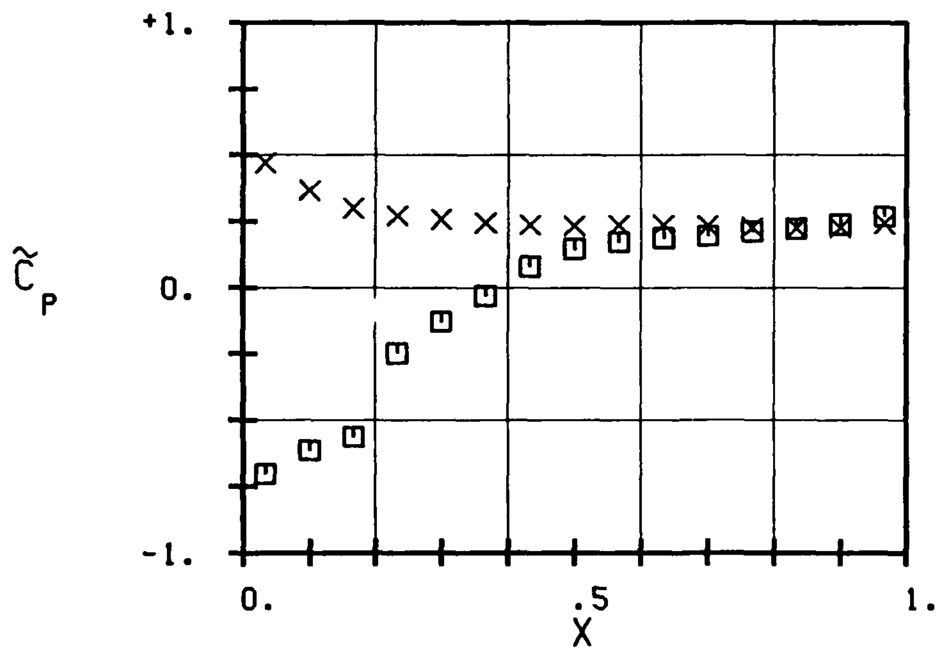

FIG. 3.5-2L: FIFTH STANDARD CONFIGURATION:
TIME AVERAGED BLADE SURFACE PRESSURE
DISTRIBUTION FOR M1=1.0 AND INCIDENCE=10 DEG.

Aeroelasticity in Turbomachine-Cascades
Fifth Standard Configuration
Time Averaged Blade Surface Pressure Distributions

$\tilde{M}_1$ (-)	0.50		0.50		0.50		0.50		0.50		0.50		0.60		0.70	
$\tilde{i}$ (^{o})	1.9		3.9		5.9		7.9		9.9		11.9		9.9		9.9	
$\tilde{P}_{t1}$ (N/m^2)	140'130		140'900		141'370		142'100		140'110		139'830		141'010		141'130	
$\tilde{P}_1$ (N/m^2)	118'020		118'540		119'080		119'470		117'900		117'600		110'480		101'880	
X (-)	$\tilde{p}/\tilde{P}_{t1}$ (-)	$\tilde{C}_p$ (-)	$\tilde{p}/\tilde{P}_{t1}$ (-)	$\tilde{C}_p$ (-)	$\tilde{p}/\tilde{P}_{t1}$ (-)	$\tilde{C}_p$ (-)	$\tilde{p}/\tilde{P}_{t1}$ (-)	$\tilde{C}_p$ (-)	$\tilde{p}/\tilde{P}_{t1}$ (-)	$\tilde{C}_p$ (-)	$\tilde{p}/\tilde{P}_{t1}$ (-)	$\tilde{C}_p$ (-)	$\tilde{p}/\tilde{P}_{t1}$ (-)	$\tilde{C}_p$ (-)	$\tilde{p}/\tilde{P}_{t1}$ (-)	$\tilde{C}_p$ (-)
Upper Surface																
0.03326	0.8067	-0.2251	0.7134	-0.8060	0.7157	-0.8031	0.7138	-0.7971	0.7321	-0.6900	0.7525	-0.5568	0.6599	-0.5708	0.5829	-0.4998
0.09979	0.8199	-0.1414	0.8039	-0.2357	0.7373	-0.6661	0.7196	-0.7607	0.7310	-0.6970	0.7507	-0.5681	0.6490	-0.6212	0.5813	-0.5055
0.16631	0.8200	-0.1408	0.8225	-0.1185	0.7904	-0.3293	0.7512	-0.5623	0.7495	-0.5803	0.7611	-0.5027	0.6664	-0.5408	0.5963	-0.4516
0.23283	0.8217	-0.1300	0.8254	-0.1002	0.8216	-0.1315	0.7897	-0.3205	0.7789	-0.3948	0.7822	-0.3700	0.6977	-0.3962	0.6365	-0.3070
0.30043	0.8233	-0.1199	0.8271	-0.0895	0.8311	-0.0712	0.8148	-0.1629	0.8025	-0.2459	0.8015	-0.2486	0.7219	-0.2845	0.6697	-0.1876
0.36695	0.8229	-0.1224	0.8296	-0.0738	0.8361	-0.0395	0.8284	-0.0775	0.8232	-0.1153	0.8206	-0.1285	0.7531	-0.1404	0.6992	-0.0816
0.43348	0.8237	-0.1174	0.8306	-0.0675	0.8377	-0.0294	0.8361	-0.0292	0.8348	-0.0422	0.8337	-0.0461	0.7653	-0.0840	0.7230	0.0040
0.50000	0.8238	-0.1167	0.8341	-0.0454	0.8430	0.0043	0.8427	0.0123	0.8456	0.0260	0.8450	0.0250	0.7876	0.0190	0.7373	0.0554
0.56652	0.8270	-0.0964	0.8375	-0.0240	0.8458	0.0220	0.8470	0.0393	0.8511	0.0607	0.8534	0.0779	0.7925	0.0416	0.7555	0.1209
0.63305	0.8269	-0.0971	0.8410	-0.0019	0.8514	0.0575	0.8534	0.0795	0.8586	0.1080	0.8585	0.1099	0.8045	0.0970	0.7616	0.1428
0.69957	0.8288	-0.0850	0.8437	0.0151	0.8536	0.0715	0.8562	0.0970	0.8626	0.1332	0.8647	0.1489	0.8119	0.1312	0.7751	0.1913
0.76609	0.8323	-0.0629	0.8514	0.0636	0.8616	0.1222	0.8644	0.1485	0.8701	0.1805	0.8730	0.2012	0.8252	0.1926	0.7863	0.2316
0.90021	0.8348	-0.0470	0.8541	0.0806	0.8658	0.1489	0.8689	0.1768	0.8742	0.2064	0.8763	0.2219	0.8235	0.1878	0.7931	0.2561
0.96674	0.8426	0.0024	0.8616	0.1279	0.8707	0.1799	0.8721	0.1969	0.8769	0.2234	0.8804	0.2477	0.8350	0.2379	0.7941	0.2597
Lower Surface																
0.09979	0.8448	0.0164	0.8685	0.1714	0.8846	0.2681	0.8897	0.3074	0.8994	0.3654	0.9077	0.4194	0.8654	0.3783	0.8271	0.3783
0.16631	0.8449	0.0170	0.8646	0.1468	0.8785	0.2294	0.8835	0.2685	[illegible]	[illegible]	0.8995	0.3678	0.8494	0.3044	0.8188	0.3485
0.23283	0.8413	-0.0058	0.8617	0.1285	0.8755	0.2104	0.8783	0.2358	[illegible]	[illegible]	0.8934	0.3295	0.8474	0.2952	0.8092	0.3139
0.30043	0.8403	-0.0122	0.8591	0.1121	0.8720	0.1882	0.8753	0.2170	[illegible]	[illegible]	0.8909	0.3137	0.8412	0.2665	0.8044	0.2967
0.36695	0.8378	-0.0280	0.8576	0.1027	0.8702	0.1768	0.8721	0.1969	[illegible]	0.2543	0.8886	0.2993	0.8381	0.2522	0.8039	0.2949
0.43348	0.8366	-0.0356	0.8555	0.0894	0.8679	0.1622	0.8708	0.1887	0.8795	0.2398	0.8878	0.2942	0.8392	0.2573	0.7972	0.2708
0.50000	0.8349	-0.0464	0.8548	0.0850	0.8661	0.1508	0.8688	0.1762	0.8788	0.2354	0.8865	0.2861	0.8328	0.2277	0.8002	0.2816
0.56652	0.8331	-0.0578	0.8527	0.0718	0.8651	0.1444	0.8678	0.1699	0.8766	0.2215	0.8859	0.2823	0.8375	0.2495	0.7929	0.2553
0.63305	0.8318	-0.0660	0.8521	0.0680	0.8631	0.1317	0.8658	0.1573	0.8756	0.2152	0.8834	0.2666	0.8295	0.2125	0.7958	0.2658
0.69957	0.8297	-0.0793	0.8500	0.0548	0.8620	0.1248	0.8649	0.1517	0.8742	0.2064	0.8802	0.2464	0.8329	0.2282	0.7905	0.2467
0.76609	0.8293	-0.0819	0.8499	0.0542	0.8606	0.1159	0.8633	0.1416	0.8725	0.1957	0.8802	0.2464	0.8270	0.2010	0.7884	0.2392
0.83262	0.8302	-0.0762	0.8496	0.0523	0.8616	0.1222	0.8642	0.1473	0.8724	0.1950	0.8789	0.2383	0.8266	0.1991	0.7902	0.2456
0.90021	0.8337	-0.0540	0.8539	0.0794	0.8631	0.1317	0.8653	0.1542	0.8723	0.1944	0.8791	0.2395	0.8286	0.2083	0.7862	0.2312
0.96674	0.8414	-0.0052	0.8590	0.1115	0.8693	0.1711	0.8707	0.1881	0.8757	0.2159	0.8810	0.2515	0.8276	0.2037	0.7967	0.2690

Table 3.5-3 (continuation on next page)

Aeroelasticity in Turbomachine-Cascades Fifth Standard Configuration Time Averaged Blade Surface Pressure Distributions										
$\tilde{M}_1$ (-)	0.80				0.91		0.90		1.00	
$\tilde{i}$ (°)	10.0				10.0				10.0	
$\tilde{p}_{t1}$ (N/m²)	140'350		200'110		140'070		199'950		199'900	
$\tilde{p}_1$ (N/m²)	92'040		131'740		82'150		118'250		105'760	
X (-)	$\tilde{p}/\tilde{p}_{t1}$ (-)	$\tilde{c}_p$ (-)	$\tilde{p}/\tilde{p}_{t1}$ (-)	$\tilde{c}_p$ (-)	$\tilde{p}/\tilde{p}_{t1}$ (-)	$\tilde{c}_p$ (-)	$\tilde{p}/\tilde{p}_{t1}$ (-)	$\tilde{c}_p$ (-)	$\tilde{p}/\tilde{p}_{t1}$ (-)	$\tilde{c}_p$ (-)
Upper Surface										
0.0333	0.4837	-0.5000	0.4911	-0.4895	0.2041	-0.9248	0.3793	-0.5191	0.1979	-0.7032
0.1000	0.4944	-0.4689	0.4991	-0.4661	0.2719	-0.7608	0.4102	-0.4435	0.2399	-0.6140
0.1667	0.5334	-0.3556	0.5351	-0.3607	0.4750	-0.2696	0.4616	-0.3177	0.2638	-0.5633
0.2333	0.5725	-0.2420	0.5618	-0.2826	0.5715	-0.0363	0.4882	-0.2526	0.4129	-0.2467
0.3000	0.6118	-0.1278	0.5920	-0.1942	0.6230	0.0883	0.5210	-0.1723	0.4690	-0.1275
0.3667	0.6442	-0.0337	0.6208	-0.1099	0.6383	0.1253	0.5532	-0.0935	0.5147	-0.0305
0.4333	0.6699	0.0410	0.6464	-0.0349	0.6443	0.1398	0.5817	-0.0237	0.5671	0.0808
0.5000	0.6886	0.0953	0.6667	0.0245	0.6500	0.1536	0.6052	0.0338	0.5979	0.1462
0.5667	0.7042	0.1406	0.6836	0.0739	0.6565	0.1693	0.6251	0.0825	0.6109	0.1738
0.6333	0.7163	0.1758	0.6976	0.1149	0.6653	0.1906	0.6415	0.1226	0.6176	0.1880
0.7000	0.7269	0.2066	0.7091	0.1486	0.6745	0.2128	0.6546	0.1547	0.6216	0.1965
0.7667	0.7356	0.2319	0.7189	0.1773	0.6820	0.2310	0.6652	0.1806	0.6296	0.2135
0.8333	0.7434	0.2545	0.7272	0.2016	0.6903	0.251	0.6747	0.2039	0.6339	0.2226
0.9000	0.7487	0.2699	0.7298	0.2092	0.6998	0.2740	0.6823	0.2225	0.6418	0.2394
0.9667	0.7078	0.1511	0.6106	-0.1397	0.6982	0.2701	0.6893	0.2396	0.6556	0.2687
Lower Surface										
0.0333	0.8398	0.5346	0.8337	0.5133	0.7983	0.5122	0.8014	0.5140	0.7508	0.4708
0.1000	0.8010	0.4219	0.8002	0.4152	0.7481	0.3908	0.7585	0.4090	0.7024	0.3681
0.1667	0.7772	0.3527	0.7751	0.3417	0.7201	0.3231	0.7285	0.3355	0.6701	0.2995
0.2333	0.7665	0.3216	0.7640	0.3093	0.7087	0.2955	0.7150	0.3025	0.6573	0.2723
0.3000	0.7593	0.3007	0.7568	0.2882	0.7021	0.2796	0.7074	0.2839	0.6506	0.2581
0.3667	0.7549	0.2879	0.7525	0.2756	0.6963	0.2656	0.7021	0.2709	0.6449	0.2460
0.4333	0.7500	0.2737	0.7487	0.2645	0.6919	0.2549	0.6977	0.2602	0.6406	0.2368
0.5000	0.7480	0.2679	0.7469	0.2592	0.6904	0.2513	0.6964	0.2570	0.6394	0.2343
0.5667	0.7480	0.2679	0.7469	0.2592	0.6907	0.2520	0.7003	0.2665	0.6406	0.2368
0.6333	0.7475	0.2664	0.7461	0.2569	0.6904	0.2513	0.7003	0.2665	0.6411	0.2379
0.7000	0.7455	0.2606	0.7439	0.2504	0.6881	0.2457	0.6963	0.2567	0.6389	0.2332
0.7667	0.7442	0.2569	0.7412	0.2425	0.6872	0.2435	0.6926	0.2477	0.6363	0.2277
0.8333	0.7440	0.2563	0.7394	0.2373	0.6879	0.2452	0.6897	0.2406	0.6355	0.2260
0.9000	0.7459	0.2618	0.7382	0.2337	0.6926	0.2566	0.6856	0.2305	0.6364	0.2279
0.9667	0.7514	0.2778	0.7394	0.2337	0.7031	0.2820	0.6861	0.2318	0.6434	0.2428

Table 5.5-5 Fifth Standard Configuration: Time Averaged Blade Surface Pressure Distributions for the 27 Recommended Aeroelastic Cases

Aeroelasticity in Turbomachine-Cascades.
Fifth Standard Configuration.
Aeroelastic test case N^{o}:______

M_1=______ • p_2/p_{t1}=______ • M_2=______ • β_1=______^{o} • β_2=______^{o} • k=______ •

$\bar{\alpha}^{(-2)}$=______ • $\bar{\alpha}^{(-1)}$=______ • $\bar{\alpha}^{(0)}$=______ • $\bar{\alpha}^{(+1)}$=______ • $\bar{\alpha}^{(+2)}$=______ • (rads)

$\sigma^{(-2)}$=______ • $\sigma^{(-1)}$=______ • $\sigma^{(0)}$=______ • $\sigma^{(+1)}$=______ • $\sigma^{(+2)}$=______ • (^{o})

a) Global Aeroelastic Coefficients

$\bar{C}_M$=______ • $\bar{C}_L$=______ • C_W=______ • Ξ =______ • (-)

Φ_M=______ • Φ_L=______ • (^{o})

b) Local Time Dependant Blade Surface Pressure Coefficients

X (-)	$C_p^{(ls)}$ (-)	$\Phi_p^{(ls)}$ (^{o})	$C_p^{(us)}$ (-)	$\Phi_p^{(us)}$ (^{o})	$\Delta\bar{C}_p$ (-)	$\Phi_{\Delta p}$ (^{o})

Table 3.5-4 Fifth Standard Configuration: Table for Presentation of the 27 Recommended Aeroelastic Cases

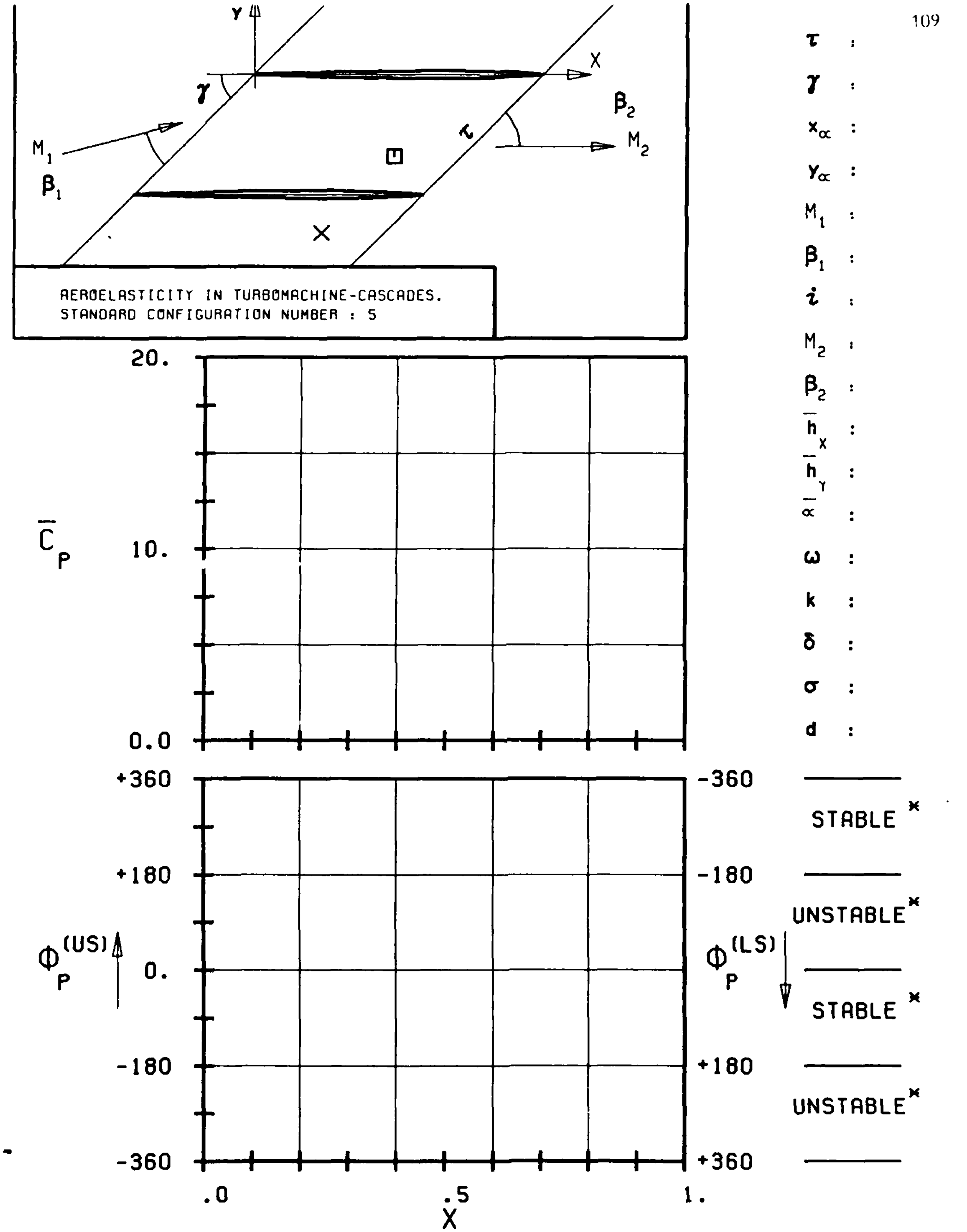

FIG. 3.5-3A: FIFTH STANDARD CONFIGURATION:
MAGNITUDE AND PHASE LEAD OF BLADE SURFACE PRESSURE COEFFICIENT.

(*: IN PITCH MODE, NOTATION VALID UPSTREAM OF PITCH AXIS)

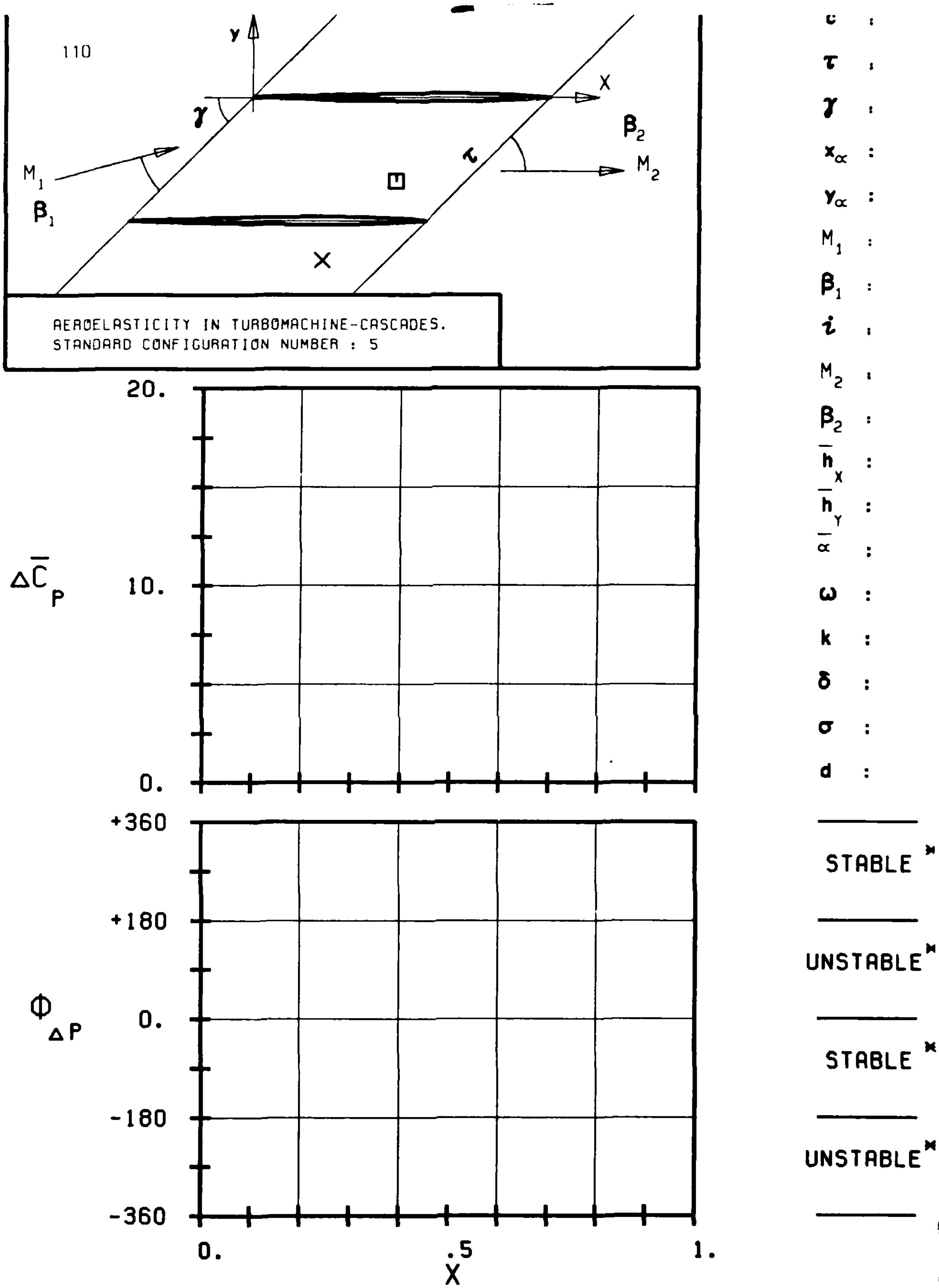

FIG. 3.5-3B: FIFTH STANDARD CONFIGURATION:
MAGNITUDE AND PHASE LEAD OF BLADE SURFACE
PRESSURE DIFFERENCE COEFFICIENT.

(*: IN PITCH MODE, NOTATION VALID UPSTREAM OF PITCH AXIS)

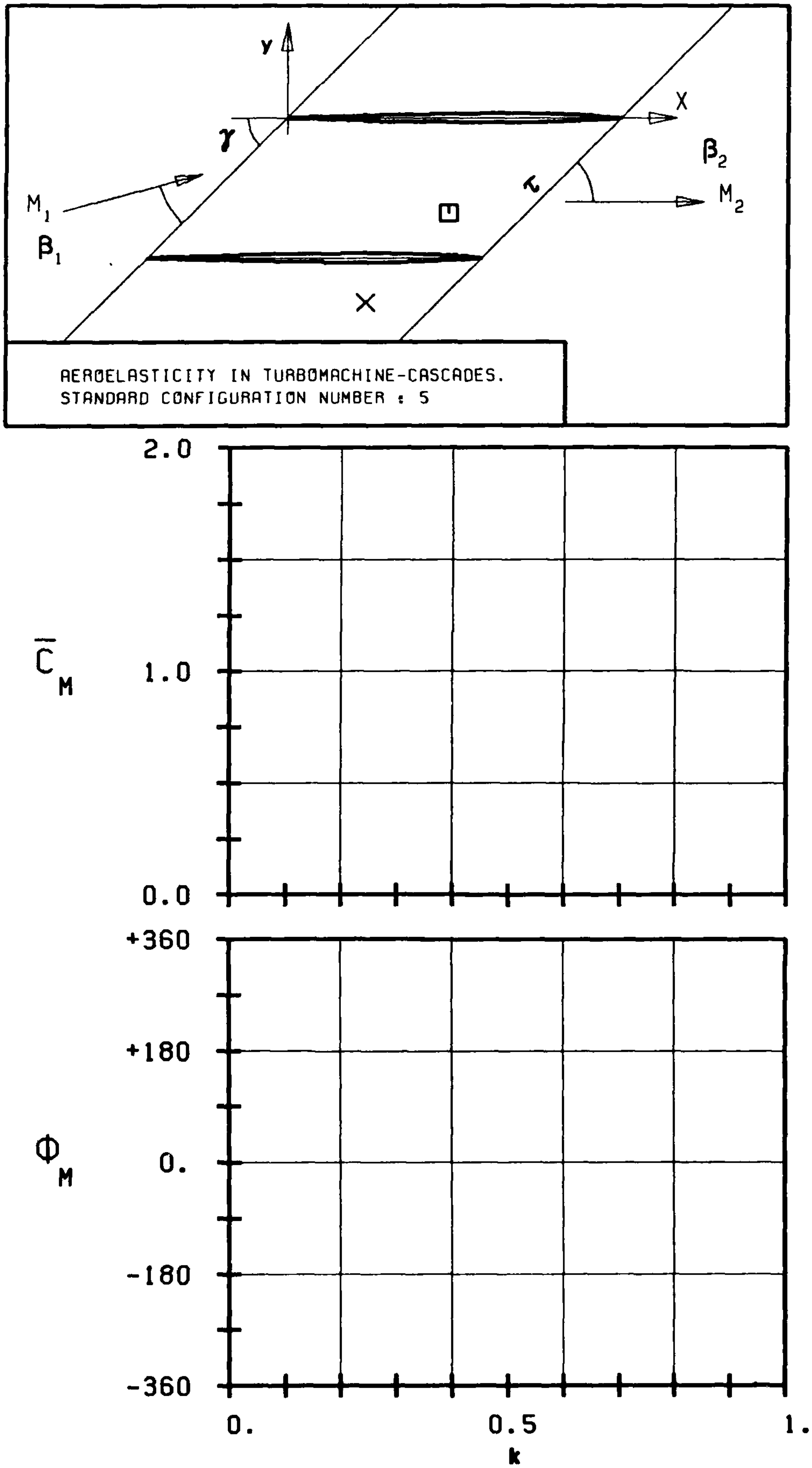

c :
τ :
γ :
x_α :
y_α :
M_1 :
β_1 :
i :
M_2 :
β_2 :
$\bar{h}_X$:
$\bar{h}_Y$:
$\bar{\alpha}$:
ω :
k :
δ :
σ :
d :

STABLE

UNSTABLE

STABLE

UNSTABLE

FIG. 3.5-3C: FIFTH STANDARD CONFIGURATION:
AERODYNAMIC MOMENT COEFFICIENT AND PHASE LEAD
IN DEPENDANCE OF REDUCED FREQUENCY.

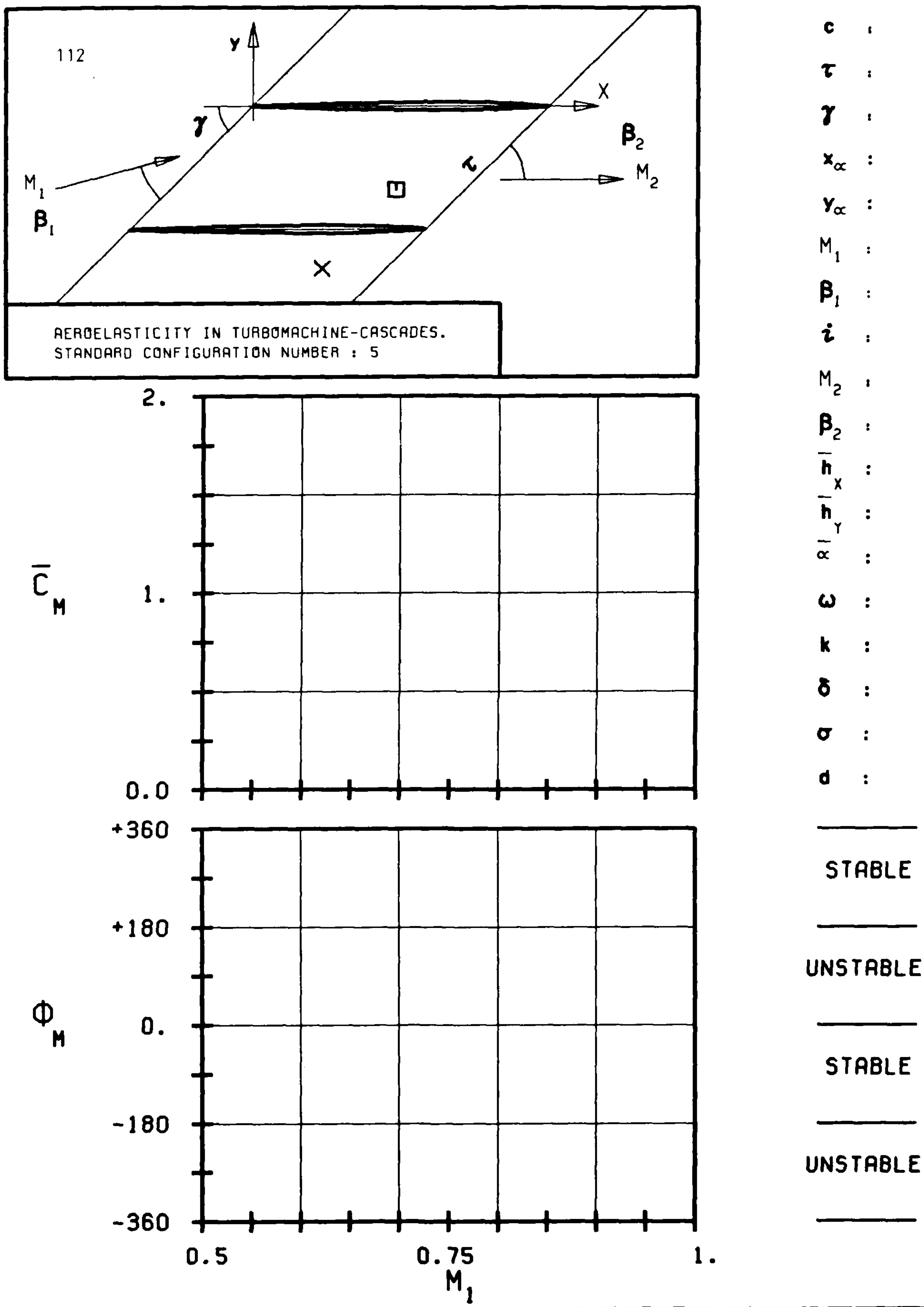

FIG. 3.5-3D: FIFTH STANDARD CONFIGURATION:
AERODYNAMIC MOMENT COEFFICIENT AND PHASE LEAD
IN DEPENDANCE OF INLET MACH NUMBER.

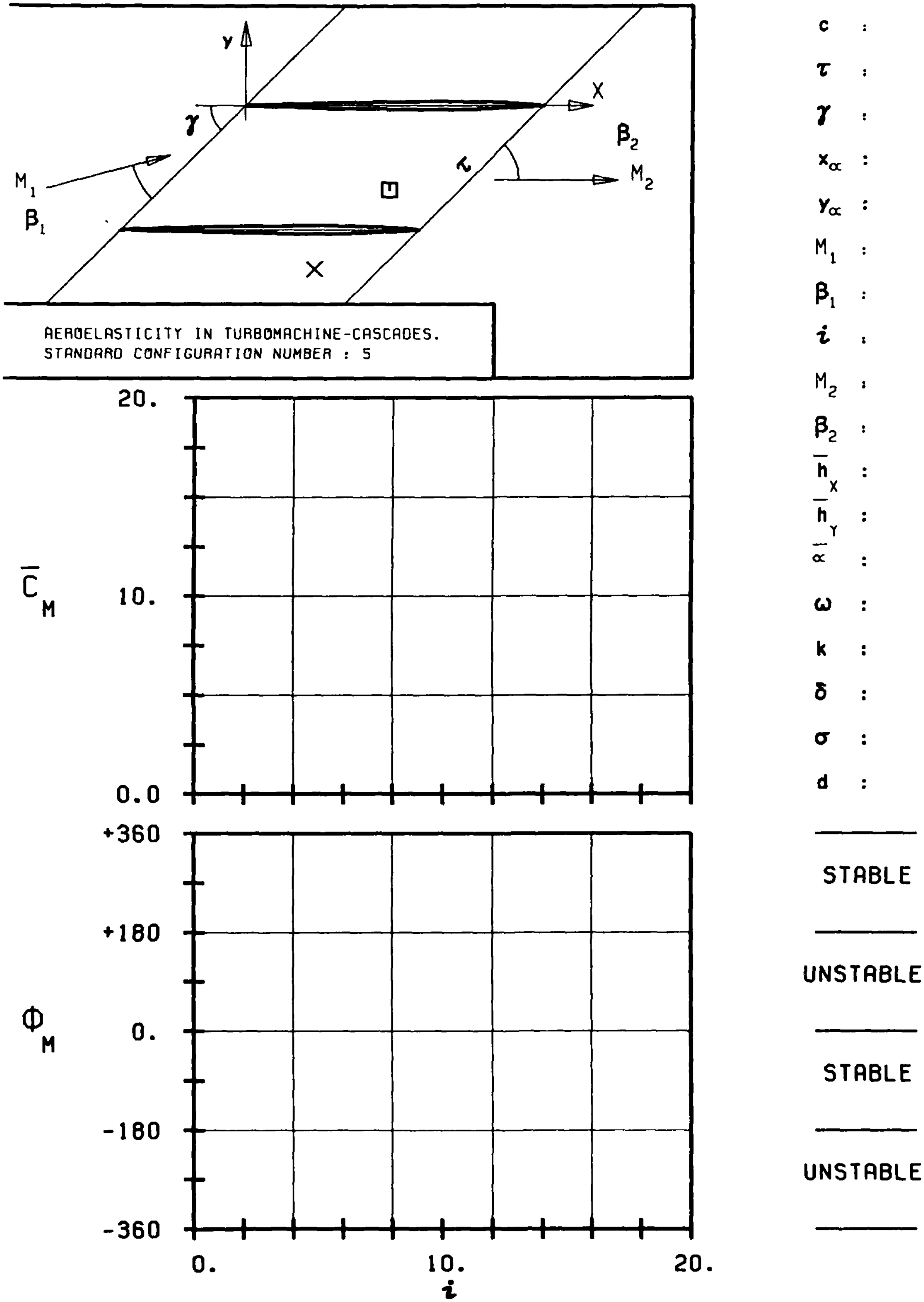

FIG. 3.5-3E: FIFTH STANDARD CONFIGURATION:
AERODYNAMIC MOMENT COEFFICIENT AND PHASE LEAD
IN DEPENDANCE OF INCIDENCE ANGLE.

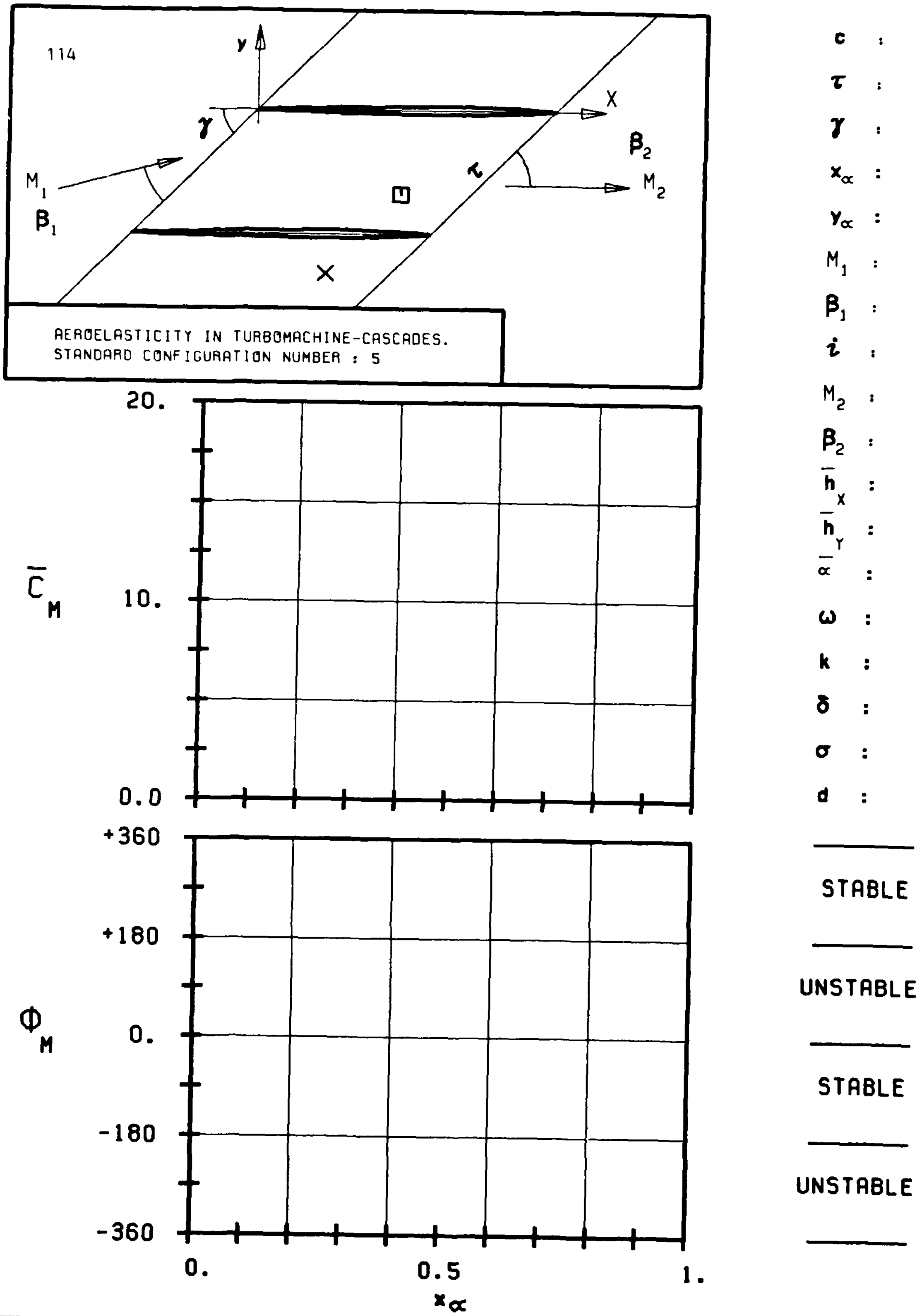

FIG. 3.5-3F: FIFTH STANDARD CONFIGURATION:
AERODYNAMIC MOMENT COEFFICIENT AND PHASE LEAD
IN DEPENDANCE OF PITCHING AXIS POSITION.

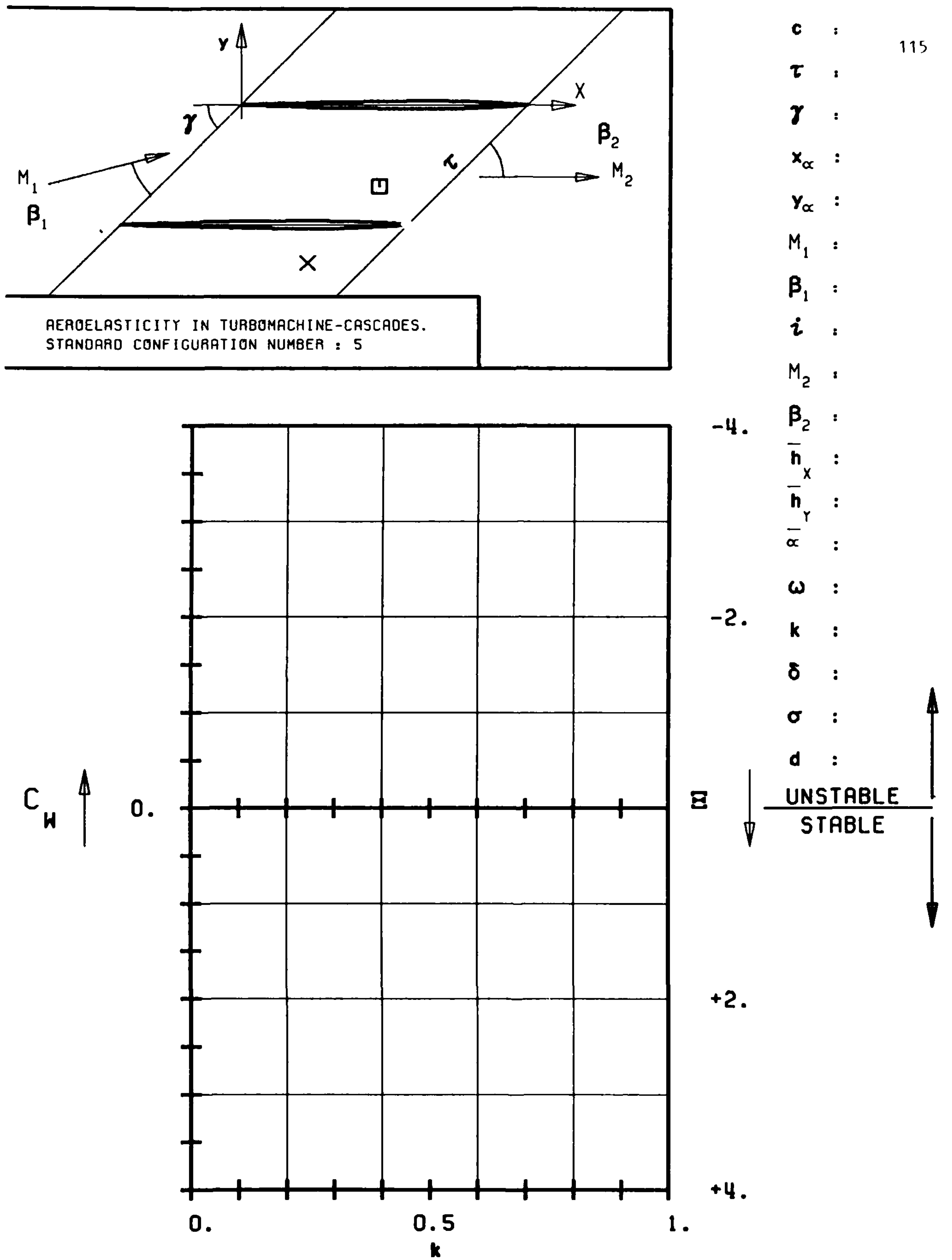

FIG. 3.5-3G: FIFTH STANDARD CONFIGURATION:
AERODYNAMIC WORK AND DAMPING COEFFICIENTS
IN DEPENDANCE OF REDUCED FREQUENCY.

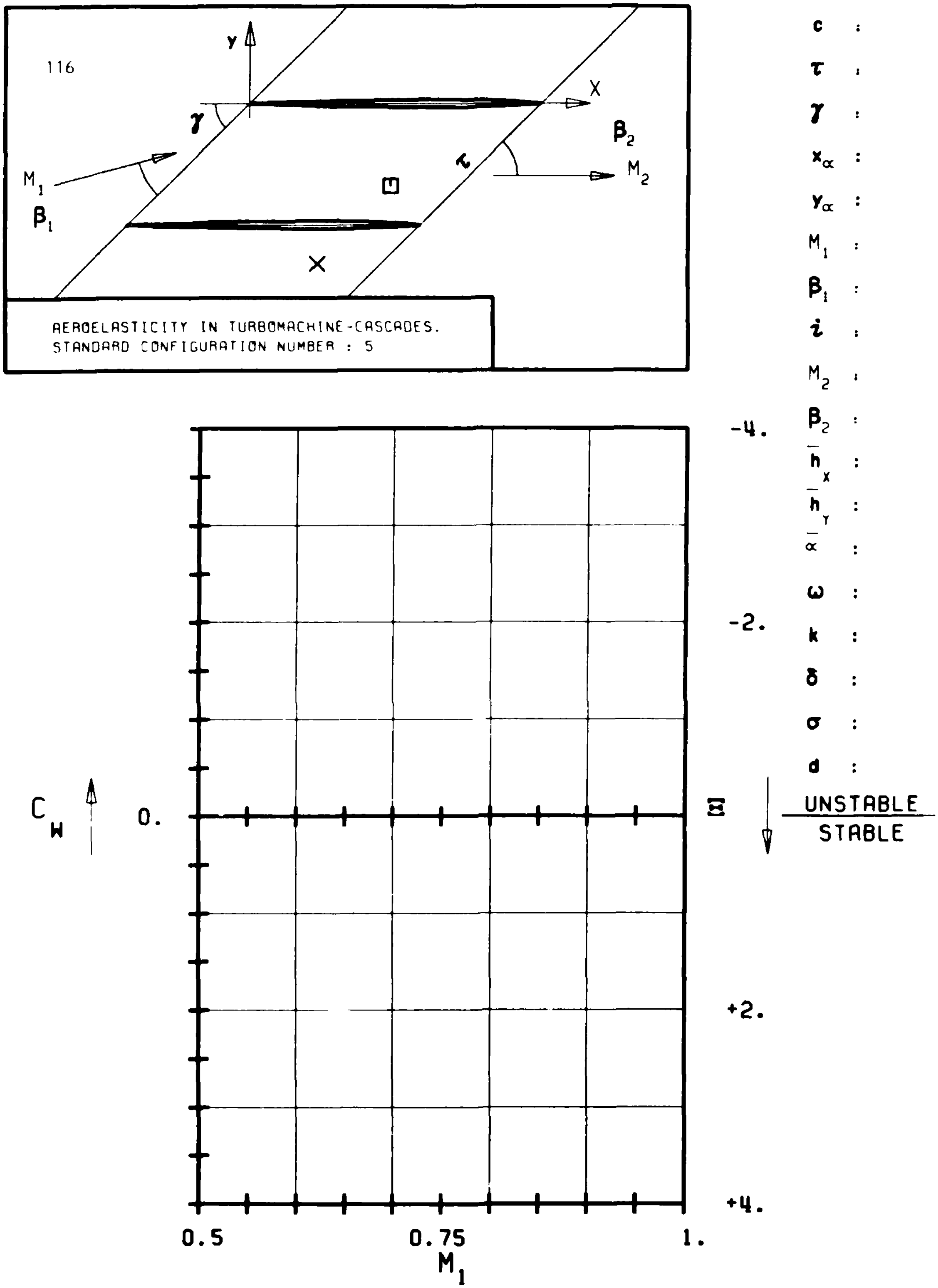

FIG. 3.5-3H: FIFTH STANDARD CONFIGURATION:
AERODYNAMIC WORK AND DAMPING COEFFICIENTS
IN DEPENDANCE OF INLET MACH NUMBER.

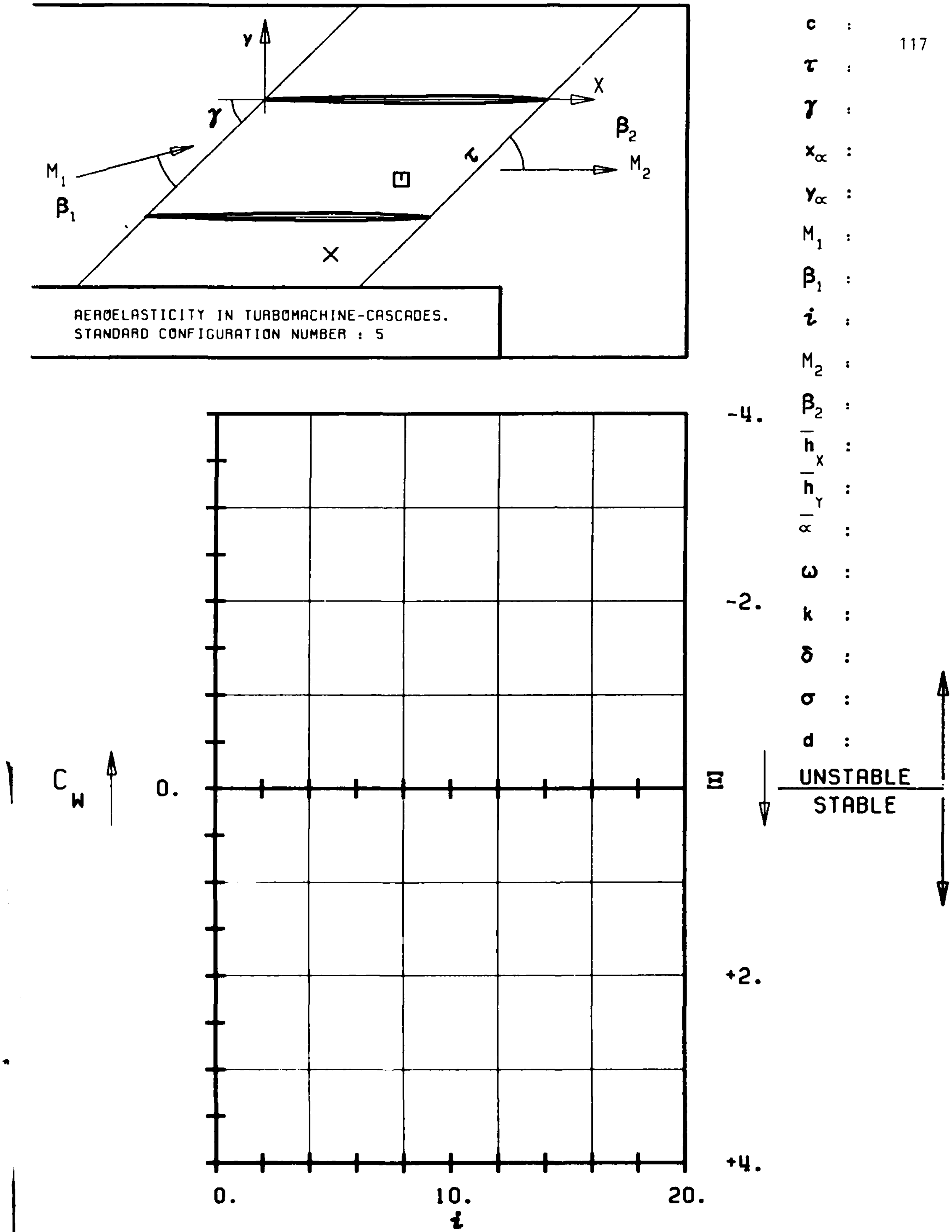

FIG. 3.5-31: FIFTH STANDARD CONFIGURATION:
AERODYNAMIC WORK AND DAMPING COEFFICIENTS
IN DEPENDANCE OF INCIDENCE ANGLE.

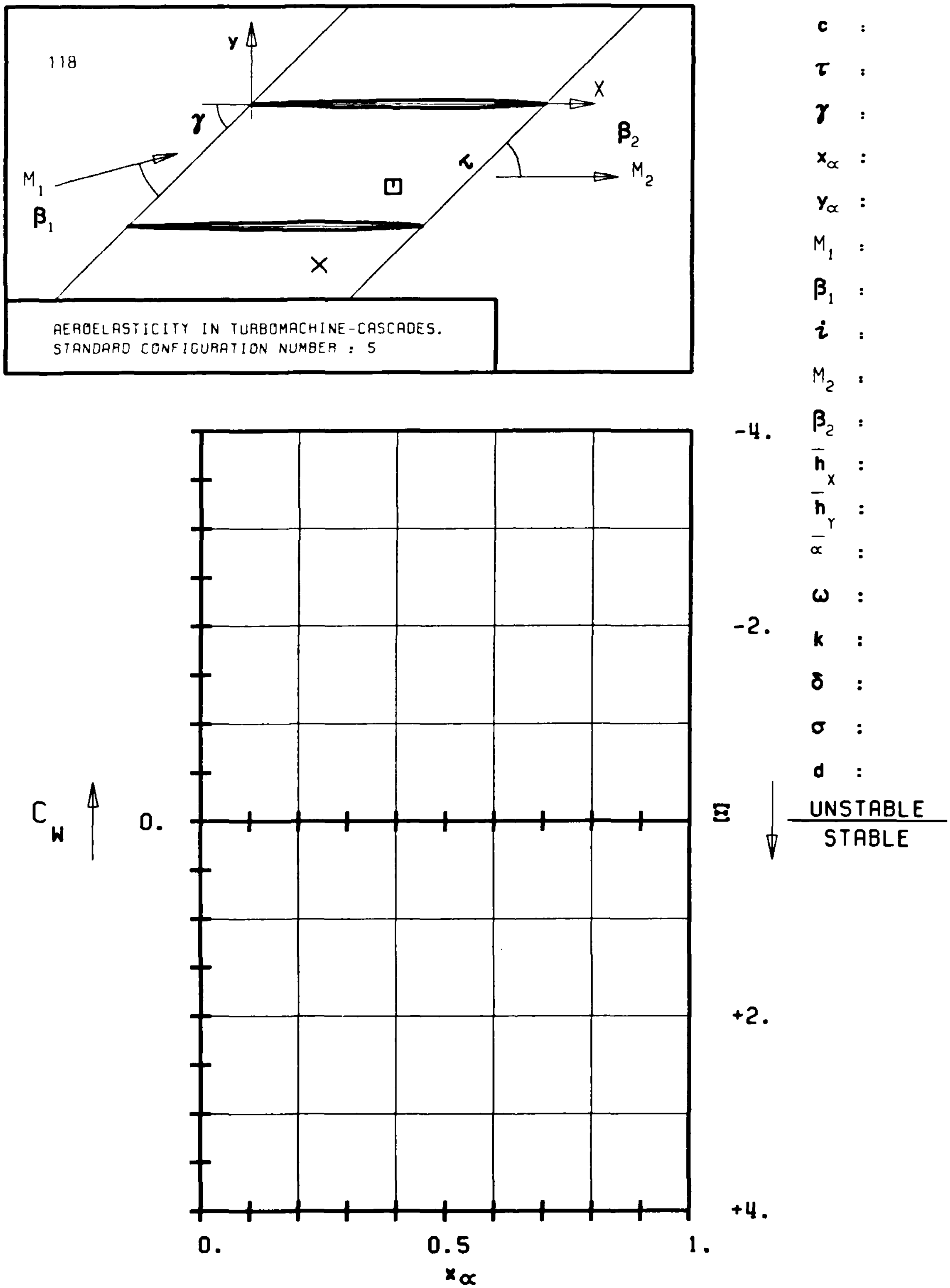

FIG. 3.5-3K: FIFTH STANDARD CONFIGURATION:
AERODYNAMIC WORK AND DAMPING COEFFICIENTS
IN DEPENDANCE OF PITCHING AXIS POSITION.

3.6 Sixth Standard Configuration

This configuration is directed towards investigations of turbine rotor blade tip sections in the transonic flow regime.

Experiments have been performed, in air, in the annular cascade test facility at the Lausanne Institute of Technology by D. Schläfli.

The cascade configuration consists of twenty vibrating low camber prismatic turbine blades. Each blade has a constant spanwise chord of c=0.0528 m and a span of 0.040 m, with 14° camber and a maximum thickness-to-chord ratio of 0.0526. The stagger angle for the experiments presented here is 16.6°, and the gap-to-chord ratio is:

0.952	(hub)
1.071	(midspan)
1.190	(tip)

The hub-tip ratio in the annular test facility is 0.80.

The cascade geometry is given in Figure 3.6-1 and the profile coordinates in Table 3.6-1.

Experiments have been performed with variable inlet flow velocity, incidence angle, expansion ratio, vibration mode shape, oscillation frequency and interblade phase angle.

Both the time averaged and time dependent instrumentation on this cascade is complete, and a large number of well documented data have been obtained.

However, due to the very thin profiles, only a limited number of pressure transducers are built into the blades, wherefore no integrations of the time dependant pressure signals to obtain global unsteady forces are performed. Instead, the self excited flutter limits of the cascade have been established for several parameters.

From the results obtained during these tests, 26 aeroelastic cases are recommended for off-design calculations. They are contained in Table 3.6-2 together with the proposal for representation of the results.

The vibration mode for all these cases is bending (δ =43.2°), and the parameters varied are inlet flow angle, expansion ratio and interblade phase angle.

The 26 aeroelastic cases correspond to 12 different time averaged settings of the cascade (see Table 3.6-2), for each of which the steady blade surface pressure distribution is given in Figures 3.6-2 and Table 3.6-3.

All experiments presented here have been performed with constant spanwise upstream flow velocities and flow angles.
It is recommended to present the results as in Figures 3.6-3 and Table 3.6-4.

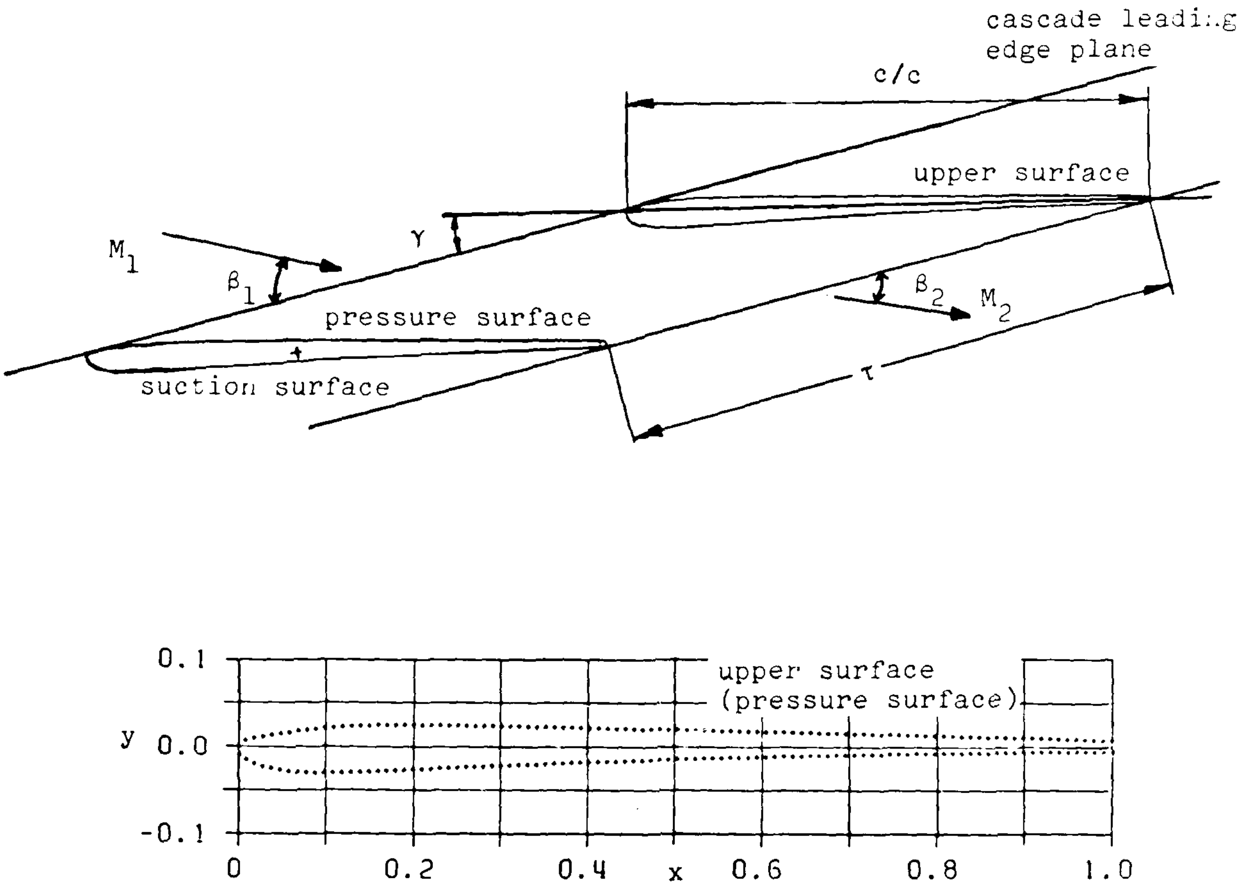

c	= 0.0528 m		γ	= 16.6°
span	= 0.040 m		camber	= 14°
τ	= 0.952	(hub)	$\frac{\text{thickness}}{\text{chord}}$	= 0.0526
	1.071	(midspan)	hub/tip	= 0.8
	1.190	(tip)		

Figure 3.6-1 Sixth Standard Configuration: Cascade Geometry

C = 0.05277 M							
UPPER SURFACE				LOWER SURFACE			
X	Y	X	Y	X	Y	X	Y
0.0000	0.0000	.5033	.0191	0.0000	0.0000	.4930	-.0151
.0078	.0063	.5135	.0189	.0008	-.0097	.5032	-.0148
.0176	.0090	.5236	.0187	.0085	-.0161	.5133	-.0145
.0275	.0109	.5338	.0185	.0178	-.0202	.5234	-.0142
.0375	.0127	.5439	.0183	.0275	-.0232	.5336	-.0138
.0475	0143	.5540	.0181	.0373	-.0256	.5437	-.0135
.0575	.0157	.5642	.0179	.0473	-.0274	.5538	-.0132
.0676	.0171	.5743	.0177	.0573	-.0288	.5640	-.0130
.0777	.0184	.5845	.0175	.0674	-.0298	.5741	-.0127
.0877	.0195	.5946	.0173	.0775	-.0305	.5843	-.0124
.0978	.0204	.6047	.0171	.0877	-.0309	.5944	-.0121
.1079	.0213	.6149	.0169	.0978	-.0311	.6045	-.0119
.1181	.0221	.6250	.0167	.1080	-.0310	.6147	-.0116
.1282	.0225	.6352	.0165	.1181	-.0307	.6248	-.0113
.1383	.0230	.6453	.0162	.1282	-.0303	.6349	-.0111
.1484	.0235	.6554	.0160	.1384	-.0298	.6451	-.0108
.1586	.0239	.6656	.0158	.1485	-.0294	.6552	-.0106
.1687	.0242	.6757	.0156	.1586	-.0289	.6654	-.0104
.1789	.0243	.6859	.0153	.1688	-.0284	.6755	-.0101
.1890	.0243	.6960	.0151	.1789	-.0278	.6856	-.0099
.1991	.0243	.7061	.0149	.1890	-.0274	.6958	-.0097
.2093	.0242	.7163	.0147	.1991	-.0269	.7059	-.0095
.2194	.0240	.7264	.0144	.2093	-.0264	.7161	-.0093
.2296	.0239	.7366	.0142	.2194	-.0259	.7262	-.0091
.2397	.0237	.7467	.0140	.2295	-.0254	.7363	-.0089
.2498	.0236	.7568	.0137	.2397	-.0250	.7465	-.0087
.2600	.0235	.7670	.0135	.2498	-.0245	.7566	-.0085
.2701	.0235	.7771	.0133	.2599	-.0240	.7668	-.0083
.2803	.0234	.7873	.0130	.2701	-.0236	.7769	-.0082
.2904	.0233	.7974	.0128	.2802	-.0232	.7870	-.0080
.3006	.0232	.8075	.0125	.2903	-.0227	.7972	-.0078
.3107	.0231	.8177	.0123	.3005	-.0223	.8073	-.0077
.3208	.0229	.8278	.0120	.3106	-.0219	.8175	-.0075
.3310	.0227	.8380	.0118	.3207	-.0214	.8276	-.0074
.3411	.0225	.8481	.0115	.3309	-.0210	.8377	-.0072
.3513	.0223	.8582	.0112	.3410	-.0206	.8479	-.0071
.3614	.0220	.8684	.0110	.3511	-.0202	.8580	-.0070
.3715	.0218	.8785	.0107	.3613	-.0198	.8682	-.0068
.3817	.0215	.8886	.0104	.3714	-.0194	.8783	-.0067
.3918	.0213	.8988	.0102	.3815	-.0190	.8884	-.0066
.4019	.0211	.9089	.0099	.3917	-.0186	.8986	-.0065
.4121	.0210	.9191	.0096	.4018	-.0183	.9087	-.0064
.4222	.0208	.9292	.0093	.4119	-.0179	.9189	-.0063
.4324	.0206	.9393	.0090	.4221	-.0175	.9290	-.0062
.4425	.0204	.9495	.0088	.4322	-.0172	.9392	-.0061
.4526	.0202	.9596	.0085	.4423	-.0168	.9493	-.0060
.4628	.0200	.9697	.0082	.4525	-.0164	.9594	-.0060
.4729	.0198	.9799	.0079	.4626	-.0161	.9696	-.0059
.4831	.0195	.9900	.0076	.4727	-.0158	.9797	-.0058
.4932	.0193	1.0002	.0073	.4829	-.0154	1.0000	-.0057

Table 3.6-1 Sixth Standard Configuration: Dimensionless Airfoil Coordinates (identical over the whole span)

Aeroelasticity in Turbomachine-Cascades
Sixth Standard Configuration

Aeroelastic Case No	Time Averaged Parameters: Isentropic inlet air velocity (a) $M_{1,is}$ (-)	Inlet flow angle β_1 (^{o})	p_2/p_1 (-)	Isentropic outlet air velocity (a) $M_{2,is}$ (-)	Time Dependant Parameters: Amplitude h^o (-)	Frequency f (Hz)	Reduced frequency k (-)	Interblade phase angle σ (^{o})	Vibration direction δ (^{o})	Recommended representation: c_p	Δc_p	C_F	C_M	Ξ
1	0.53	20.0	0.27	1.63	0.0030	226	0.068	0	43.2	1	2	3	6	9
2	↓	↓	↓	↓	↓	↓	↓	+45	↓	-	-	↓	↓	↓
3	↓	↓	↓	↓	↓	↓	↓	+90	↓	1	2	↓	↓	↓
4	↓	↓	↓	↓	↓	↓	↓	+135	↓	-	-	↓	↓	↓
5	↓	↓	↓	↓	↓	↓	↓	-180	↓	1	2	↓	↓	↓
6	↓	↓	↓	↓	↓	↓	↓	-135	↓	-	-	↓	↓	↓
7	↓	↓	↓	↓	↓	↓	↓	-90	↓	1	2	↓ ,4,5	↓ ,7,8	↓ ,10,11
8					↓	↓		-45	↓	-	-			
9	0.52	20.0	0.50	1.20	↓	↓	0.092	-90	↓	1	2	4	7	10
10	0.52	20.0	0.54	1.14	↓	↓	0.097	↓	↓		↓	↓	↓	↓
11	0.52	19.8	0.62	1.02	↓	↓	0.108	↓	↓					
12	0.52	19.8	0.65	0.98	↓	↓	0.113	0	↓	1	2	3	6	9
13	↓	↓	↓	↓	↓	↓	↓	+45	↓	-	-	↓	↓	↓
14	↓	↓	↓	↓	↓	↓	↓	+90	↓	1	2	↓	↓	↓
15	↓	↓	↓	↓	↓	↓	↓	+135	↓	-	-	↓	↓	↓
16	↓	↓	↓	↓	↓	↓	↓	-180	↓	1	2	↓	↓	↓
17	↓	↓	↓	↓	↓	↓	↓	-135	↓	-	-	↓	↓	↓
18	↓	↓	↓	↓	↓	↓	↓	-90	↓	1	2	↓ ,4	↓ ,7	↓ ,10
19					↓	↓		-45	↓	-	-			
20	0.40	24.9	0.26	1.60	↓	↓	0.069	-90	↓	-	-	5	8	11
21	0.39	27.4	0.26	1.61	↓	↓	0.066	↓	↓	-	-	4,5	7,8	10,11
22	0.39	27.2	0.35	1.40	↓	↓	0.079	↓	↓	-	-	↓ -	↓ -	↓ -
23	0.39	27.2	0.37	1.37	↓	↓	0.080	↓	↓	-	-	↓	↓	↓
24	0.37	27.7	0.61	0.95	↓	↓	0.116	↓	↓	-	-	↓	↓	↓
25	0.37	27.5	0.69	0.85			0.130	↓		-	-	↓	↓	↓
26	0.30	27.9	0.85	0.57			0.193			-	-			

NOTES: a) Isentropic Mach numbers

1) c_p as a function of x
2) Δc_p " " " " x
3) C_F " " " " σ
4) C_F " " " " $M_{2,is}$
5) C_F " " " " β_1
6) C_M as a function of σ
7) C_M " " " " $M_{2,is}$
8) C_M " " " " β_1
9) Ξ " " " " σ
10) Ξ " " " " $M_{2,is}$
11) Ξ " " " " β_1

Table 3.6-2 Sixth Standard Configuration: 26 Recommended Aeroelastic Cases

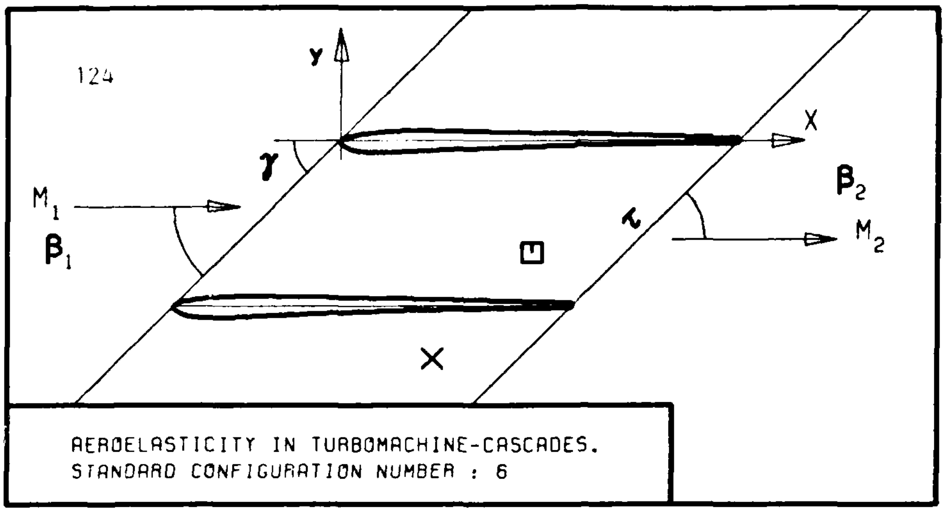

c :
τ :
γ :
x_α :
y_α :
M_1 :
β_1 :
i :
M_2 :
β_2 :
$\bar{h}_X$:
$\bar{h}_Y$:
$\bar{\alpha}$:
ω :
k :
δ :
σ :
d :

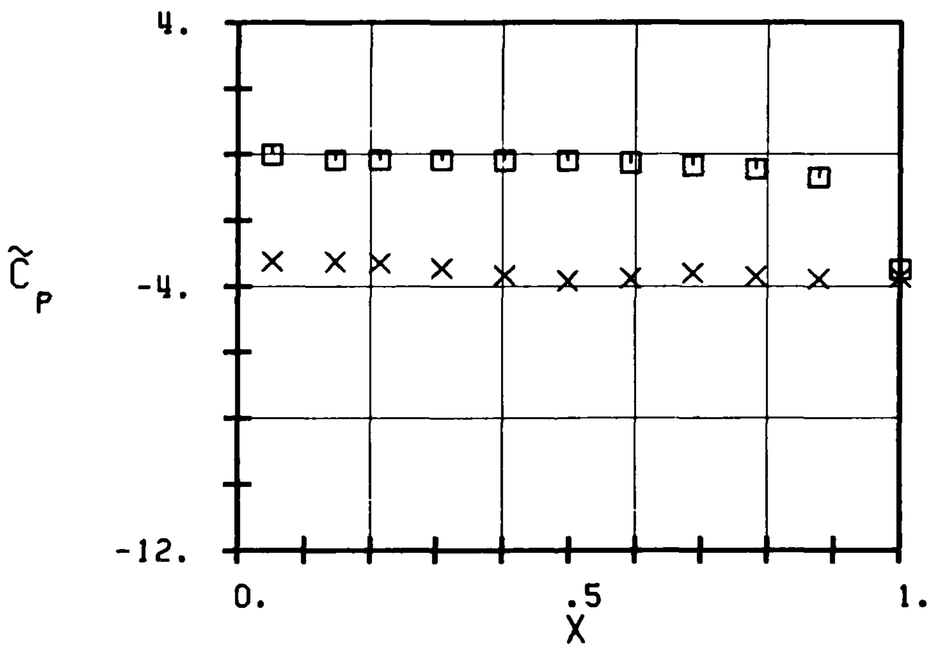

FIG. 3.6-2A: SIXTH STANDARD CONFIGURATION.
TIME AVERAGED BLADE SURFACE PRESSURE
COEFFICIENT FOR B1=20 DEG AND M2(IS)=1.63

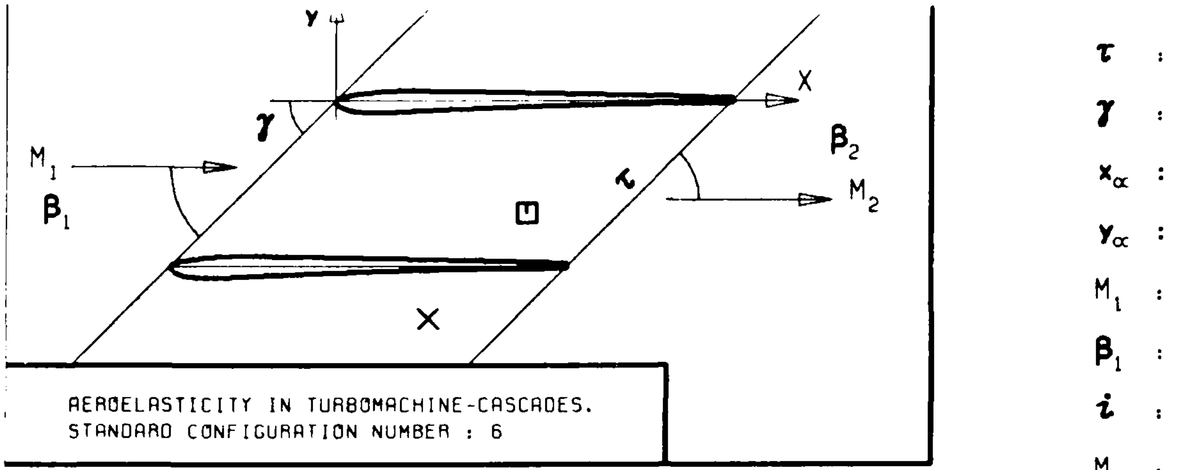

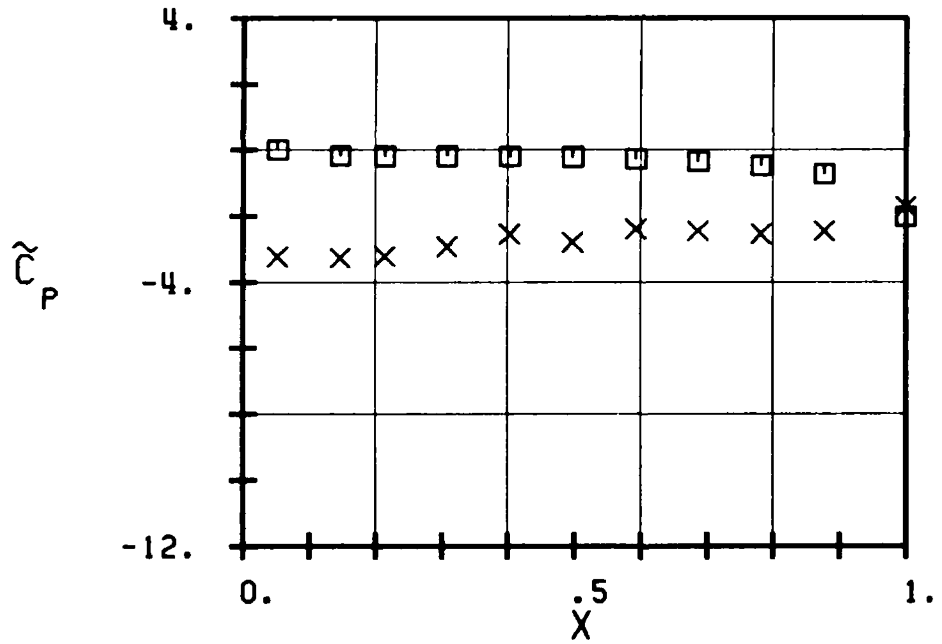

FIG. 3.6-28: SIXTH STANDARD CONFIGURATION.
TIME AVERAGED BLADE SURFACE PRESSURE
COEFFICIENT FOR B1=20 DEG AND M2(IS)=1.20

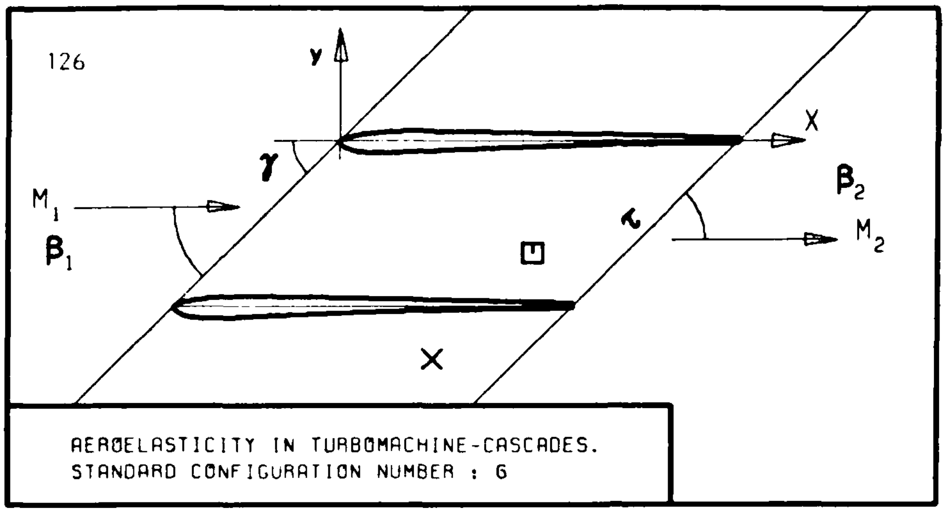

c :
τ :
γ :
x_α :
y_α :
M_1 :
β_1 :
i :
M_2 :
β_2 :
$\bar{h}_X$:
$\bar{h}_Y$:
$\bar{\alpha}$:
ω :
k :
δ :
σ :
d :

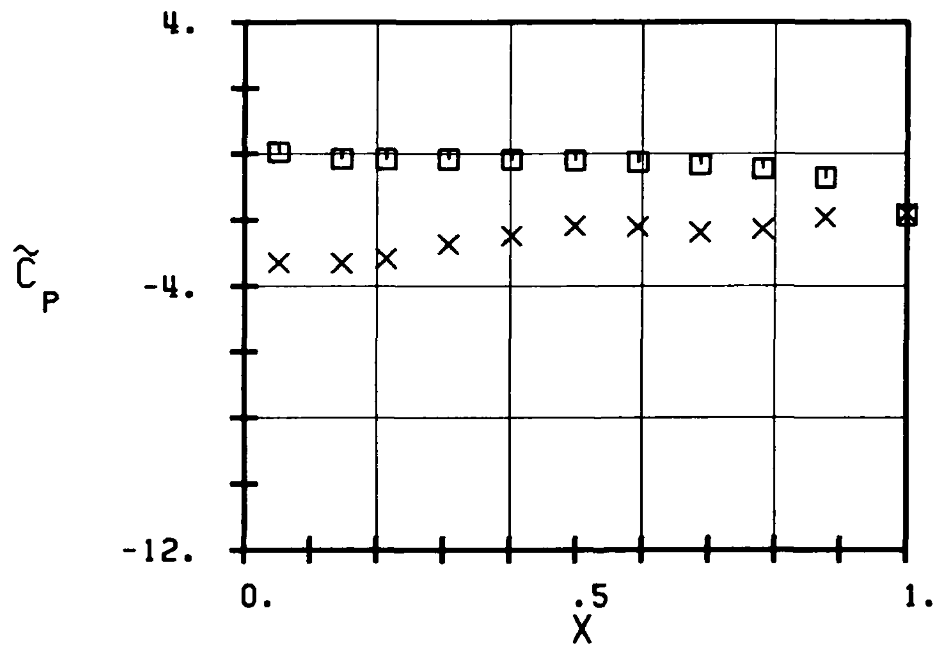

FIG. 3.6-2C: SIXTH STANDARD CONFIGURATION.
TIME AVERAGED BLADE SURFACE PRESSURE
COEFFICIENT FOR B1=20 DEG AND M2(IS)=1.14

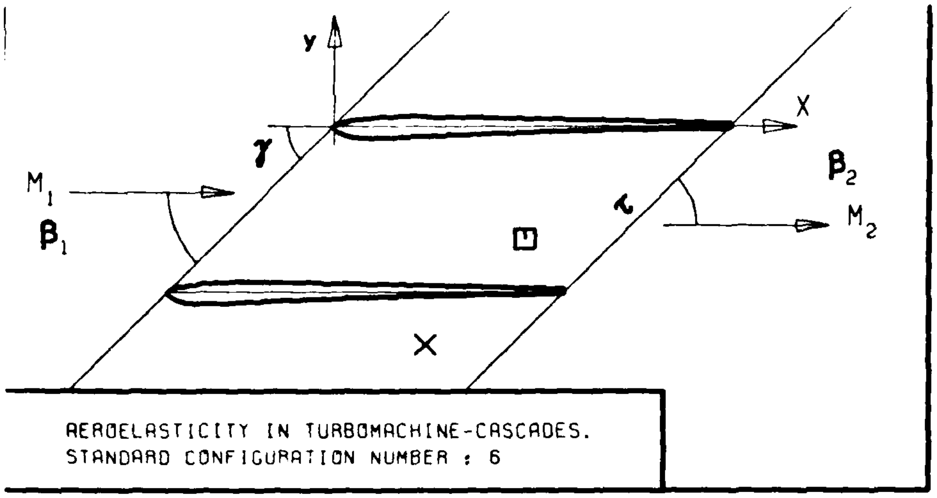

c	:
τ	:
γ	:
x_α	:
y_α	:
M_1	:
β_1	:
i	:
M_2	:
β_2	:
$\bar{h}_X$	:
$\bar{h}_Y$	:
$\bar{\alpha}$	:
ω	:
k	:
δ	:
σ	:
d	:

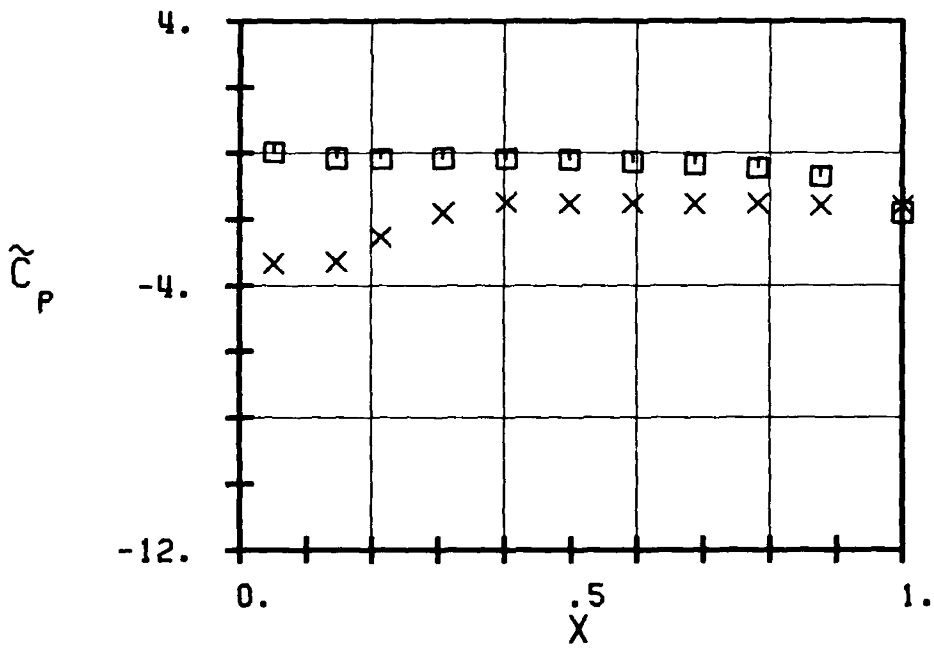

FIG. 3.6-20: SIXTH STANDARD CONFIGURATION.
TIME AVERAGED BLADE SURFACE PRESSURE
COEFFICIENT FOR B1=20 DEG AND M2(IS)=1.02

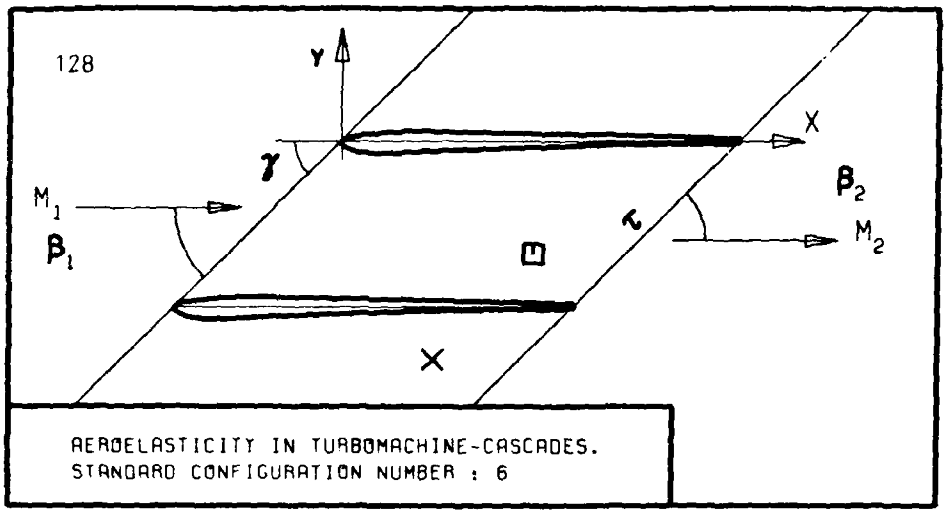

c :
τ :
γ :
x_α :
y_α :
M_1 :
β_1 :
i :
M_2 :
β_2 :
$\bar{h}_X$:
$\bar{h}_Y$:
$\bar{\alpha}$:
ω :
k :
δ :
σ :
d :

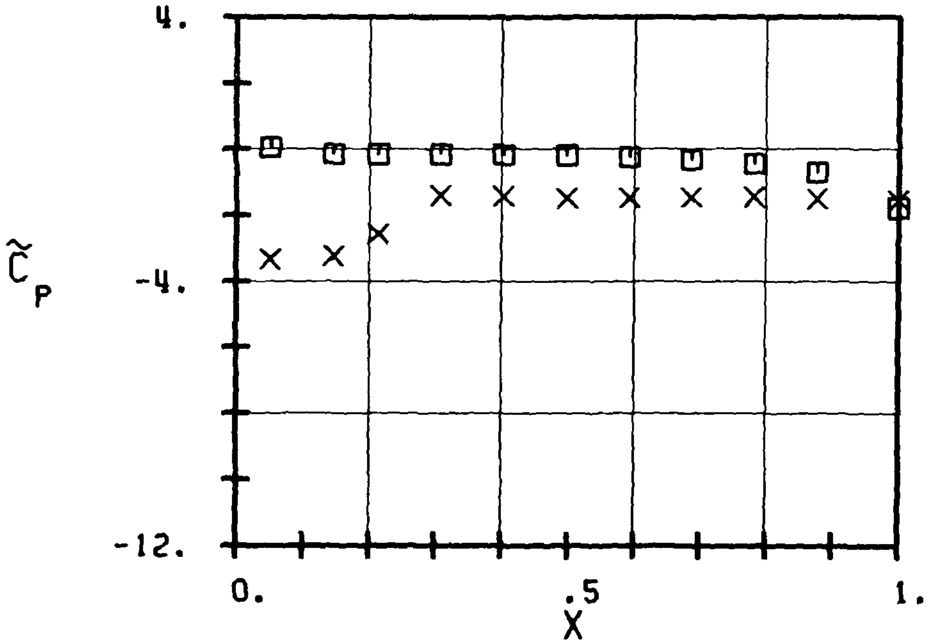

FIG. 3.6-2E: SIXTH STANDARD CONFIGURATION.
TIME AVERAGED BLADE SURFACE PRESSURE
COEFFICIENT FOR B1=20 DEG AND M2(IS)=0.98

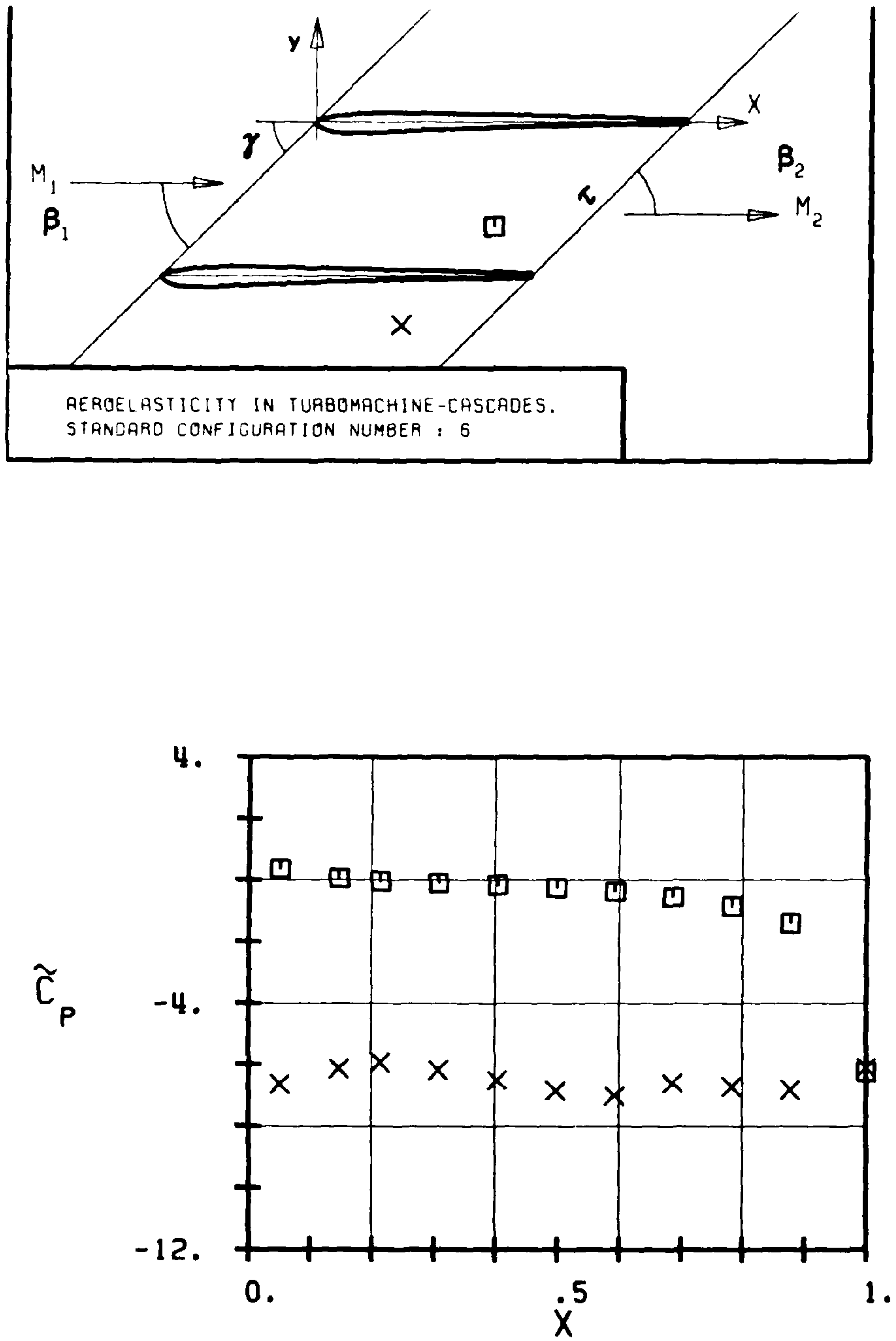

c :
τ :
γ :
x_α :
y_α :
M_1 :
β_1 :
i :
M_2 :
β_2 :
$\bar{h}_X$:
$\bar{h}_Y$:
$\bar{\alpha}$:
ω :
k :
δ :
σ :
d :

FIG. 3.6-2F: SIXTH STANDARD CONFIGURATION.
TIME AVERAGED BLADE SURFACE PRESSURE
COEFFICIENT FOR B1=25 DEG AND M2(IS)=1.60

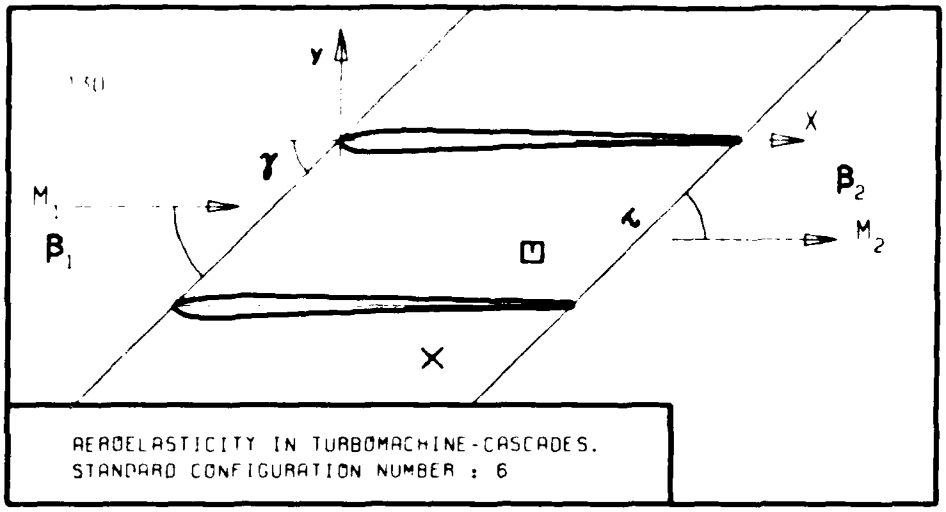

c :
τ :
γ :
x_α :
y_α :
M_1 :
β_1 :
i :
M_2 :
β_2 :
$\bar{h}_X$:
$\bar{h}_Y$:
$\bar{\alpha}$:
ω :
k :
δ :
σ :
d :

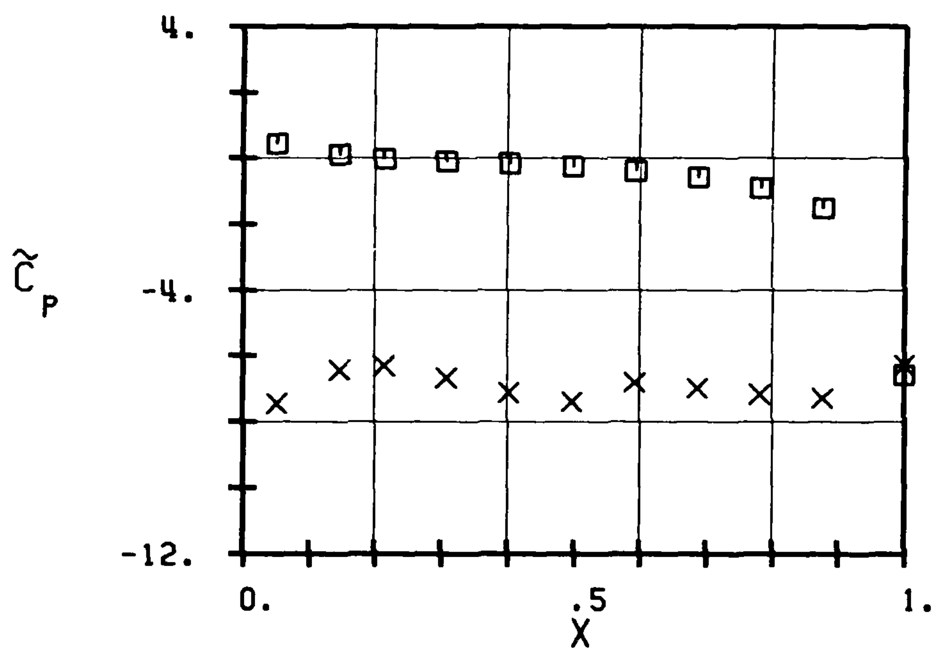

FIG. 3.6-2G: SIXTH STANDARD CONFIGURATION.
TIME AVERAGED BLADE SURFACE PRESSURE
COEFFICIENT FOR B1=27 DEG AND M2(IS)=1.61

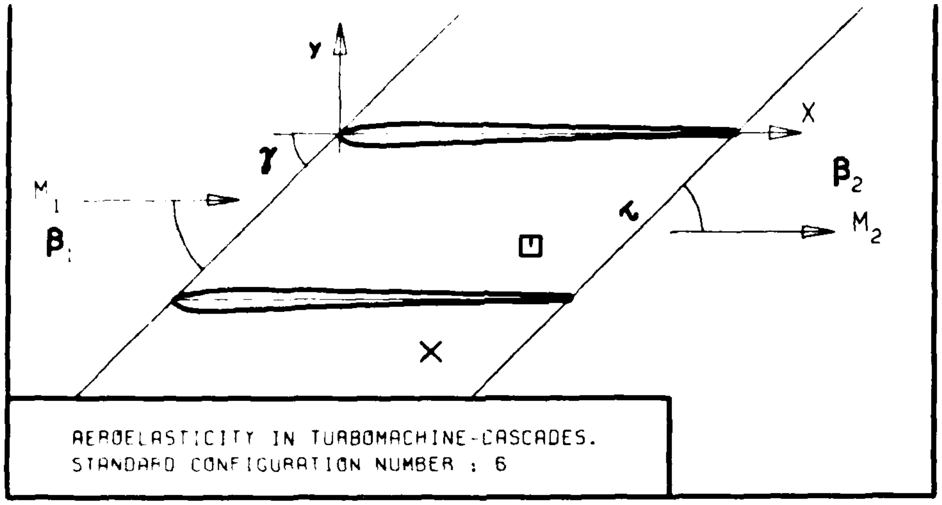

c :
τ :
γ :
x_α :
y_α :
M_1 :
β_1 :
i :
M_2 :
β_2 :
$\bar{h}_X$:
$\bar{h}_Y$:
$\bar{\alpha}$:
ω :
k :
δ :
σ :
d :

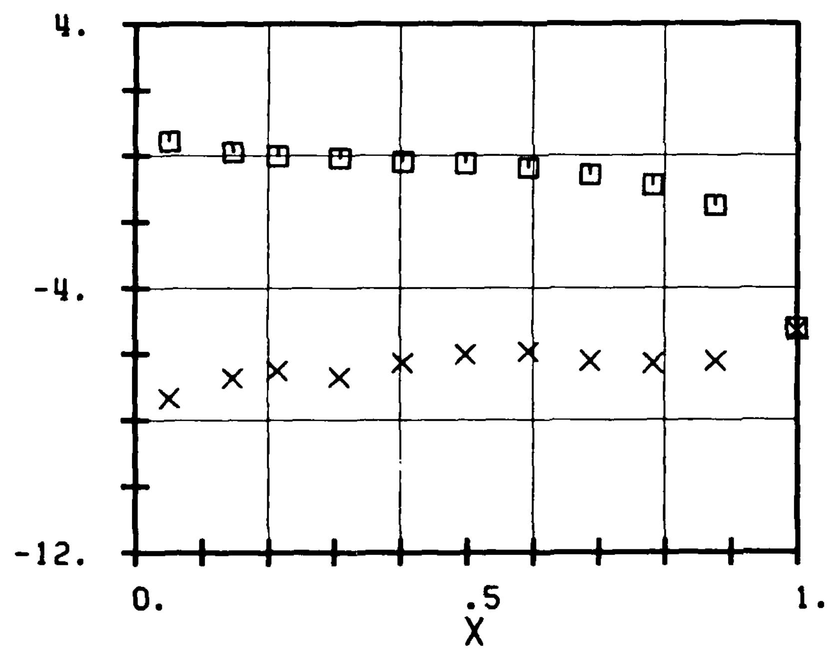

FIG. 3.6-2H: SIXTH STANDARD CONFIGURATION.
TIME AVERAGED BLADE SURFACE PRESSURE
COEFFICIENT FOR B1=27 DEG AND M2(IS)=1.40

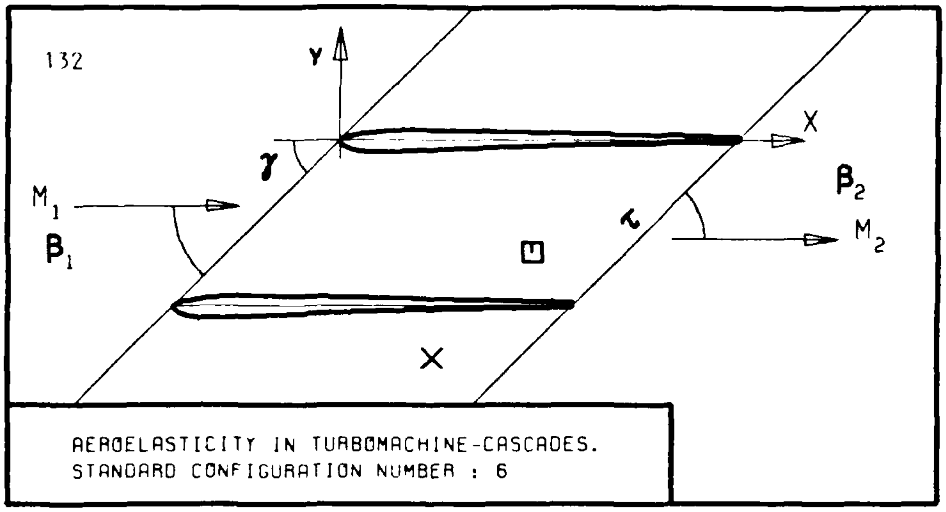

c :
τ :
γ :
x_α :
y_α :
M_1 :
β_1 :
i :
M_2 :
β_2 :
$\bar{h}_X$:
$\bar{h}_Y$:
$\bar{\alpha}$:
ω :
k :
δ :
σ :
d :

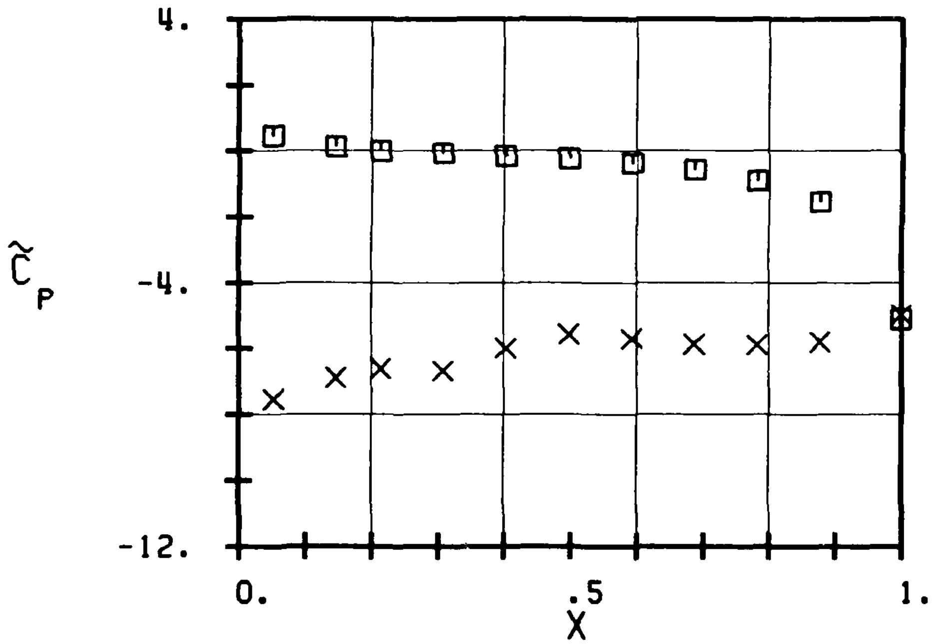

FIG. 3.6-21: SIXTH STANDARD CONFIGURATION.
TIME AVERAGED BLADE SURFACE PRESSURE
COEFFICIENT FOR B1=27 DEG AND M2(IS)=1.37

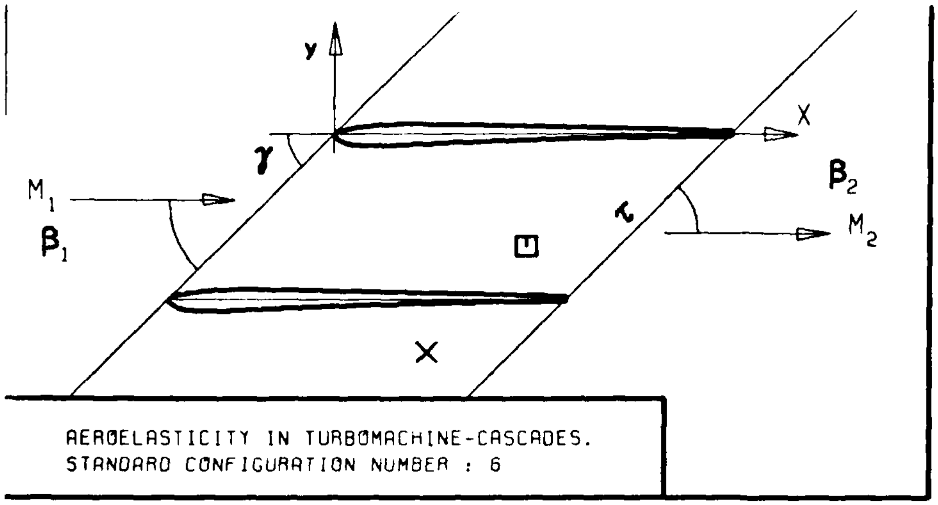

c :
τ :
γ :
x_α :
y_α :
M_1 :
β_1 :
i :
M_2 :
β_2 :
$\bar{h}_X$:
$\bar{h}_Y$:
$\bar{\alpha}$:
ω :
k :
δ :
σ :
d :

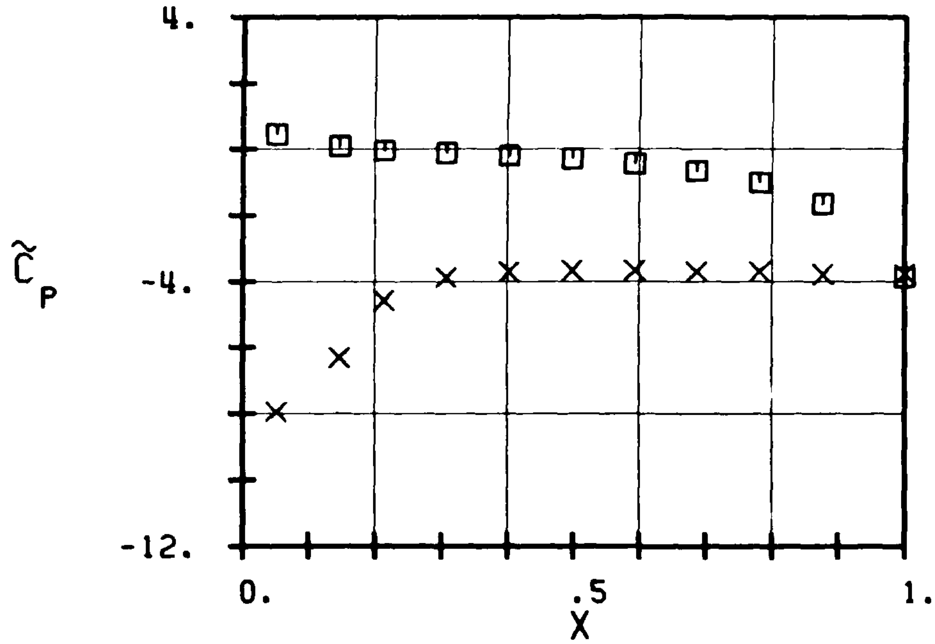

FIG. 3.6-2K: SIXTH STANDARD CONFIGURATION.
TIME AVERAGED BLADE SURFACE PRESSURE
COEFFICIENT FOR B1=28 DEG AND M2(IS)=0.95

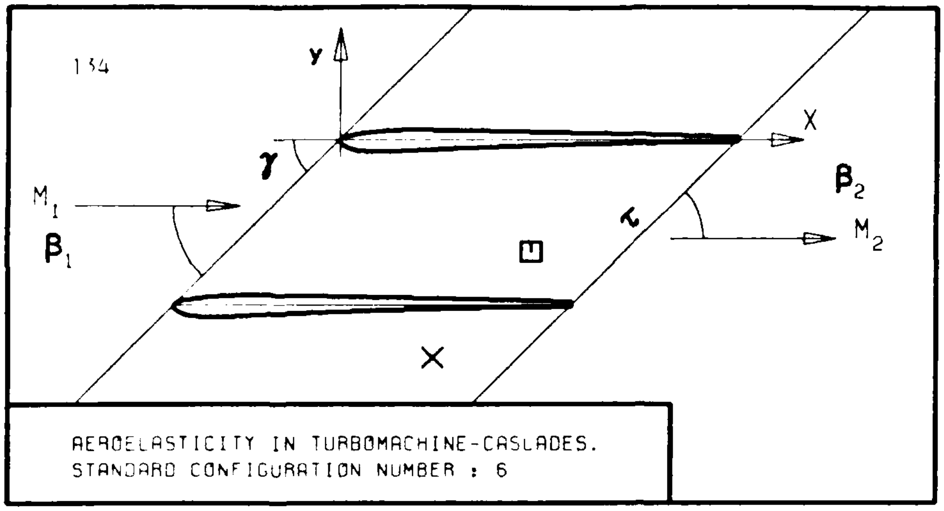

c :
τ :
γ :
x_α :
y_α :
M_1 :
β_1 :
i :
M_2 :
β_2 :
$\bar{h}_X$:
$\bar{h}_Y$:
$\bar{\alpha}$:
ω :
k :
δ :
σ :
d :

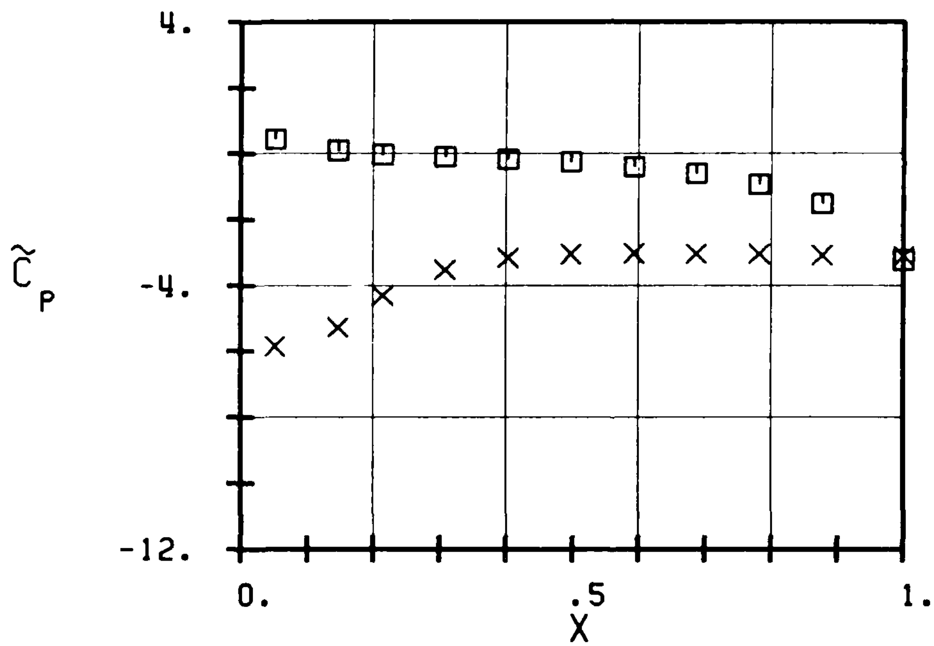

FIG. 3.6-2L: SIXTH STANDARD CONFIGURATION.
TIME AVERAGED BLADE SURFACE PRESSURE
COEFFICIENT FOR B1=28 DEG AND M2(IS)=0.85

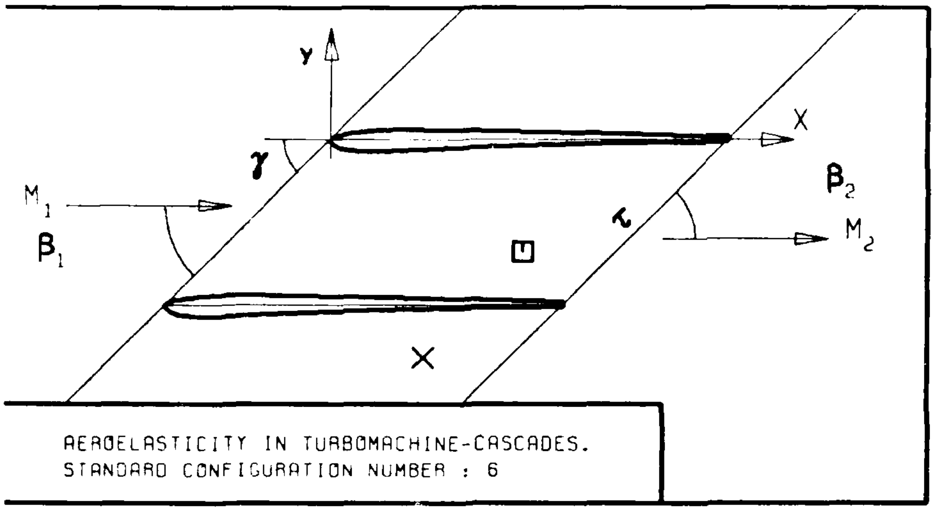

c :
τ :
γ :
x_α :
y_α :
M_1 :
β_1 :
i :
M_2 :
β_2 :
$\bar{h}_X$:
$\bar{h}_Y$:
$\bar{\alpha}$:
ω :
k :
δ :
σ :
d :

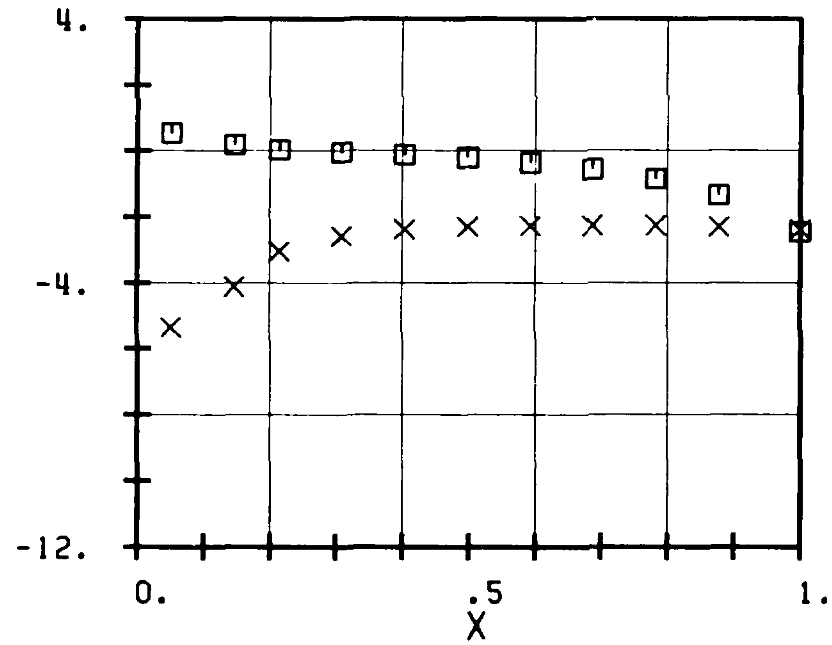

FIG. 3.6-2M: SIXTH STANDARD CONFIGURATION.
TIME AVERAGED BLADE SURFACE PRESSURE
COEFFICIENT FOR B1=28 DEG AND M2(IS)=0.57

Aeroelasticity in Turbomachine-Cascades Sixth Standard Configuration Time Averaged Blade Surface Pressure Distributions												
Aeroelastic case No	1 - 8	9	10	11	12 - 19	20	21	22	23	24	25	26
$\tilde{M}_{1is}$ (-)	0.53	0.52	0.52	0.52	0.52	0.40	0.39	0.39	0.39	0.37	0.37	0.30
$\tilde{\beta}_1$ (°)	20	20	20	20	20	25	27	27	27	28	28	28
$\tilde{p}_2/\tilde{p}_1$ (-)	0.27	0.50	0.54	0.62	0.65	0.26	0.26	0.35	0.37	0.61	0.69	0.85
$\tilde{M}_{2is}$ (-)	1.63	1.20	1.14	1.02	0.98	1.60	1.61	1.40	1.37	0.95	0.85	0.57
$\tilde{p}_{t1}$ (N/m²)	269'900	272'900	273'700	275'000	275'800	260'100	269'700	270'500	270'400	273'100	276'700	294'800
x (-)	$\tilde{c}_p$ (-)	$\tilde{c}_p$ (-)	$\tilde{c}_p$ (-)	$\tilde{c}_p$ (-)	$\tilde{c}_p$ (-)	$\tilde{c}_p$ (-)	$\tilde{c}_p$ (-)	$\tilde{c}_p$ (-)	$\tilde{c}_p$ (-)	$\tilde{c}_p$ (-)	$\tilde{c}_p$ (-)	$\tilde{c}_p$ (-)
Upper surface (pressure surface)												
0.052	-0.005	0.004	0.057	0.035	0.056	0.357	0.433	0.440	0.456	0.457	0.111	0.543
0.147	-0.166	-0.174	-0.142	-0.154	-0.141	0.061	0.104	0.112	0.125	0.095	0.093	0.179
0.214	-0.177	-0.187	-0.160	-0.165	-0.160	-0.036	-0.022	-0.007	-0.004	-0.038	-0.033	0.035
0.308	-0.168	-0.180	-0.155	-0.162	-0.152	-0.094	-0.089	-0.075	-0.072	-0.111	-0.093	-0.040
0.403	-0.183	-0.193	-0.171	-0.175	-0.165	-0.159	-0.163	-0.179	-0.152	-0.193	-0.171	-0.116
0.498	-0.202	-0.215	-0.190	-0.197	-0.184	-0.242	-0.241	-0.228	-0.233	-0.284	-0.252	-0.208
0.593	-0.263	-0.277	-0.252	-0.262	-0.247	-0.375	-0.385	-0.373	-0.378	-0.442	-0.402	-0.364
0.687	-0.335	-0.350	-0.326	-0.331	-0.321	-0.549	-0.579	-0.571	-0.578	-0.654	-0.606	-0.561
0.782	-0.455	-0.474	-0.455	-0.455	-0.448	-0.845	-0.904	-0.900	-0.913	-1.008	-0.931	-0.861
0.877	-0.707	-0.734	-0.720	-0.710	-0.706	-1.397	-1.511	-1.519	-1.544	-1.659	-1.521	-1.341
1.000	-3.493	-2.019	-1.862	-1.812	-1.786	-6.227	-6.570	-5.243	-5.114	-3.881	-3.232	-2.451
Lower surface (pressure surface))												
0.052	-3.244	-3.233	-3.298	-3.335	-3.327	-6.635	-7.447	-7.332	-7.546	-7.958	-5.816	-3.338
0.147	-3.255	-3.264	-3.309	-3.279	-3.232	-6.126	-6.427	-6.725	-6.890	-6.302	-5.272	-4.116
0.214	-3.297	-3.217	-3.162	-2.537	-2.554	-5.921	-6.302	-6.496	-6.616	-4.580	-4.309	-3.035
0.308	-3.451	-2.927	-2.740	-1.812	-1.400	-6.173	-6.663	-6.698	-6.677	-3.878	-3.528	-2.590
0.403	-3.678	-2.547	-2.479	-1.487	-1.422	-6.491	-7.114	-6.272	-5.989	-3.708	-3.167	-2.382
0.498	-3.842	-2.794	-2.175	-1.523	-1.483	-6.838	-7.389	-6.007	-5.574	-3.668	-3.019	-2.306
0.593	-3.767	-2.399	-2.208	-1.517	-1.481	-7.000	-6.804	-5.940	-5.711	-3.669	-3.028	-2.277
0.687	-3.602	-2.459	-2.368	-1.526	-1.472	-6.596	-6.976	-6.207	-5.871	-3.700	-3.045	[illegible]
0.782	-3.701	-2.541	-2.278	-1.517	-1.452	-6.715	-7.163	-6.280	-5.882	-3.708	-3.037	-2.260
0.877	-3.775	-2.459	-1.921	-1.582	-1.507	-6.809	-7.278	-6.216	-5.791	-3.701	-3.085	-2.306
1.000	-3.759	-1.719	-1.807	-1.591	-1.552	-6.083	-6.283	-5.289	-4.966	-3.771	-3.111	-2.376

Note: The pressures at x= 1.000 are the trailing edge pressures measured on two different blades.

Table 3.6-3 Sixth Standard Configuration: Time Averaged Blade Surface Pressure Distribution for the 26 Recommended Aeroelastic Cases

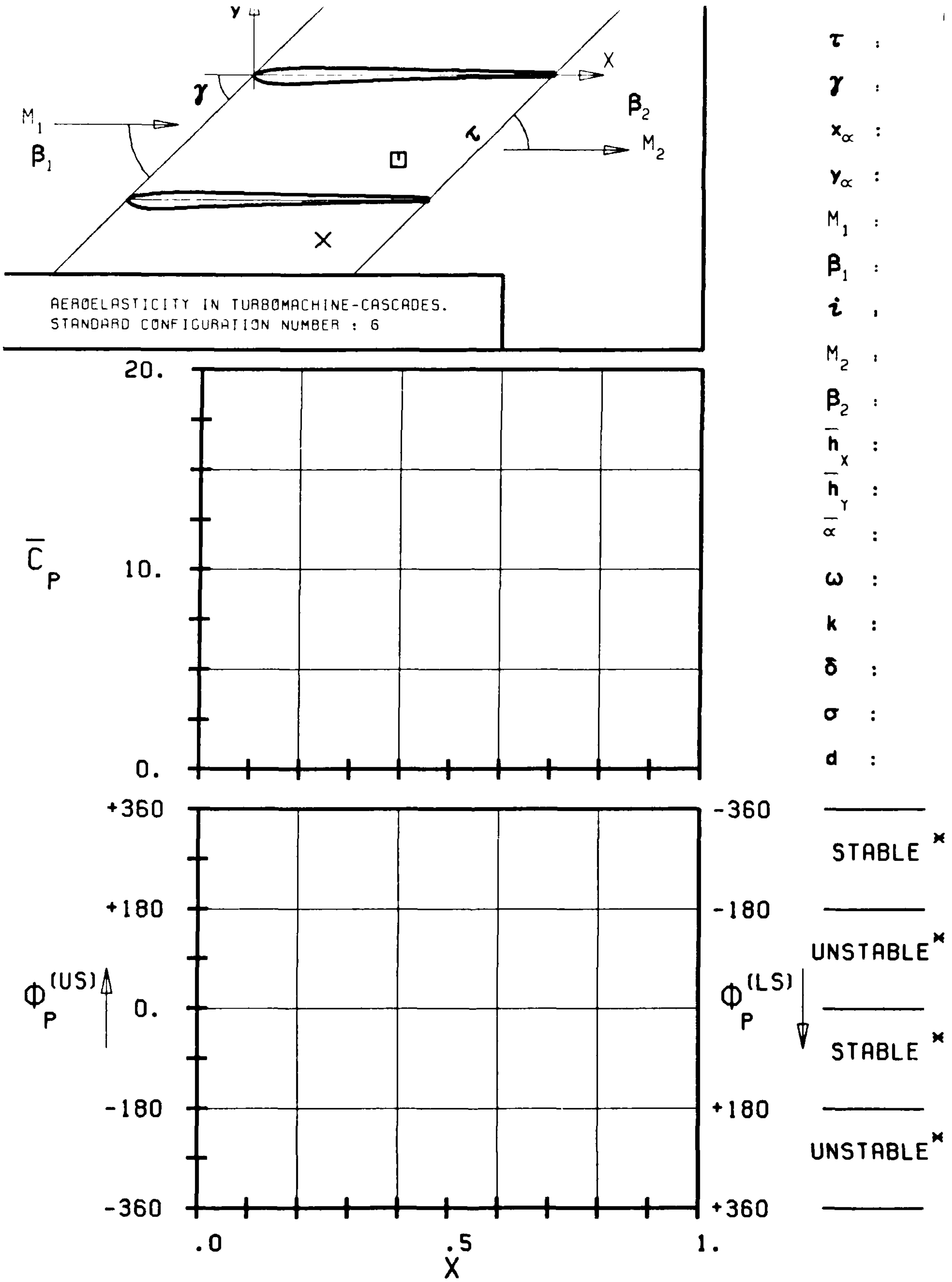

FIG. 3.6-3A: SIXTH STANDARD CONFIGURATION.
MAGNITUDE AND PHASE LEAD OF UNSTEADY BLADE SURFACE PRESSURE COEFFICIENT.

(*: IN PITCH MODE, NOTATION VALID UPSTREAM OF PITCH AXIS)

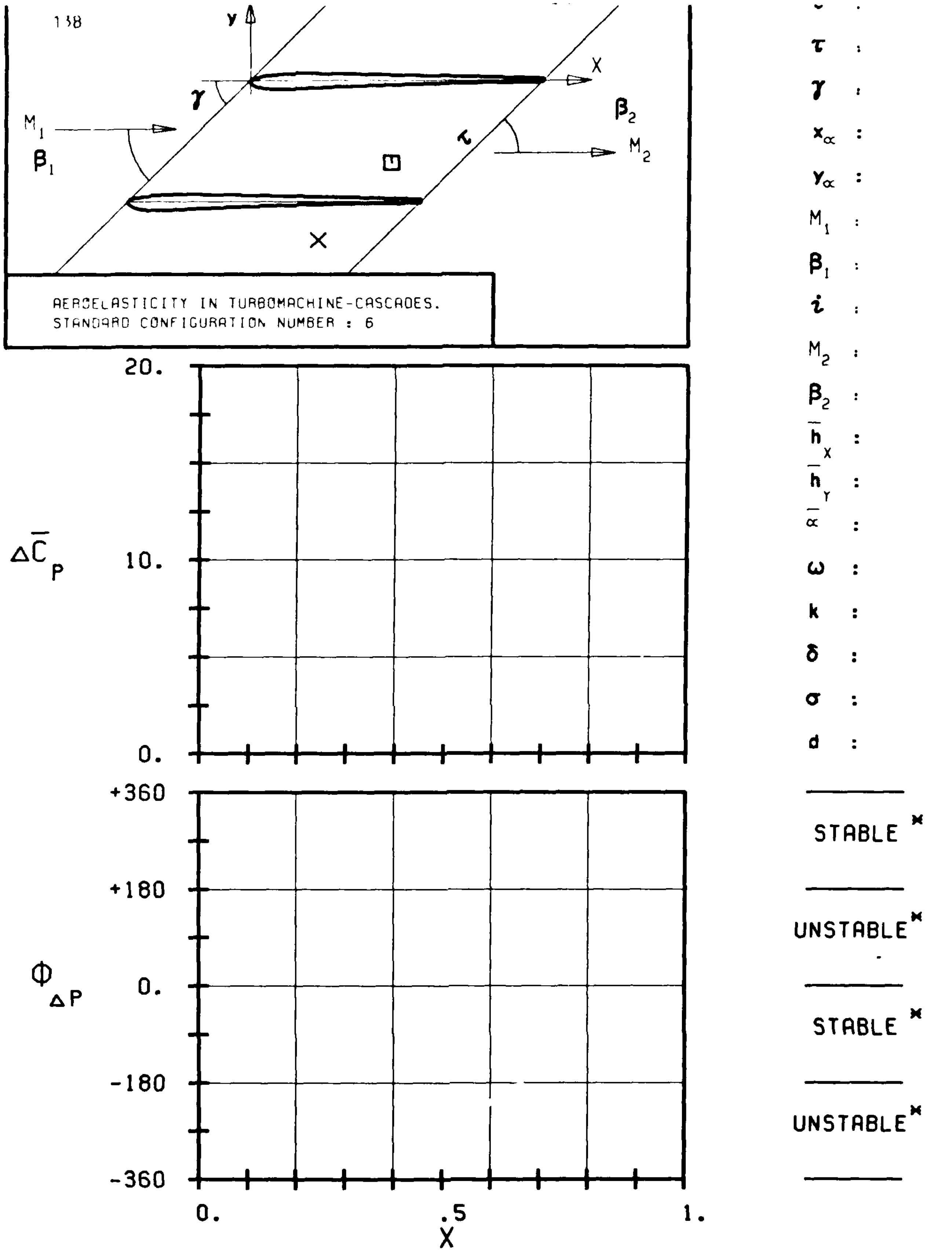

FIG. 3.6-3B: SIXTH STANDARD CONFIGURATION.
MAGNITUDE AND PHASE LEAD OF UNSTEADY BLADE SURFACE PRESSURE DIFFERENCE COEFFICIENT.
(*: IN PITCH MODE, NOTATION VALID UPSTREAM OF PITCH AXIS)

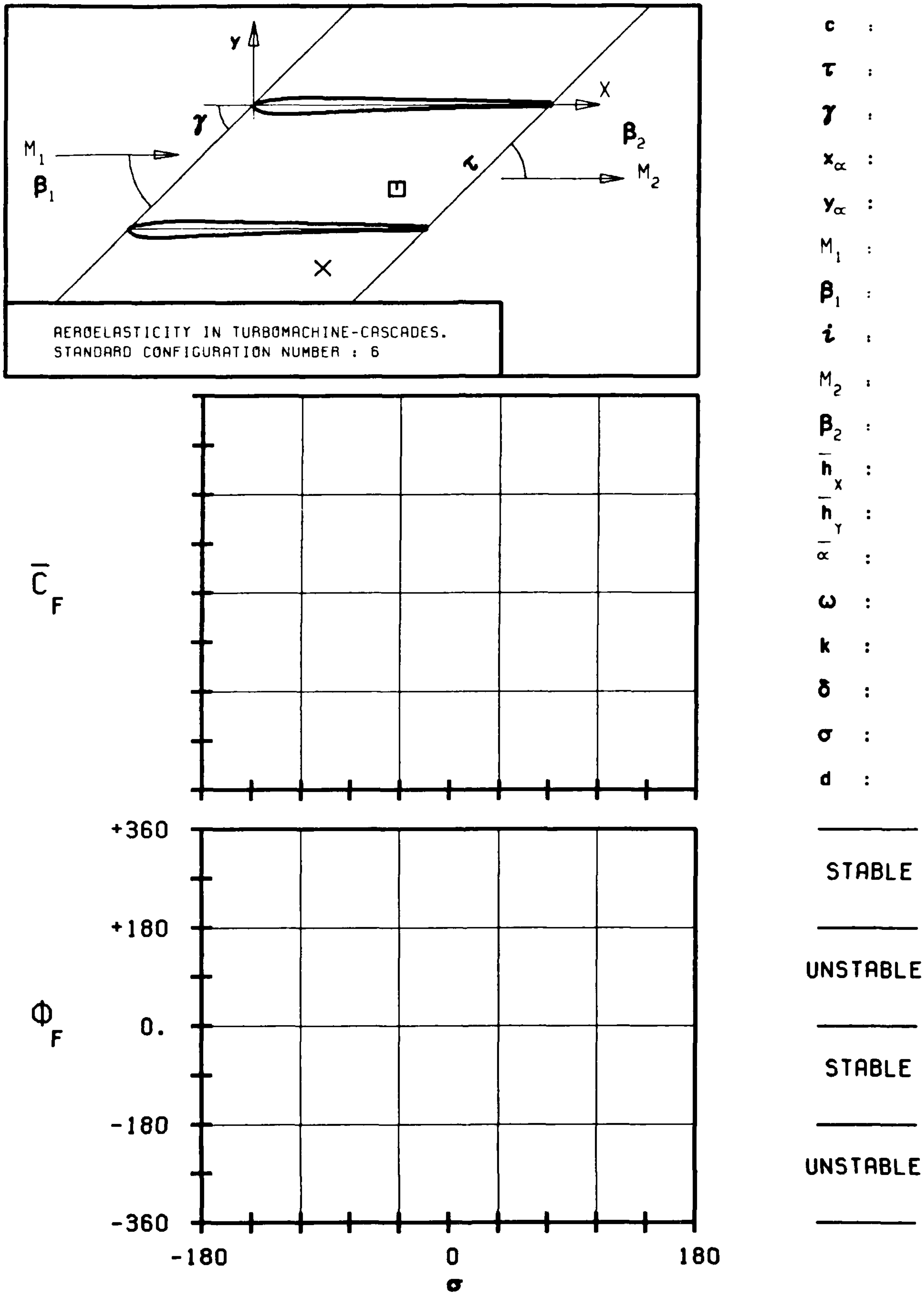

FIG. 3.6-3C: SIXTH STANDARD CONFIGURATION.
AERODYNAMIC FORCE COEFFICIENT AND PHASE LEAD
IN DEPENDANCE OF INTERBLADE PHASE ANGLE.

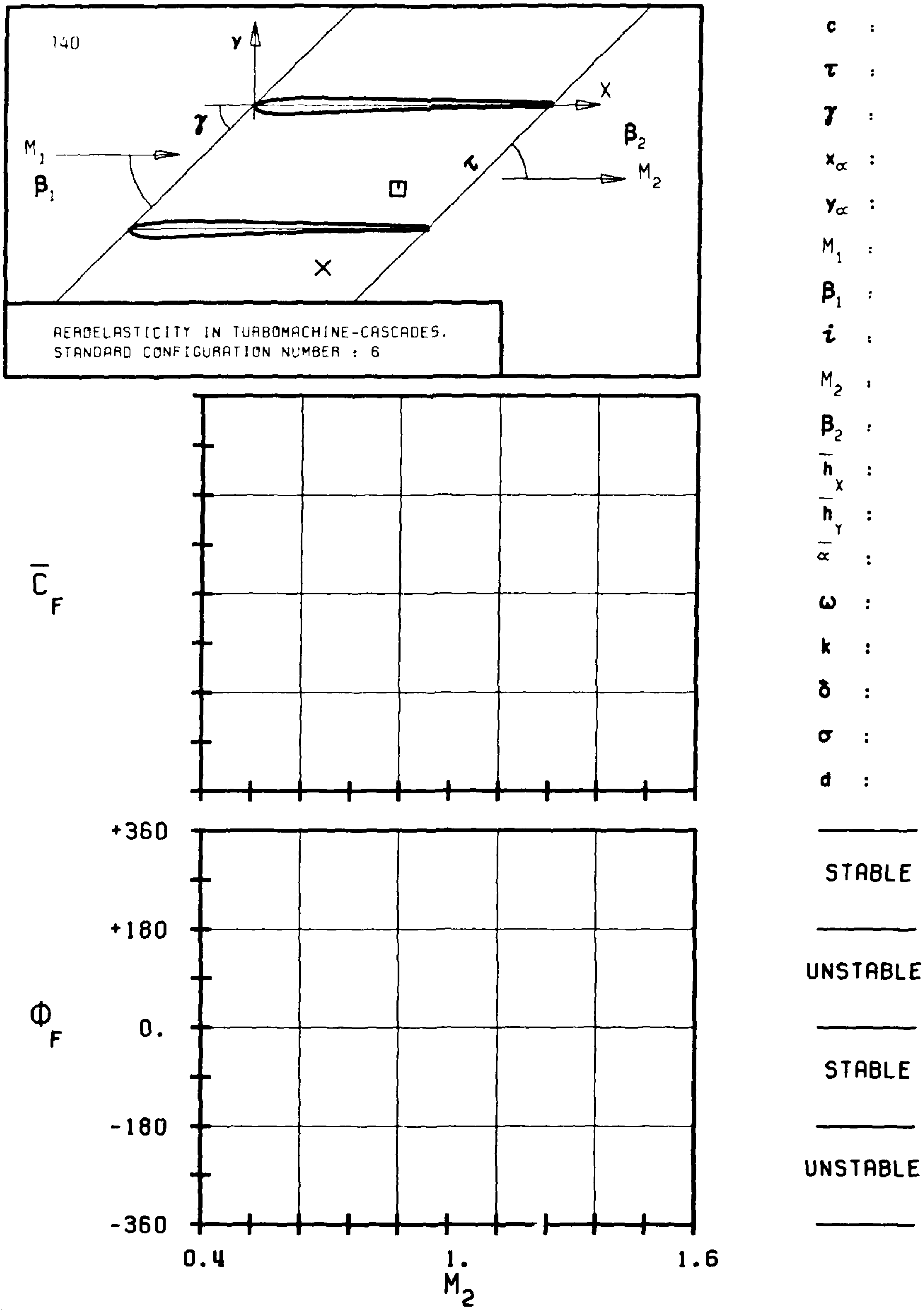

FIG. 3.6-3D: SIXTH STANDARD CONFIGURATION.
AERODYNAMIC FORCE COEFFICIENT AND PHASE LEAD
IN DEPENDANCE OF OUTLET ISENTROPIC VELOCITY M2(IS).

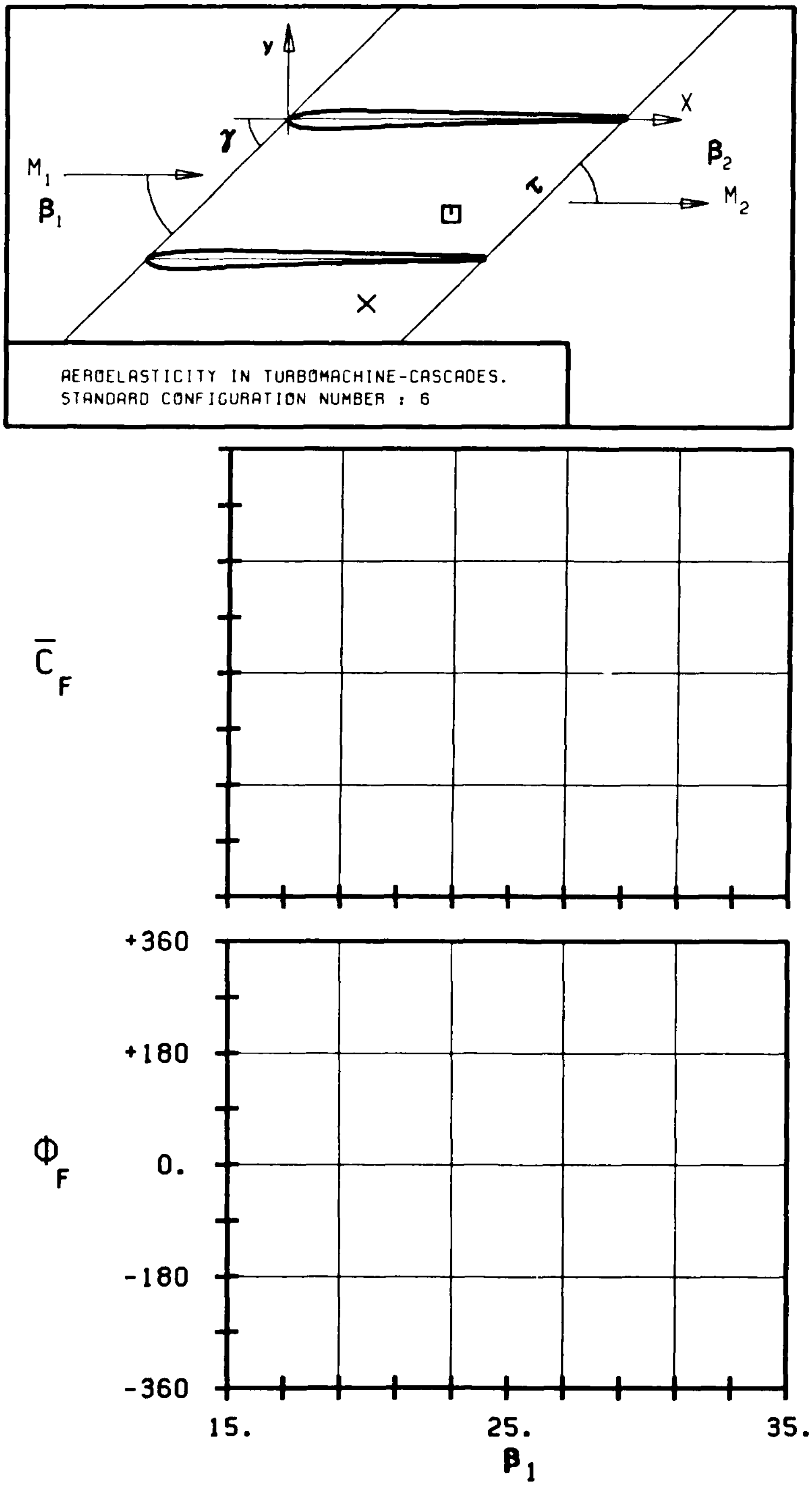

c :
τ :
γ :
x_α :
y_α :
M_1 :
β_1 :
i :
M_2 :
β_2 :
$\bar{h}_X$:
$\bar{h}_Y$:
$\bar{\alpha}$:
ω :
k :
δ :
σ :
d :

STABLE

UNSTABLE

STABLE

UNSTABLE

FIG. 3.6-3E: SIXTH STANDARD CONFIGURATION.
AERODYNAMIC FORCE COEFFICIENT AND PHASE LEAD
IN DEPENDANCE OF INLET FLOW ANGLE BETA1.

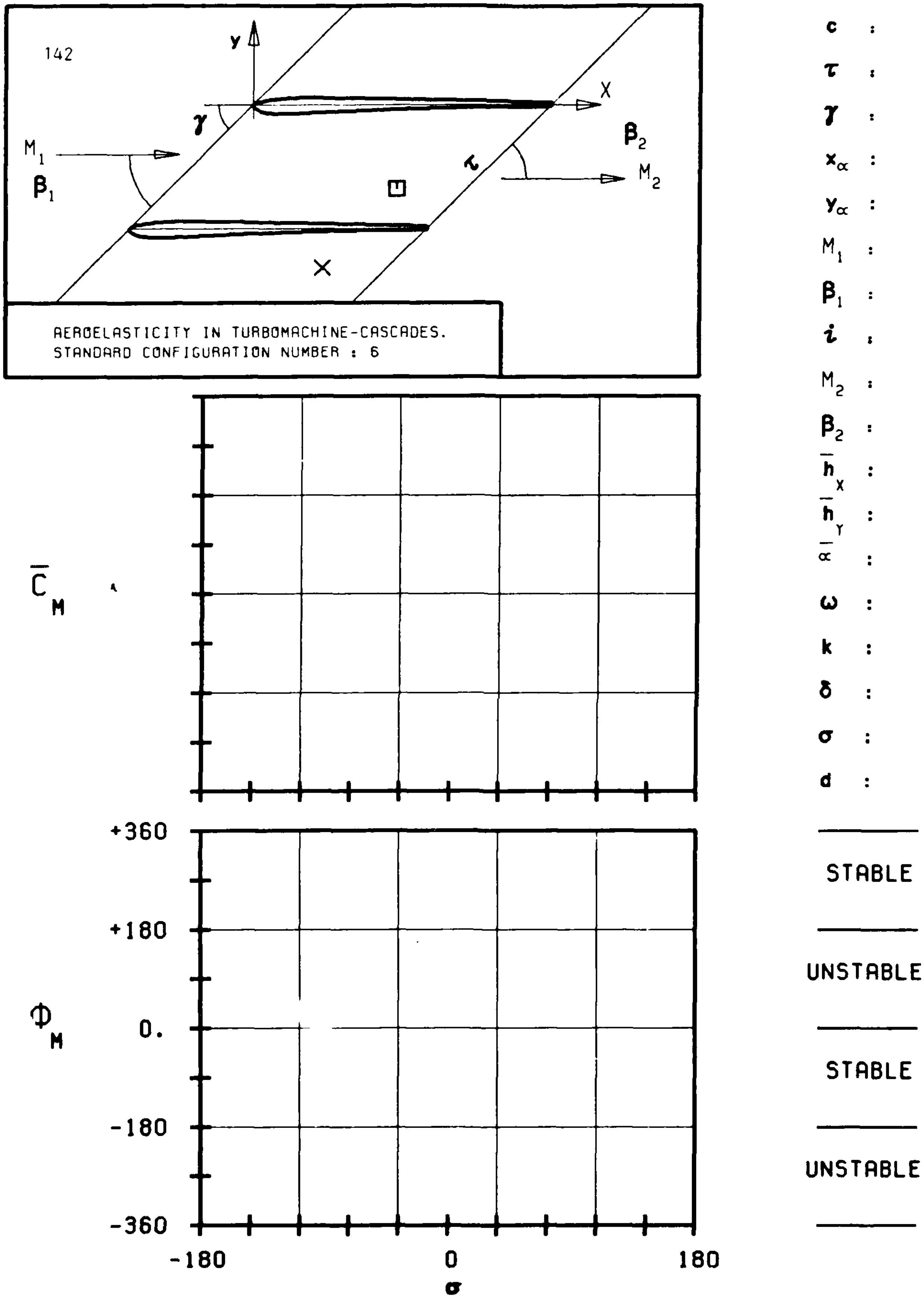

FIG. 3.6-3F: SIXTH STANDARD CONFIGURATION.
AERODYNAMIC MOMENT COEFFICIENT AND PHASE LEAD
IN DEPENDANCE OF INTERBLADE PHASE ANGLE.

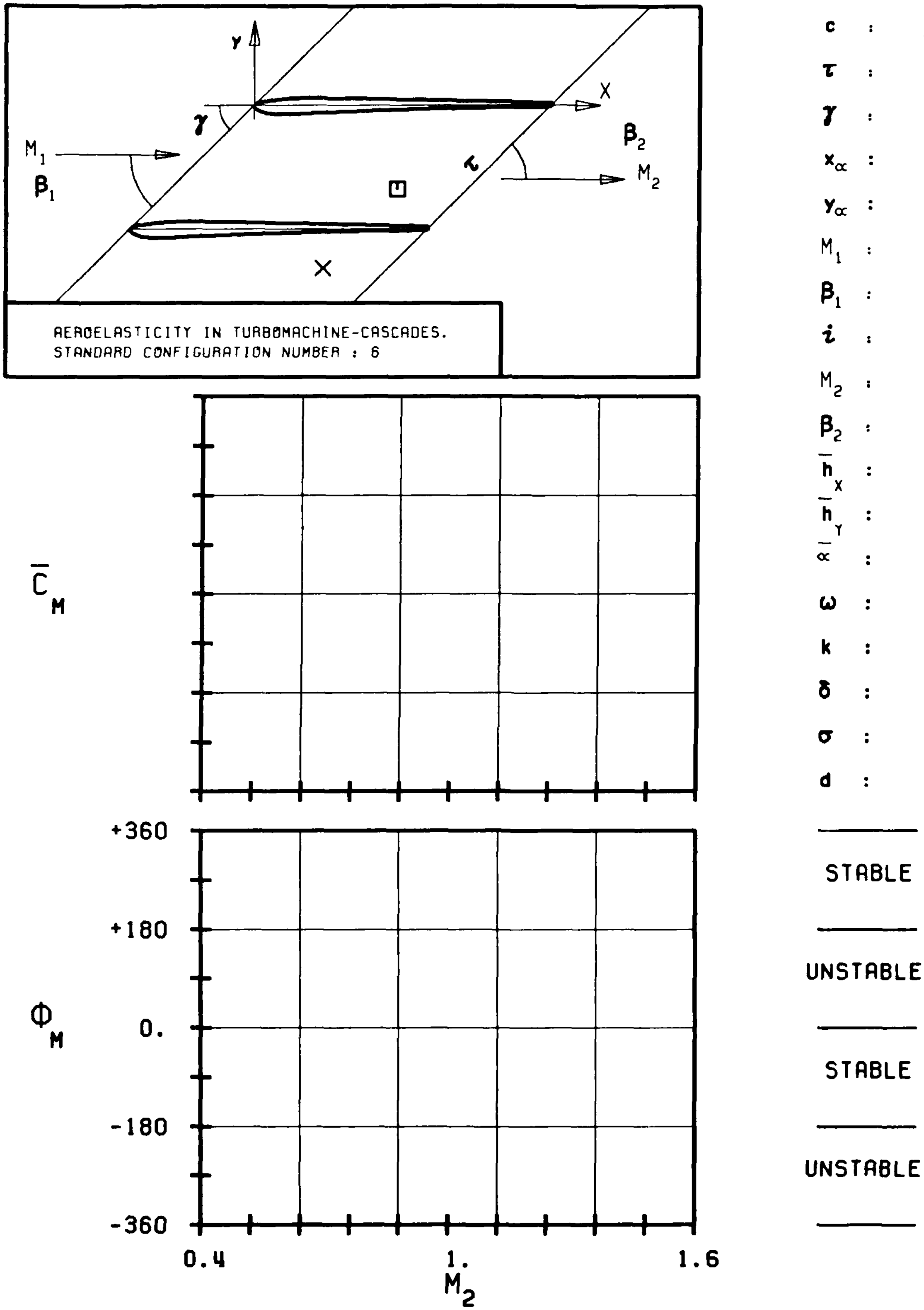

FIG. 3.6-36: SIXTH STANDARD CONFIGURATION.
AERODYNAMIC MOMENT COEFFICIENT AND PHASE LEAD
IN DEPENDANCE OF OUTLET ISENTROPIC VELOCITY M2(IS).

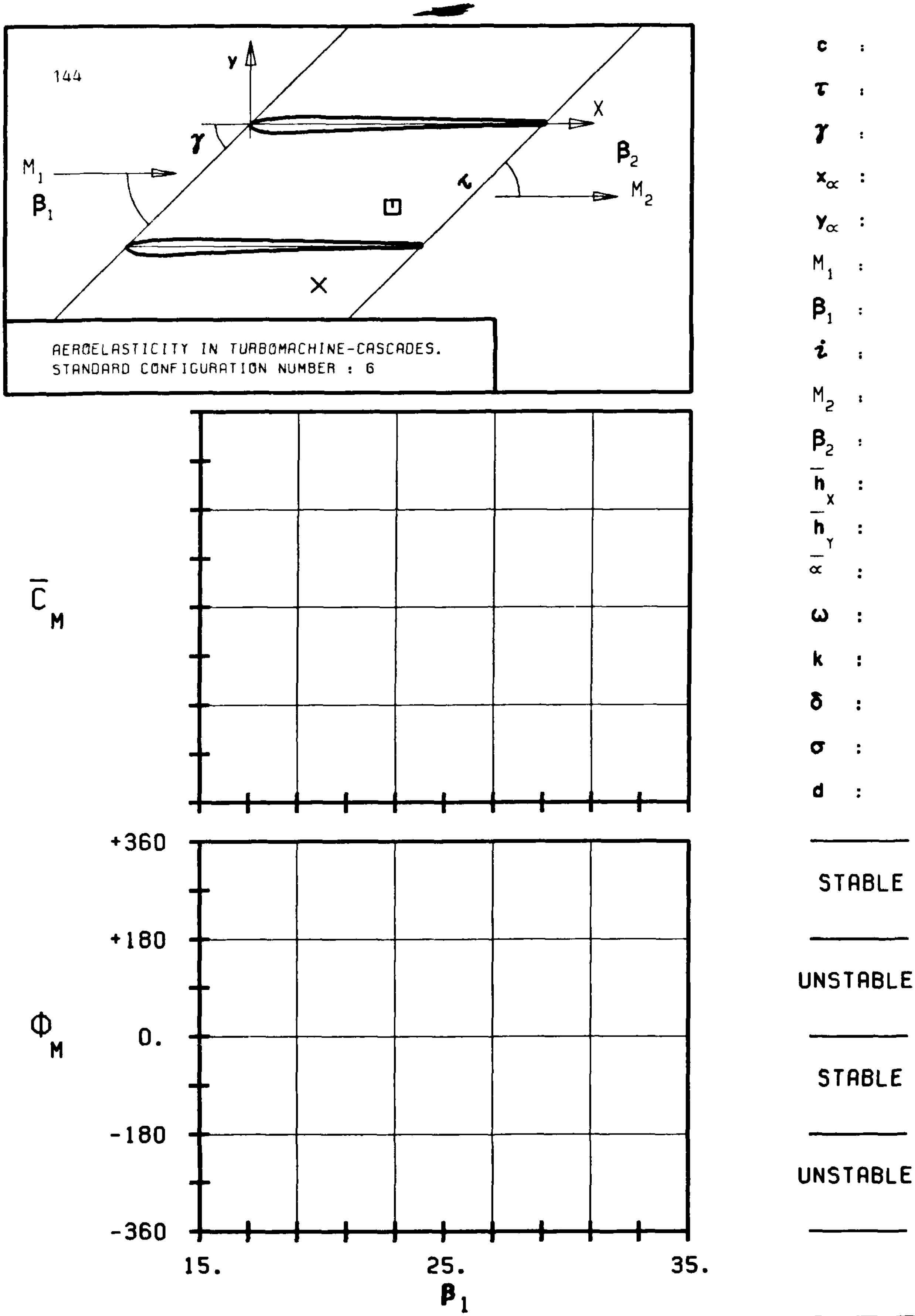

FIG. 3.6-3H: SIXTH STANDARD CONFIGURATION.
AERODYNAMIC MOMENT COEFFICIENT AND PHASE LEAD
IN DEPENDANCE OF INLET FLOW ANGLE BETA1.

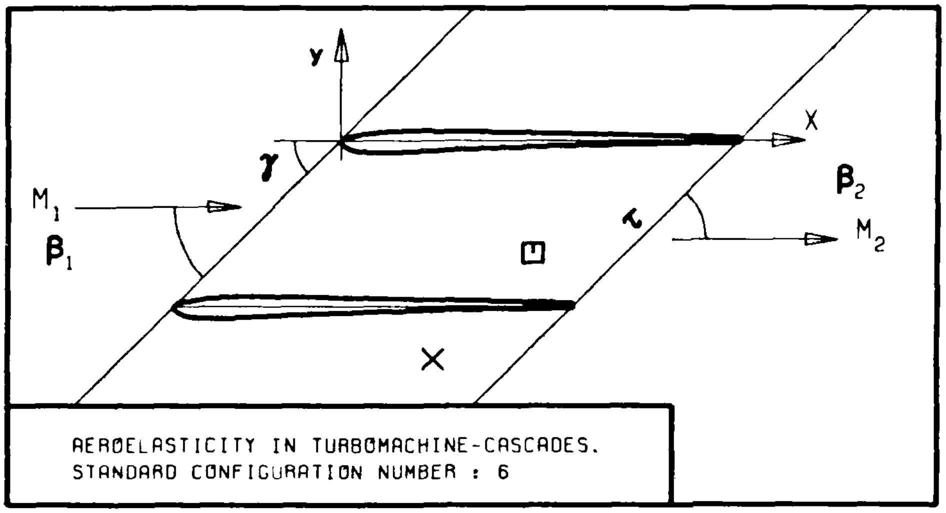

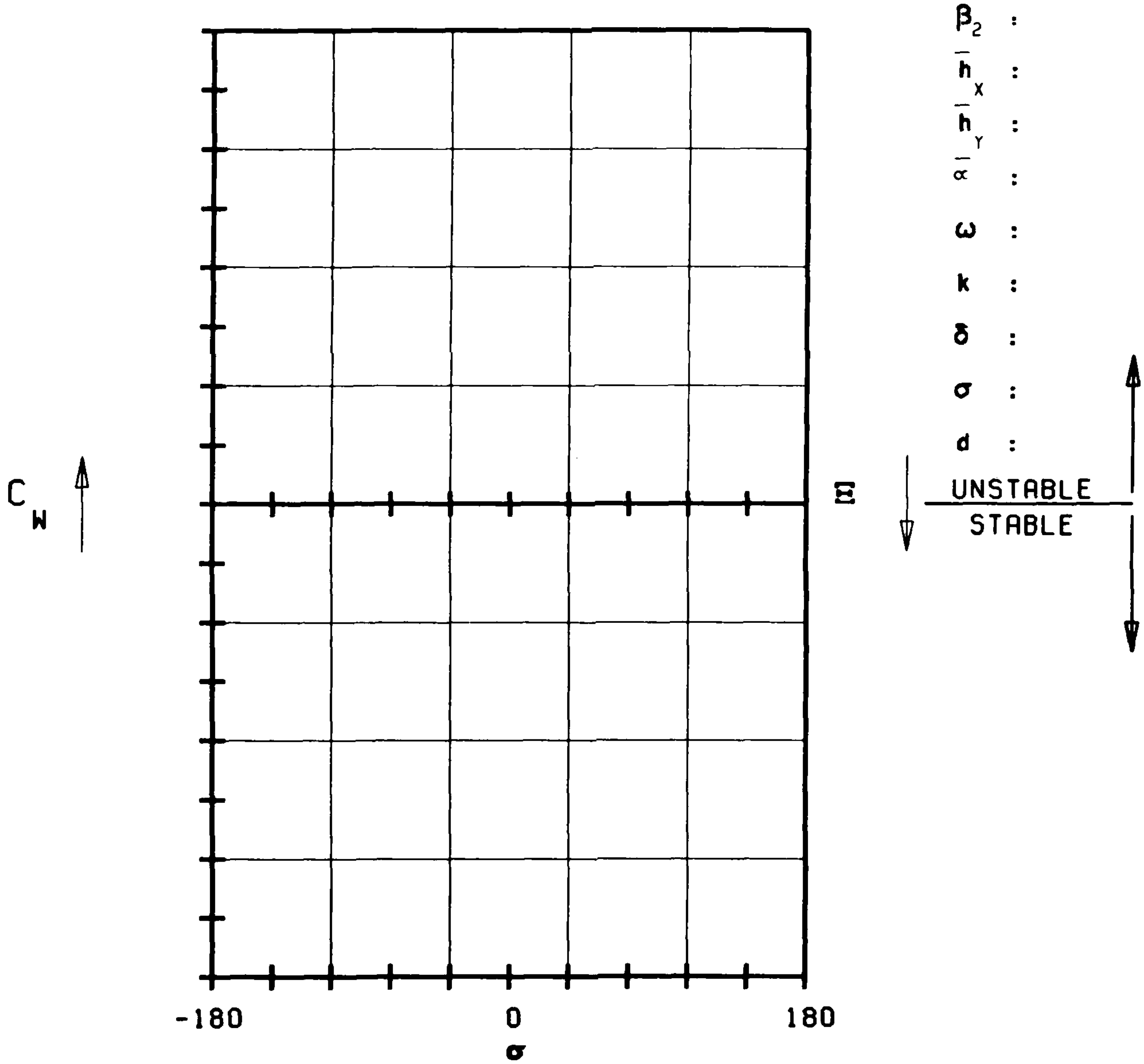

c :
τ :
γ :
x_α :
y_α :
M_1 :
β_1 :
i :
M_2 :
β_2 :
$\bar{h}_X$:
$\bar{h}_Y$:
$\bar{\alpha}$:
ω :
k :
δ :
σ :
d :

FIG. 3.6-31: SIXTH STANDARD CONFIGURATION.
AERODYNAMIC WORK AND DAMPING COEFFICIENTS
IN DEPENDANCE OF INTERBLADE PHASE ANGLE.

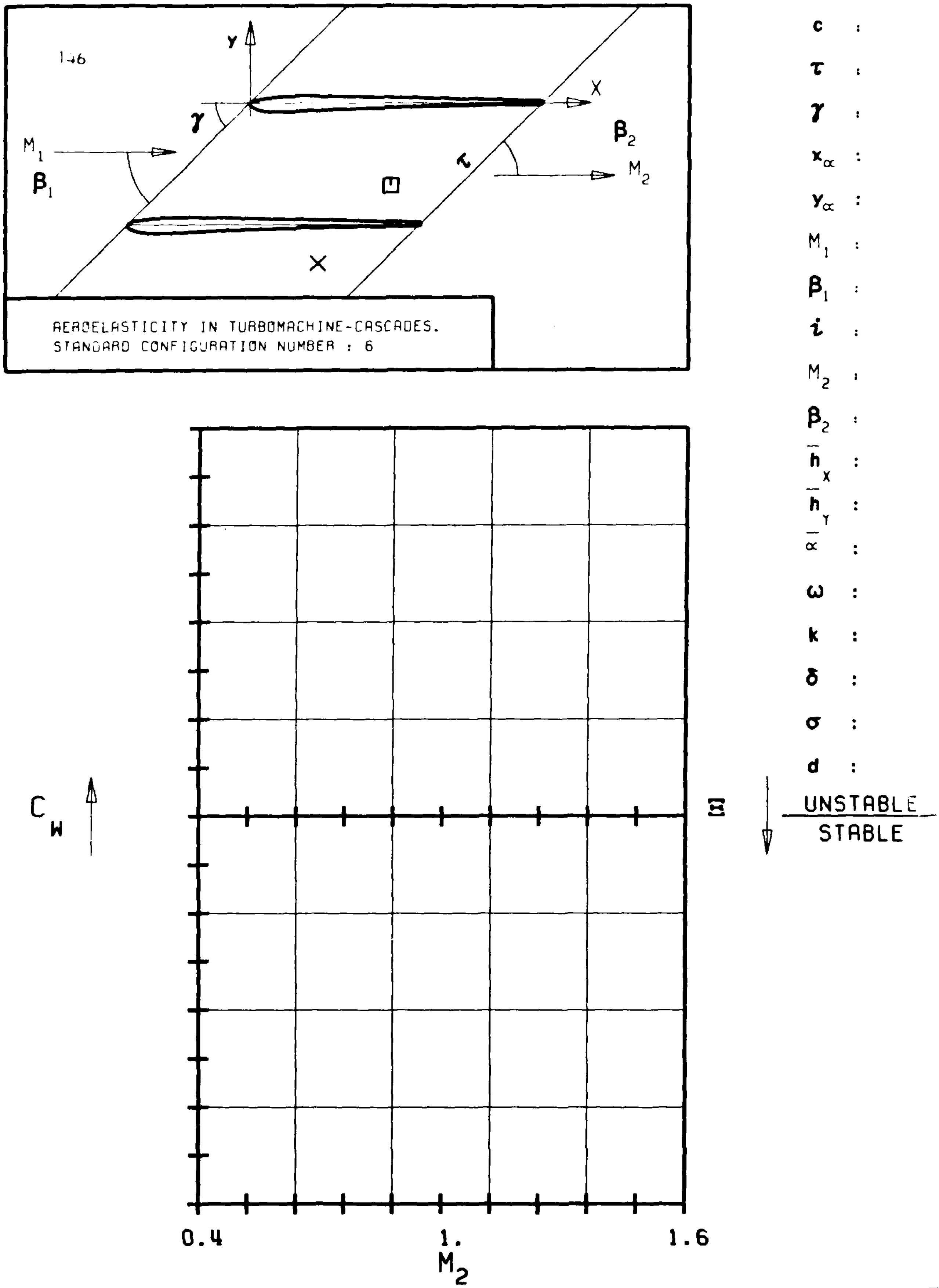

FIG. 3.6-3K: SIXTH STANDARD CONFIGURATION.
AERODYNAMIC WORK AND DAMPING COEFFICIENTS
IN DEPENDANCE OF OUTLET ISENTROPIC VELOCITY M2(IS)

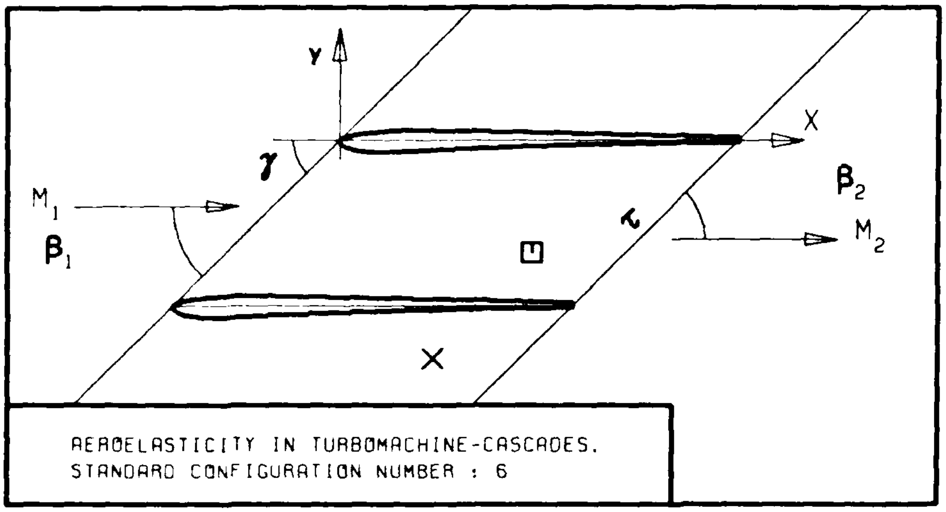

c :
τ :
γ :
x_α :
y_α :
M_1 :
β_1 :
i :
M_2 :
β_2 :
$\bar{h}_X$:
$\bar{h}_Y$:
$\bar{\alpha}$:
ω :
k :
δ :
σ :
d :

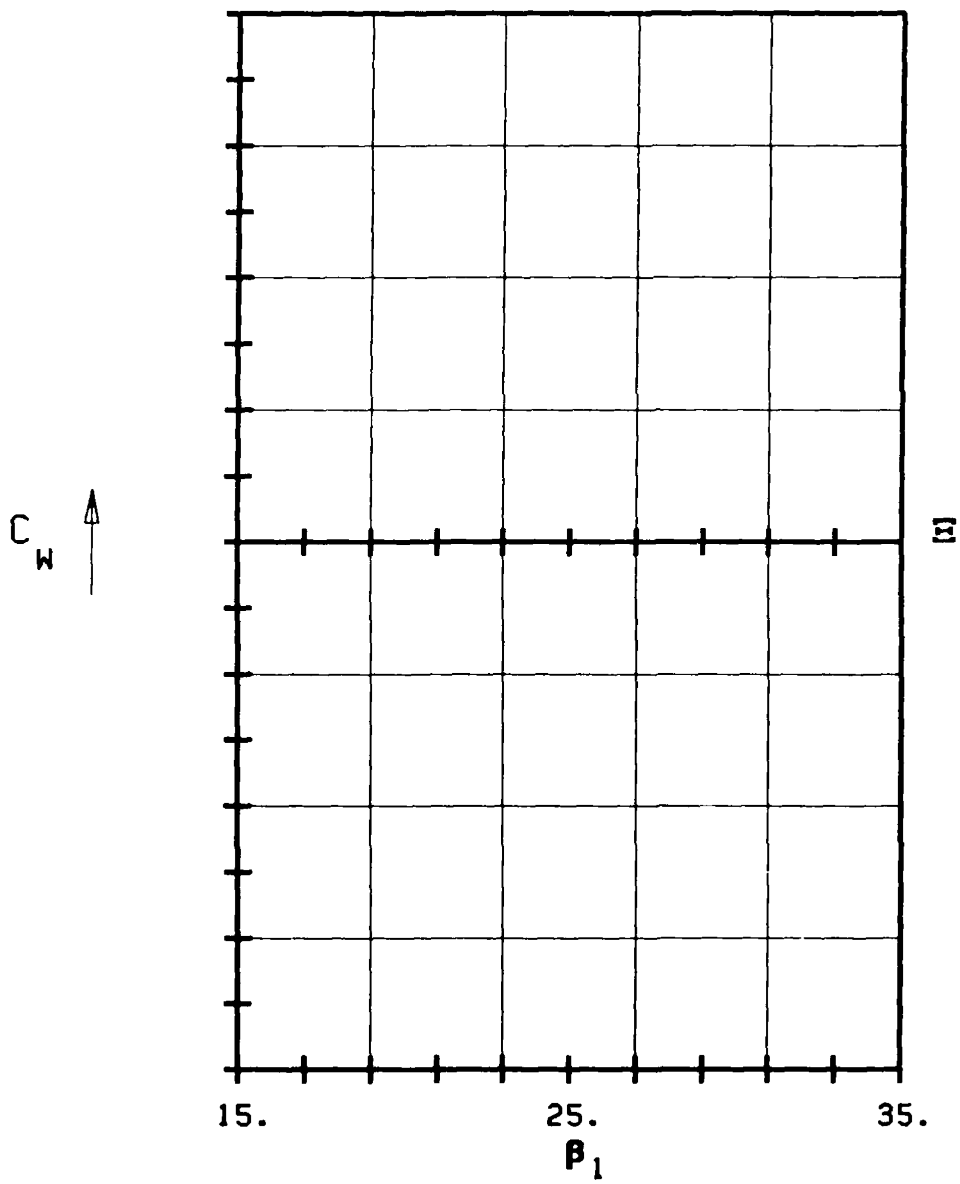

UNSTABLE
STABLE

FIG. 3.6-3L: SIXTH STANDARD CONFIGURATION.
AERODYNAMIC WORK AND DAMPING COEFFICIENTS
IN DEPENDANCE OF INLET FLOW ANGLE BETA1.

Aeroelasticity in Turbomachine-Cascades.
Sixth Standard Configuration.
Aeroelastic test case N^{o}: ______

M_1=______ • p_2/p_{t1}=______ • M_2=______ • β_1=______^{o} • β_2=______^{o} • k=______ •

$\bar{\alpha}^{(-2)}$=______ • $\bar{\alpha}^{(-1)}$=______ • $\bar{\alpha}^{(0)}$=______ • $\bar{\alpha}^{(+1)}$=______ • $\bar{\alpha}^{(+2)}$=______ • (rads)

$\sigma^{(-2)}$=______ • $\sigma^{(-1)}$=______ • $\sigma^{(0)}$=______ • $\sigma^{(+1)}$=______ • $\sigma^{(+2)}$=______ • $(^{o})$

a) Global Aeroelastic Coefficients

$\left\{\begin{array}{l}\bar{C}_M=\_\_\_\_\_\_ \\ \Phi_M=\_\_\_\_\_\_\end{array}\right.$ • $\left\{\begin{array}{l}\bar{C}_L=\_\_\_\_\_\_ \\ \Phi_L=\_\_\_\_\_\_\end{array}\right.$ • C_W=______ • Ξ=______ • (-) $(^{o})$

b) Local Time Dependant Blade Surface Pressure Coefficients

X (-)	$C_p^{(ls)}$ (-)	$\Phi_p^{(ls)}$ $(^{o})$	$C_p^{(us)}$ (-)	$\Phi_p^{(us)}$ $(^{o})$	$\Delta\bar{C}_p$ (-)	$\Phi_{\Delta p}$ $(^{o})$

Table 3.6-4 Sixth Standard Configuration: Table for Presentation of the 26 Recommended Aeroelastic Cases

3.7 Seventh Standard Configuration

The seventh standard configuration has been tested in the Detroit Diesel Allison rectilinear air test facility, and the results are included herein by courtesy of the sponsoring agent, D.R. Boldman at NASA Lewis Research Center. The configuration is representative for tip sections of fan stages of turboreactors (multiple circular arc transonic profiles). Each blade has a chord of c=0.0762 m and a span of 0.0762 m, with a -1.30° net camber and a maximum thickness-to-chord ratio of 0.034. The gap-to-chord ratio is 0.855 and the stagger angle 28.45°.

The cascade geometry is given in Figure 3.7-1 and the profile coordinates in Table 3.7-1.

The airfoils oscillates in pitching mode about a pivot axis at (0.50, 0.00), with a frequency in the range between 710 Hz and 730 Hz. The pitching amplitude of the reference blade lies between 0.06° and 0.2°, depending upon the test conditions, with some scatter in the motion amplitudes between neighbouring blades.

Both the time averaged and time dependant instrumentation on this cascade is extensive, and data have been obtained for different interblade phase angles and axial velocity ratios.

From the tests, 44 aeroelastic cases are selected as recommended test cases. They are contained in Table 3.7-2, together with a proposal for representation of the results.

The 44 aeroelastic cases correspond to four different time averaged settings of the cascade. The time averaged blade surface pressure distributions for these nominal settings are given in Table 3.7-3 and Figures 3.7-2.

The recommended representations of the results from the seventh standard configuration allows detailed comparison of the local time dependant blade surface pressures and trends of global effects, such as moment coefficient and aerodynamic damping coefficient, in dependance of interblade phase angle and axial velocity ratio. If possible, the results should be represented as in Figures 3.7-3 and Table 3.7-4.

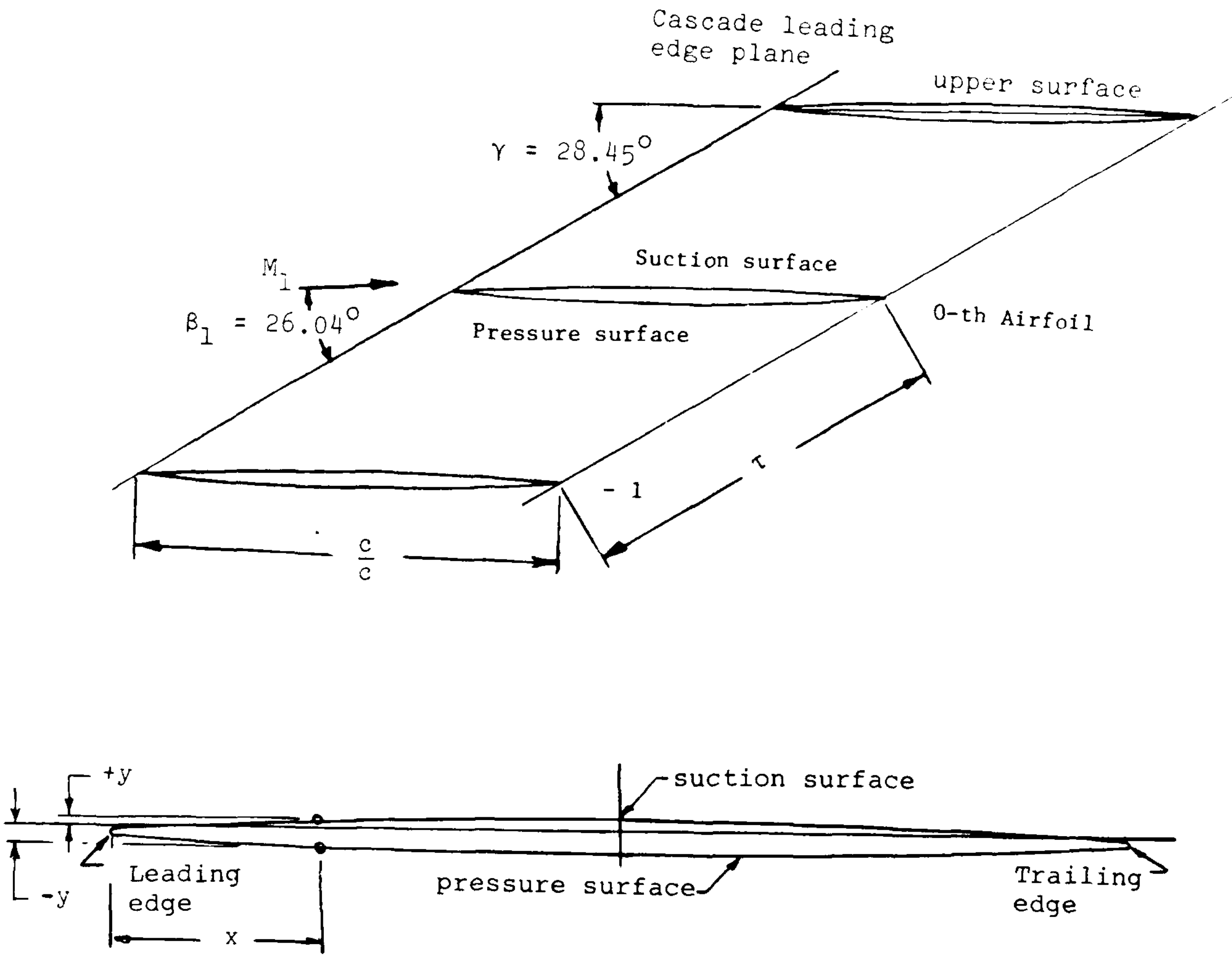

c	= 0.0762 m	τ	= 0.855
span	= 0.0762 m	(x_α, y_α)	= (0.5,0.)
camber	= -1.30°	$\frac{\text{thickness}}{\text{chord}}$	= 0.034
γ	= 28.45°		

Figure 3.7-1 Seventh Standard Configuration: Cascade Geometry

C = 0.0762 m (3.00 in)			
Upper surface (SUCTION SURFACE)		Lower surface (PRESSURE SURFACE)	
X	+Y	X	-Y
0	-0.0029	0	0.0029
0.0026	-0.0004	0.0027	0.0056
0.0278	0.0015	0.0279	0.0066
0.0655	0.0041	0.0657	0.0079
0.1032	0.0065	0.1035	0.0092
0.1410	0.0087	0.1412	0.0103
0.1788	0.0107	0.1790	0.0113
0.2165	0.0124	0.2168	0.0123
0.2543	0.0139	0.2546	0.0131
0.2921	0.0152	0.2923	0.0138
0.3299	0.0162	0.3301	0.0144
0.3551	0.0168	0.3552	0.0148
0.3929	0.0175	0.3930	0.0152
0.4307	0.0179	0.4308	0.0155
0.4685	0.0181	0.4685	0.0158
0.5063	0.0181	0.5063	0.0159
0.5441	0.0179	0.5440	0.0159
0.5820	0.0174	0.5818	0.0158
0.6198	0.0167	0.6195	0.0156
0.6576	0.0158	0.6573	0.0153
0.6828	0.0150	0.6824	0.0151
0.7205	0.0137	0.7202	0.0146
0.7583	0.0122	0.7580	0.0140
0.7961	0.0105	0.7958	0.0133
0.8338	0.0087	0.8336	0.0124
0.8716	0.0067	0.8714	0.0112
0.9093	0.0047	0.9092	0.0098
0.9471	0.0026	0.9470	0.0082
0.9848	0.0003	0.9848	0.0063
0.9974	-0.0005	0.9974	0.0057
1.0000	-0.0029	1.0000	0.0029
L.E. RADIUS/C= 0.0027			
T.E. RADIUS/C= 0.0027			

Table 3.7-1 Seventh Standard Configuration: Dimensionless Airfoil Coordinates

Case No	Time Averaged Parameters: Inlet Air Velocity (-) M_1	Inlet Flow Angle (°) β_1	P_{t2}/P_{t1} (-)	P_2/P_1 (-)	Outlet Air Velocity (-) M_2	Outlet Flow Angle (°) β_2	Time Dependent Parameters: Amplitudes $\bar{h}^{(-2)}/\bar{\alpha}^{(0)}$	$\bar{h}^{(-1)}/\bar{\alpha}^{(0)}$	$\bar{\alpha}^{(0)}$ (rad)	$\bar{h}^{(+1)}/\bar{\alpha}^{(0)}$	$\bar{h}^{(+2)}/\bar{\alpha}^{(0)}$	Frequency (Hz) f	Reduced Frequency (-) k	Interblade phase angles, Measured: $\sigma^{(-2)}$ (°)	$\sigma^{(-1)}$ (°)	$\sigma^{(0)}$ (°)	$\sigma^{(+1)}$ (°)	Nominal: $\sigma^{(+2)}$ (°)	Recommended representation: C_p	ΔC_p	C_L	C_M	
1	1.315	26.0	0.958	1.04	1.25	27.2	0.76	0.52	0.00122	1.27	0.00	725	0.44		-173	-187	-178	-180	1	2		3	7
2	↓	↓	↓	↓	↓	↓	0.87	0.20	0.00112	0.67	↓	714	0.43		-91	-65	-81	-80	↓	↓		↓	↓
3	↓	↓	↓	↓	↓	↓	0.34	0.61	0.00379	0.75	↓	724	0.44		+4	+6	-8	0	↓	↓		↓	↓
4	↓	↓	↓	↓	↓	↓	0.31	0.26	0.00197	0.69	↓	725	0.44		+26	+35	+31	+30	↓	↓		↓	↓
5	↓	↓	↓	↓	↓	↓	0.71	0.78	0.00206	0.32	↓	745	0.45		+48	+53	+54	+50	↓	↓		↓	↓
6	↓	↓	↓	↓	↓	↓	0.56	0.59	0.00187	0.97	↓	724	0.44		+91	+91	+84	+90	↓	↓		↓	↓
7	1.315	26.0	0.957	1.45	0.99	26.4	1.21	0.85	0.00131	0.60	0.00	724	0.44		-172	-168	-165	-170	1	2		3	7
8	↓	↓	↓	↓	↓	↓	0.54	0.44	0.00178	0.34	↓	725	0.44		-66	-69	-61	-66	↓	↓		↓	↓
9	↓	↓	↓	↓	↓	↓	0.64	0.96	0.00202	1.11	↓	724	0.44		-4	+8	-5	0	↓	↓		↓	↓
10	↓	↓	↓	↓	↓	↓	0.36	0.65	0.00386	0.50	↓	724	0.44		+66	+59	+60	+60	↓	↓		↓	↓
11	↓	↓	↓	↓	↓	↓	0.66	0.96	0.00227	0.73	↓	725	0.44		+92	+74	+86	+85	↓	↓		↓	↓
12	↓	↓	↓	↓	↓	↓	0.35	0.40	0.00129	0.25	↓	725	0.44		+96	+115	+98	+100	↓	↓		↓	↓
13	1.315	26.0	0.958	1.04	1.25	27.2	1.	1.	0.00349	1.	1.	725	0.44	←	←	0	→	→	1	2	5,6	3,4	7,8
14	↓	↓	↓	↓	↓	↓	↓	↓	↓	↓	↓	↓	↓	←	←	+45	→	→	-	-	↓	↓	↓
15	↓	↓	↓	↓	↓	↓	↓	↓	↓	↓	↓	↓	↓	←	←	+90	→	→	1	2	↓	↓	↓
16	↓	↓	↓	↓	↓	↓	↓	↓	↓	↓	↓	↓	↓	←	←	+120	→	→	-	-	↓	↓	↓
17	↓	↓	↓	↓	↓	↓	↓	↓	↓	↓	↓	↓	↓	←	←	+180	→	→	1	2	↓	↓	↓
18	↓	↓	↓	↓	↓	↓	↓	↓	↓	↓	↓	↓	↓	←	←	-45	→	→	-	-	↓	↓	↓
19	↓	↓	↓	↓	↓	↓	↓	↓	↓	↓	↓	↓	↓	←	←	-90	→	→	1	2	↓	↓	↓
20	↓	↓	↓	↓	↓	↓	↓	↓	↓	↓	↓	↓	↓	←	←	-120	→	→	-	-	↓	↓	↓
21	1.315	26.0	0.956	1.20	1.14	26.6	1.	1.	0.00349	1.	1.	725	0.44	←	←	0	→	→	-	-	5,6	3,4	7,8
22	↓	↓	↓	↓	↓	↓	↓	↓	↓	↓	↓	↓	↓	←	←	+45	→	→	-	-	↓	↓	↓
23	↓	↓	↓	↓	↓	↓	↓	↓	↓	↓	↓	↓	↓	←	←	+90	→	→	1	2	↓	↓	↓
24	↓	↓	↓	↓	↓	↓	↓	↓	↓	↓	↓	↓	↓	←	←	+120	→	→	-	-	↓	↓	↓
25	↓	↓	↓	↓	↓	↓	↓	↓	↓	↓	↓	↓	↓	←	←	+180	→	→	-	-	↓	↓	↓
26	↓	↓	↓	↓	↓	↓	↓	↓	↓	↓	↓	↓	↓	←	←	-45	→	→	-	-	↓	↓	↓
27	↓	↓	↓	↓	↓	↓	↓	↓	↓	↓	↓	↓	↓	←	←	-90	→	→	1	2	↓	↓	↓
28	↓	↓	↓	↓	↓	↓	↓	↓	↓	↓	↓	↓	↓	←	←	-120	→	→	-	-	↓	↓	↓
29	1.315	26.0	0.956	1.34	1.05	26.7	1.	1.	0.00349	1.	1.	725	0.44	←	←	0	→	→	-	-	5,6	3,4	7,8
30	↓	↓	↓	↓	↓	↓	↓	↓	↓	↓	↓	↓	↓	←	←	+45	→	→	-	-	↓	↓	↓
31	↓	↓	↓	↓	↓	↓	↓	↓	↓	↓	↓	↓	↓	←	←	+90	→	→	1	2	↓	↓	↓
32	↓	↓	↓	↓	↓	↓	↓	↓	↓	↓	↓	↓	↓	←	←	+120	→	→	-	-	↓	↓	↓
33	↓	↓	↓	↓	↓	↓	↓	↓	↓	↓	↓	↓	↓	←	←	+180	→	→	-	-	↓	↓	↓
34	↓	↓	↓	↓	↓	↓	↓	↓	↓	↓	↓	↓	↓	←	←	-45	→	→	-	-	↓	↓	↓
35	↓	↓	↓	↓	↓	↓	↓	↓	↓	↓	↓	↓	↓	←	←	-90	→	→	1	2	↓	↓	↓
36	↓	↓	↓	↓	↓	↓	↓	↓	↓	↓	↓	↓	↓	←	←	-120	→	→	-	-	↓	↓	↓
37	1.315	26.0	0.957	1.45	0.99	26.4	1.	1.	0.00349	1.	1.	725	0.44	←	←	0	→	→	-	-	5,6	3,4	7,8
38	↓	↓	↓	↓	↓	↓	↓	↓	↓	↓	↓	↓	↓	←	←	+45	→	→	-	-	↓	↓	↓
39	↓	↓	↓	↓	↓	↓	↓	↓	↓	↓	↓	↓	↓	←	←	+90	→	→	1	2	↓	↓	↓
40	↓	↓	↓	↓	↓	↓	↓	↓	↓	↓	↓	↓	↓	←	←	+120	→	→	-	-	↓	↓	↓
41	↓	↓	↓	↓	↓	↓	↓	↓	↓	↓	↓	↓	↓	←	←	+180	→	→	-	-	↓	↓	↓
42	↓	↓	↓	↓	↓	↓	↓	↓	↓	↓	↓	↓	↓	←	←	-45	→	→	-	-	↓	↓	↓
43	↓	↓	↓	↓	↓	↓	↓	↓	↓	↓	↓	↓	↓	←	←	-90	→	→	1	2	↓	↓	↓
44	↓	↓	↓	↓	↓	↓	↓	↓	↓	↓	↓	↓	↓	←	←	-120	→	→	-	-	↓	↓	↓

NOTES 1) $C_p = f(x)$ 2) $\Delta C_p = f(x)$ 3) $C_M = f(\sigma)$ 4) $C_M = f(M_2)$ 5) $C_L = f(\sigma)$ 6) $C_L = f(M_2)$ 7) [illegible] $= f(\sigma)$ 8) [illegible] $= f(M_2)$

Table 3.7-2 Seventh Standard Configuration: 44 Recommended Aeroelastic Test Cases

Aeroelasticity in Turbomachine - Cascades Seventh Standard Configuration Time Averaged Blade Surface Pressure Distributions									
$\tilde{M}_1$ (-)	1.315		1.315		1.315		1.315		
$\tilde{\beta}_1$ (°)	26.0		26.0		26.0		26.0		
$\tilde{p}_2/\tilde{p}_1$ (-)	1.04		1.20		1.35		1.45		
$\tilde{p}_{t2}/\tilde{p}_{t1}$ (-)	0.958		0.956		0.956		0.957		
$\tilde{M}_2$ (-)	1.25		1.14		1.05		0.99		
$\tilde{\beta}_2$ (°)	27.2		26.6		26.7		26.4		
X (-)	$\tilde{p}/\tilde{p}_{t1}$ (-)	$\tilde{C}_p$ (-)	$\tilde{p}/\tilde{p}_{t1}$ (-)	$\tilde{C}_p$ (-)	$\tilde{p}/\tilde{p}_{t1}$ (-)	$\tilde{C}_p$ (-)	X (-)	$\tilde{p}/\tilde{p}_{t1}$ (-)	$\tilde{C}_p$ (-)
Upper surface									
0.0500	0.365	0.016	0.373	0.028	0.362	0.011	0.0482	0.374	0.029
0.1500	0.377	0.034	0.380	0.039	0.364	0.014	0.1481	0.405	0.078
0.2500	0.382	0.042	0.378	0.036	0.362	0.011	0.2486	0.380	0.039
0.3250	0.375	0.031	0.381	0.040	0.366	0.017	0.3242	0.377	0.034
0.4000	0.354	-0.002	0.352	-0.005	0.336	-0.029	0.3995	0.347	-0.012
0.5200	0.319	-0.056	0.317	-0.059	0.302	-0.082	0.5201	0.310	-0.070
0.6000	0.301	-0.084	0.292	-0.098	0.277	-0.121	0.5999	0.303	-0.081
0.7500	0.315	-0.062	0.317	-0.059	0.327	-0.043	0.7503	0.339	-0.025
0.9553	0.353	-0.003	0.330	-0.039	0.345	-0.016	0.8597	0.454	0.153
0.9615	0.367	0.019	0.382	0.042	0.457	0.158	0.9604	0.531	0.273
Lower surface									
0.0500	0.412	0.088	0.407	0.081	0.408	0.082	0.0474	0.539	0.271
0.1500	0.345	-0.016	0.338	-0.026	0.338	-0.026	0.1464	0.548	0.299
0.2000	0.320	-0.054	0.315	-0.062	0.313	-0.065	0.1963	0.518	0.253
0.2500	0.301	-0.084	0.298	-0.088	0.279	-0.118	0.2465	0.490	0.209
0.3250	0.364	0.014	0.371	0.025	0.381	0.040	0.3221	0.519	0.254
0.4000	0.373	0.028	0.381	0.040	0.415	0.093	0.3961	0.501	0.226
0.4800	0.384	0.045	0.372	0.026	0.514	0.247	0.4770	0.496	0.219
0.6000	0.299	-0.087	0.361	0.009	0.479	0.192	0.5984	0.439	0.130
0.7500	0.313	-0.065	0.373	0.028	0.445	0.140	0.7483	0.453	0.152
0.8500	0.298	-0.088	0.408	0.082	0.464	0.169	0.8491	0.462	0.166
Compare figure	372A		372B		372C		372D		

Table 3.7-3 Seventh Standard Configuration: Time Averaged Blade Surface Pressure Distribution for the 44 Recommended Aeroelastic Cases

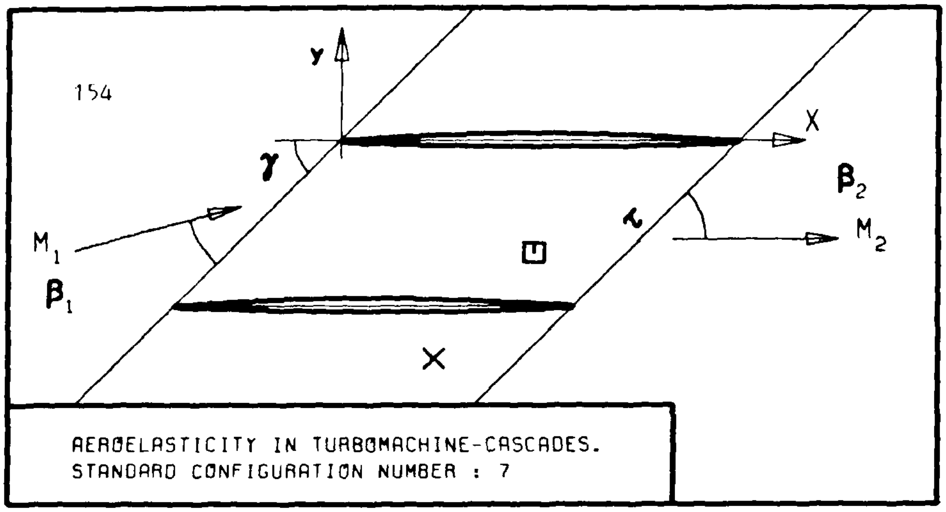

c :

τ :

γ :

x_α :

y_α :

M_1 :

β_1 :

i :

M_2 :

β_2 :

$\bar{h}_X$:

$\bar{h}_Y$:

$\bar{\alpha}$:

ω :

k :

δ :

σ :

d :

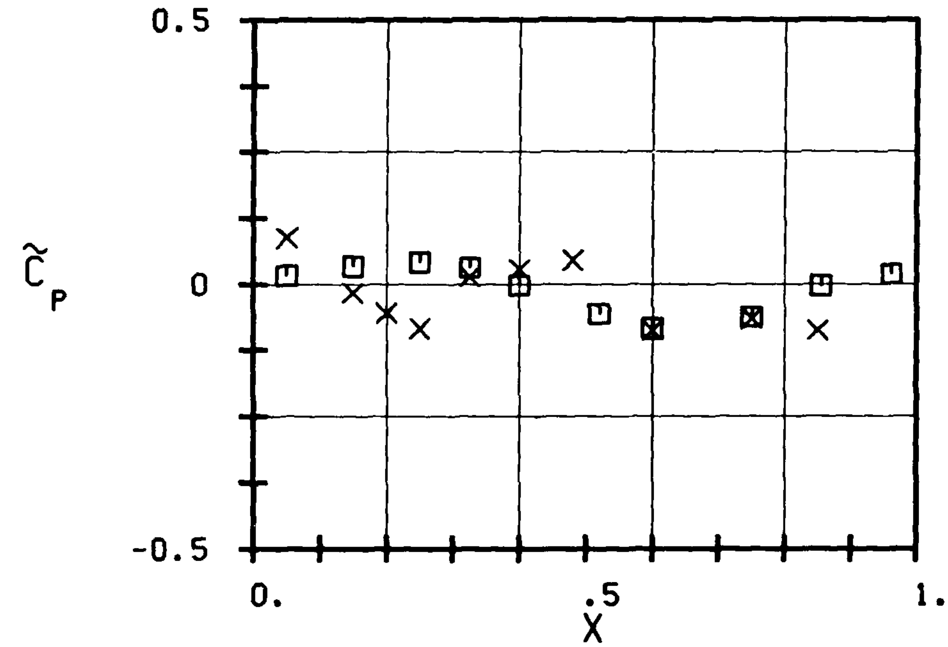

FIG. 3.7-2A: SEVENTH STANDARD CONFIGURATION:
TIME AVERAGED BLADE SURFACE PRESSURE
DISTRIBUTION FOR OUTLET VELOCITY M2=1.25 .

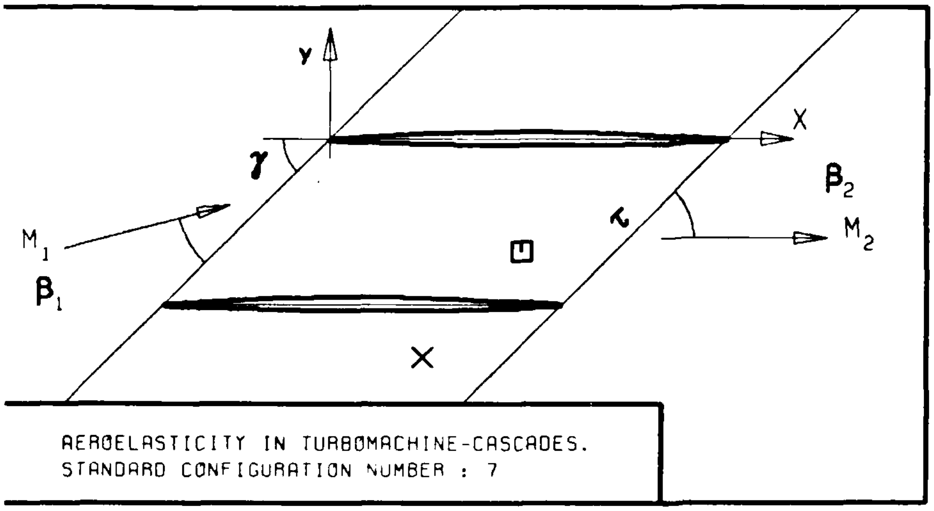

c :
τ :
γ :
x_α :
y_α :
M_1 :
β_1 :
i :
M_2 :
β_2 :
$\bar{h}_x$:
$\bar{h}_y$:
$\bar{\alpha}$:
ω :
k :
δ :
σ :
d :

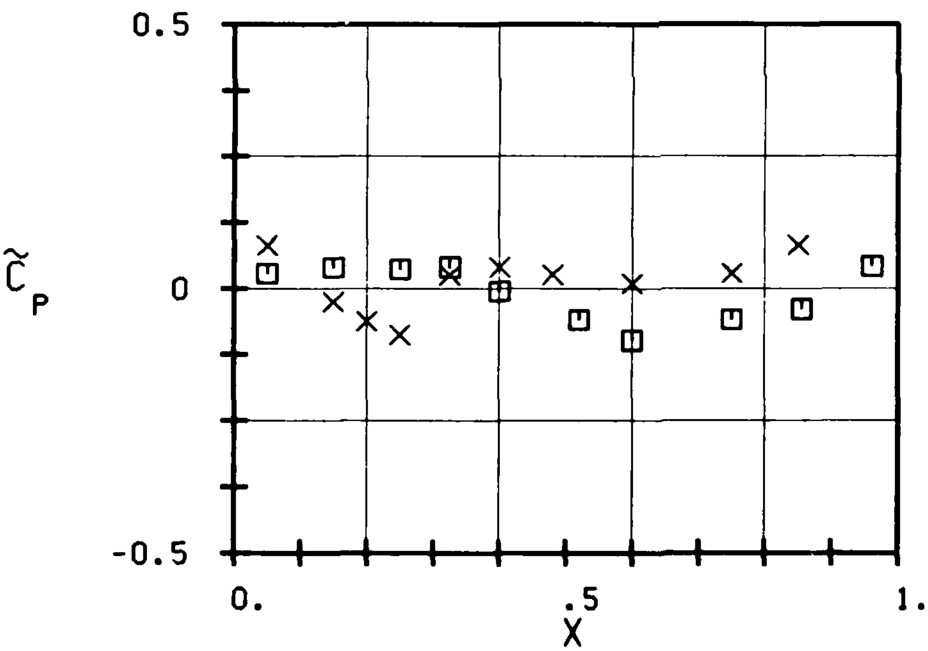

FIG. 3.7-28: SEVENTH STANDARD CONFIGURATION:
TIME AVERAGED BLADE SURFACE PRESSURE
DISTRIBUTION FOR OUTLET VELOCITY M2=1.14 .

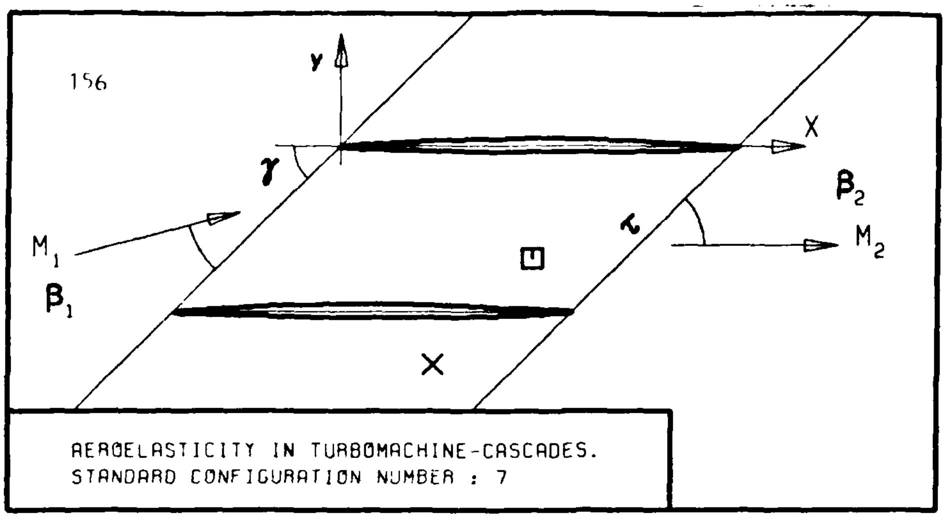

c	:
τ	:
γ	:
x_α	:
y_α	:
M_1	:
β_1	:
i	:
M_2	:
β_2	:
$\bar{h}_X$	:
$\bar{h}_Y$	:
$\bar{\alpha}$	:
ω	:
k	:
δ	:
σ	:
d	:

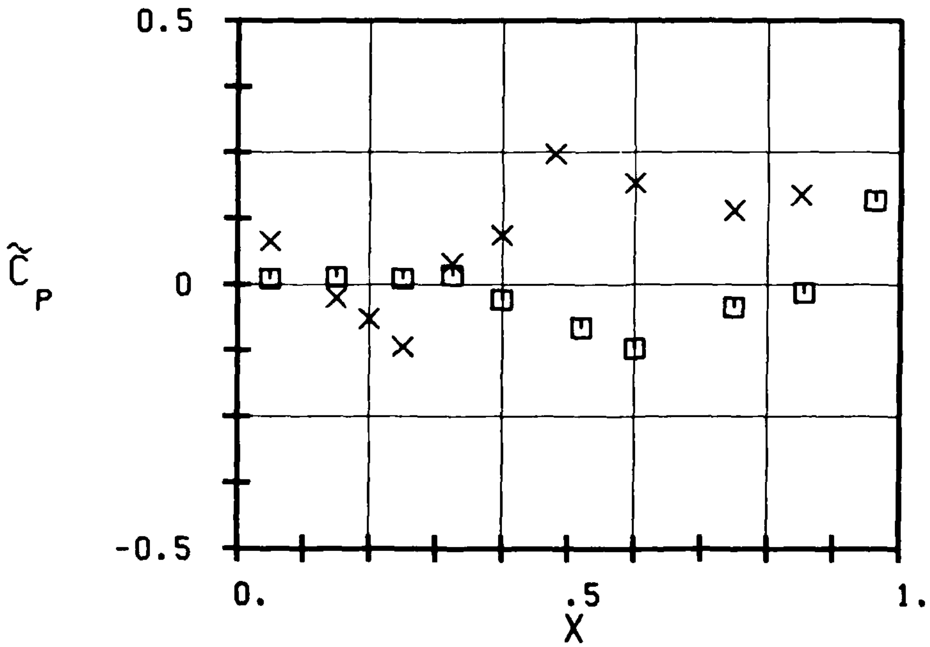

FIG. 3.7-2C: SEVENTH STANDARD CONFIGURATION:
TIME AVERAGED BLADE SURFACE PRESSURE
DISTRIBUTION FOR OUTLET VELOCITY M2=1.05 .

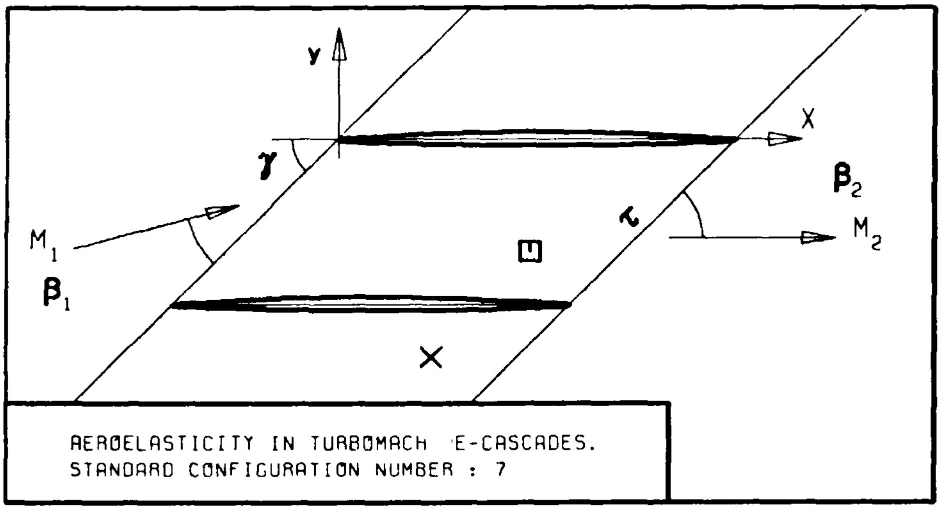

c :
τ :
γ :
x_α :
y_α :
M_1 :
β_1 :
i :
M_2 :
β_2 :
$\bar{h}_X$:
$\bar{h}_Y$:
$\bar{\alpha}$:
ω :
k :
δ :
σ :
d :

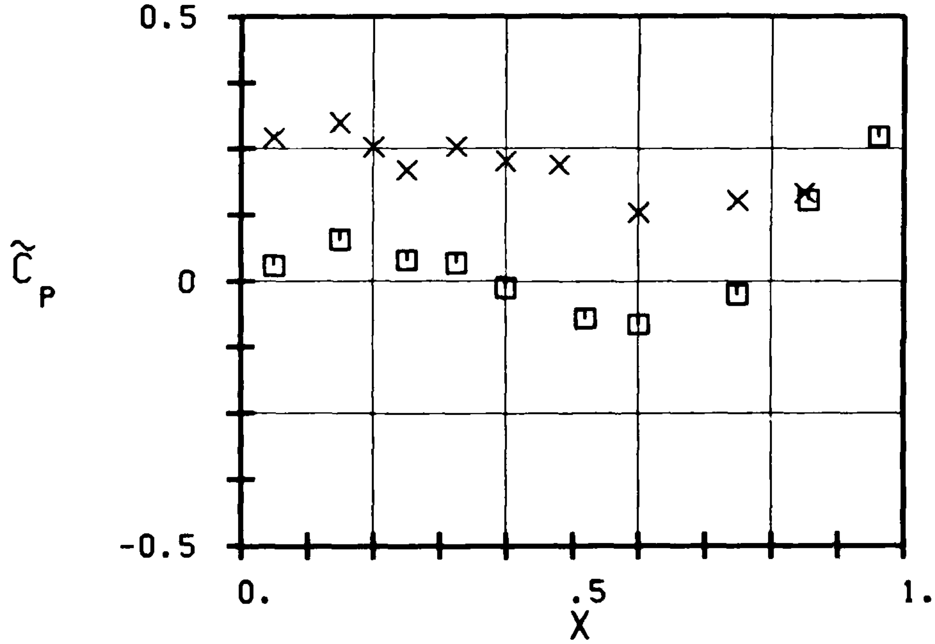

FIG. 3.7-2D: SEVENTH STANDARD CONFIGURATION:
TIME AVERAGED BLADE SURFACE PRESSURE
DISTRIBUTION FOR OUTLET VELOCITY M2=0.99 .

Aeroelasticity in Turbomachine-Cascades.
Seventh Standard Configuration:
Aeroelastic test case N^o:_______

M_1=______ • p_2/p_{t1}=______ • M_2=______ • β_1=_____^{o} • β_2=_____^{o} • k=______ •

$\bar{\alpha}^{(-2)}$=_____ • $\bar{\alpha}^{(-1)}$=_____ • $\bar{\alpha}^{(0)}$=_____ • $\bar{\alpha}^{(+1)}$=_____ • $\bar{\alpha}^{(+2)}$=_____ • (rads)

$\sigma^{(-2)}$=_____ • $\sigma^{(-1)}$=_____ • $\sigma^{(0)}$=_____ • $\sigma^{(+1)}$=_____ • $\sigma^{(+2)}$=_____ • (^{o})

a) Global Aeroelastic Coefficients

$\bar{C}_M$=______ • $\bar{C}_L$=______ • C_W=______ • Ξ =______ • (-)

Φ_M=______ • Φ_L=______ • (^{o})

b) Local Time Dependant Blade Surface Pressure Coefficients

X (-)	$C_p^{(ls)}$ (-)	$\Phi_p^{(ls)}$ (^{o})	$C_p^{(us)}$ (-)	$\Phi_p^{(us)}$ (^{o})	$\Delta\bar{C}_p$ (-)	$\Phi_{\Delta p}$ (^{o})

Table 3.7-4 Seventh Standard Configuration: Table for Presentation of the 44 Recommended Aeoelastic Test Cases

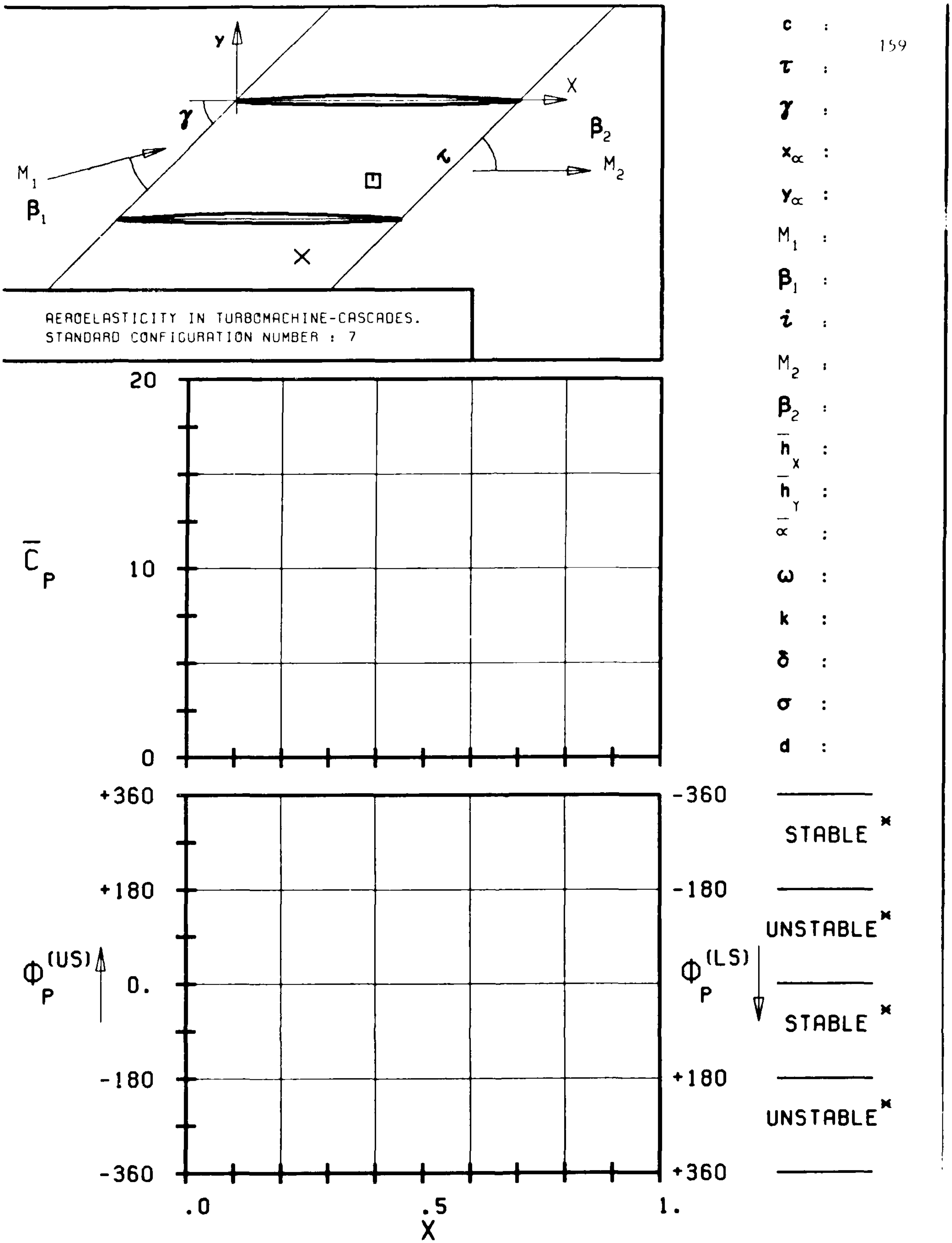

FIG. 3.7-3A: SEVENTH STANDARD CONFIGURATION:
MAGNITUDE AND PHASE LEAD OF BLADE SURFACE
PRESSURE COEFFICIENT.

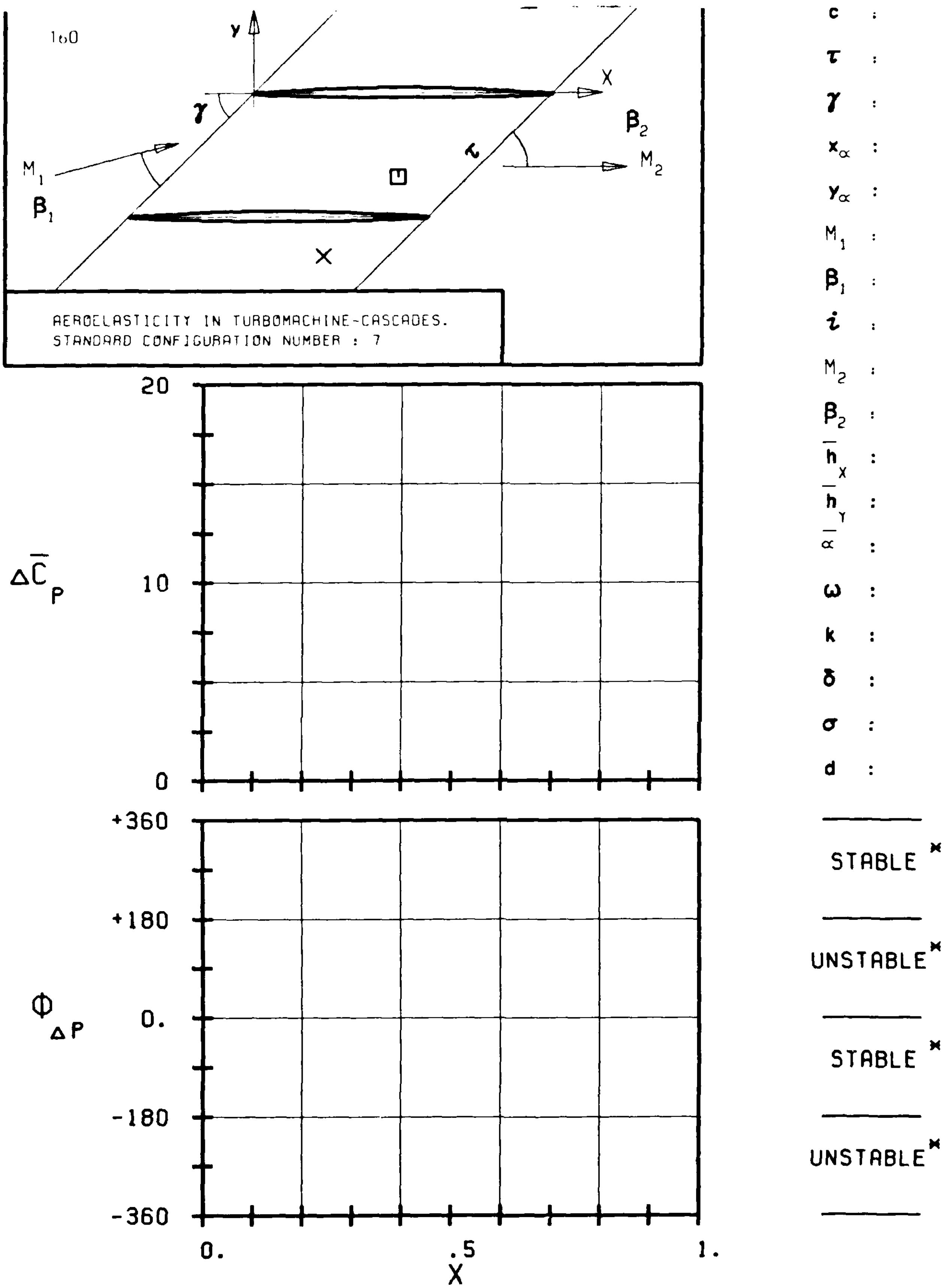

FIG. 3.7-3B: SEVENTH STANDARD CONFIGURATION: MAGNITUDE AND PHASE LEAD OF BLADE SURFACE PRESSURE DIFFERENCE COEFFICIENT.

(*: IN PITCH MODE, NOTATION VALID UPSTREAM OF PITCH AXIS)

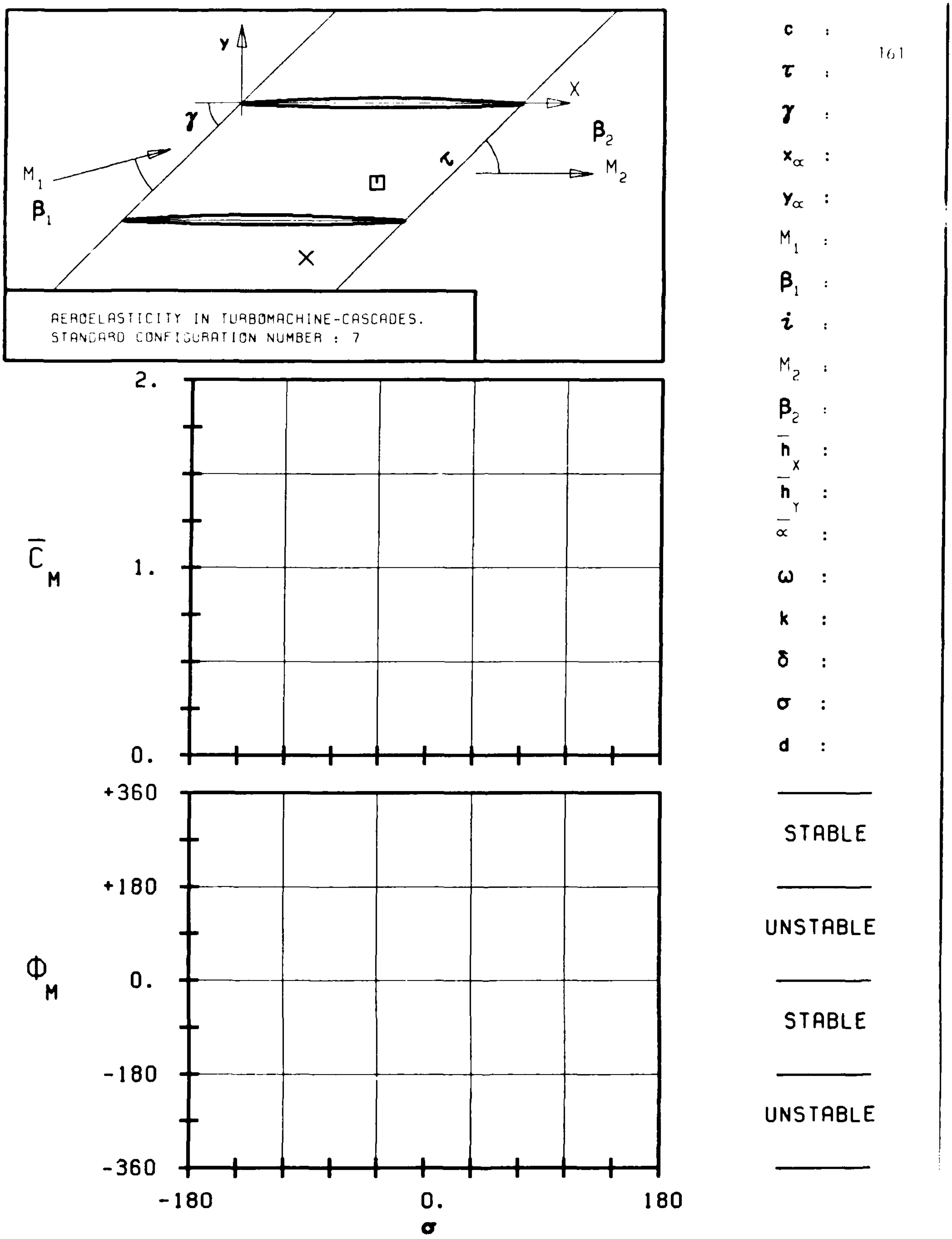

FIG. 3.7-3C: SEVENTH STANDARD CONFIGURATION:
AERODYNAMIC MOMENT COEFFICIENT AND PHASE LEAD
IN DEPENDANCE OF INTERBLADE PHASE ANGLE.

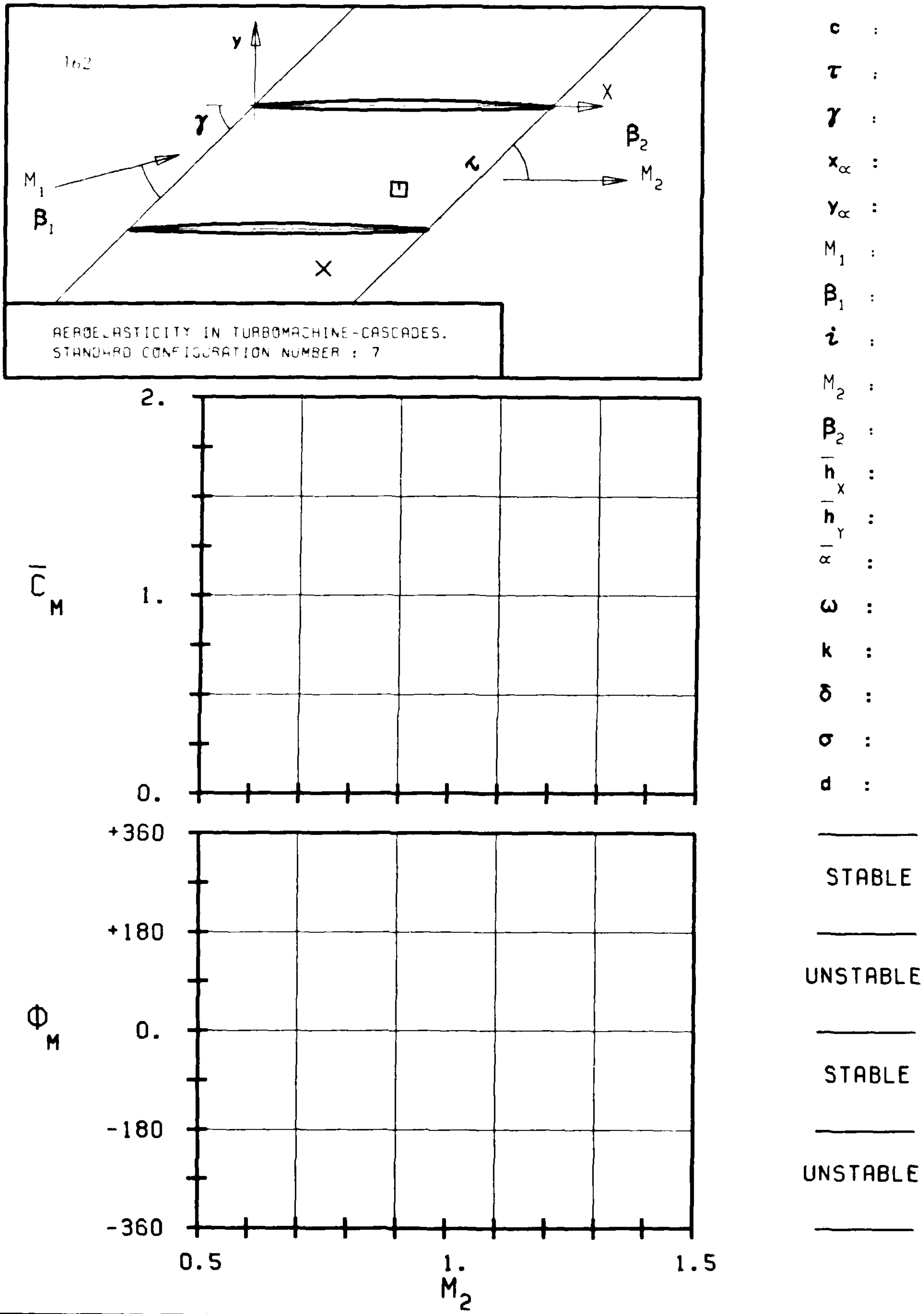

FIG. 3.7-3D: SEVENTH STANDARD CONFIGURATION:
AERODYNAMIC MOMENT COEFFICIENT AND PHASE LEAD
IN DEPENDANCE OF OUTLET MACH NUMBER.

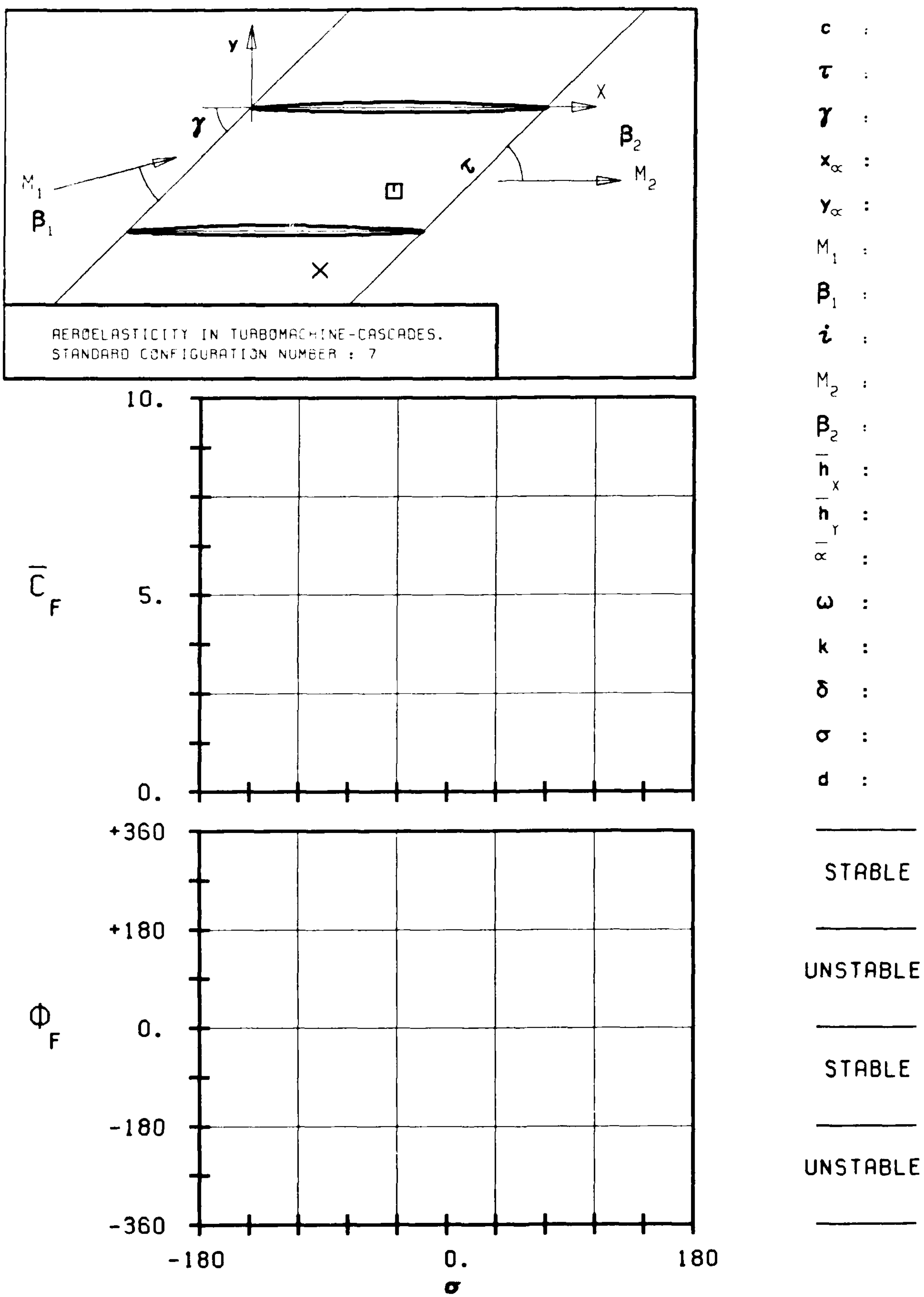

FIG. 3.7-3E: SEVENTH STANDARD CONFIGURATION:
AERODYNAMIC FORCE COEFFICIENT AND PHASE LEAD
IN DEPENDANCE OF INTERBLADE PHASE ANGLE.

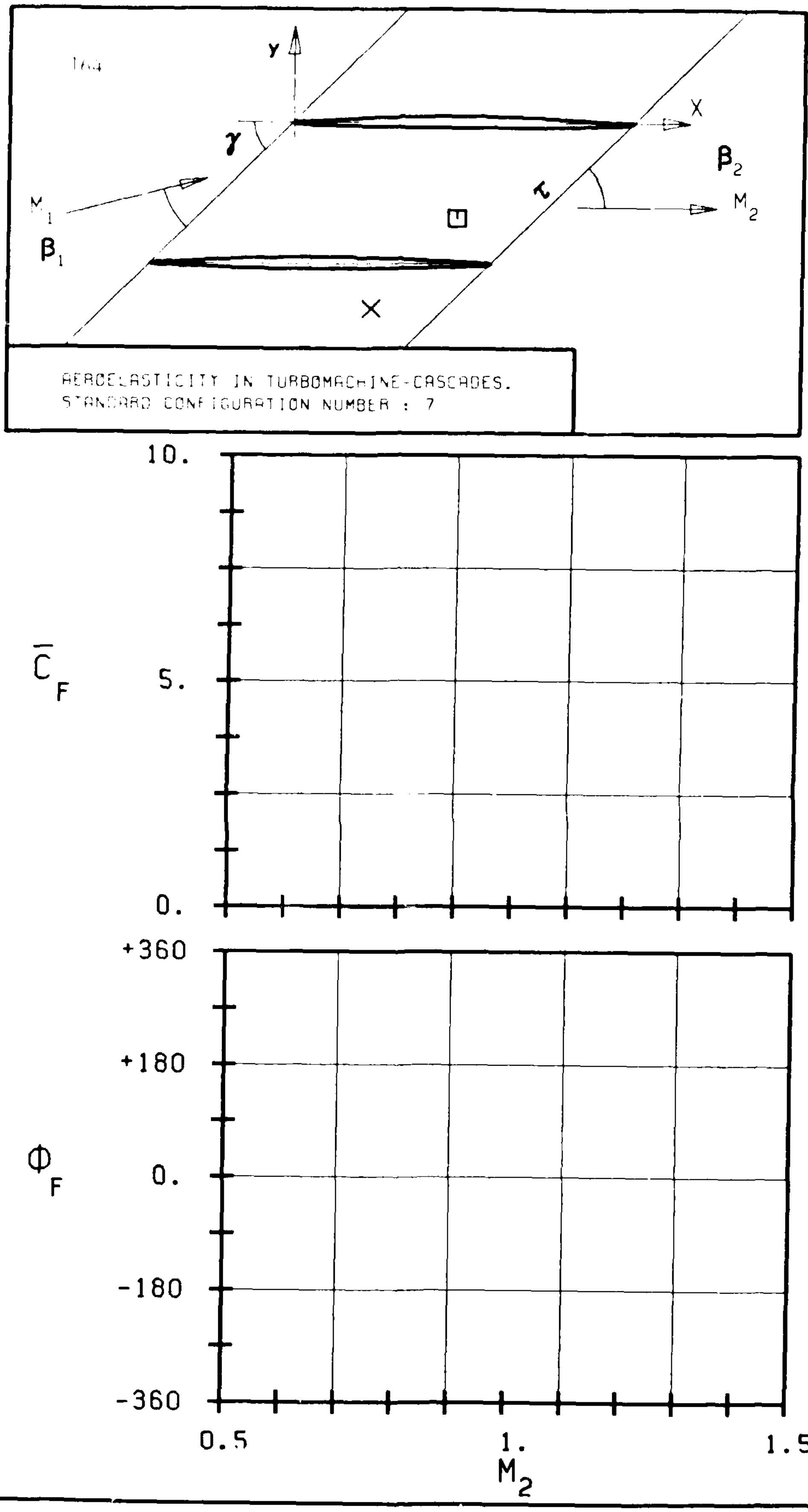

FIG. 3.7-3F: SEVENTH STANDARD CONFIGURATION:
AERODYNAMIC FORCE COEFFICIENT AND PHASE LE[illegible]
IN DEPENDANCE OF OUTLET MACH NUMBER.

c
τ
γ
x_c
y_c
M_1
β_1
i
M_2
β_2
$\bar{h}_X$
$\bar{h}_Y$
$\bar{\alpha}$
ω
k
δ
σ
d
S
UNS
S
UNS

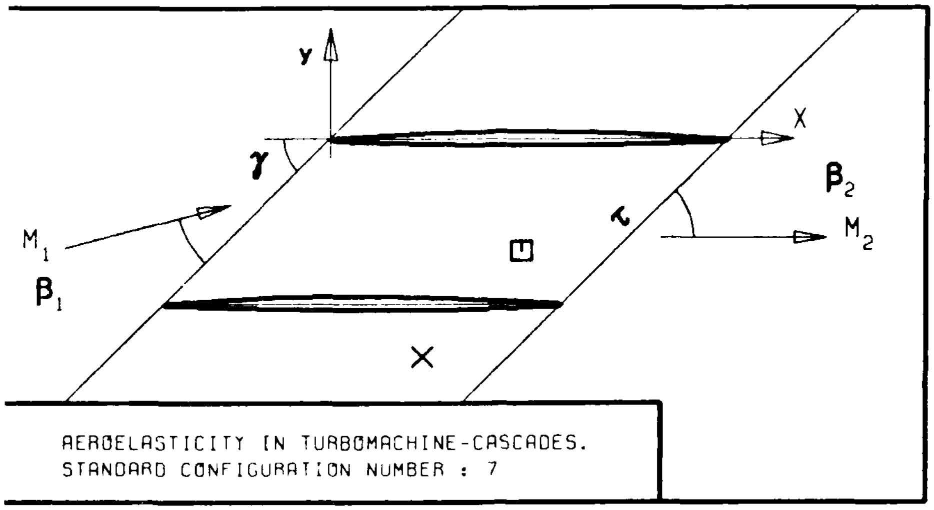

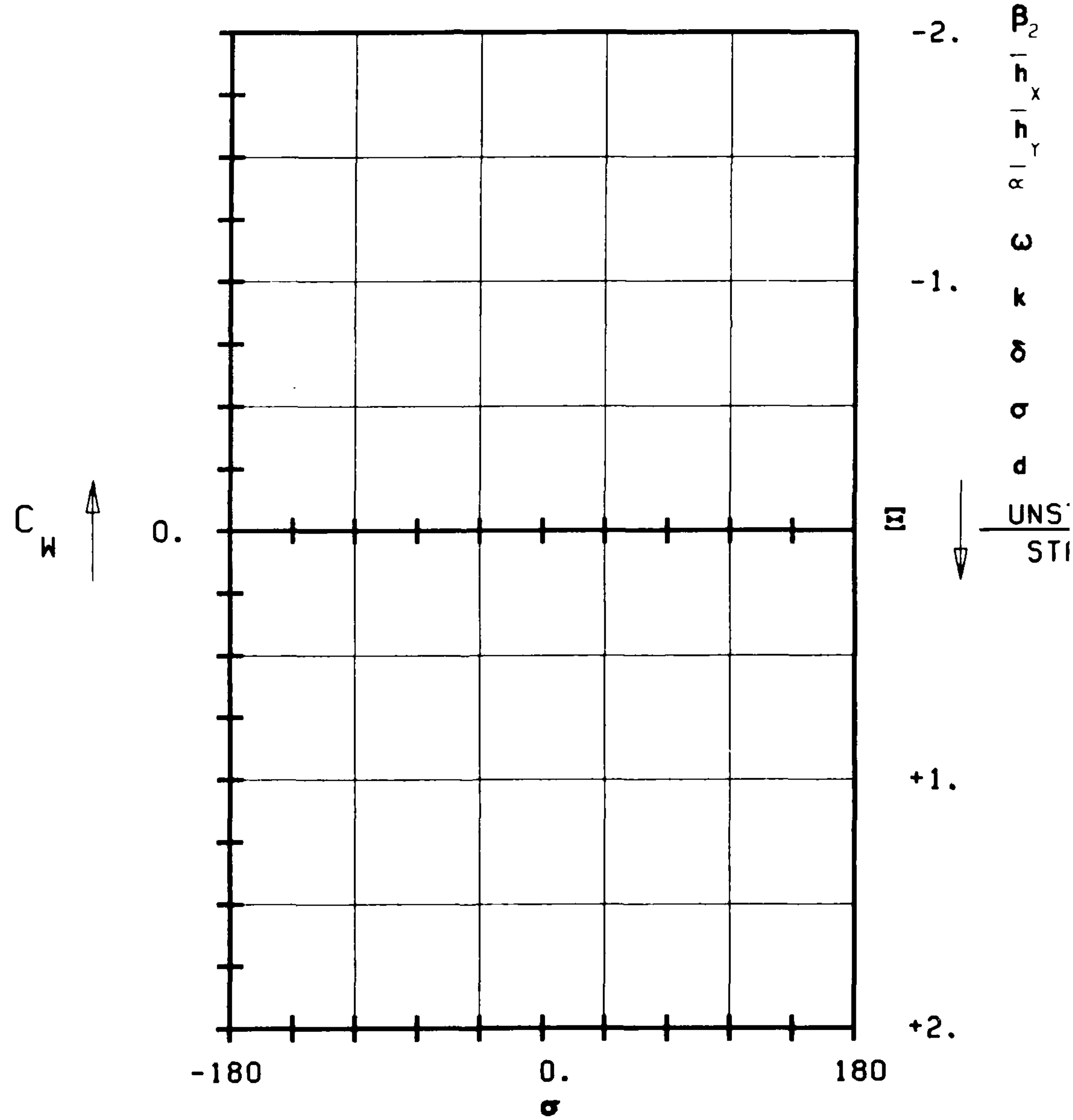

FIG. 3.7-3G: SEVENTH STANDARD CONFIGURATION:
AERODYNAMIC WORK AND DAMPING COEFFICIENTS
IN DEPENDANCE OF INTERBLADE PHASE ANGLE.

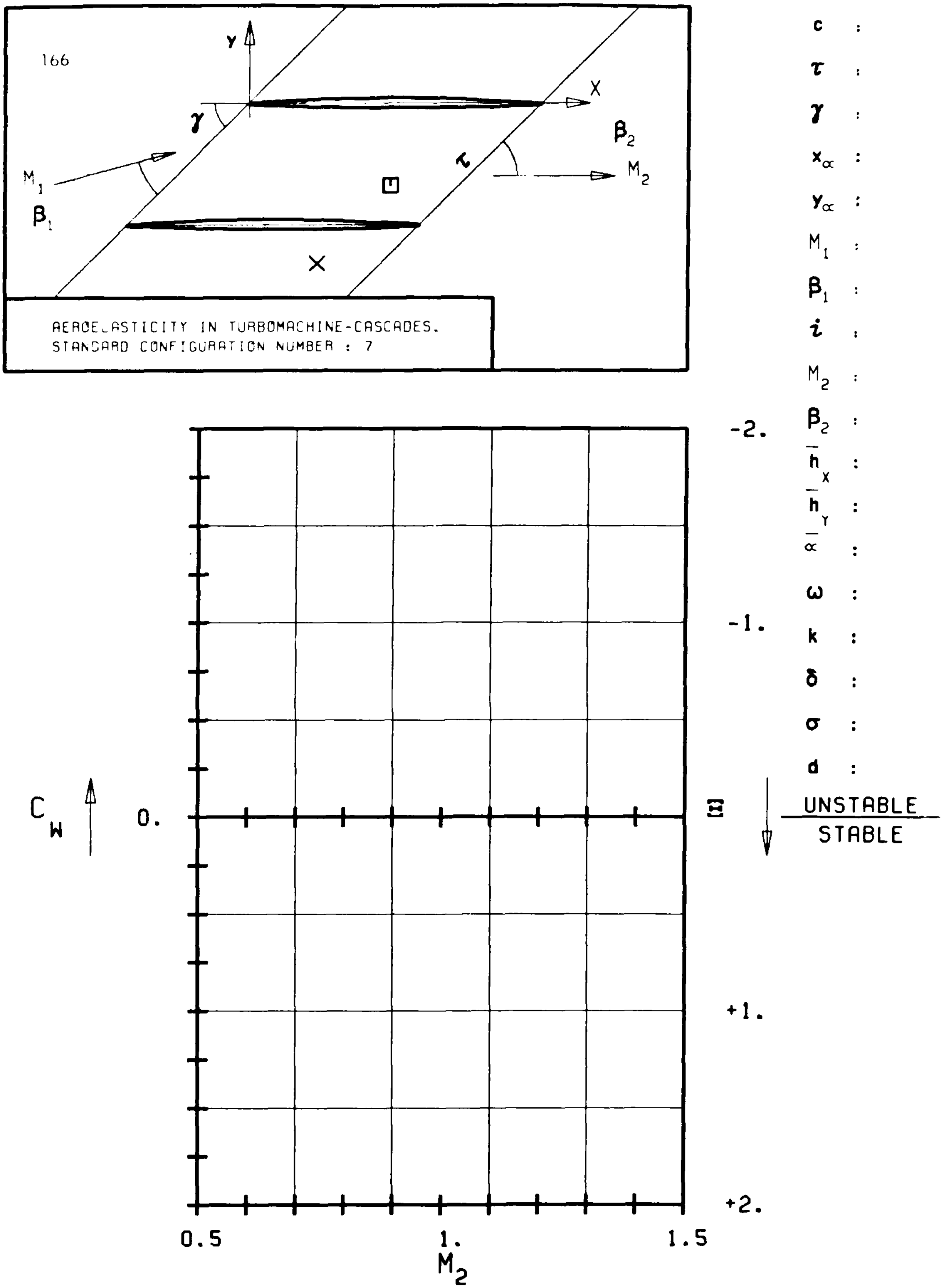

FIG. 3.7-3H: SEVENTH STANDARD CONFIGURATION:
AERODYNAMIC WORK AND DAMPING COEFFICIENTS
IN DEPENDANCE OF OUTLET MACH NUMBER.

3.8 Eighth Standard Configuration

The eighth and ninth standard configurations are directed towards the investigation of basic aeroelastic phenomena and influence of thickness effects on numerical calculations, especially in the transonic flow region.

Configuration number eighth considers a two-dimensional cascade of flat plates. Theoretical analysis of such unsteady configurations have been performed for many years now, but the problem is still of large interest, mainly due to the following factors:

- o In modern compressors, operating in the transonic and supersonic flow regimes, the actual blades are rather thin and have a low camber. They can thus mostly be fairly well approximated as flat plates.
- o Supersonic two-dimensional flat plate prediction models are often one of the main aeroelastic tools used by the designer of large turboreactors.
- o In the incompressible flow domain, analytical flat plate solutions are available.
- o It is possible to establish, with different theories and for the purpose of the present comparative work, the aeroelastic response of a flat plate cascade over the whole Mach number range from incompressible to supersonic flow conditions.
- o The strip theory assumption should be validated, in the transonic flow domain, in a fairly simple case. This requires validation not only of theoretical results, but also of two dimensional and quasi three-dimensional experimental data on thin airfoils.

In this chapter, the main emphasize will be laid upon the change in the aeroelastic behaviour of the cascade in dependance of inlet flow velocity, pressure ratio through the cascade, stagger angle and solidity. The unsteady blade surface pressure distributions will thus only be compared in detail for a few aeroelastic cases.

It is assumed that the two-dimensional airfoils oscillates in pitch about mid chord (0.5, 0.), with an amplitude of 2° (0.0349 rad).

As the main interest for this configuration lies in the variation of the time averaged parameters the calculations should be performed, at zero mean incidence, with a constant interblade phase angle of 90° and with a fairly high reduced frequency, k=1.0.

The cascade configuration is given in Figure 3.8-1 and a recommendation

for 35 aeroelastic cases to be calculated is given in Table 3.8-1. If possible, the results should be represented as in Figures and Tables 3.8-2. The 35 aeroelastic cases are situated in different velocity domains, wherefore it is not expected that one single program can calculate all cases. However, it would be of interest for the comparisons if all participants could calculate the cases their program(s) can handle.

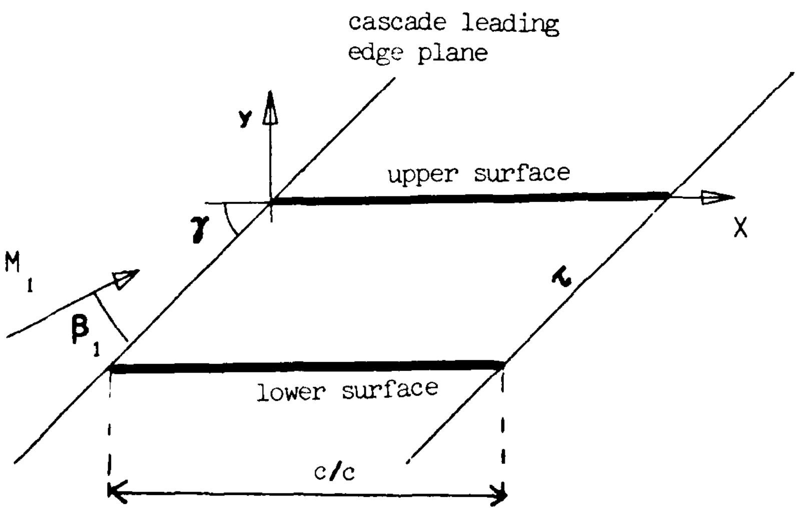

Flat plates

c	= 0.1 m	$\bar{\alpha}$ = 2.0° (0.0349 rad)
camber	= 0°	σ = 90°
(x_α, y_α)	= (0.5,0.)	k = 1.0
i	= 0°	

Figure 3.8-1 Eighth Standard Configuration: Cascade Geometry

Aeroelastic Case No	$\tilde{M}_{-\infty}$ (-)	$\tilde{i}_{-\infty}$ (°)	Normal shock ?	(°)	$\tilde{i}$ (-)	Recommended Representation c_p	Δc_p	C_M	[illegible]
1	Incompressible	0		30	0.75	1	2	3,4	6,7
2				45		-	-		
3				60		-	-		
4	↓			90		-	-	↓	↓
5	0.5			30		-	-	4	7
6	0.6					-	-		
7	0.7					-	-		
8	0.8					1	2	3, ,5	6, ,8
9	0.9					-	-		
10	0.95			↓		-	-	↓	↓
11	0.8			45		-	-	3	6
12				60		-	-		
13				90	↓	-	-	↓	↓
14				30	0.5	-	-	5	8
15	↓				1.0	-	-	↓	↓
16	1.1		-		0.75	-	-	4	7
17			at L.E.			-	-		
18	↓		at T.E.			-	-		
19	1.2		-			-	-		
20			at L.E.			-	-		
21	↓		at T.E.			-	-		
22	1.3		-			1	2	,5	,8
23			at L.E.					3, ,5	6, ,8
24	↓		at T.E.			↓	↓		
25	1.4		-			-	-		
26			at L.E.			-	-		
27	↓		at T.E.			-	-		
28	1.5		-			-	-		
29			at L.E.			-	-		
30	↓		at T.E.		↓	-	-	↓	↓
31	1.3		-		0.5	1	2	5	8
32			-		1.0				
33			at L.E.	↓	0.5				
34					1.0				
35	↓	↓	↓	45	0.75	↓	↓	↓	↓

Notes :

1) c_p as a function of x
2) Δc_p " " " " x
3) C_M " " " " γ
4) C_M " " " " M_1
5) C_M as a function of τ
6) Ξ " " " " γ
7) Ξ " " " " M_1
8) " " " " τ

Table 3.8-1 Eighth Standard Configuration: 35 Recommended Aeroelastic Cases

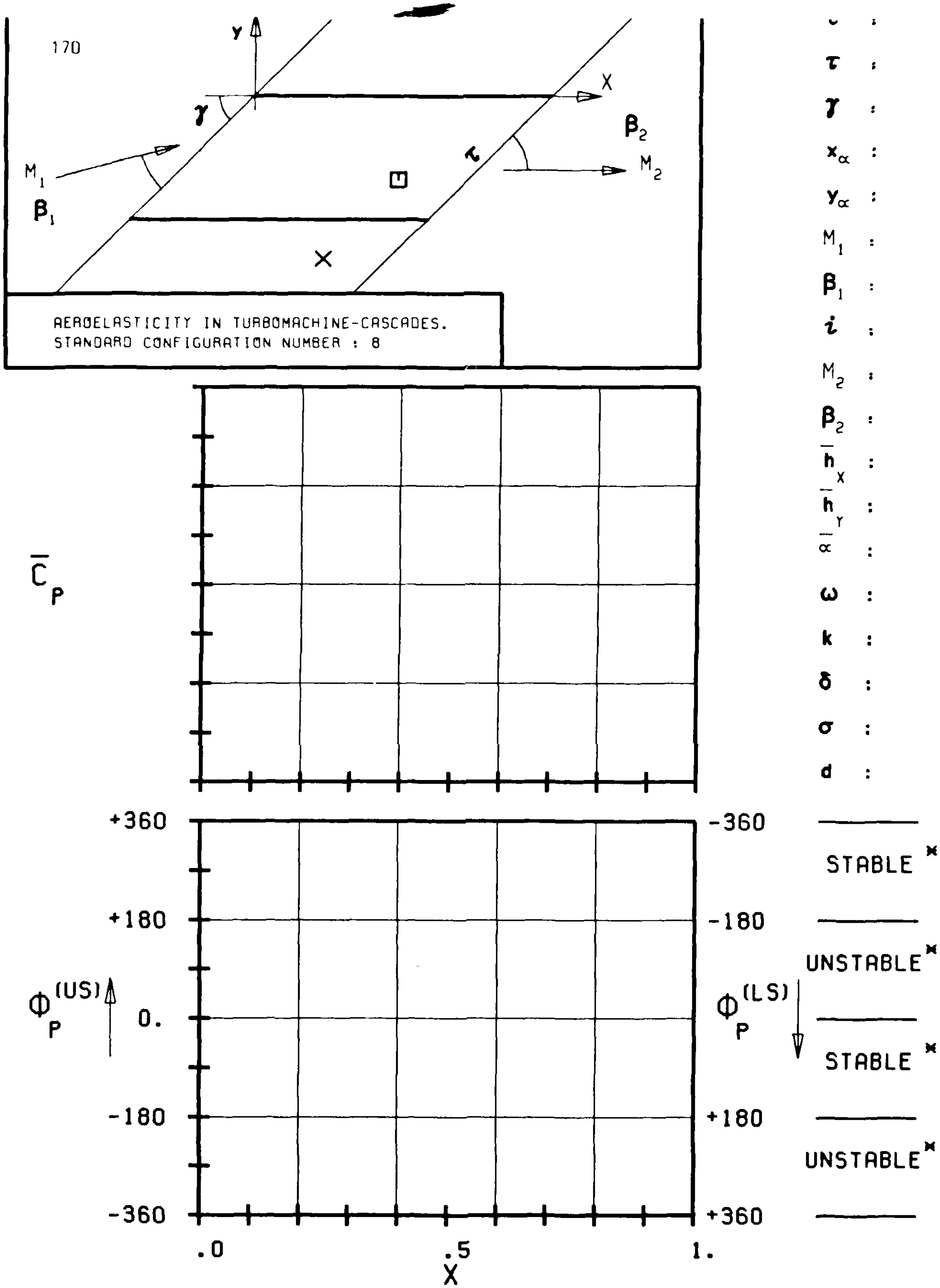

FIG. 3.8-2A: EIGHTH STANDARD CONFIGURATION.
MAGNITUDE AND PHASE LEAD OF UNSTEADY BLADE SURFACE PRESSURE DISTRIBUTION.

(*: IN PITCH MODE, NOTATION VALID UPSTREAM OF PITCH AXIS)

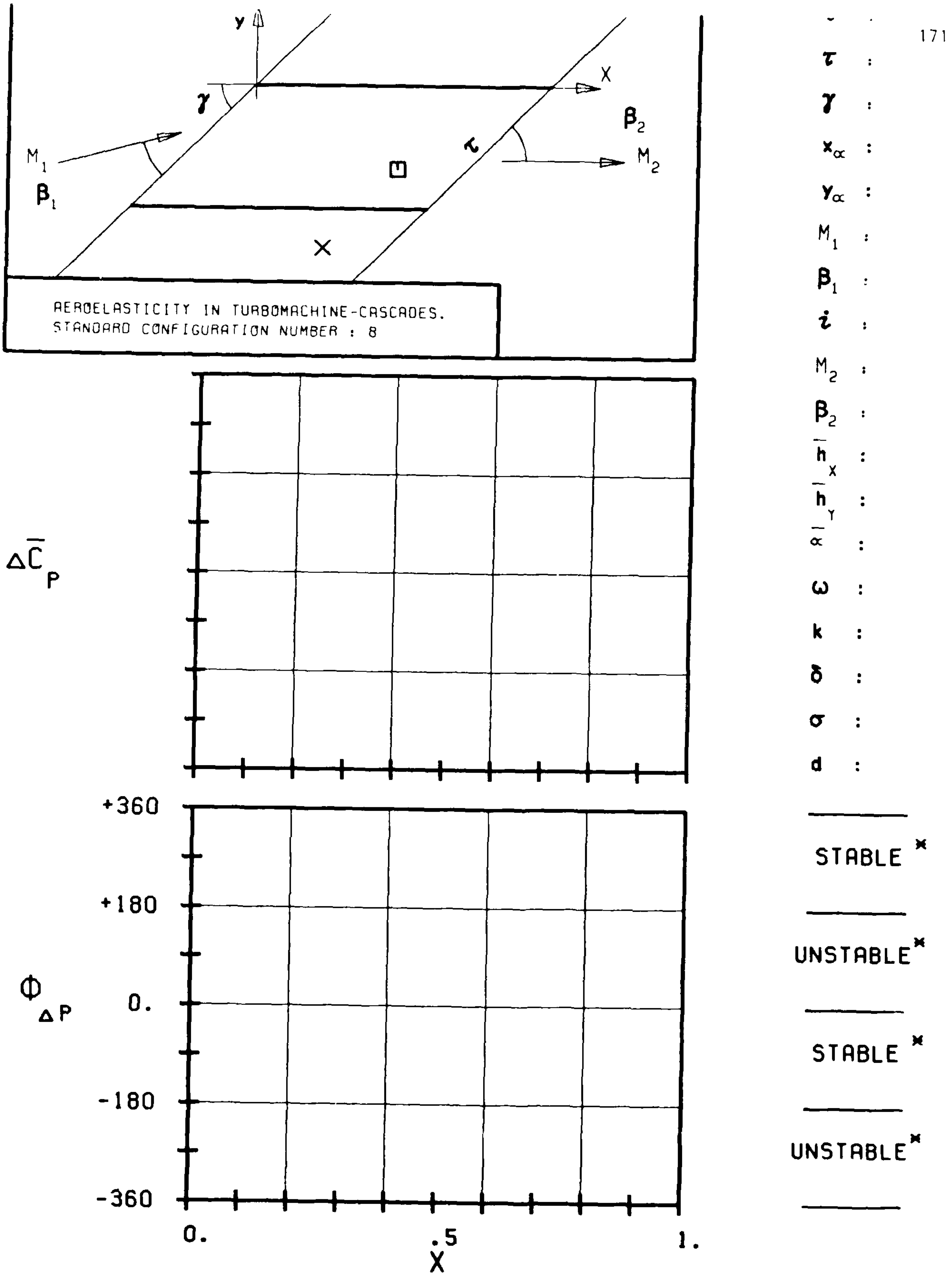

FIG. 3.8-2B: EIGHTH STANDARD CONFIGURATION.
MAGNITUDE AND PHASE LEAD OF UNSTEADY BLADE SURFACE PRESSURE DIFFERENCE DISTRIBUTION.

(*: IN PITCH MODE, NOTATION VALID UPSTREAM OF PITCH AXIS)

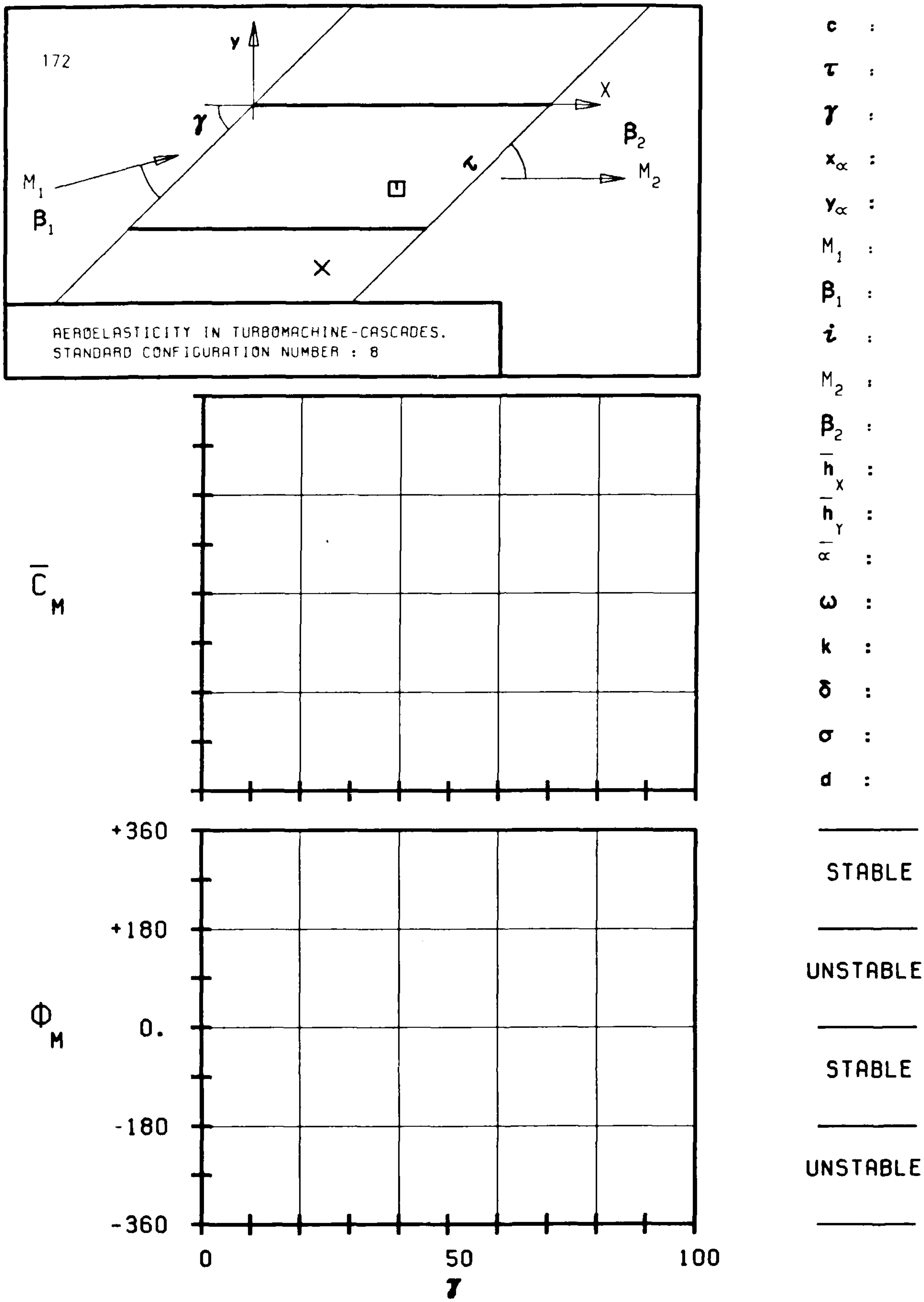

FIG. 3.8-2C: EIGHTH STANDARD CONFIGURATION.
AERODYNAMIC MOMENT COEFFICIENT AND PHASE LEAD
IN DEPENDANCE OF STAGGER ANGLE.

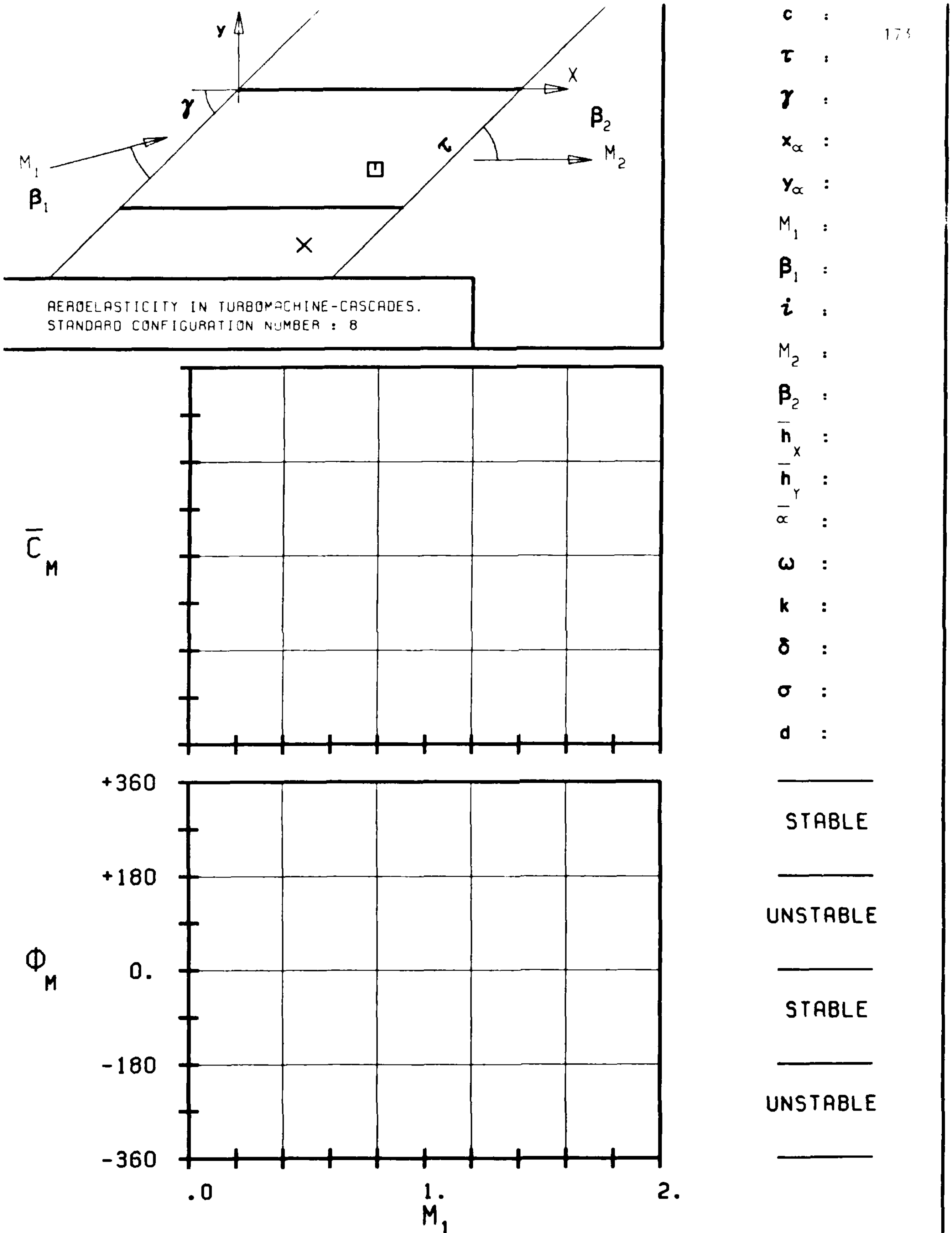

FIG. 3.8-20: EIGHTH STANDARD CONFIGURATION.
AERODYNAMIC MOMENT COEFFICIENT AND PHASE LEAD
IN DEPENDANCE OF INLET MACH NUMBER.

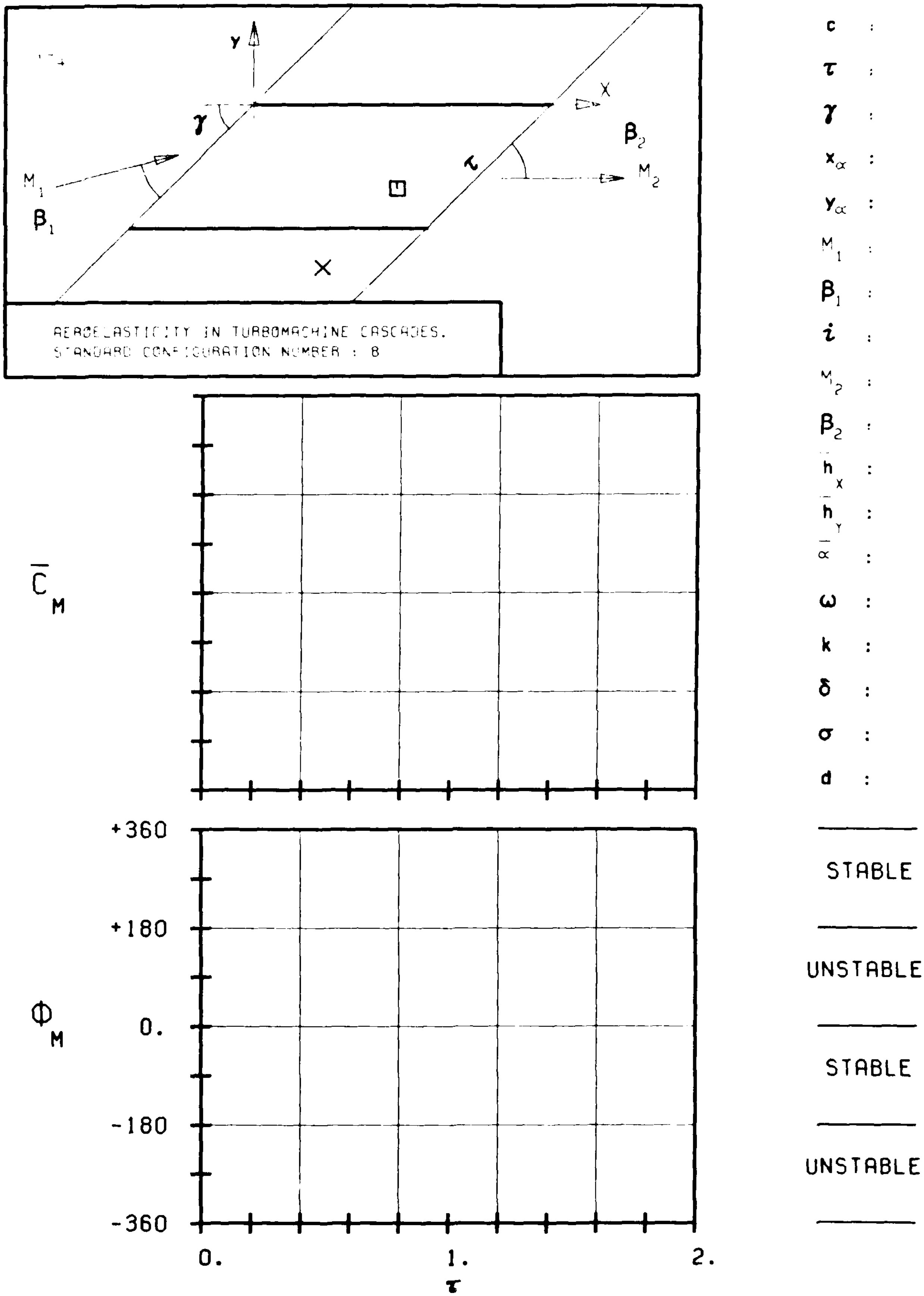

FIG. 3.8-2E: EIGHTH STANDARD CONFIGURATION. AERODYNAMIC MOMENT COEFFICIENT AND PHASE LEAD IN DEPENDANCE OF SOLIDITY.

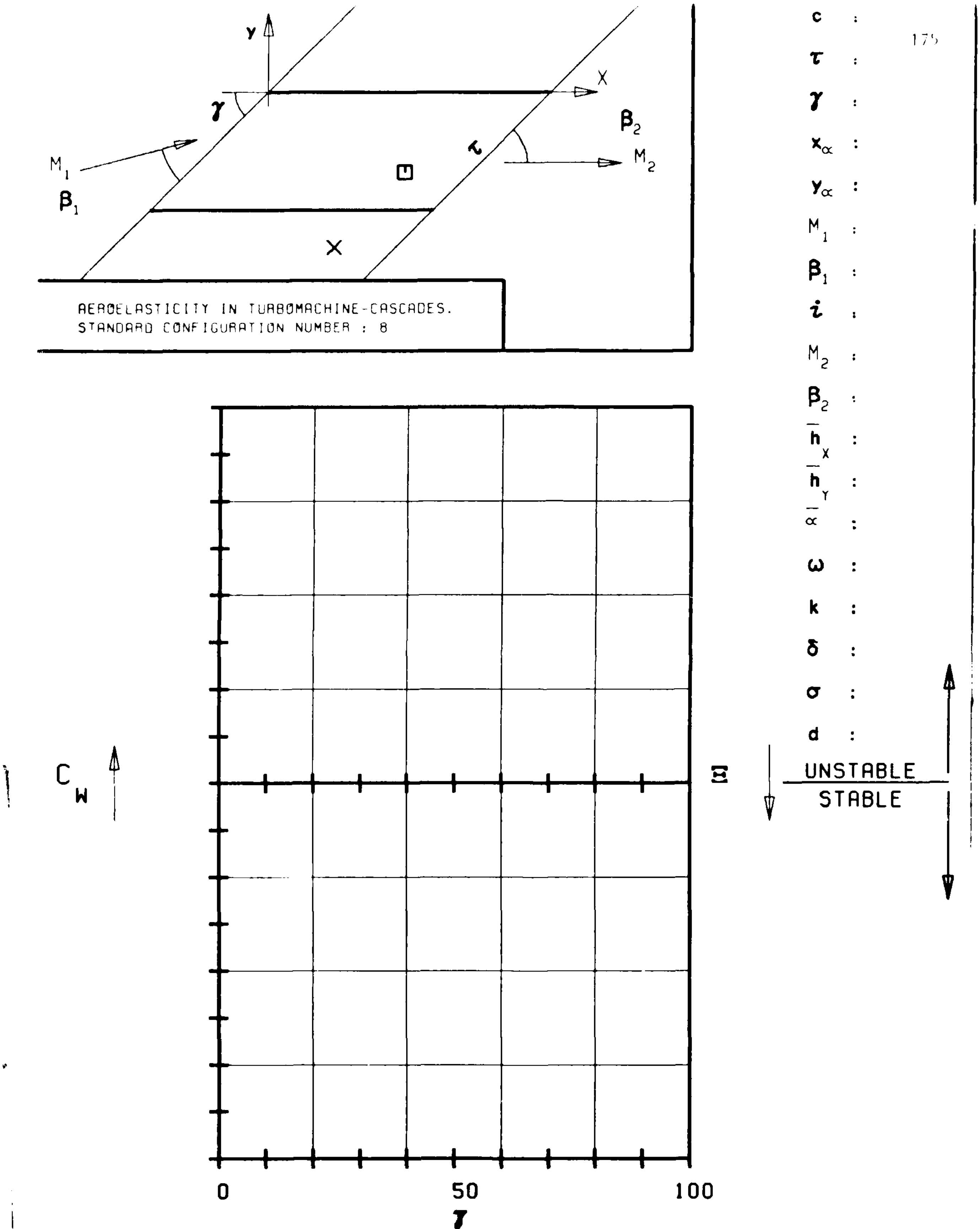

FIG. 3.8-2F: EIGHTH STANDARD CONFIGURATION.
AERODYNAMIC WORK AND DAMPING COEFFICIENTS
IN DEPENDANCE OF STAGGER ANGLE.

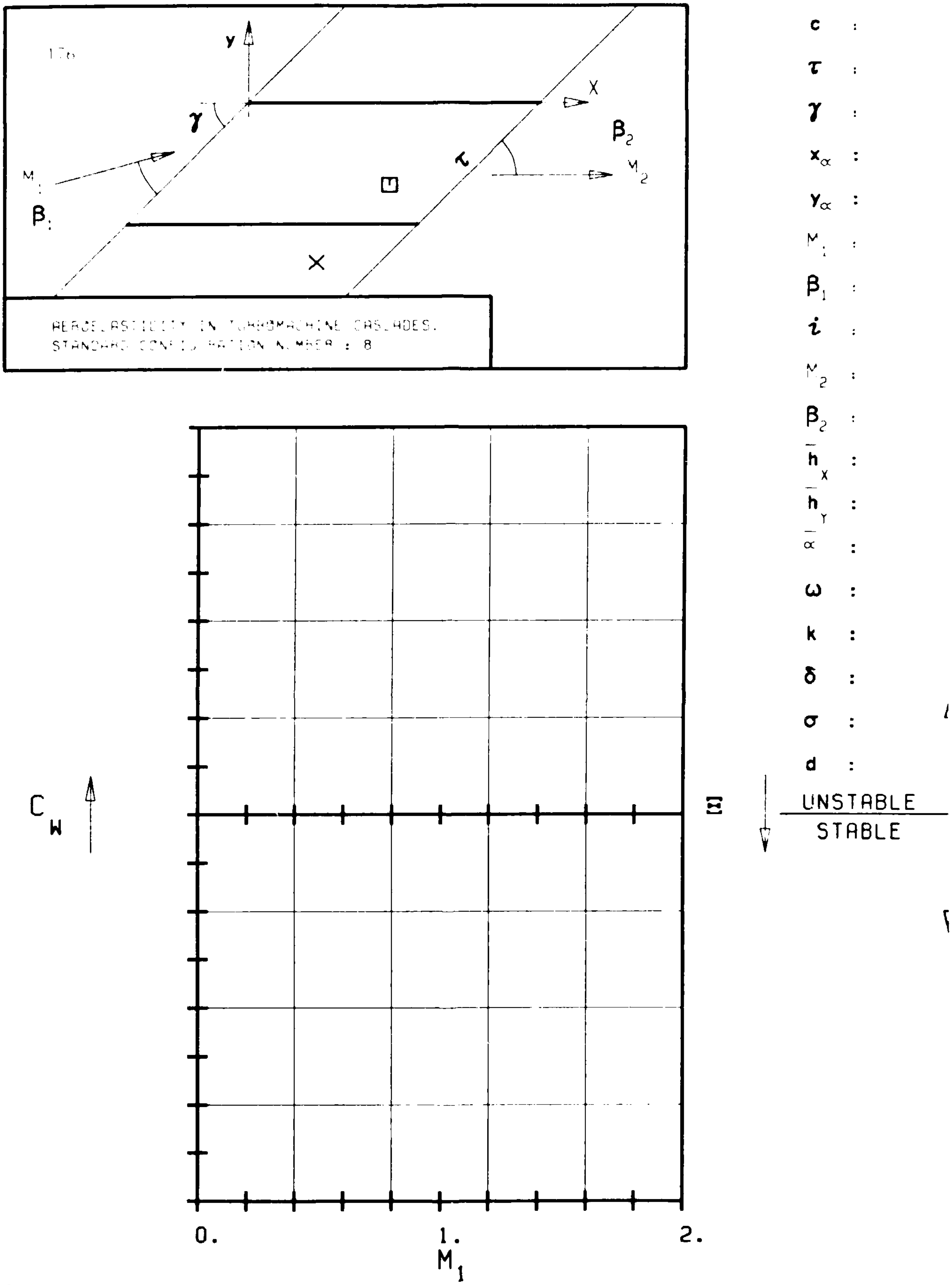

FIG. 3.8-2G: EIGHTH STANDARD CONFIGURATION.
AERODYNAMIC WORK AND DAMPING COEFFICIENTS
IN DEPENDANCE OF INLET MACH NUMBER.

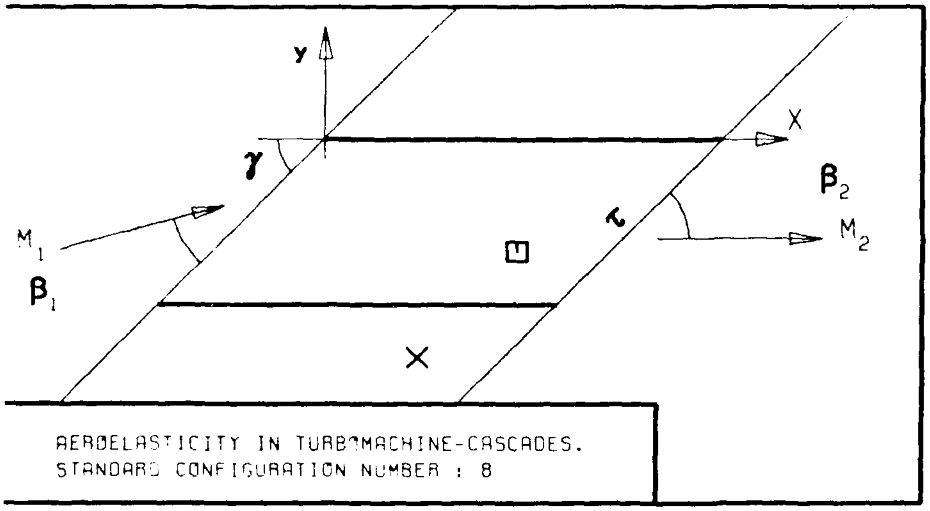

c :
τ :
γ :
x_α :
y_α :
M_1 :
β_1 :
i :
M_2 :
β_2 :
$\bar{h}_X$:
$\bar{h}_Y$:
$\bar{\alpha}$:
ω :
k :
δ :
σ :
d :

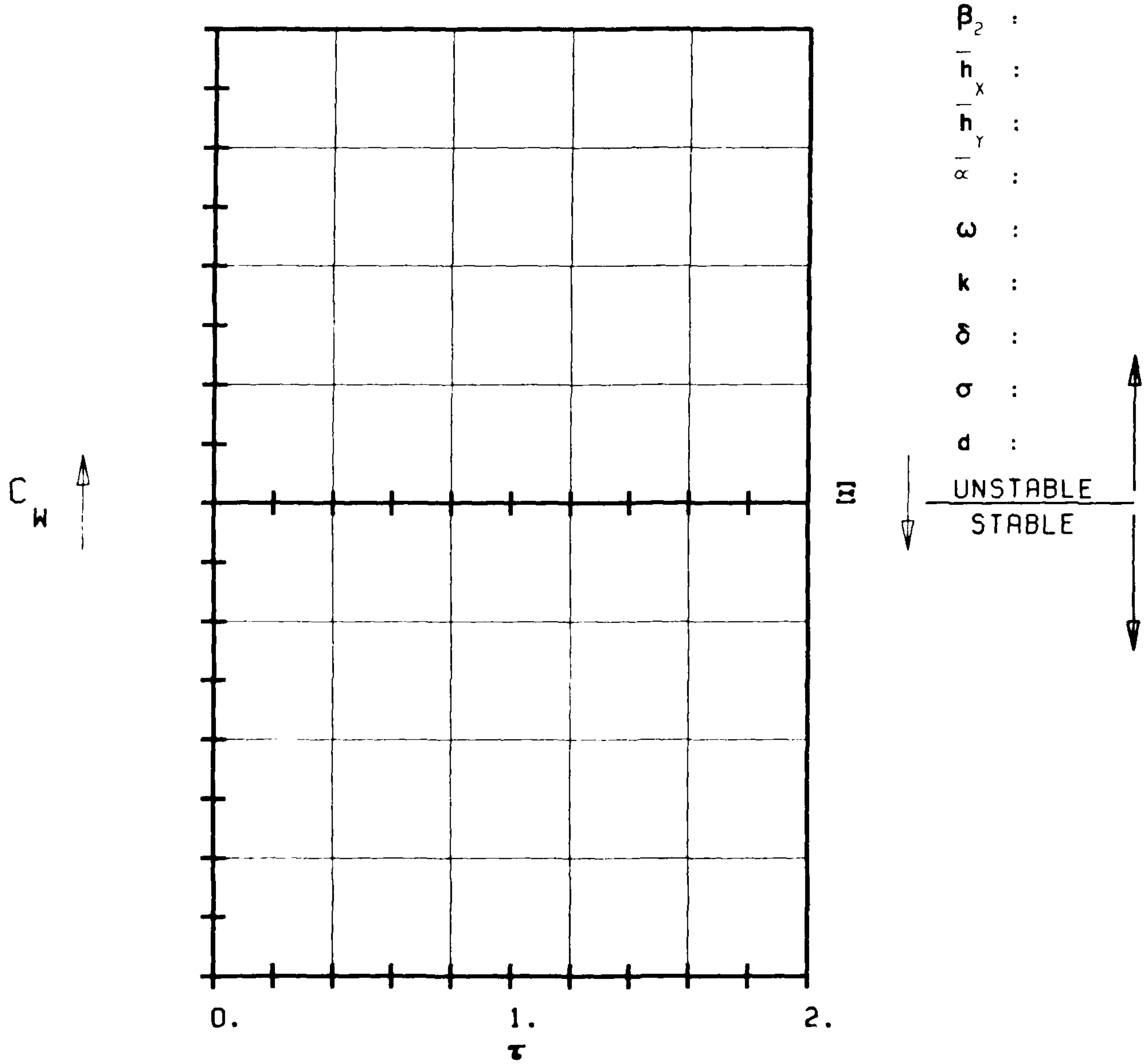

FIG. 3.8-2H: EIGHTH STANDARD CONFIGURATION.
AERODYNAMIC WORK AND DAMPING COEFFICIENTS
IN DEPENDANCE OF SOLIDITY.

Aeroelasticity in Turbomachine-Cascades. Eighth Standard Configuration							
Flat plates at zero incidence $(x_\alpha, y_\alpha) = (0.5, 0.0)$. $\alpha = 0.0349$ rad. $\sigma = 90^o$. $k = 1.0$.							
Aeroelastic Case №	$\tilde{M}_1$ (-)	Normal shock ?	γ (^{o})	τ (-)	$\overline{C}_M$ (-)	ϕ_M (^{o})	C_W

Table 5.8-2 a Eighth Standard Configuration: Table for Representa
of the 35 Recommended Aeroelastic Test Cases

Aeroelasticity in Turbomachine-Cascades.
Eighth Standard Configuration.
Aeroelastic test case N^o:______

Flat plates at zero mean incidence.
$(x_\alpha, y_\alpha)=(0.5,0.)$. $\bar{\alpha}=0.0349$ rad. $\sigma=90^o$. $k=1.0$.
$M_1=$ _____. Shock at _____. $\gamma=$ _____ ^{o}. $\tau=$ _____.

a) Global Aeroelastic Coefficients

$\bar{C}_M=$ ______	$\bar{C}_L=$ ______	$C_W=$ ______	$\Xi=$ ______	(-)
$\Phi_M=$ ______	$\Phi_L=$ ______			(^{o})

b) Local Time Dependant Blade Surface Pressure Coefficients

X (-)	$C_p^{(ls)}$ (-)	$\Phi_p^{(ls)}$ (^{o})	$C_p^{(us)}$ (-)	$\Phi_p^{(us)}$ (^{o})	$\Delta\bar{C}_p$ (-)	$\Phi_{\Delta p}$

Table 3.8-2 b Eighth Standard Configuration: Table for Representati
of the 35 Recommended Aeroelastic Cases

3.9 Ninth Standard Configuration

The ninth standard configuration is selected to be a continuation of the flat plate investigation. The emphasize is now placed upon blade thickness influence, especially in the high subsonic flow region, on the numerical results from the different prediction models.
To this end, a symmetric circular-arc profile, with thickness/chord ranging from 0.01 to 0.10, is defined (see Figure 3.9-1).
Apart from the profile thickness, the influence of inlet Mach number on the aeroelastic response of the cascade will be investigated.
For this configuration, the same vibration mode, reduced frequency and interblade phase angle as in the eighth configuration (1.0 and 90° resp.) are choosen. The stagger angle has been defined to be 30°, mainly to allow for realistic conditions at high velocities. This stagger angle may in some computations introduce influence of distorted calculation grids, wherefore it is of importance to give indications about the computational scheme together with the numerical results.
In the configuration, 24 aeroelastic cases are defined for comparison (see table 3.9-1). The incidence in the subsonic cases is 0°. For the supersonic cases, the unique incidence is calculated with a program based upon the method of characteristics. The 11 supersonic cases are defined as to have attached leading edge shock waves, and they should be calculated with supersonic throughflow. The results should be represented as in Figures 3.9-2 and in Table 3.9-2.
As for the eighth configuration, it is here not the purpose to calculate all the cases with the same prediction model. It is instead proposed that the participants calculate the cases their programs can handle, whereafter the different results will be compared and analysied.

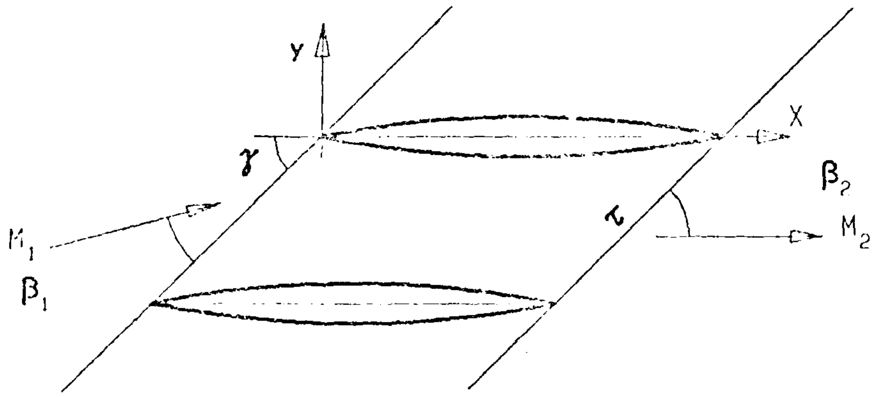

Symmetric Circular Arc Profiles.

Maximum Thickness at x = 0.5.

Vibration in pitch around $(x_\alpha, y_\alpha) = (0.5, 0.)$

$\alpha = 2.0^0$ (0.0349 rad)

$c = 0.1$ m

$\tau = 0.75$

$d = \dfrac{\text{thickness}}{\text{chord}} = 0.01 \div 0.1$

$k = 1.0$

$i = 0^0$

camber $= 0^0$

$\gamma = 30^0$

Figure 3.9-1 Ninth Standard Configuration: Cascade Geometry

Aeroelastic Case	$\tilde{M}_{-}$ (-)	$\tilde{i}_{-}$ [a] (°)	ε (°)	d (-)	Recommended Representation: C_p	ΔC_p	C_M	[illegible]
1	Incompressible	[illegible]	[illegible]	[illegible]	1	2	3,4	5,6
2				[illegible]				
3				0.02				
4				[illegible]				
5	[illegible]			[illegible]				
6				[illegible]				
7				[illegible]				
8	[illegible]			[illegible]				
9				[illegible]				
10				[illegible]				
11				[illegible]				
12	[illegible]			[illegible]				
13				[illegible]				
14	[illegible]	[illegible]		[illegible]				
15	[illegible]	[illegible]		[illegible]				
16		1.49		0.02				
17		2.22		[illegible]				
18	1.4	[illegible]		0.01				
19		1.61		0.02				
20		2.33		0.03				
21		3.13		[illegible]				
22	1.5	1.71		[illegible]				
23		3.32		0.04				
24		[illegible]		[illegible]				

Note : a) In supersonic flow, the unique incidence is calculated with the method of characteristics

b) All cases should be calculated with the least possible backpressure

1) C_p as a function of x

2) ΔC_p " " " " x

3) C_M " " " " M_1

4) C_M as a function of d

5) [illegible] " " " " M_1

6) [illegible] " " " " d

Table 3.9.1 [illegible] Recommended Aeroelastic Cases [illegible], the throughflow is supersonic

Aeroelasticity in Turbomachine-Cascades.
Ninth Standard Configuration.
Aeroelastic test case N^{o}:______

Symmetric circular arc profiles at zero mean incidence.
$(x_\alpha, y_\alpha) = (0.5, 0.)$. $\tau = 0.75$. $\gamma = 30^{o}$. $\sigma = 90^{o}$. $k = 1.0$. $\bar{\alpha} = 0.0349$ rad.
$M_1 =$ _____. $d =$ _____.

a) Global Aeroelastic Coefficients

$\bar{C}_M =$ ______	$\bar{C}_L =$ ______	$C_W =$ ______	$\bar{\Xi} =$ ______	(-)
$\Phi_M =$ ______	$\Phi_L =$ ______			(^{o})

b) Local Time Dependant Blade Surface Pressure Coefficients

x (-)	$C_p^{(ls)}$ (-)	$\Phi_p^{(ls)}$ (^{o})	$C_p^{(us)}$ (-)	$\Phi_p^{(us)}$ (^{o})	$\Delta\bar{C}_p$ (-)	$\Phi_{\Delta p}$ (^{o})

Table 5.9.2 Ninth Standard Configuration: Recommended Representation of the 24 Aeroelastic Cases.

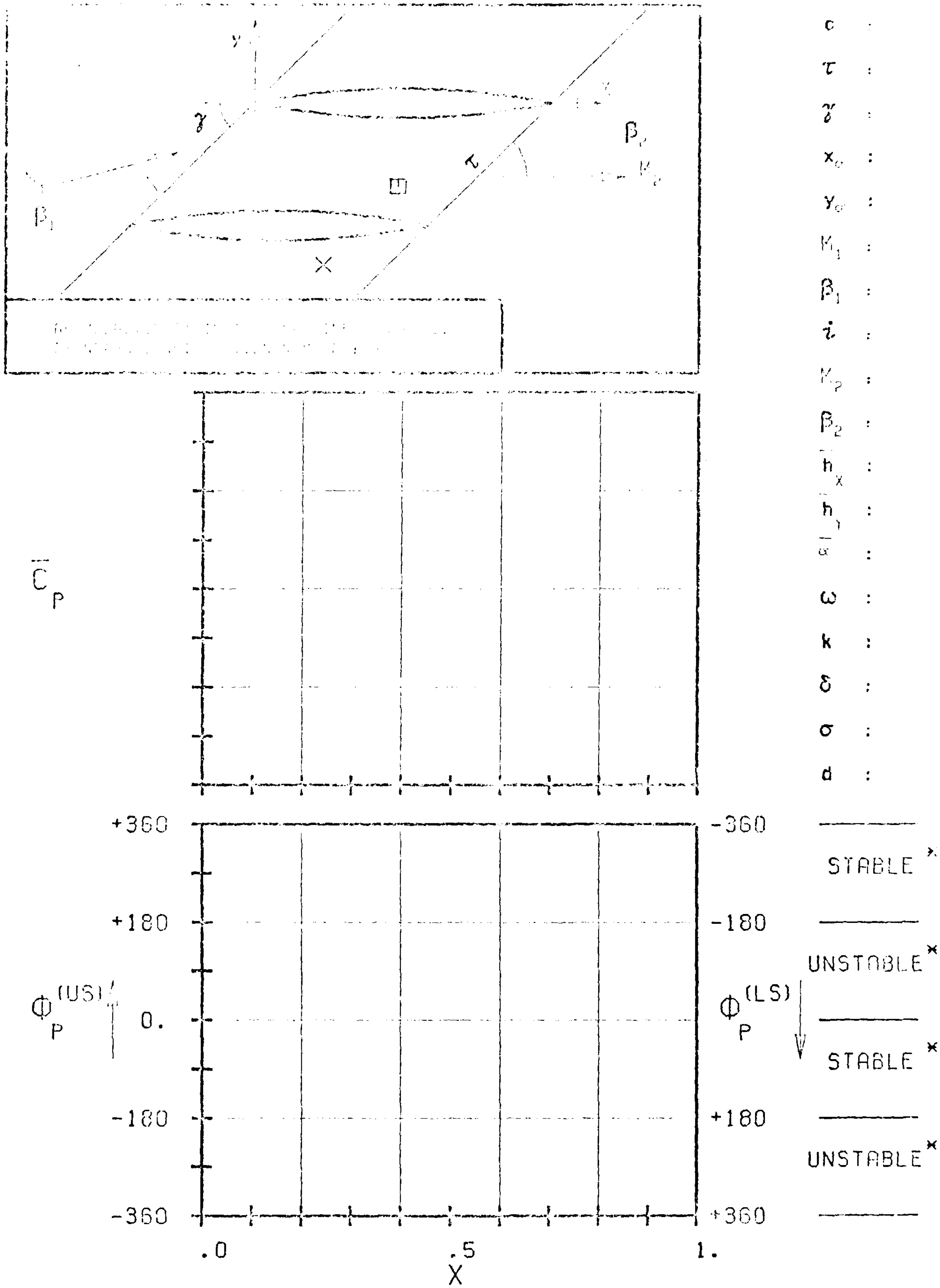

FIG. 3.9-2A: NINTH STANDARD CONFIGURATION.
MAGNITUDE AND PHASE LEAD OF UNSTEADY BLADE
SURFACE PRESSURE COEFFICIENT.

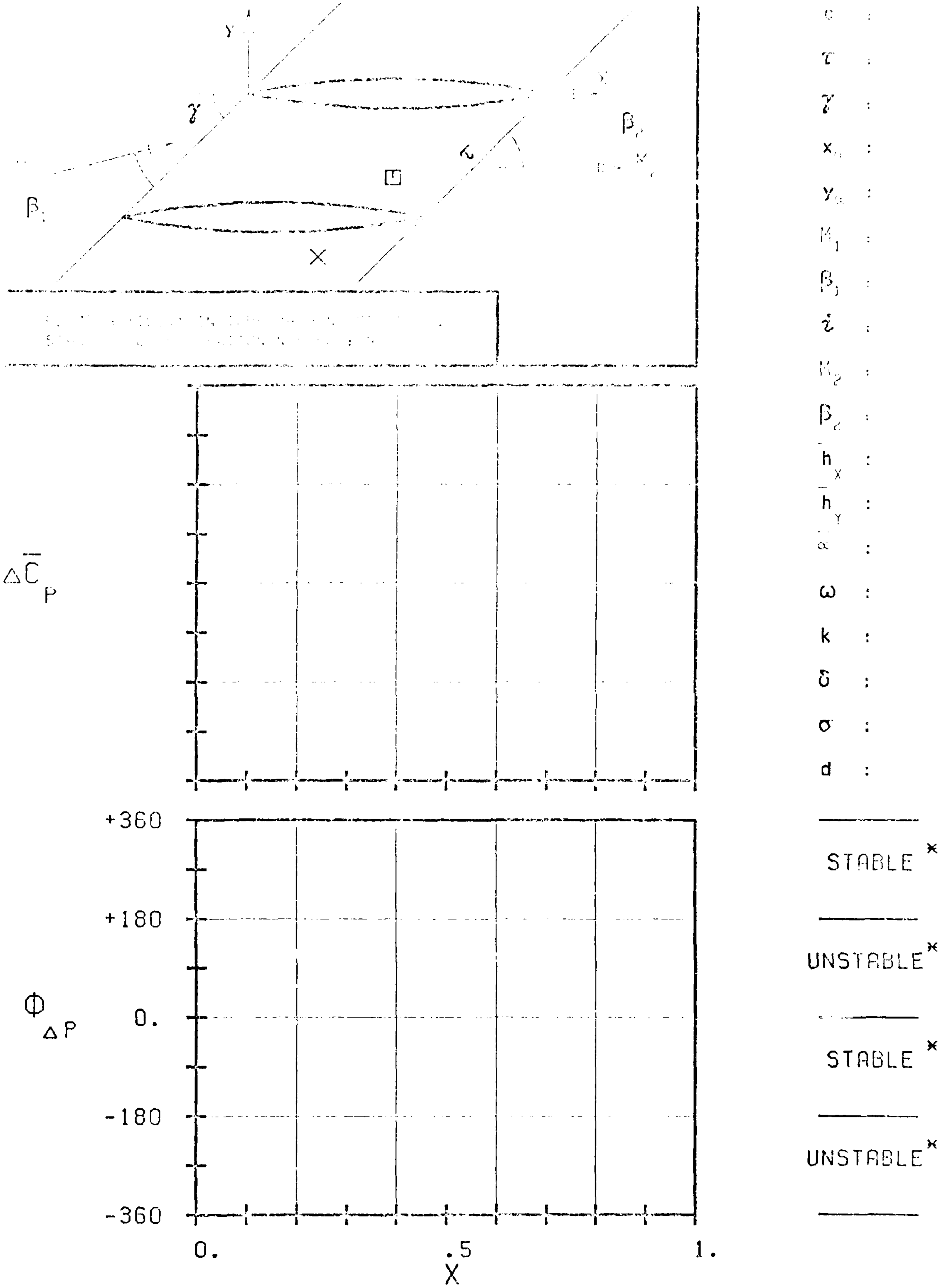

FIG. 3.9-28: NINTH STANDARD CONFIGURATION.
MAGNITUDE AND PHASE LEAD OF UNSTEADY BLADE
SURFACE PRESSURE DIFFERENCE COEFFICIENT.

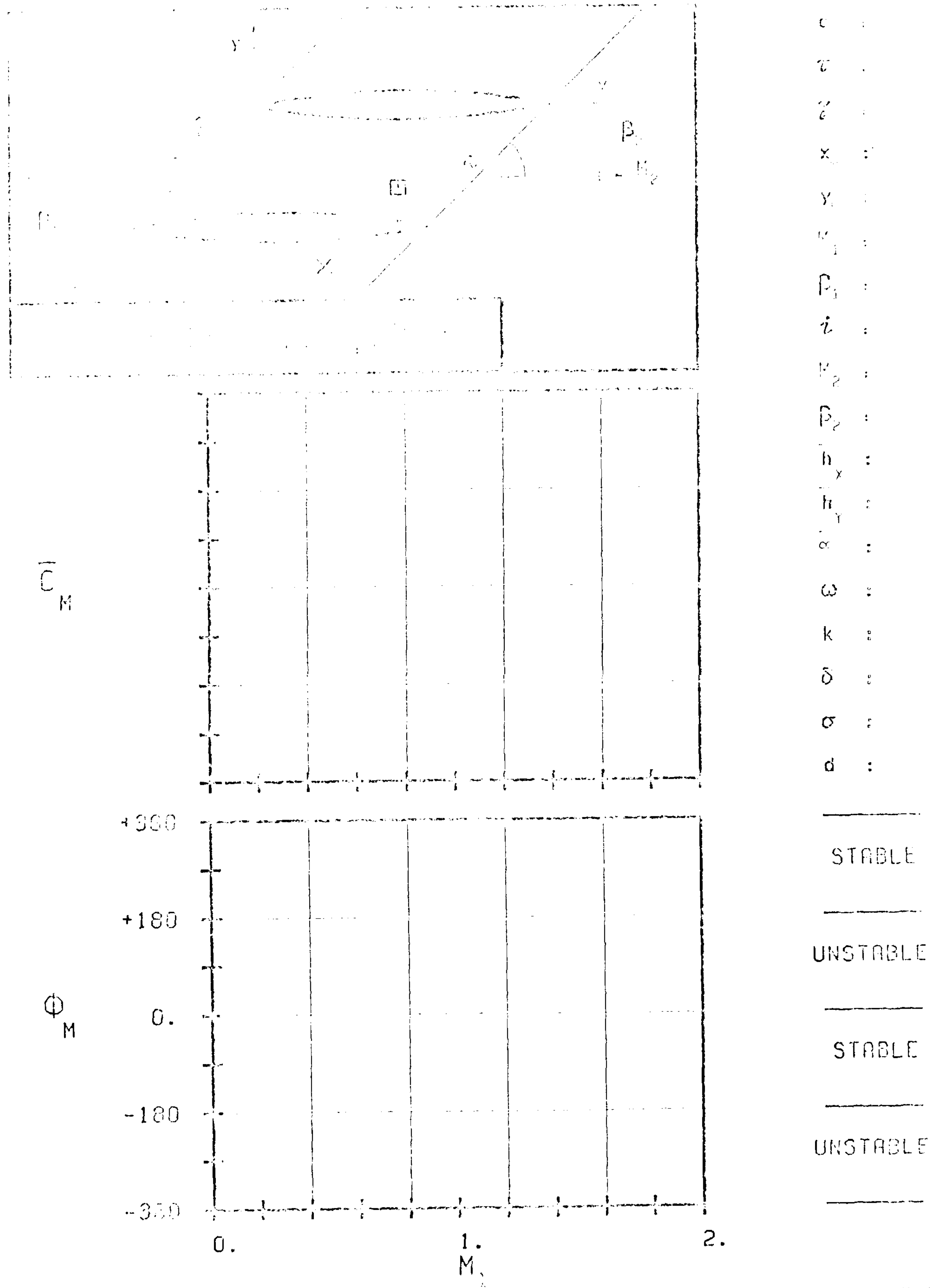

FIG. 3.9-20: NINTH STANDARD CONFIGURATION.
AERODYNAMIC MOMENT COEFFICIENT AND PHASE LEAD
IN DEPENDENCE OF INLET MACH NUMBER.

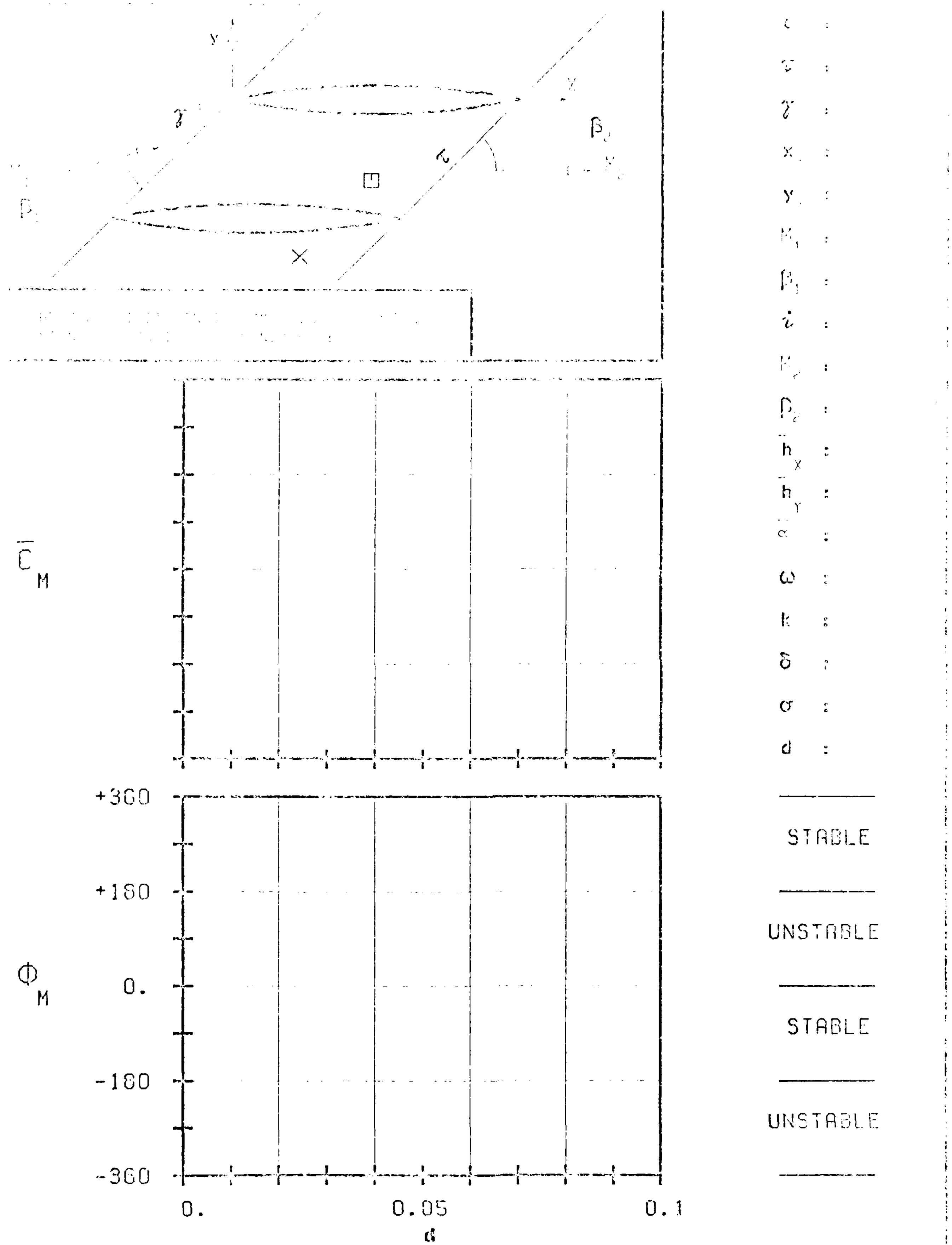

FIG. 3.9-20: NINTH STANDARD CONFIGURATION
AERODYNAMIC MOMENT COEFFICIENT AND PHASE LEAD
IN DEPENDANCE OF BLADE THICKNESS.

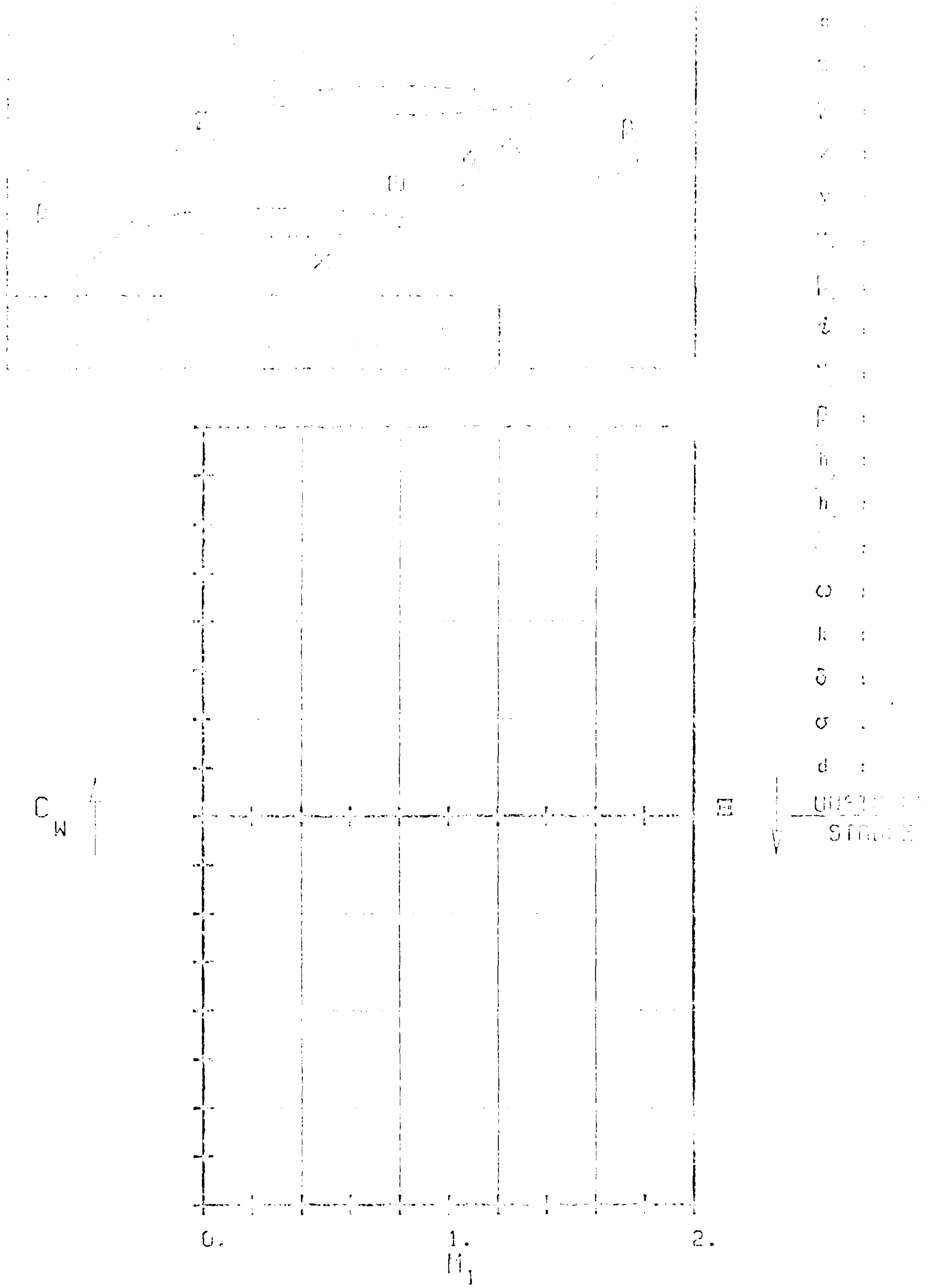

FIG. 3.9-26: [illegible]
[illegible]
IN [illegible] OF INLET MACH [illegible]


0.
0.05
0.1
d

4 Proposed Calculation of the Standard Configurations

As the present comparative study is directed towards the validation of prediction models for aeroelastic investigations in turbomachines and to establish the state-of-art of this research, it is important that as many models as possible are compared with each other and with the experimental data. To this end, all researchers interested in the field of aeroelasticity in turbomachines are invited to participate in the project and to, if a prediction model is available at their institution, predict the aeroelastic behaviour of the standard configuration(s) of their choice.

If anyone is interested in performing calculations on the standard configurations the profile coordinates (on cards) together with the diagrams to be used for representation of the corresponding configuration can be obtained upon request. Furthermore, as soon as someone has performed the first "blind test" predictions, he will receive the experimental data. It is hoped that he may then analyse the results and prepare a contribution to be presented at the Third Symposium on "Aeroelasticity in Turbomachines" (1984), in which the method and the results are explained, and in which eventual discrepancies between the theoretical and experimental results are analysied. Simultaneously, he will also have the possibility to, if wished, refine some of the results.

The participants may at any time withdraw their results. All the information we have received regarding this calculation will then be returned, and no reference will be made to the results in the report covering the comparison between the prediction models and the experiments.

However, if the results are not withdrawn, they will be compared to and presented with the experimental data at the 1984 Symposium on Aeroelasticity. At the same occasion, the state-of-art of flutter prediction models will be discussed.

[illegible]

[illegible]

[illegible]

[illegible]

[illegible]

[illegible]

[illegible]

AD-A141 904 TWO-DIMENSIONAL AND QUASI THREE-DIMENSIONAL EXPERIMENTAL STANDARD CONFIGU..(U) ECOLE POLYTECHNIQUE FEDERALE DE LAUSANNE (SWITZERLAND) LAB DE.. 3/3

UNCLASSIFIED T FRANSSON ET AL. 30 SEP 83 F/G 20/4 NL

END
DATE
FILMED
7 84
DTIC

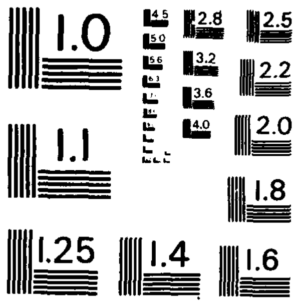

MICROCOPY RESOLUTION TEST CHART
NATIONAL BUREAU OF STANDARDS-1963-A

Aeroelasticity in Turbomachine-Cascades			
Participants with experimental data		Participants with predicition models	
Country / Institution	Name	Country / Institution	Name
USA		USA	
United Technologies Research Center	F.O. Carta	Physical Sciences Inc.	N.H. Kemp
NASA Lewis Research Center	D.R. Boldman	United Technologies Research Center	J.M. Verdon/J.R. Caspar
Westinghouse	Z. Kovatz	NASA Lewis Research Center	M.E. Goldstein/W.H. Braun/ F.B. Molls
Massachussetts Institute of Techn[illegible].	[illegible]. Crawley	University of Notre Dame	H. Atassi
Stevens Institute of Technology	[illegible]. Sisto	University of Tennesse Space	J. Caruthers/M. Kurosaka
Detroit Diesel Allison	R.L. Jay	Massachussetts Institute of Techn.	E.F. Crawley
		Naval Postgraduate School	M.F. Platzer/K. Vogeler
		Nielsen Engineering and Research Inc.	D. Nixon
		General Electric	R. Jutras
		University of California	P. Friedmann
		Princeton University	O. Bendiksen
Japan		Japan	
Tokyo University	S. Kaji/H. Tanaka/Y.Tanida	Tokyo University	H. Shoji/S. Kaji/H. Tanaka/ Y. Tanida
Toshiba	T. Araki		
Mitsubishi	S. Takahara/M. Honjo	Kuyushu University	M. Namba
Ishikawajima-Harima Heavy Industries	S. Nagana	Mitsubishi	S. Takahara
National Aerospace Lab.	H. Kobayashi		
United Kingdom		United Kingdom	
Cambridge University	D.S. Whitehead/R.J. Grant M. Davies	Cambridge University	D.S. Whitehead/S.N. Smith
Rolls - Royce	D.G. Halliwell	Imperial College	M. Graham
France		France	
ONERA	J.Girault/E.Szechenyi	ONERA	P. Salaün
West Germany		West Germany	
DFVLR	P. Bublitz/H. Triebstein	DFVLR	V. Carstens
Technische Hochschule Aachen	H.E. Gallus/K. Vogeler/ K.D. Broichhausen	Technische Hochschule Aachen	H.E. Gallus/K. Vogeler
KWU	D. Bohn		
Switzerland		Switzerland	
Brown Boveri	A. Kirschner	Lausanne Institute of Technology	A. Bölcs/T.H. Fransson
Lausanne Institute of Technology	A. Bölcs/M. Degen/ D. Schläfli		
		Italy	
		Florence University	F. Martelli

Table 4.1-1 Present Participation in the Project "Aeroelasticity in Turbomachine-Cascades"

	Institution	Name	Classification Number	Test case	Remarks
A	Tokyo University, Japan	Kaji	[illegible]	Yes	• 2-dimensional isolated airfoils. This problem is treated in an AGARD Workshop (/1/).
	Tokyo University, "	Tanida	[illegible]	Y	
	Tokyo University, "	Tanaka, H.	[illegible]	Y	
	TH Aachen, Germany	Gallus/Vogeler	[illegible]	N	
	DFVLR-Göttingen, Germany	Triebstein	[illegible]	Y	
B	ONERA, France	Girault	[illegible]	No	• 2-dimensional or quasi 2-dimensional aeroelastic investigations in linear cascades
	Detroit Diesel Allison, Indianapolis, USA	Jay	[illegible]	Y	
	DFVLR-Göttingen, Germany	Schlitz	[illegible]	Y	
	DFVLR-Göttingen, "	Triebstein	[illegible]	Y	
	Toshiba-Kawasaki, Japan	Araki	[illegible]	Y	
	ONERA, France	Szechenyi	[illegible]	N	
	Tokyo University, Japan	Tanida	[illegible]	Y	
	Tokyo University, "	Tanaka, H.	[illegible]	Y	
	United Technologies, USA	Carta	[illegible]	Y	
	NASA-Lewis, USA	Boldman/Ball	[illegible]	Y	
	Westinghouse-Pittsbourgh, USA	Kovatz	31	N	
	Mitsubishi-Nagasaki, Japan	Takahara	[illegible]	N	
C	EPF-Lausanne, Switzerland	Fransson/Schläfli	[illegible]	Y	• Quasi 2-dimensional aeroelastic investigations in annular cascades
	EPF-Lausanne, "	Fransson/Schläfli	[illegible]	Y	
	National Aerospace Lab., Tokyo, Japan	Kobayashi	12	Y	
	Whittle Lab., Cambridge, U.K.	Davies	14	N	
	Whittle Lab., Cambridge, "	Whitehead/Grant	[illegible]	Y	
	Brown Boveri, Baden, Switzerland	Kirschner	21	Y	
	TH Aachen, Germany	Gallus	[illegible]	N	
D	MIT, Massachussets, USA	Crawley	1	Y	• Fully 3-dimensional aeroelastic investigations in real machines. + No fully 3-D calculation methods exists presently, wherefore we hope to treat this at a later time.
	Rolls-Royce, Derby, U.K.	Halliwell	3	Y	
	ONERA, France	Szechenyi	[illegible]	N	
	Stevens Institute, Hoboken, USA	Sisto	33		
	Ishikawajima-Harima Heavy Ind., Tokyo, Japan	Nagano	34	N	
	Kraftwerk Union AG, Mühlheim/Ruhr, Germany	Bohn	29	Y	
E	Detroit Diesel Allison, Indianapolis, USA	Jay	4	Y	• Non-vibrating blades. Pressure fluctuations due to wake interactions or acoustic resonances. + In order to exploit to the maximum the comparison between different theories and experiments, a very restricted number of test cases concerning aeroelastic phenomena will be choosen. We hope however to investigate this theme at a later time.
	Mitsubishi, Takasago, Japan	Honjo	[illegible]	Y	
	TH Aachen, Germany	Gallus/Broichhausen	[illegible]	Y	
	TH Aachen, "	Gallus	[illegible]	Y	
	TH Aachen, "	Gallus	[illegible]	Y	
F	Whittle Lab., Cambridge, U.K.	Whitehead			• Exact solutions + Small perturbations, inviscid.
	Physical Science Co, Massachussets, USA/ ?, Japan/ ?, Japan	Kemp/Ohashi/Shoji			
	University of Cambridge, U.K.	Smith			

▨ = Not appropriate

Table 1: Classification of the 34 sets of experimental data and some exact solutions, from which the test cases will be choosen.

The scope of the present work is limited to two-dimensional or quasi two-dimensional configurations (parts 'B','C' and 'F' above).

Table 4.1-2a Classification of Present Participation in the Experimental Part of the Project

Institution	Name	Classification number	Cascade				Profile				Configuration			Flow: Fluid		Flow: Mach regime					Flutter flow field			Kinematics: Excitation		Kinematics: Motion				Mode				Magnitude		Results			
			Isolated airfoil	Linear cascade	Annular cascade	Real machine	Flat plate	Thickness	Camber	Twist	2 - Dimensional	Quasi 3-Dimensional	3 - Dimensional	Inviscid	Viscous	Incompressible	Subsonic	Supersonic	Sub - Supersonic	Super - Subsonic	No stall	Partially stalled	Fully stalled	Forced	Selfexcited	Harmonic	Non-harmonic	Interblade phase = 0	Interblade phase ≠ 0	None (gust)	Bending	Torsion	Coupled	Small disturbance	Fully unsteady	Force/Moment	Stability/Stability limits	Unsteady blade press.	Unsteady isobars
Physical Sciences Inc. University of Tokyo	Kemp Shoji	1		x			x				x			x		x					x			x		x		x		x	x	x		x		x		x	
Cambridge University	Whitehead/Smith	2		x			x				x			x		x	x				x			x		x		x	x	x	x	x		x		x		x	
Cambridge University	Whitehead	3		x			x				x			x				x			x			x		x		x	x	x	x	x		x		x		x	
Cambridge University	Whitehead	4		x			x	x	x		x			x		x	x				x			x		x		x	x		x	x		x		x		x	
Cambridge University	Whitehead	5		x			x	x	x					x		x	x	x	x	x	x			x		x		x	x		x	x		x		x		x	
United Technologies	Verdon/Caspar	6		x			x	x	x		x			x		x	x		x		x			x		x		x	x		x	x		x		x		x	
United Technologies	Verdon	7		x			x				x			x				x			x			x		x		x	x		x	x		x		x		x	
University of Tokyo	Kaji	8		x			x		x		x			x			x			x	x	x		x		x		x	x		x			x		x			
ONERA	Salaün	9			x		x			x			x	x			x				x			x		x		x	x		x	x		x		x			
ONERA	Salaün	10			x		x			x			x	x				x			x			x		x		x	x		x	x		x					
ONERA	Salaün	11		x			x			x	x			x				x			x			x		x		x	x		x	x		x		x			
NASA LeRC	Braun/Molls/Goldstein	12		x			x				x			x						x	x			x		x		x	x		x	x		x		x		x	
NASA LeRC	"	13		x				x	x		x			x						x	x			x		x		x	x		x	x		x		x		x	
Kyushu University	Namba	14		x			x	x	x		x			x				x			x			x		x		x	x		x	x		x		x	x	x	
Florence University	Martelli	15		x				x	x		x			x					x		x			x		x								x					
Florence University	Martelli	16		x				x	x		x			x			x				x			x		x				x				x		x		x	
Technische Hochschule Aachen	Gallus/Vogeler	17		x			x	x			x			x				x			x			x		x		x	x		x	x		x		x		x	
Nielsen Engineering and Research, Inc.	Nixon	18		x				x	x		x			x			x		x		x			x		x		x	x		x	x		x		x	x	x	
University of Tennessee	Caruthers	19		x				x	x		x			x			x				x			x		x	x	x	x	x	x	x	x	x				x	
University of California	Friedmann	20		x			x				x	x		x		x				x	x			x					x				x	x	x				
Lausanne Inst. of Technology	Fransson	21		x			x	x	x		x			x		x	x				x			x		x		x			x				x	x		x	x

Table 4.1-2 b Classification of Present Participation in the Theoretical Part of the Project

Acknowledgement

This research project is sponsored in part by the United States Air Force under Grants AFOSR 81-0251, AFOSR 83-0063 with Dr. Anthony Amos as program manager, and in part by the Lausanne Institute of Technology. The authors express their thanks to all the research collegues who are participating in the project. It is needless to say that without their understanding, patience and good will, these standard configurations would never have been compiled.

References

|1| "Aéroélasticité dans les turbomachines"
Proceedings of the Symposium held in Paris, France, 1976
Revue Mécanique Française, Numéro spécial 1976

|2| P. Suter (Editor) "Aeroelasticity in Turbomachines"
Proceedings of the Symposium held in Lausanne, Sept. 8-12, 1980.
Communication du Laboratoire de Thermique Appliquée N° 10, Lausanne Institute of Technology, Switzerland

|3| F.O. Carta "Unsteady Gapwise Periodicity of Oscillating Cascaded Airfoils"
ASME Paper 82-GT-286, 1982

|4| J.M. Verdon, J.R. Caspar "Development of a linear Unsteady Aerodynamic Analysis for Finite-Deflection Subsonic Cascades"
AIAA Paper 81-1290, 1981

|5| Y.C. Fung "An introduction to the Theory of Aeroelasticity"
Dover Publications, Inc., New-York, 1969, page 82

|6| H. Ashley, R.L. Bisplinghoff "Principles of Aeroelasticity"
Dover Publications, Inc., New-York, 1969, page 202

|7| F.O. Carta "Coupled Blade-Disk-Shroud Flutter Instabilities in Turbojet Engine Motors"
Journal of Engineering for Power, July 1967, p.p. 419-426

|8| S.R. Bland (Coordinator) "AGARD Two-Dimensional Aeroelastic Configurations"
AGARD Advisory Report N° 156, 1979

|9| J.M. Verdon, J.E. Mc Cune — "Unsteady Supersonic Cascade in Subsonic Axial Flow" AIAA Journal Vol. 13, Nº 2, 1975, pp. 193-201

|10| S. Fleeter — "Aeroelasticity Research for Turbomachine Applications". Journal of Aircraft, Vol.16, Nº 5, 1979

Appendix: Aeroelasticity in Turbomachine-Cascades

To be returned to

Mr. Torsten Fransson
Laboratoire de Thermique Appliquée
Ecole Polytechnique Fédérale de Lausanne
CH-1015 LAUSANNE
Switzerland

Are you interested in participating in the project on Aeroelasticity in Turbomachine-Cascades and will you perform calculations upon some of the standard configurations? __________

Which configuration(s) and aeroelastic cases will you calculate? __________

____

____

____

Would you like to obtain the profile coordinates on cards for these configurations? __________

Are you interested in receiving the aeroelastic test cases for standard configuration number 4 when they are available? __________

Name : ____________________

Affiliation : ____________________

Address : ____________________

____

____

____

Telephone : ____________________

Telex : ____________________